NASA Contractor Report 189628

ANALYSIS OF SYSTEMS HARDWARE FLOWN ON LDEF - RESULTS OF THE SYSTEMS SPECIAL INVESTIGATION GROUP

H. W. Dursch, W. S. Spear, E. A. Miller, G. L. Bohnhoff-Hlavacek, and J. Edelman

BOEING DEFENSE & SPACE GROUP
Seattle, Washington

DISTRIBUTION STATEMENT A
Approved for public release;
Distribution Unlimited

Contract NAS1-19247
April 1992

19980309 109

National Aeronautics and
Space Administration

Langley Research Center
Hampton, Virginia 23665-5225

DTIC QUALITY INSPECTED 4

PLEASE RETURN TO:

BMD TECHNICAL INFORMATION CENTER
BALLISTIC MISSILE DEFENSE ORGANIZATION
7100 DEFENSE PENTAGON
WASHINGTON D.C. 20301-7100

U5688

Accession Number: 5688

Publication Date: Apr 01, 1992

Title: Analysis of Systems Hardware Flown on LDEF-Results of the Systems Special Investigation Group

Personal Author: Dursch, H.W.; Spear, W.S.; Miller, E.A. et al.

Corporate Author Or Publisher: Boeing Defense & Space Group, PO Box 3999, Seattle, WA 98124
Report Number: NASA Contractor Report 189628

Report Prepared for: NASA, Langley Research Center, Hampton, VA 23665

Descriptors, Keywords: LDEF LEO Spacecraft

Pages: 00298

Cataloged Date: May 25, 1995

Document Type: HC

Number of Copies In Library: 000001

Record ID: 30051

National Aeronautics and
Space Administration

Goddard Space Flight Center
Greenbelt, Maryland
20771

NASA

Reply to Attn of: 720

April 24, 1992

Dear Colleague:

This report summarizes the work and results of the LDEF Systems Special Investigation Group (Systems SIG) through the November - December 1991 time frame. Information contained herein also includes appropriate information generated by the other Special Investigation Groups (i.e., Materials, Radiation, and Debris), Data Groups, and Principal Investigators. We request that any comments, corrections, suggestions, etc. that you might have concerning the document be sent to myself or Harry Dursch at Boeing.

If additional funding support is obtained by the Systems SIG, it is our desire to update this document with data to be presented at the Second LDEF Post-Retrieval Symposium scheduled for June 1992.

The work of the Systems SIG is unique in the total LDEF effort in that there is not a clearly identified discipline home within NASA nor any professional association specifically associated with the Systems SIG's wide-ranging areas of interest. To accomplish the objectives of the Systems SIG, therefore, required the hard work and dedication of individuals on the LDEF Systems SIG who were drawn from various discipline areas at the NASA Centers, several DOD laboratories, and CNES in France. I would like to thank all members of the Systems SIG for their support as well as those in the LDEF Science Office and the LDEF Experimenters that contributed so much to the effort. Additional thanks and appreciation are due to Harry Dursch and his dedicated support team at Boeing Defense and Space Group. They have worked well with the complete LDEF community and have done an excellent job. I would also like to take this opportunity to also offer special thanks to Joel Edelman for his truly outstanding efforts on behalf of the LDEF Systems SIG and the LDEF effort in general. Joel's efforts with respect to the LDEF Newsletter speak for themselves, and have successfully captured the attention and admiration of many both within and outside the LDEF Community.

James B. Mason
Chairman, LDEF Systems SIG

FOREWORD

This report describes the work accomplished under "LDEF Systems Special Investigation Group Support" contracts NAS1-18224, Task 15 (October 1989 through January 1991) and NAS1-19247 Task 2 (May 1991 through December 1991). Sponsorship for these two programs was provided by National Aeronautics and Space Administration, Langley Research Center, Hampton, Virginia and The Strategic Defense Initiative Organization, Key Technologies Office, Washington D.C.

Mr. Lou Teichman, NASA Langley Research Center, was the NASA Task Technical Monitor. Dr. James Mason, Goddard Space Flight Center, was the System Special Investigation Group Chairman. The Materials & Processes Technology organization of the Boeing Defense & Space Group was responsible for completing both contracts. The following Boeing (unless otherwise noted) personnel provided critical support throughout the program.

Sylvester Hill	Program Manager
Harry Dursch	Technical Leader
Joel Edelman (LDEF Corporation)	Thermal and LDEF Newsletter
Dr. Steve Spear	Mechanical Testing and Analysis
Emmett Miller	Electrical Testing and Analysis
Dr. Gary Pippin	Materials

The following Boeing personnel provided critical support during the program.

Gail Bohnhoff-Hlavacek	Optics and Optical Database
Dave Smith	Wire Harness Testing
Dr. Chris Johnson	Batteries
Bruce Keough	Lubricants and Seals
Dr. Robert Burgess	Solar Cells
Russ Crutcher	Contamination
Roger Bourassa	Atomic Oxygen and Solar Environment
Ken Mellott	Fasteners
Pete George	Composites

We would also like to acknowledge the contributions made to this report by Mr. Tom See, Lockheed Engineering and Sciences Company and Dr. Tom Parnell, MSFC.

The successful completion of this contract would not have been achieved without the advice and contributions of the System SIG members, LDEF Project Office Staff, LDEF Ground Operations Team, and LDEF Experimenters. These individuals helped make this program a success.

Preceding Page Blank

Systems Special Investigation Report
February, 1992
Table of Contents

	Page
1.0 EXECUTIVE SUMMARY	1
2.0 INTRODUCTION	9
2.1 LDEF Mission	9
2.2 Systems Special Investigation Group	22
3.0 LDEF ENVIRONMENT	25
3.1 Meteoroid and Debris	25
3.2 Ionizing Radiation	33
3.3 Atomic Oxygen	35
3.4 Solar	38
3.5 Thermal Environment	40
3.6 Contamination	44
4.0 SYSTEMS TEST RESULTS	47
4.1 Mechanical Systems	47
4.1.1 Primary Structure	47
4.1.2 End Support Beam	49
4.1.3 Fasteners	54
4.1.3.1 Primary Structure Fasteners	54
4.1.3.2 Tray Clamp Fasteners	54
4.1.3.3 Experimenter Fasteners	69
4.1.3.4 Velcro	70
4.1.3.5 Coldwelding	74
4.1.3.5.1 LDEF Coldwelding Experiment	74
4.1.3.5.2 Coldwelding Summary	74
4.1.4 Mechanisms	77
4.1.4.1 Environment Exposure Control Canisters	77
4.1.4.2 FRECOPA Canisters	81
4.1.4.3 Experimenter Mechanisms	83
4.1.5 Magnetically Anchored Viscous Damper	84
4.1.6 Grapples	87
4.1.7 Lubricants and Greases	89
4.1.8 Seals	95
4.1.9 Composites	99
4.1.10 Mechanical Systems Lessons Learned	103

Page

4.2 Electrical Systems 105
4.2.1 Experiment Initiate System 107
4.2.2 Experiment Power and Data System 113
4.2.3 Batteries 116
4.2.3.1 $LiSO_2$ 116
4.2.3.2 LiCF 123
4.2.3.3 NiCd 127
4.2.4 Wire Harness 131
4.2.5 Failure Analysis of A0038: Interstellar Gas Experiment 134
4.2.6 Failure Analysis of A0187-1: Chemistry of Micrometeoroids 138
4.2.7 Solar Cells 139
4.2.8 Experiment Electronic Systems 155
4.2.9 Electrical Systems Lessons Learned 160

4.3 Thermal Systems 162
4.3.1 Hardware Flown 162
4.3.2 Thermal Systems Lessons Learned 163
4.3.2.1 Thermal System Observations 163
4.3.2.2 Thermal Control Coatings 165
4.3.2.3 Thermal Control Blankets 171
4.3.2.4 Heat Pipes 176
4.3.2.5 Radiometers, Calorimeters, Reflectometers 178
4.3.3 Unresolved Issues 178

4.4 Optical Systems 181
4.4.1 Optical Systems-Related Concerns 181
4.4.2 LDEF Optical Hardware and Systems Lessons Learned 182
4.4.2.1 Uncoated Optical Materials 183
4.4.2.2 Coated Optical Materials 188
4.4.2.3 Solar Cells 196
4.4.2.4 Fiber Optics 198
4.4.2.5 Detectors 200
4.4.2.6 Reflectometers and Radiometers 200
4.4.2.7 Optical Sources 201
4.4.2.8 Lessons Learned—Additional Remarks 203
4.4.3 Optical Experiments Database 204

5.0 REFERENCES 205

APPENDIXES:
A. Hardware Flown on LDEF 216
B. Survey of Current Research in Optical Systems: Contamination Control 226
C. Optics Database User's Guide 228
D. Paper Copy of Systems SIG Optical Database 232

ACRONYM LIST

AFB	Air Force Base
AFWL	Air Force Weapons Lab
Ah	Ampere-hour
AO	Atomic Oxygen
BR/TDF	Bi-directional Reflection/Transmission Distribution Function
BRDF	Bi-directional Reflection Distribution Function
BSF	Back Surface Field
BSR	Back Surface Reflector
CAA	Chromic Acid Anodize
CNS	Centre National d'Etudes Spatiales
CRES	Corrosion Resistant Steel
CTE	Coefficient of Thermal Expansion
DAC	Digital-to-Analog Converter
DMA	Dynamic Mechanical Analysis
EAROM	Electrically Alterable Read Only Memory
EDX	Energy Dispersion X-ray
EECC	Environment Exposure Control Canisters
EEPROM	Electrically Erasable Programmable Read Only Memory
BOL	Beginning of Life
EIS	Experiment Initiate System
EPDM	Ethylene Propylene Diene Monomer
EPDS	Experiment Power and Data System
ESB	End Support Beam
ESD	Electro Static Discharge
FRECOPA	French Cooperative Passive Payload
FTIR	Fourier Transform Infrared Spectroscopy
GEOS	Geostationary Earth Observation Satellite
GMA	Gas Metal Arc
GSFC	Goddard Space Flight Center
HEPP	Low Temperature Heat Pipe Experiment Package
HVPS	High Voltage Power Supply
I-V	Current-Voltage
IGE	Interstellar Gas Experiment
Isc	Short-Circuit Current
ITO	Indium Tin Oxide
JSC	Johnson Space Center
KSC	Kennedy Space Center
LaRC	Langley Research Center
LDEF	Long Duration Exposure Facility
LEO	Low Earth Orbit
LiCF	Lithium Carbon Monofluoride
$LiSO_2$	Lithium Sulfur Dioxide
LPE	Liquid Phase Epitaxy
M&D	Meteoroid and Debris
MLI	Multi-Layer Insulation
MSFC	Marshall Space Flight Center
MTM	Magnetic Tape Module

NA	Not Applicable
NASA	National Aeronautics and Space Administration
NBR	Acrylonitrile Butadiene Rubber
NiCd	Nickel Cadmium
ORU	Orbital Replacement Unit
OTS	Orbitial Test Satellite
Pmp	Maximum Power Point
PTFE	Polytetrafluoroethylene
QCM	Quartz Crystal Microbalance
RMS	Remote Manipulator System
SAEF-II	Spacecraft Assembly and Encapsulation Facility
SAMPLE	Solar Array Passive LDEF Experiment
SEM	Scanning Electron Microscope
SIG	Special Investigation Group
SMM	Solar Maximum Mission
SSF	Space Station Freedom
TCSE	Thermal Control Surfaces Experiment
THP	Transporter Heat Pipe
TMA	Thermo Mechanical Analysis
UV	Ultraviolet
VDA	Vapor Deposited Aluminum
Voc	Open Circuit Voltage

1.0 EXECUTIVE SUMMARY

The Long Duration Exposure Facility (LDEF) is a large, low-cost, reusable, unmanned spacecraft which accommodated technology, science, and applications experiments for long-term exposure to the space environment (ref. 1). Specifically, LDEF was designed to transport experiments into space via the Space Shuttle, free-fly in low Earth orbit (LEO) for an extended period of time, and then be retrieved by a later Shuttle flight. LDEF was passively stabilized, making it an excellent platform to measure the effects of various LEO environments.

LDEF was deployed by the Shuttle Challenger on April 7, 1984 for a planned 10-month to 1-year mission carrying 57 different experiments. These experiments ranged from the study of the LEO environment to determining the effect of long-term space exposure on tomato seeds. Because of schedule changes and the loss of Challenger, LDEF was not retrieved until January 12, 1990 after spending 69 months in orbit. During these 69 months, LDEF completed 32,422 orbits of Earth and travelled almost 750,000,000 nmi. After LDEF was retrieved and prior to being berthed in the Shuttle cargo bay, a detailed photographic survey and visual inspection was performed. Following the Shuttle landing at Edwards AFB and the ferry flight to Kennedy Space Center (KSC), the deintegration process began. This process was initiated with the removal of LDEF from the Shuttle Columbia on January 27, 1990 and ended 4 months later with the LDEF structure being placed in storage.

The extended duration of the LDEF mission and the successful retrieval presented a unique opportunity to study the long-term effects of space exposure on the more than 10,000 specimens carried by the various experiments. There have been only two other instances of NASA hardware being retrieved from space after similar long-term exposures. The modular attitude control system and the coronagraph/polarimeter main electronics box were returned by the Solar Maximum Repair Mission (same mission that deployed LDEF) after 50 months of exposure (ref. 2) and the Surveyor 3 camera and other miscellaneous hardware were retrieved during the Apollo XII mission after 30 months on the lunar surface (ref. 3).

Because of the extended mission length, the science and engineering interest extended beyond the original individual experiment objectives. Four Special Investigation Groups (SIG) were formed by the LDEF Project Office to perform the deintegration of LDEF and post-flight analysis of hardware. These four SIGs were the Meteoroid and Debris, Induced Radiation, Material, and Systems SIGs. The Systems SIG was chartered to investigate the effects of the extended mission on both LDEF systems and experiment systems and to coordinate and integrate all systems analysis.

LDEF systems hardware was divided into three categories: LDEF Standalone, LDEF Shared, and Experimenter Hardware. The Standalone Hardware was provided by the LDEF Project Office and included the LDEF primary structure, viscous damper, rigidize-sensing grapple, flight releasable grapple, and the Experiment Initiate System. The LDEF Shared Hardware was also provided by the LDEF Project Office but was distributed to individual experimenters for support of their experiment objectives. This hardware consisted of five Environment Exposure Control Cannisters, seven data

acquisition systems (Experiment Power and Data Systems), the experiment trays, and ninety-two lithium-sulfur-dioxide batteries. The Experimenter Hardware consisted of the unique hardware developed by the individual experimenters for use within the confines of their own experiments. This hardware consisted of a wide variety of systems and system components including fiber optics, high voltage power supplies, fasteners, seals, solar cells, heat pipes, etc.

The approach to the testing of hardware by the System SIG has always emphasized the testing of each system at its highest practicable level of assembly. The results at this level provided the direction for further testing in the form of either nominal or anomalous behavior. The results from the system functional test then provided a clear set of directions for subsequent testing and/or failure analysis of subsytems or components. At this time the Systems SIG has performed or supported high level system functional tests on almost all LDEF and experiment systems.

The Systems SIG divided the investigations into four major engineering disciplines represented by the LDEF hardware: electrical, mechanical, thermal, and optical systems. Almost all functional testing of the active experiments has been completed and the results are documented within this report. System component hardware is currently being evaluated by either Boeing or the various experimenters. This document integrates the results to date of the ongoing testing and analysis. These integrated results include those that have been generated outside of the Systems SIG or other SIGs, e.g. by the experimenters on their respective experiments. Testing and analysis of systems-related hardware will continue beyond the release of this document. It is hoped that this document will be updated to include all future results, but the status of the funding required to perform this task is currently uncertain.

To disseminate LDEF information to the spacecraft community, the Systems SIG has completed the following activities: (1) distribution of a semi-quarterly newsletter containing updates on current results from all aspects of the various ongoing LDEF evaluations. Because of the newsletter's popularity (currently at 2000 copies), the LDEF Project Office has assumed responsibility of this activity; (2) development and release of standardized test plans for systems-related hardware (ref. 8), (3) release of the Systems SIG Interim Report in January 1991 (ref. 10); and (4) release of this report.

The following paragraphs summarize the major Systems findings to date. All of these findings are discussed in further detail in section 4. 0. To provide the necessary background for the findings presented in sec. 4.0, this document contains the following sections; a description of LDEF and the LDEF retrieval mission (secs. 2.0 and 2.1); a description of the objectives and approach of the Systems SIG (sec. 2.2); and brief summaries of the various LEO environments encountered by LDEF (sec. 3.0).

General Observations:

LDEF carried a remarkable variety of mechanical, electrical, thermal, and optical systems, subsystems, and components. A total of 19 of the 57 experiments flown on LDEF contained functional systems that were active on-orbit. Almost all the other experiments possessed at least a few specific components of interest to the Systems SIG (adhesives, seals, fasteners, optical hardware, etc.).

No system anomalies occurred that indicate any new fundamental limitations to extended mission lifetimes in LEO. However, shielding from the effects of atomic oxygen, micrometeoroids, space debris, and ultraviolet radiation must be considered.

There were several major system anomalies. However, the analysis to date has indicated that none of these can be solely attributed to the long-term exposure to LEO. Design, workmanship, and lack of pre-flight testing have been identified as the primary causes of all system failures.

The combination of any of the individual low Earth orbit environmental factors such as UV, atomic oxygen, thermal cycling, meteoroid and/or debris impacts and contamination can produce synergistic conditions that may accelerate the onset and rate of degradation of space exposed systems and materials

The most detrimental contamination process during LDEF's mission was the outgassing and redeposition of molecular contaminants which resulted in a brown film on the surfaces of LDEF. This brown film was widely dispersed over the trailing rows and both the Earth and space ends. Thermal control surfaces, optics hardware and solar cells were most susceptible to this contamination. Ram facing surfaces appeared "clean" due to atomic oxygen attack (i.e., cleaning) of the brown film.

Atomic oxygen erosion was observed on exterior surfaces at up to 100 degrees from the ram direction. This was due to the thermal component of the oxygen molecular velocity plus the effects of co-rotation of the atmosphere. Roughly 54% of the atomic oxygen exposure was accumulated during the last 6 months of the LDEF mission. The rapid increase in atomic oxygen fluence at the end of the mission was a result of both increasing solar activity and decaying orbit altitude.

Mechanical:

The LDEF deintegration team and several experimenters noted severe fastener and hardware removal difficulties during post-flight activities. The Systems SIG has investigated all reported instances, and in all cases the difficulties were attributed to galling during installation or post-flight removal. To date, no evidence of coldwelding has been found. Correct selection of materials and lubricants as well as proper mechanical procedures are essential to ensure successful on-orbit or post-flight installation and removal of hardware.

The finding of no coldwelding indicated a need to review previous on-orbit coldwelding experiments and on-orbit spacecraft anomalies to determine whether the absence of coldwelding on LDEF was to be expected. The results of this investigation showed that there have been no documented cases of a significant on-orbit coldwelding event occurring on U.S. spacecraft. There have been a few documented cases of seizure occurring during on-orbit coldwelding experiments. However, the seized materials had been selected for the experiment because of their susceptibility to coldweld during vacuum testing on Earth. This susceptibility was enhanced by effective pre-flight cleanliness procedures.

The majority of seals and lubricants used on LDEF were designed as functioning components of experiments and were, therefore, both shielded and hermetically sealed from exposure to the LEO environment. Post-flight testing has shown nominal behavior for these seals and lubricants. However, several lubricants were exposed to the LEO environment as experiment specimens. Post-flight analysis showed a range of results for these specimens ranging from nominal behavior to complete loss of lubricant, depending on the particular lubricant and its location on LDEF.

With few exceptions, adhesives performed as expected. Several experimenters noted that the adhesives had darkened in areas that were exposed to UV. The most obvious adhesive failure was the loss of four solar cells bonded to an aluminum substrate using an unfilled epoxy. Two cells were on a leading edge tray and the other two were bonded to a trailing edge tray. No adhesive remained on the two leading edge tray but some remained on the trailing edge tray. This indicated that the bond failed at the cell/adhesive interface and then the adhesive was attacked by atomic oxygen. Possible causes of failure include poor surface preparation and/or thermal expansion mismatch between the solar cell substrate and the aluminum mounting plate.

The viscous damper, used to provide stabilization of LDEF from deployment caused oscillations, performed as designed and exhibited no signs of degradation. The damper has undergone extensive post-flight testing and has been returned to NASA LaRC in a flight ready condition.

Both the rigidize-sensing grapple, used by the RMS to activate the active experiments prior to deployment, and the flight-releasable grapple, used by the RMS to deploy and retrieve LDEF, worked as designed. The grapples are currently awaiting functional testing to determine their post-flight condition.

The most significant finding for the fiber-reinforced organic composites was the atomic oxygen erosion of leading edge specimens. While the measured erosion was not unexpected, the detailed comparison of ground based predictions vs actual recession rates has not been completed. A thin protective coating of nickel and SiO_2 was used on leading edge specimens to successfully prevent this erosion.

Electrical:

Electrical/mechanical relays continue to be a design concern. Two of the most significant LDEF active system failures involved relay failures. The Interstellar Gas Experiment was one of the more complex experiments on LDEF, with seven "cameras" located on four trays. Each camera contained five copper-beryllium foil plattens, which were to sequentially rotate out of their exposed position at pre-determined intervals. This experiment was never initiated due to a failure of the experiment's master initiate relay. The Thermal Control Surfaces Experiment recorded on-orbit optical properties of various thermal control coatings using a four-track Magnetic Tape Module. The latching relay which switched track sets failed to operate when switching from track 3 to track 4. Consequently, portions of the early flight data on track 1 were overwritten and lost.

The Experiment Initiate System (EIS) provided the initiate signal to the active experiments which directed them to turn on their power and begin their operational programs. Post-flight inspection and testing, using the original ground support equipment, showed the condition of the EIS to be nominal.

NASA supplied seven Experiment Power and Data Systems (EPDS) to record on-orbit generated data. All EPDS units were similar, consisting of a Data Processor and Control Assembly (DPCA), a tape recorder (the Magnetic Tape Module), and two $LiSO_2$ batteries, all of which were attached to a mounting plate designed to fit into the backside of the experiment tray. The EPDS components were not directly exposed to the exterior environment, being protected by their mounting plate and by external thermal shields. Although simple compared with today's data systems, the EPDS contained many elements common to most such systems, including various control and "handshake" lines, programmable data formats and timing, and a data storage system. EPDS electronic components were procured to MIL-SPEC-883, Class B standards, and were not rescreened prior to installation. Data analysis and post-flight functional testing showed that all EPDS functioned normally during and after the LDEF flight.

Three different types of batteries were used on LDEF: lithium-sulfur-dioxide ($LiSO_2$), lithium carbon monofluoride (LiCF), and nickel-cadmium (NiCd) batteries. NASA provided a total of 92 $LiSO_2$ batteries that were used to power all but three of the active experiments flown on LDEF. Ten LiCF batteries were used by the two active NASA MSFC experiments. One NiCd battery, continuously charged by a four-array panel of solar cells, was used to power an active experiment from NASA GSFC. A loss of overcharge protection resulted in the development of internal pressures which caused bulging of the NiCd cell cases. However, post-flight testing showed that the battery still has the capability to provide output current in excess of the cell manufacturer's rated capacity of 12.0 ampere-hours. All the LiCF and $LiSO_2$ batteries met or exceeded expected lifetimes.

LDEF provided valuable knowledge concerning the viability of using various solar cells and solar cell encapsulants (adhesives and coverglass materials). Coverglass materials such as ceria doped microsheet and fused silica withstood this particular environment. Measurable degradation of some widely used antireflection

coatings was observed. Results from some low cost materials such as silicone, Teflon, and polyimide indicated that these materials will require additional research before full-scale replacement of the conventional encapsulants (fused silica coverglass and DC 93500 adhesive) is justified. Micrometeoroid and debris impacts will continue to be a significant solar cell performance degradation mechanism. Solar cell performance degradation due to the deposition of contamination on the surfaces was also well documented. However, the majority of electrical characterization and analysis of on-orbit data remains to be completed.

Pyrotechnic devices, flown on Experiment A0038, were successfully fired during post-retrieval ground testing.

Thermal:

The change in performance of a wide variety of thermal control coatings and surfaces was moderate, with a few exceptions. A significant amount of these changes has been attributed to contamination effects. Certain metals (esp. chromic acid anodize aluminum), ceramics, coatings (YB-71, Z-93, PCB-Z), aluminum coated stainless steel reflectors, composites with inorganic coatings (Ni/SiO_2), and siloxane-containing polymers exhibited spaceflight environment resistance that is promising for longer missions. Other thermal control and silicone based conformal coatings, uncoated polymers and polymer matrix composites, metals (Ag, Cu) and silver Teflon thermal control blankets and second surface mirrors displayed significant environmental degradation. In addition, post-flight measurements may be optimistic because of bleaching effects from the ambient environment.

The results of thermal measurements on different samples of the same materials made at different laboratories have proven to be remarkably consistent and in agreement, lending additional credibility to the results. Confidence in designers' thermal margins for longer flight missions has been increased.

One of the most notable observations made during the on-orbit photo survey was the loose silverized Teflon thermal blankets located on a space end experiment. Tape was used to hold the edges of the thermal blankets to the experiment tray frame. The blankets apparently shrunk in flight causing the blankets to detach from the frame. Portions of the tape were attached to both the blanket and frame, indicating that the tape had failed in tension. Post-flight adhesion testing showed that the tape retained adequate adhesive properties.

Initial functional tests were performed for each of the three heat pipe experiments flown on the LDEF, and the heat pipe systems were found to be intact and fully operational. No heat pipe penetration occurred due to micrometeoroid or debris impact.

Actual measured temperatures within the interior of the LDEF ranged from a low of 39°F to a maximum of 134°F and were well within design specifications. External thermal profiles varied greatly, depending on orientation, absorptance/emittance, and material mounting and shielding. The thermal stability of the LDEF adds to the

accuracy of existing thermal models and enhances our ability to model the LDEF thermal history, as well as other spacecraft.

The loss of specularity of silver Teflon thermal blankets, one of the earliest observations noted at the time of retrieval, was determined to have had no significant effect on the thermal performance of those materials. This loss of specularity is the result of first surface erosion and roughening by atomic oxygen.

The thermal performance (absorptance/emittance) of many surfaces was degraded by both line-of-sight and secondary contamination. The specific contamination morphology in various locations was affected by ultraviolet radiation and atomic oxygen impingement. Overall, the macroscopic changes in thermal performance from contamination appear to be moderate at worst. Limited measurements on surfaces from which the contamination was removed post flight suggest that the surfaces beneath the contamination layers have undergone minimal thermal degradation.

Over 50% of all LDEF's exterior surfaces were chromic acid anodized (CAA) aluminum. Extensive optical testing of LDEF's CAA aluminum tray clamps was performed because of their wide distribution around the LDEF and representation of a complete spectrum of spaceflight environmental exposures. The tray clamps provided a complete picture of the spaceflight environmental effects on this surface treatment. Comparison of front-side (exposed), backside (shielded) and control clamps showed slight changes in the optical properties. However, the variations in absorptance and emittance have been attributed to the inherent variability in anodizing, to variations in measurements, and to the effects of on-orbit contamination deposited on tray clamp surfaces.

Betacloth which was exposed to the atomic oxygen flux was seen to have been cleansed of the many minute fibers that normally adorn its surface. This has been observed to have no measurable effect on the thermal performance of the betacloth, although some associated contamination issues are raised.

Optical:

Contaminant films and residue were widespread in their migration over LDEF and onto optical experiment surfaces, especially due to the decomposition and outgassing of several materials, at least two possible sources being identified as those from the vehicle itself, as well as those materials used in some of the experiments.

Four experiments flew fiber optics and a fifth experiment evaluated fiber optic connectors. Four of these five experiments recorded on-orbit data using the NASA provided EPDS. Overall the fiber optics performed well on-orbit, with little or no degradation to optical performance. Most environmental effects were confined to the protective sheathing. However, one fiber optic bundle was struck by a meteoroid or debris particle causing discontinuity in the optical fiber. Preliminary data has indicated the need for additional study of the temperature effects on fiber optical performance. Post-flight testing performed on fiber optics flown on the Fiber Optic Exposure

Experiment showed an increase in loss with decreasing temperature, becoming much steeper near the lower end of their temperature range.

Four LDEF experiments contained a variety of detectors. Most detectors were not degraded by the space exposure, with one notable exception. The triglycine sulfide had a 100% detectivity failure rate on both the control and flight samples.

Several types of optical sources were flown on LDEF including solid and gas lasers, flashlamps, standard lamps, and LEDs. To date, the results indicate that most optical sources operated nominally except for two gas lasers (HeNe and CO_2) which would not fire during post-flight testing and a flickering deuterium lamp arc. During post-flight testing of the two gas lasers, no laser action could be obtained from the tubes. The characteristics of the tubes suggested that the mixture of fill gas had changed during the period between pre-flight and post flight tests. This result is consistent with changes expected due to gas diffusion through the glass tube. The tubes were in good physical condition, and survived the launch and recovery phases without apparent degradation.

Micrometeoroid and debris impacts on optical surfaces caused localized pitting, punctures, cracking, crazing, and delaminations.

Spectral radiation from both solar and earth albedo sources was indicated both in the modifications of surface coating materials (chemical decomposition caused by ultraviolet radiation). This was particularly noticeable on an experiment located on the trailing edge where the holographic gratings had a 30% to 40% degradation of reflectivity from exposure to solar radiation and cosmic dust. Experimenters also noted that changes to coating interfaces as a result of infrared absorption may have contributed to mechanical stresses and failures from thermal cycling.

Atomic oxygen had a major effect in the oxidation of many physically "soft" materials, including optical coatings and thin films, as well as oxidation of uncoated, metallic reflective coatings (copper and silver). In general, "hard" uncoated optical materials were found to be resistant to the LEO environment.

Synergistic conditions of degradation resulted from the multiple and combined effects of environmental factors; for instance, UV and atomic oxygen attacked, changed, or even eroded away some of the overlaying contamination, modifying the broadband and spectral content of optical inputs to the sample beneath .

An LDEF Optical Experiment Database was created (using Filemaker Pro database software) that provides for quick and easy access to available experimenter's optic's related findings. The database contains a file for each of the LDEF experiments that possessed optical hardware (database currently contains 29 files). Each file contains various fields that identify the optical hardware flown, describe the environment seen by that hardware, summarizes experimenter findings and list references for additional information. A paper copy of this database is contained in Appendix D of this report.

2.0 INTRODUCTION

2.1 LDEF MISSION (Refs. 4,5)

The Long Duration Exposure Facility was developed by NASA's Office of Aeronautics and Space Technology and the Langley Research Center to provide a means of exposing a variety of experiments to the low Earth orbit (LEO) space environment. LDEF was designed and fabricated at Langley in the late 1970s as a passive satellite which is reusable for planned repeat missions. The LDEF is a 14-ft-diameter by 30-ft-long aluminum structure with the cylindrical cross section of a 12-sided regular polygon. The structure is designed with 72 bays around its circumferential surface, 8 bays at the space oriented end, and 6 bays at the Earth-oriented end (fig. 2.1-1). Each bay contained one tray which was clamped to the LDEF structure. Figure 2.1-2 describes the tray numbering system used to identify specific tray locations. The experiments were totally self-contained in either the 3-ft by 4-ft trays mounted in each circumferential bay or the 2.5-ft by 2.5-ft trays mounted at the ends. Figure 2.1-3 is an on-orbit retrieval photograph of several experiments showing the trays/experiments mounted on the LDEF structure.

There were a total of 57 different experiments mounted in the 86 trays facing outward from the LDEF structure. Some experiments used more than one tray and others used as little as 1/6 of a tray. Specific experiments included exposure to the LEO environment of thermal control coatings, composites, solar array materials and solar cells, fiber optics, infrared detectors, high-altitude balloon materials, electronic components, and solid rocket materials. Other experiments were designed to study heat pipes, the ability to grow crystals during long exposure to low gravity, and investigate the LEO environment including atomic oxygen, meteoroid and space debris, interstellar gas, radiation, and cosmic rays. Millions of tomato seeds were also flown on LDEF and then distributed to schools for use in projects to determine if any mutations occurred due to the long-term LEO exposure. Figure 2.1-4 is the complete list of experiments and their experiment number and figure 2.1-5 shows the location of each experiment. Reference 5 provides a detailed discussion for each of the 57 experiments. Due to the extended exposure, the LDEF structure and the various experiment support systems became an unplanned experiment. All welds, fasteners, wire harnesses, trunnions, attitude stabilization systems, experiment initiate systems, etc., were examined to determine if the extended exposure had any effect on the hardware that made up the LDEF structure.

LDEF was a passive satellite with no telemetry of data to Earth during the mission. However, several experiments required on-orbit collection of data. An Experiment Power and Data System (EPDS) was developed by Langley to record these data onto a magnetic tape for post-flight analysis. Seven EPDSs were flown, with some experiments sharing a specific unit. An Experiment Exposure Control Cannister (EECC) was developed to provide contamination protection of experiment specimens during deployment and retrieval. Five of these canisters were flown with all five opening at day 14 of the mission and then closing after day 297. Both of these experiment-support subsystems utilized $LiSO_2$ batteries developed specifically for the LDEF mission. All the experiment support hardware was mounted on the backside of the trays, which shielded the hardware from direct exposure to the LEO environment.

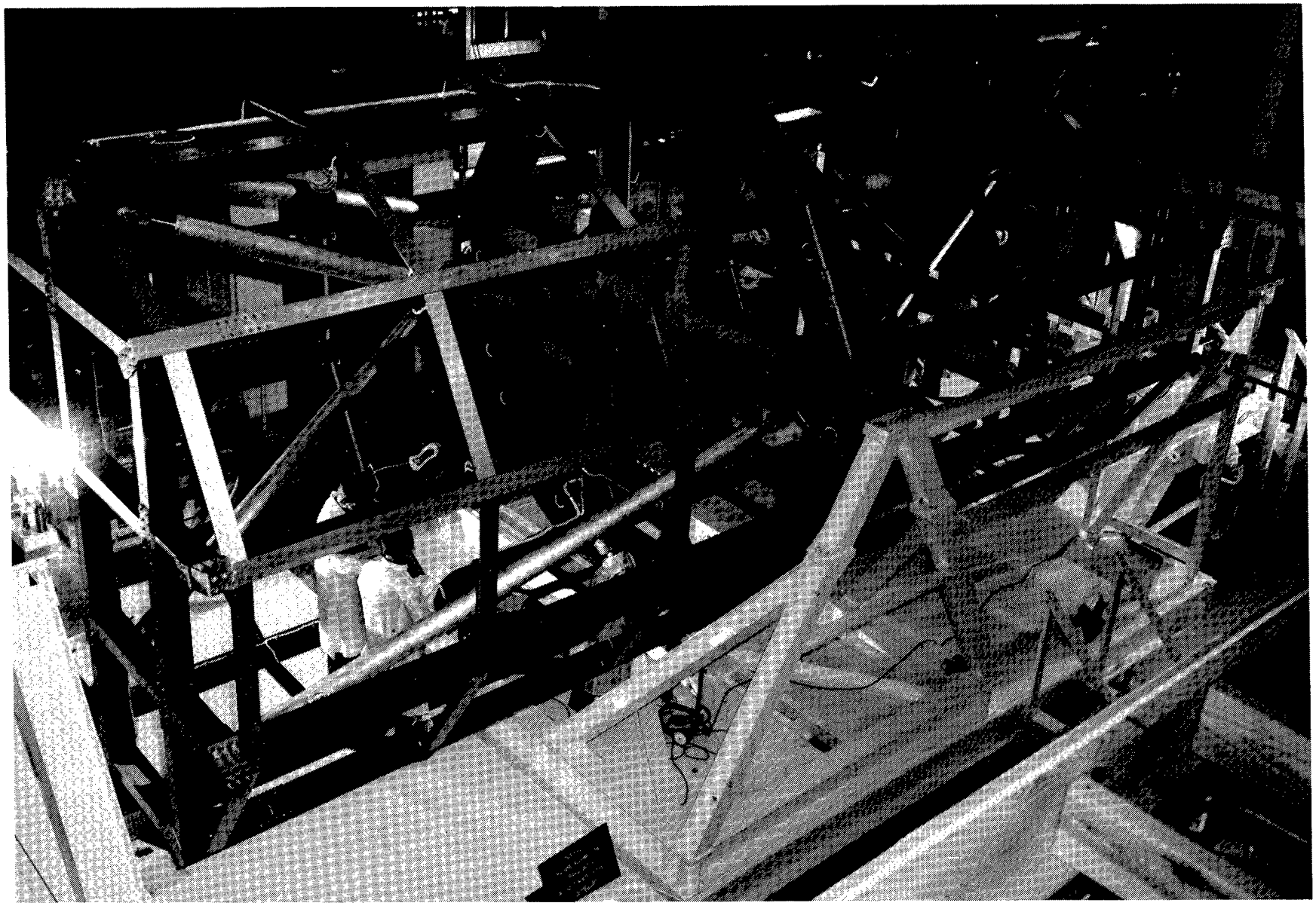

Figure 2.1-1. LDEF Structure

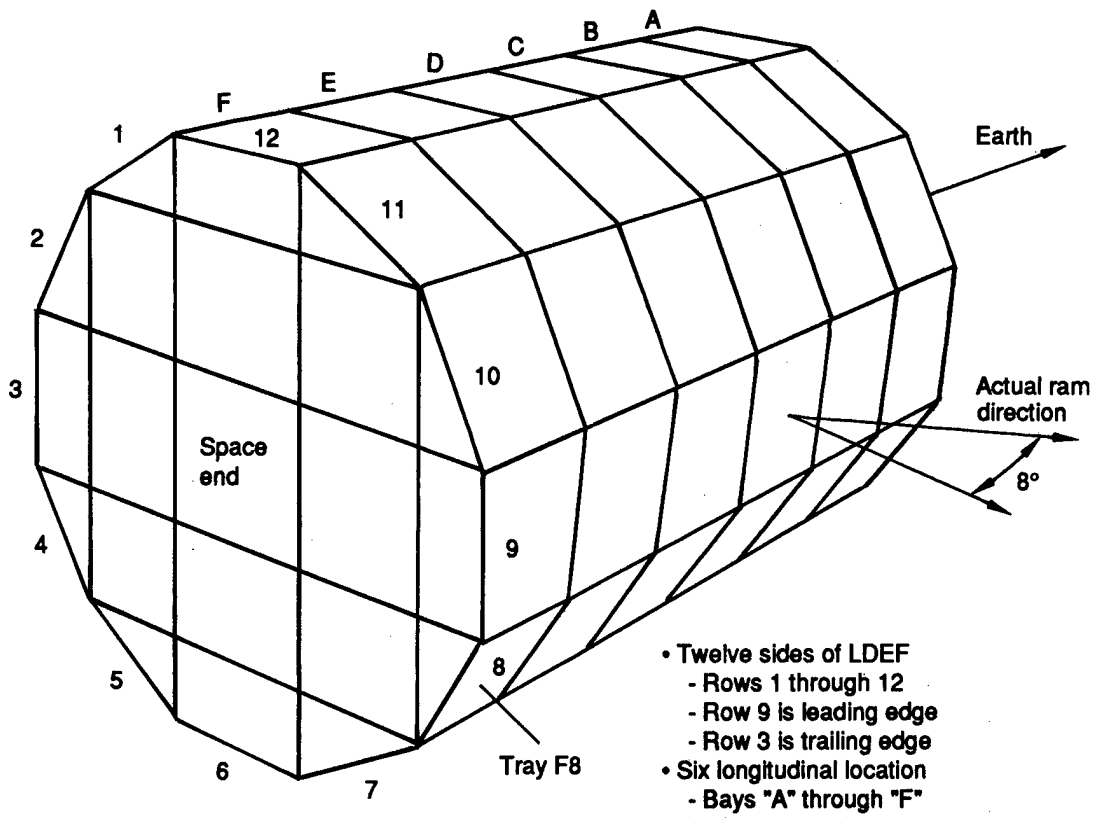

- Twelve sides of LDEF
  - Rows 1 through 12
  - Row 9 is leading edge
  - Row 3 is trailing edge
- Six longitudinal location
  - Bays "A" through "F"
- Earth end bays in
  - "G" identifier
- Space end bays
  - "H" identifier

Example:
Tray F8 is located 38° from ram (30° +8° offset) and adjacent to space end

Figure 2.1-2. Tray Numbering System

Figure 2.1-3. Photograph Taken During LDEF Retrieval Showing Trays/Experiments Mounted to LDEF

ELECTRONICS & OPTICS

- Holographic Data Storage Crystals
- Infrared Multilayer Filters
- Pyroelectric Infrared Detectors
- Metal Film and Multilayers
- Vacuum-Deposited Optical Coatings
- Ruled and Holographic Gratings
- Optical Fibers and Components
- Earth Radiation Budget Experiment Components
- Solar Radiation On Glasses
- Quartz Crystal Oscillators
- Active Optical System Components
- Fiber Optic Data Transmission
- Fiber Optics Systems
- Space Environments Effects

HEAT PIPES & THERMAL SYSTEM

- Variable Conductance Heat Pipe
- Low-Temperature Heat Pipe
- Transverse Flat-Plate Heat Pipe
- Thermal Measurements

MATERIALS & COATINGS

- Crystal Growth
- Radar Phased-Array Antenna
- Atomic Oxygen Outgassing
- Atomic Oxygen Interaction
- High-Toughness Graphite Epoxy
- Composite Materials For Space Structures
- Epoxy Matrix Composites
- Composite Materials
- Graphite-Polymide and Graphite-Epoxy
- Polymer Matrix Composites
- Spacecraft Materials
- Balloon Materials Degradation
- Thermal Control Surfaces
- Textured and Coated Surfaces
- Metallic Materials Under Ultravacuum

SCIENCE

- Interstellar Gas
- Ultra-Heavy Cosmic Ray Nuclei
- Heavy Ions
- Trapped-Proton Energy Spectrum
- Heavy Cosmic Ray Nuclei
- Linear Energy Transfer Spectrum
- Microabrasion Package
- Meteoroid Impact Craters
- Dust Debris Collection
- Chemistry Of Micrometeoroids
- Measurements of Micrometeoroids
- Interplanetary Dust
- Space Debris Impact
- Meteoroid Damage to Spacecraft
- Biostack
- Seeds In Space
- Student Seeds Experiment

POWER & PROPULSION

- High Voltage Drainage
- Sol.ar Array Materials
- Advanced Photovoltaics
- Coatings and Solar Celols
- Solid Rocket Materials

Figure 2.1-4. List of Experiments (Including Experiment Number) Flown on LDEF

Trailing edge

Leading edge

Bay / Row	A	B	C		D	E	F
1	A0175	S0001	Grapple		A0178	S0001	S0001
2	A0178	S0001	A0015, A0187, M0006		A0189, A0172, S0001	A0178	P0004, P0006
3	A0187	A0138	A0023, A0034, A0114, A0201		M0003, M0002	A0187, S1002	S0001
4	A0178	A0054	S0001		M0003	S0001	A0178
5	S0001	A0178	A0178	P0003, P0005	A0178	S0050, A0044, A0135	S0001
6	S0001	S0001	A0178		A0201, S0001	A0023, S1006, S1003, M0002	A0038
7	A0175	A0178	S0001		A0178	S0001	S0001
8	A0171	S0001, A0056, A0147	A0178		M0003	A0187	M0004
9	S0069	S0010, A0134	A0023, A0034, A0114, A0201		M0003, M0002	S0014	A0076
10	A0178	S1005	Grapple		A0054	A0178	S0001
11	A0187	S0001	A0178		A0178	S0001	S0001
12	S0001	A0201	S0109		A0023, A0019, A0180	A0038	S1001

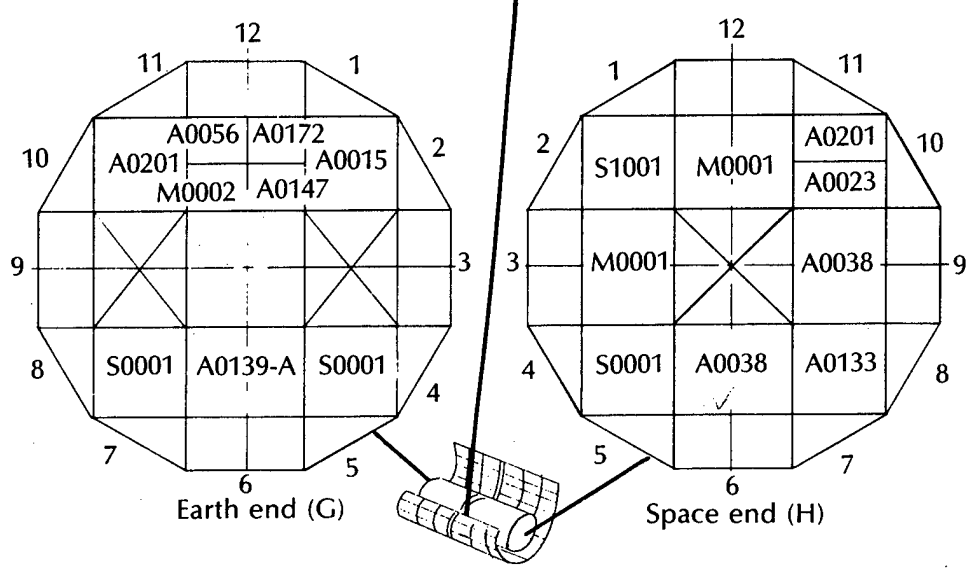

Figure 2.1-5. Location of Experiment on LDEF

The LDEF, weighing 21,400 lbs, was placed in orbit by the Shuttle Challenger on April 7, 1984 at a 482-km nearly circular orbit with a 28.4-deg inclination. LDEF was gravity-gradient stabilized and mass loaded so that one end of the LDEF was always pointed at Earth and one side (leading edge) was always oriented into the orbit path (ram) direction. The actual orientation was slightly offset from the planned orientation. LDEF ended up rotated around its long axis such that the leading edge (row 9) was offset from the ram direction by about 8 deg (fig. 2.1-2). This orientation remained constant throughout the entire mission. LDEF also used a viscous damper which was designed to gradually eliminate the destabilizing oscillations imparted to LDEF during deployment.

Plans at the time of deployment called for Challenger to retrieve LDEF in early 1985 after a 10-month to 1-year mission. Due to Shuttle rescheduling and the loss of Challenger, LDEF was not retrieved until January 12, 1990, after 2106 days and 32,422 orbits in LEO orbit. By this time LDEF's orbit had degraded to 340 km. Any major slide in the launch of the retrieval mission would have jeopardized retrieval as LDEF was predicted to reenter the Earth's atmosphere by mid March 1990. Figure 2.1-6 shows LDEF's altitude versus days after deployment (ref. 6). It is apparent from this figure that the LDEF orbit was nearly stable for the first 4 years of the mission and then began to decay at an increasing rate. Also of interest is that LDEF's range of altitudes approximates the orbital ranges currently planned for Space Station Freedom (333 km to 492 km).

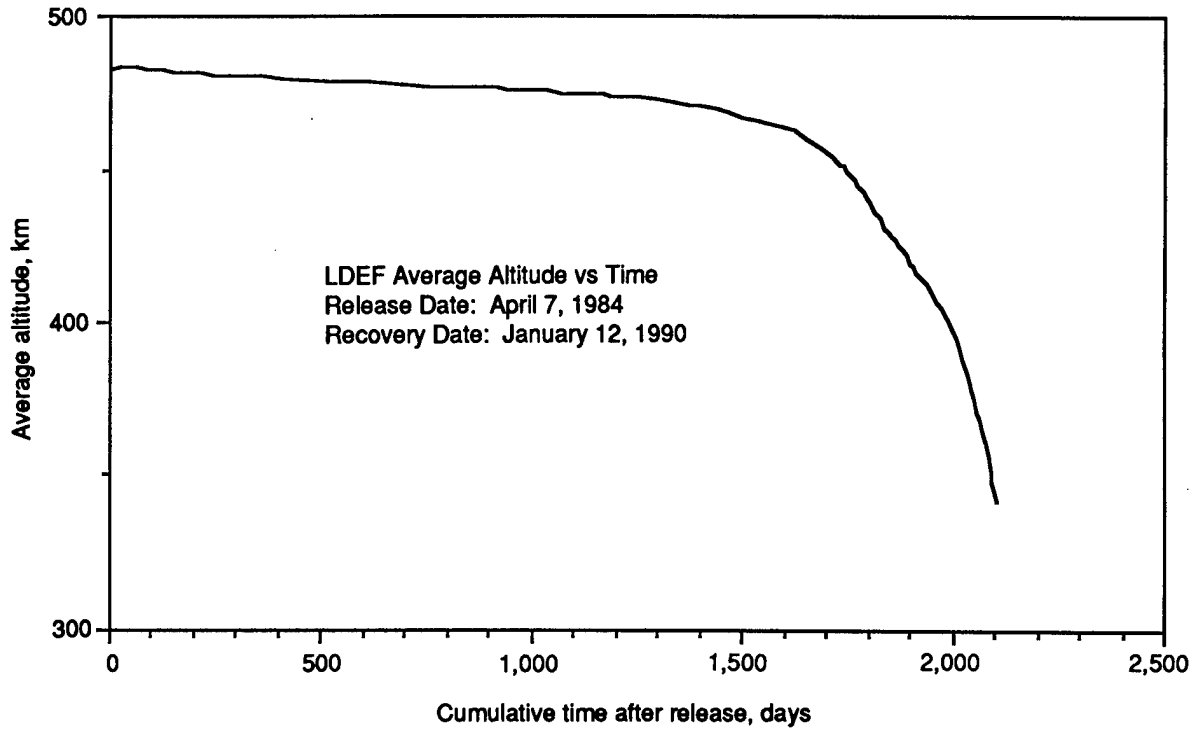

Figure 2.1-6. LDEF Average Orbital Altitude Versus Time After Release

During the retrieval operations, the approach (fig. 2.1-7) and grapple (fig. 2.1-8) of LDEF by the Shuttle Columbia were performed such that Shuttle plume impingement on LDEF was prevented. After LDEF was grappled and prior to the berthing, a 4-1/2 hr photographic survey was performed using the Remote Manipulator System (RMS) to maneuver LDEF. All surfaces were surveyed. Figure 2.1-9 shows rows 9 and 10 being surveyed and figure 2.1-10 is an on-orbit close-up of a specific experiment (S0069). One of the reasons the photo survey was was performed was to distinguish between the effects of the space exposure and the effects of the shuttle landing and ferry flight from Edwards AFB to KSC. Figures 2.1-11 and 2.1-12 show the results of these effects. Both photos are of experiment M0003, tray D9 with figure 2.1-11 being an on-orbit photograph and figure 2.1-12 a photo of tray D9 after removal from LDEF at KSC. Note the on-orbit presence of severe particle contamination in the upper half of tray D9 that had accumulated during the 69-month mission. By the time the tray was processed at KSC, this contamination had disappeared.

Following the ferry flight, LDEF was removed from Columbia at KSC and then transported to the Spacecraft Assembly and Encapsulation Facility (SAEF-2). SAEF-2 was maintained in a controlled temperature and humidity environment and at a class 100,000 cleanliness level (figure 2.1-13). After inspections, photo survey, and radiation measurements were completed, LDEF was ready for individual tray removals, as shown in figure 2.1-14. Each tray went through a thorough examination prior to leaving SAEF-2. Photographs from all angles were taken both while the tray was still on LDEF and then following removal. This was followed by determination of the size and location of all meteoroid and space debris impacts greater than 0.3 mm in diameter (ref. 7). The batteries used to power the active experiments were checked for leaks, removed, and post-flight voltages determined. Several experiments underwent Normarski analysis (optical image contrast enhancement). Following completion of all required examinations, the trays were sent to the principal investigators' laboratories for testing and analysis.

Following removal of the last tray, the LDEF structure underwent extensive analysis. This included evaluation of the welds, structural fastener assemblies, wire harnessing, and meteoroid and debris evaluation of the exterior structure surfaces. The almost 4-month deintegration was completed by the middle of May 1990 with the LDEF, looking like a picked-over turkey carcass, being placed into storage at KSC.

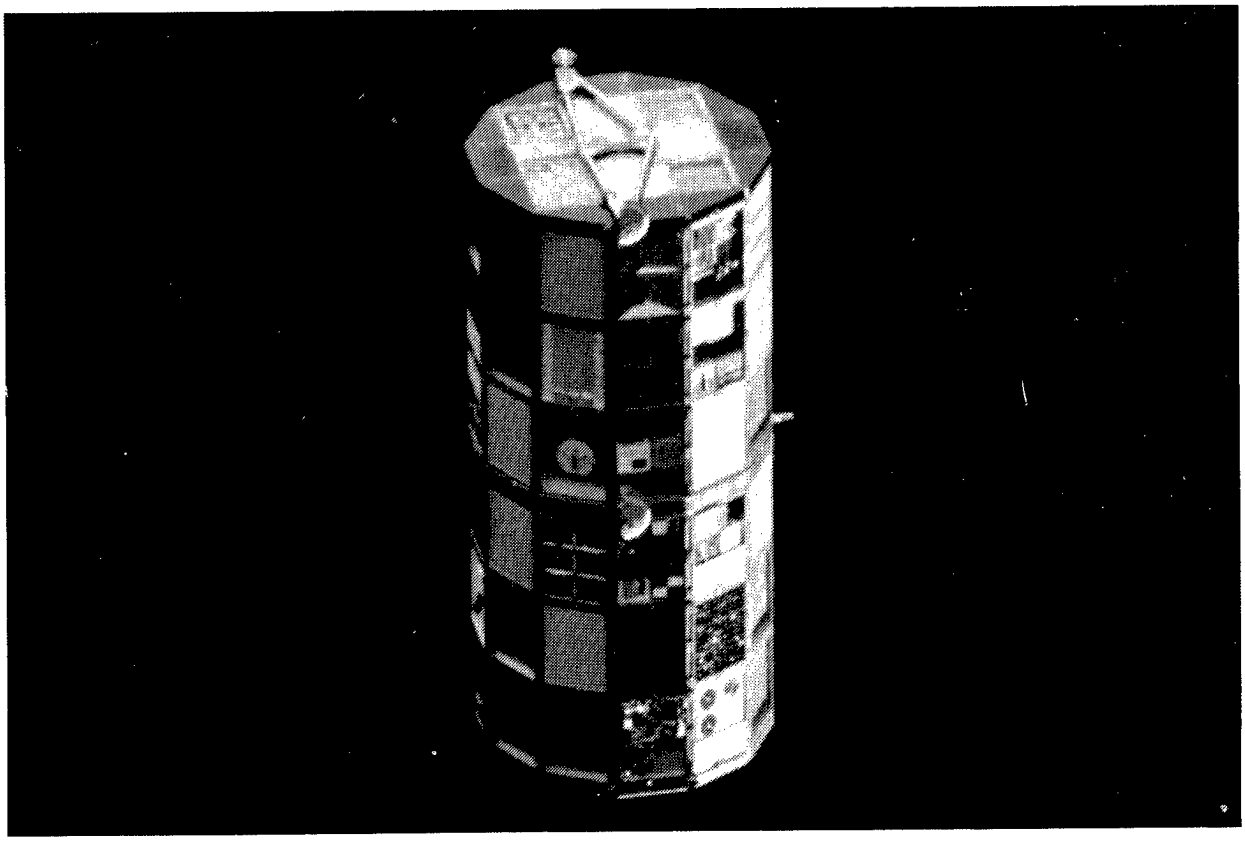

Figure 2.1-7. Approach of LDEF by Shuttle Columbia

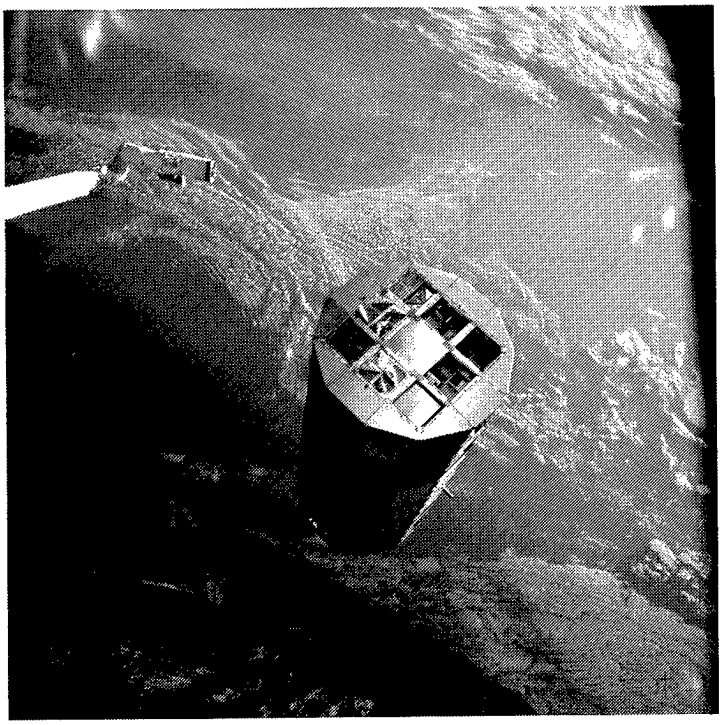

Figure 2.1-8. Grappling of LDEF

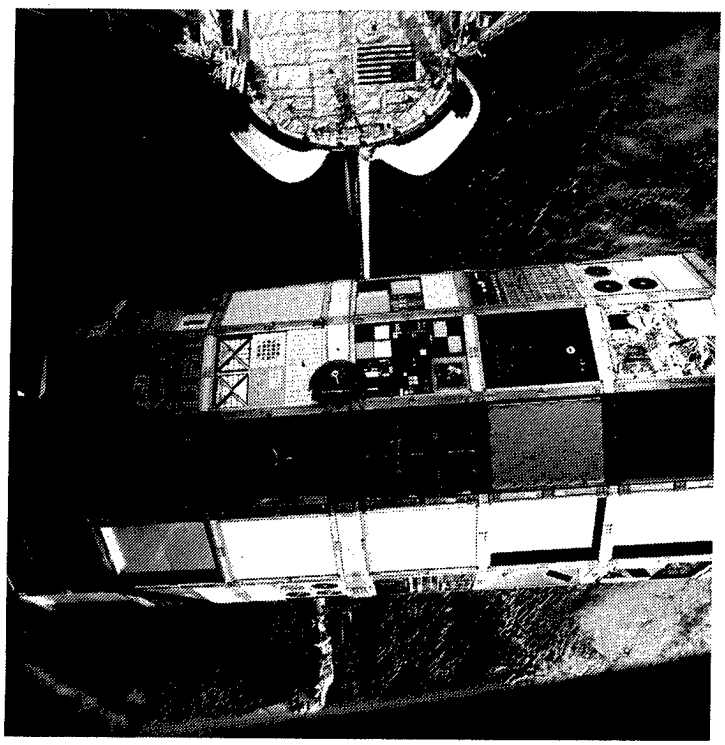

Figure 2.1-9. Rows 9 and 10 Undergoing Visual Inspection and Photographic Survey

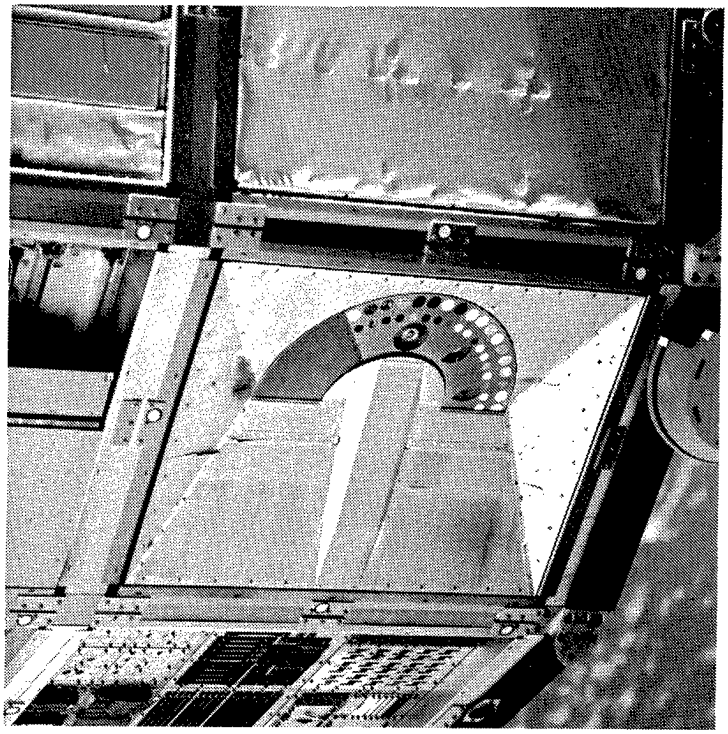

Figure 2.1-10. Experiment S0069 Undergoing Visual Inspection and Photographic Survey

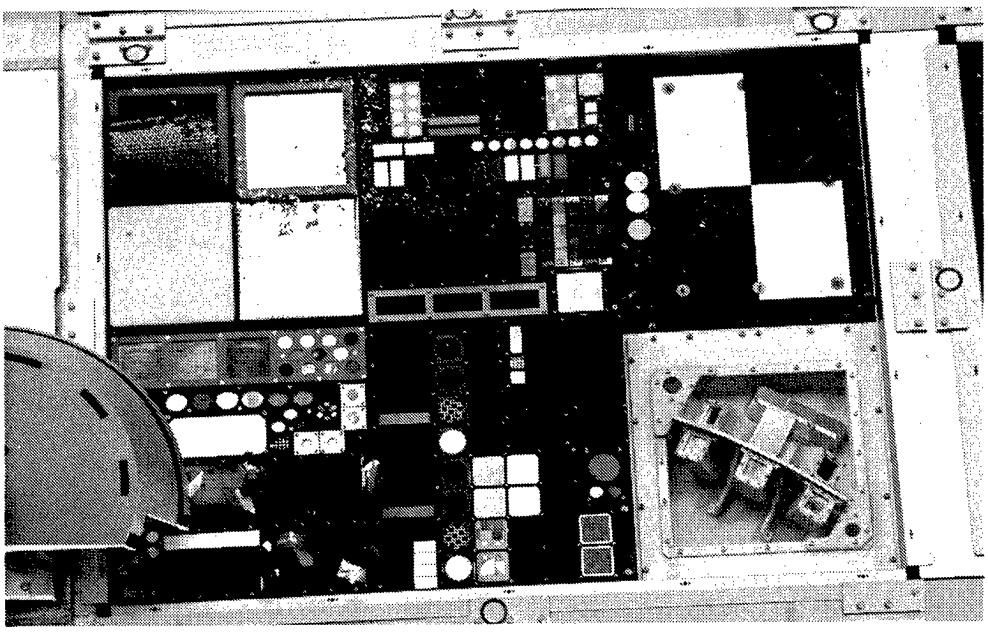

Figure 2.1-11. On-Orbit Photograph of Tray D9

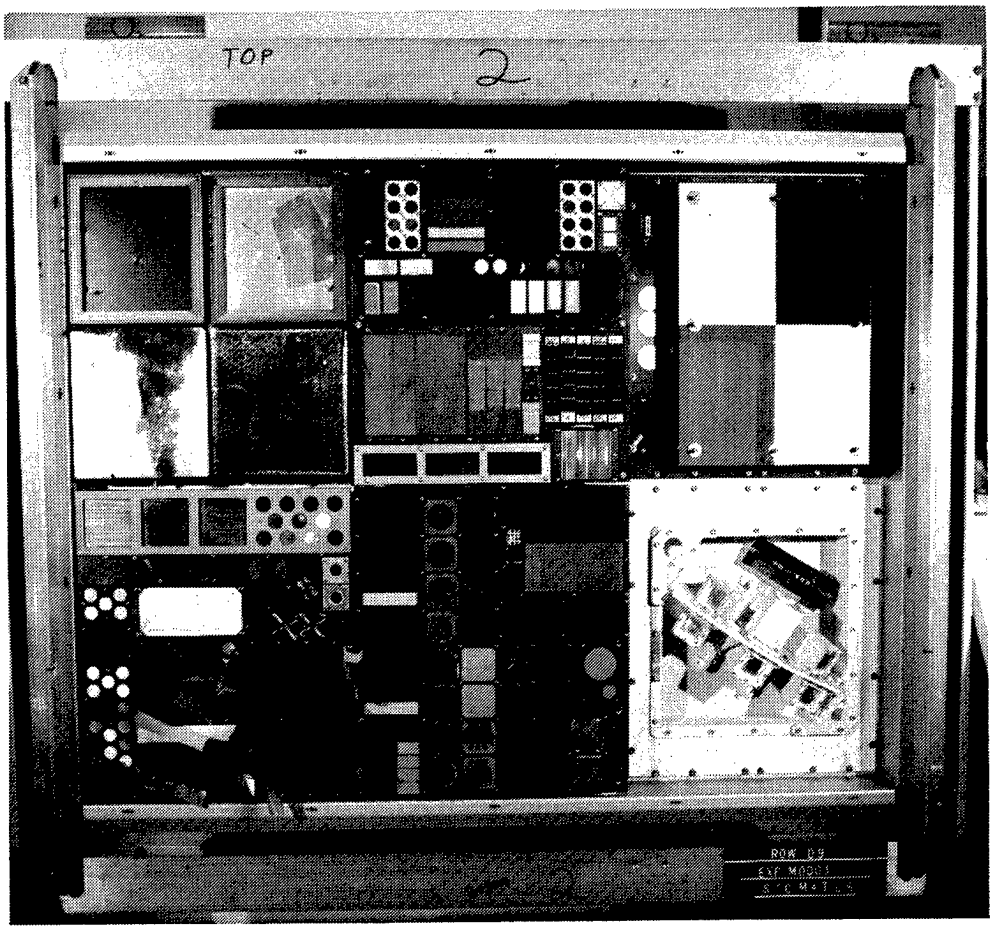

Figure 2.1-12. Photograph of Tray D9 Following Removal From LDEF

Figure 2.1-13. LDEF in SAEF-2 During Deintegration

Figure 2.1-14. Removal of an Experiment From LDEF

2.2 SYSTEMS SPECIAL INVESTIGATION GROUP

Because of LDEF's extended mission, the science and engineering interest extended beyond the original experiment objectives. In response to this interest, the LDEF Project Office commissioned four Special Investigation Groups (SIG) to expand the post-flight investigative effort beyond the scope of the original experiments. The SIGs formed for this effort were the Induced Radiation, Meteoroid and Debris, Materials, and Systems SIGs. This report documents the results of the Systems SIG investigation.

The Systems SIG is chaired by Dr. James B. Mason at NASA Goddard Space Flight Center, and the Systems SIG Committee includes members from eight NASA field centers, the Department of Defense, the Strategic Defense Initiative Organization, and the European Space Agency (fig. 2.2-1). To assist the Systems SIG in meeting its objectives, a task was assigned to Boeing Aerospace & Electronics to provide the required personnel and testing facilities.

The Systems SIG was chartered to -

a. Investigate the effects of the 69-month exposure to the LEO space environment on LDEF and experiment systems.
b. Coordinate the data from the analysis of the LDEF and experiment systems into a single LDEF document.

LDEF hardware of interest to the Systems SIG investigation included hardware provided by the LDEF Project Office, such as the LDEF structure, as well as unique hardware used by individual experimenters to support their experiments, such as a particular lubricant or an electronics package.

The initial effort for the Systems SIG was the identification of systems hardware on LDEF that was pertinent to the Systems investigation. The largest portion of hardware was associated with the so-called "active" experiments, which were those requiring battery power for systems which were designed to perform functions during the mission. Examples of these systems include the EPDSs, EECCs, both the active and passive grapples, viscous damper, Experiment Initiate System (EIS), and the clam shells used on the Chemistry of Micrometeoroids Experiment. Most of these types of systems were available to the Systems SIG as they were not an integral part of any experiment. Other hardware of interest was the isolated passive components which were included as experiment specimens, such as bandpass filters, or ancillary items such as fasteners.

The hardware of interest included an enormous diversity of components. The management of this hardware was facilitated by the division into four major engineering disciplines: mechanical, electrical, thermal, and optical. This division has been carried throughout the program, from the development of test plans to this final report. In order to assist the investigation process, the Systems SIG developed a set of standardized test plans for each of these four discipline areas (ref. 8). These plans were designed to be used by either the Systems SIG or the experimenters in their testing and analysis of systems hardware.

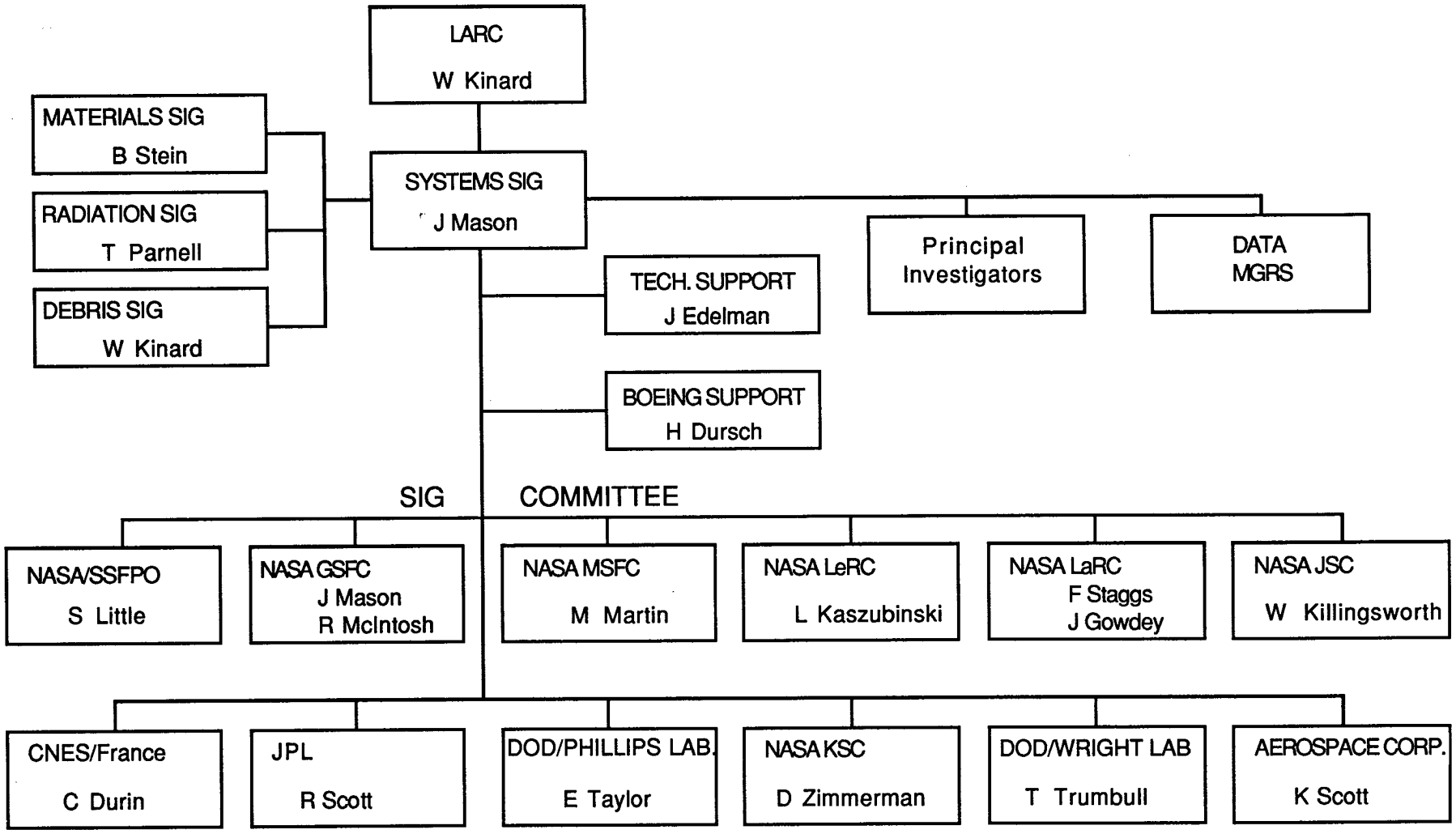

Figure 2.2-1. LDEF Systems SIG Organization

The approach to the testing of hardware by the System SIG has always emphasized the testing of each system at its highest practicable level of assembly. The results at this level provided the direction for further testing in the form of either nominal or anomalous behavior. The results from the system functional test then provided a clear set of directions for subsequent testing and/or failure analysis of subsytems or components. At this time the Systems SIG has performed or supported high level system functional tests on almost all LDEF and experiment systems. Included are inspection and functional testing of the EIS and two EPDS during deintegration at KSC and numerous system functional tests on hardware conducted at experimenter or Boeing facilities.

The process of developing systems data from the identified hardware of interest has, because of the diverse origins of the hardware, involved a diverse group of investigators, including experimenters, other SIGs, the LDEF Project Office, and System SIG contractors. The largest amount of System SIG data was developed by Boeing Aerospace & Electronic's personnel because of the combination of direct access to hardware and direct funding of support personnel. A second set of data, labeled "Systems SIG inspired," is comprised of results obtained by experimenters who performed testing recommended by the the Systems SIG. The final type is the data developed by the experimenters and other investigative groups in the course of their own investigations.

The culmination of the data-gathering process is the dissemination of the results. To accomplish this, the Systems SIG developed a three-point plan (ref. 9). The first component was the distribution of a semi-quarterly newsletter to the LDEF community. The purpose of this activity has been to provide the earliest possible updates on current results from all aspects of the LDEF evaluation. The distribution of this newsletter has increased eight-fold from its inception to a current mailing of over 2000 copies. Because of the newsletter's popularity, the LDEF Project Office has assumed responsibility for the continuation of this activity. The second component was the release of the Systems SIG Interim Report in January 1991 (ref. 10). The report documented the deintegration from a systems standpoint and provided a status of the testing and analysis of hardware that took place in 1990. The third component is the release of this report.

3.0 LDEF ENVIRONMENT

This section is designed to provide the reader with a summary of the following environments encountered by LDEF: meteoroid and debris, radiation, atomic oxygen, solar, thermal, and contamination. Because LDEF's orientation was constant throughout the entire mission, it provided an excellent platform to study the effects of these environments, either individually or synergistically.

The results of the individual and/or synergistic effects are shown in figure 3.0-1. The surfaces of certain white thermal control paints remained visually unchanged when exposed to ultraviolet radiation and atomic oxygen (leading edge environment) but became uniformly darker when exposed to only the ultraviolet (trailing edge environment). The top photo of tray D4 (near trailing edge) shows the browned thermal control cover on the right third of the tray. Cross-sections of paint specimens of the A-276 paint show the brown layer thickness to be typically about 2-microns thick. The color change, which is induced by the solar UV, is due to rearrangement of the chemical structure of the organic binder in the paint. It was not caused by contamination deposition. By contrast, the identical coating used on tray D8 (near leading edge) thermal cover still appears white. However, examination of the this A-276 paint shows that the organic binder has been oxidized and removed by atomic oxygen and the outer layers of paint contain only pigment and inorganic filler.

3.1 METEOROID AND DEBRIS

LDEF exposed a total surface area of ~130 m^2 for 69 months, which is almost two orders of magnitude larger than all previous opportunities combined (ref. 11). This significance was clearly recognized prior to LDEF's retrieval, and is the primary reason for the establishment of the Meteoroid and Debris SIG (M&D SIG). M&D SIG members participated in the deintegration of LDEF at KSC by scanning and photodocumenting all LDEF space-exposed surfaces; a special emphasis was placed on those surfaces that were not initially intended to be investigated for impact features. The results of the M&D SIG KSC activities are discussed in reference 12.

The bombardment effects of a non-spinning platform encountering an (assumed) isotropic cloud of hypervelocity particles in LEO are akin to raindrops hitting the windshield of a moving vehicle (i.e., more particles are encountered in the forward-facing direction than in the rearward-facing direction). The velocity distribution of the impactors varies from "fast" in the forward-facing (leading-edge) direction, to "slow" in the opposing (trailing-edge) direction, because particle and spacecraft velocities are added vectorially. For LDEF, the mean encounter velocities range, on average, from ~20 to 11 km/s for surfaces facing the leading- and trailing-edge directions, respectively, while the effective fluxes (at constant projectile size) between these orientations may differ by a factor of 10 (refs. 13,14,& 15).

The size of any crater or penetration hole depends on a number of physical properties of both the target and projectile material, and on the projectile's mass and impact velocity. An impactor will generate a crater of different sizes on LDEF, depending on location, because of the different encounter velocities. The quantitative

(See color photograph on p. 291)

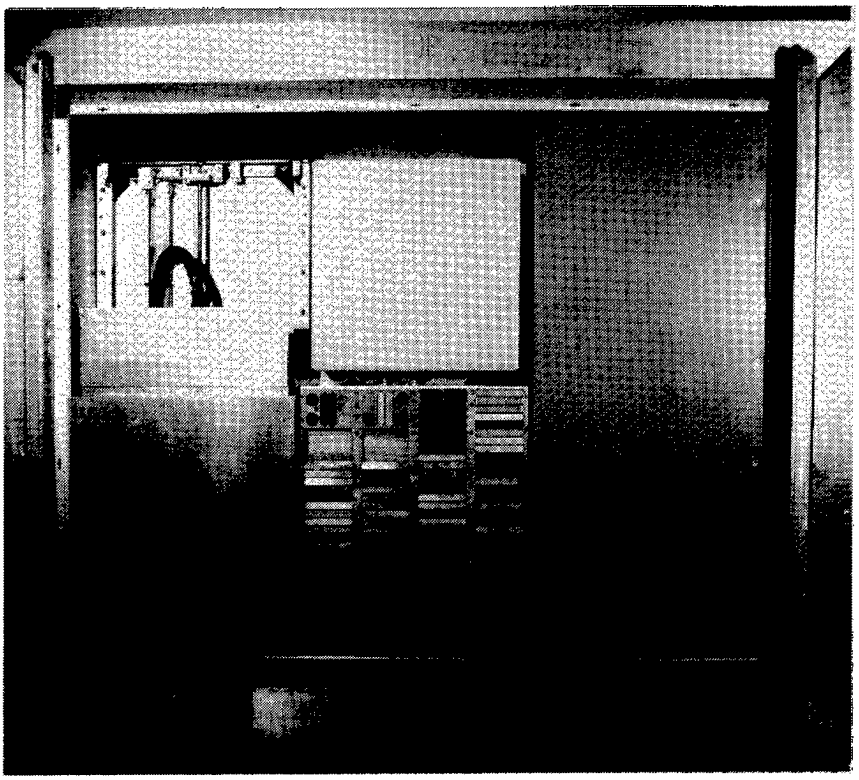

Near Trailing Edge

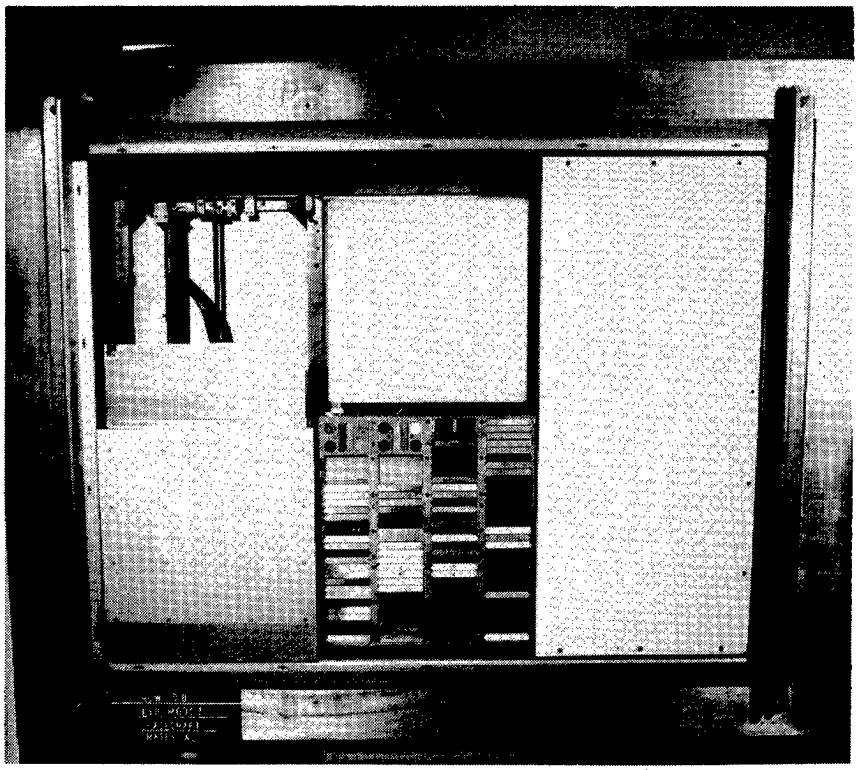

Near Leading Edge

Figure 3.0-1. Effect of Solar UV on Thermal Control Coatings

relationships among these parameters are known for a few LDEF materials, but only over a restricted range of initial conditions. Specifically, the prevalent impact velocities in LEO are beyond current laboratory capabilities for most impactors >10 μm in diameter.

To fully exploit LDEF's potential in contributing to dynamic issues of the particle environment it is necessary to study surfaces that are manufactured from identical materials and that are widely distributed over the entire spacecraft. Such considerations identify LDEF's aluminum structural frame and the A0178 silverized Teflon thermal blankets as the most outstanding materials for study (in addition to those afforded by dedicated and well-calibrated micrometeoroid and debris experiments). LDEF's structural frame was manufactured from 6061-T6 aluminum and had a total exposed surface area of ~15.4 m^2. LDEF's individual structural members represent impact "detectors" of a single material type pointing in 26 well-defined directions, each possessing >0.5 m^2 of surface area.

Although not exposed in all 26 directions, identical silverized Teflon thermal blankets associated with the 16 A0178 experiment trays and the one P0004/P0006 experiment tray provided another material type that was widely distributed around the circumference of the spacecraft. All rows except 3, 9, and 12 contained at least one of these blankets. Each blanket exposed ~1.2 m^2 of surface area.

Figure 3.1-1 illustrates the morphology and associated diameter measurement for typical impact features encountered on the two materials discussed. Crater and penetration-hole diameters refer to center-of-rim to center-of-rim dimensions. Reference 12 describes the morphologies of craters and penetration holes, many of the latter were typically characterized by various colored ring-like, delamination features of variable widths, crispness, spacings, scaled diameters and absolute ring numbers.

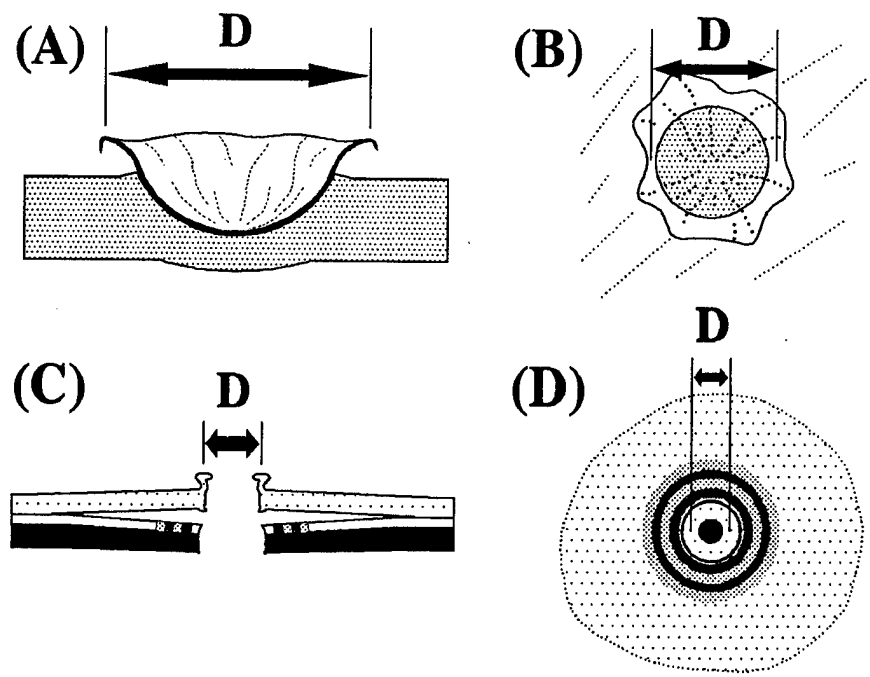

Figure 3.1-1. Drawings of typical crater (A & B) and penetration-hole (C & D) morphologies encountered, and associated measured diameters for features in the aluminum LDEF frame and A0178 thermal blankets, respectively.

Cut-off diameters of 500 μm for craters in infinite halfspace targets, and 300 μm for penetration holes in thermal blankets, were chosen by the M&D SIG for detailed photodocumentation at KSC. This dual-size threshold was employed due to the differing processes associated with hypervelocity impacts into foils versus materials of much greater thickness, and was applied rigorously and systematically to all LDEF surfaces. In addition, the total number of impact structures between these cut-off diameters and ~50 μm in diameter, as observed with the naked eye, were counted and recorded as a single, cumulative number. The M&D SIG survey of LDEF yielded ~35,000 impacts >50 μm in diameter, which must constitute a minimum value, and included ~4,000 larger structures that were documented individually and that represent a quantitative account of LDEF's "large" impact features.

Table 3.1-1 shows the distribution of impact features on LDEF. The values listed do not represent a complete count of the number of impact features on LDEF because (1) many surfaces were examined but the exact locations of the <0.3 mm and/or <0.5 mm diameter features were not recorded (whether they resided on the experimental surfaces or the tray flanges) and (2) during the first several days of M&D SIG documentation activities, only those features that were photodocumented were counted. Thus, the number of features listed in the various categories represent only those features known to exist on that particular surface type, while the "Totals" column depicts the total number of known impacts counted in the various size categories, regardless of their locations.

The cumulative size-frequency distributions and spatial densities of these large craters and penetration holes are illustrated in figure 3.1-2, grouped into specific viewing directions identified by LDEF row. Unfortunately, the total number of events is still generally small, leading to poor statistics and large scatter in the data. Two-sigma (95% confidence level) error bars (not illustrated for the sake of clarity in fig. 3.1-2) revealed that the effective crater-production rates depend on instrument orientation and that the relative size-frequency distributions could be identical.

Figure 3.1-3 illustrates the data from figure 3.1-2 in polar coordinates (on logarithmic scales). Figure 3.1-4 illustrates the same data in histogram form, both in absolute and relative terms, the latter after normalization to the maximum spatial densities observed on the Row 10 intercostals (crater density) and thermal blankets

Table 3.1-1. Distribution of Impact Features on LDEF

	CLAMPS, BOLTS & SHIMS	TRAY FLANGES	EXPERI-MENTAL SURFACES	LDEF FRAME	THERMAL BLANKETS	TOTALS
<0.3 mm	NA	NA	158	NA	*2831	3069
>0.3 mm	NA	NA	172	NA	+625	797
<0.5 mm	1318	1923	14171	5171	NA	27385
>0.5 mm	161	419	2106	432	NA	3118
TOTALS	1479	2342	16687	5603	3456	34336

* - Count is incomplete; the <0.3 mm diameter features were not counted on F02, C05, C06 and D07

\+ - Count is incomplete; the ≥0.3 mm diameter features from F02 not included.

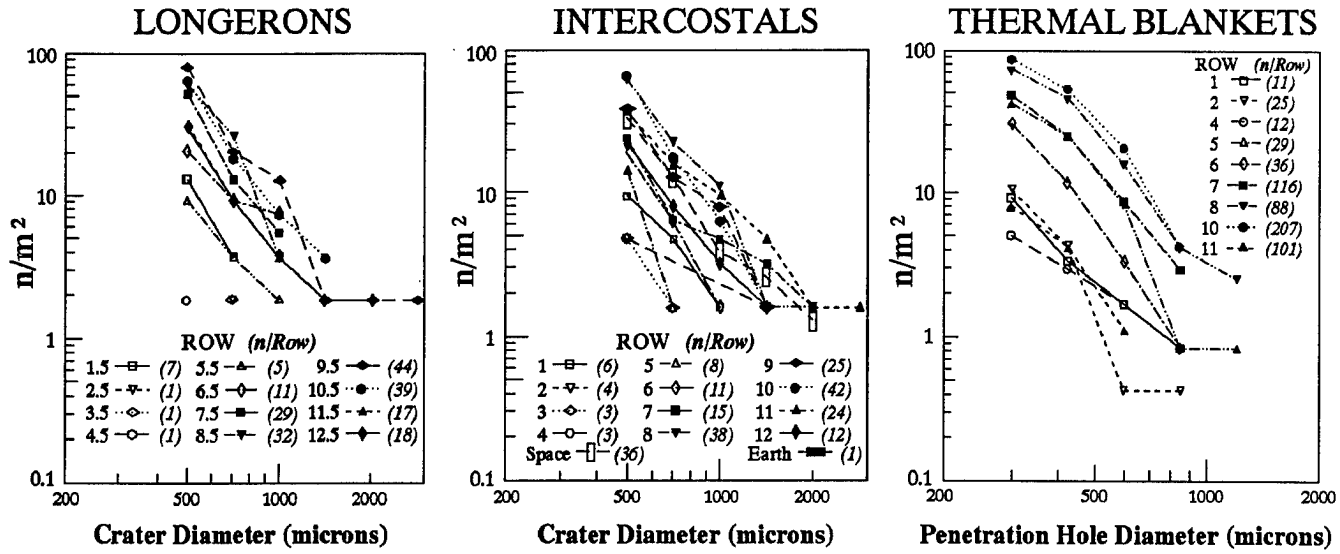

Figure 3.1-3. Absolute spatial density (plotted in polar coordinates on logarithmic scales) of impact features (N/m^2) observed on frame components and thermal blankets.

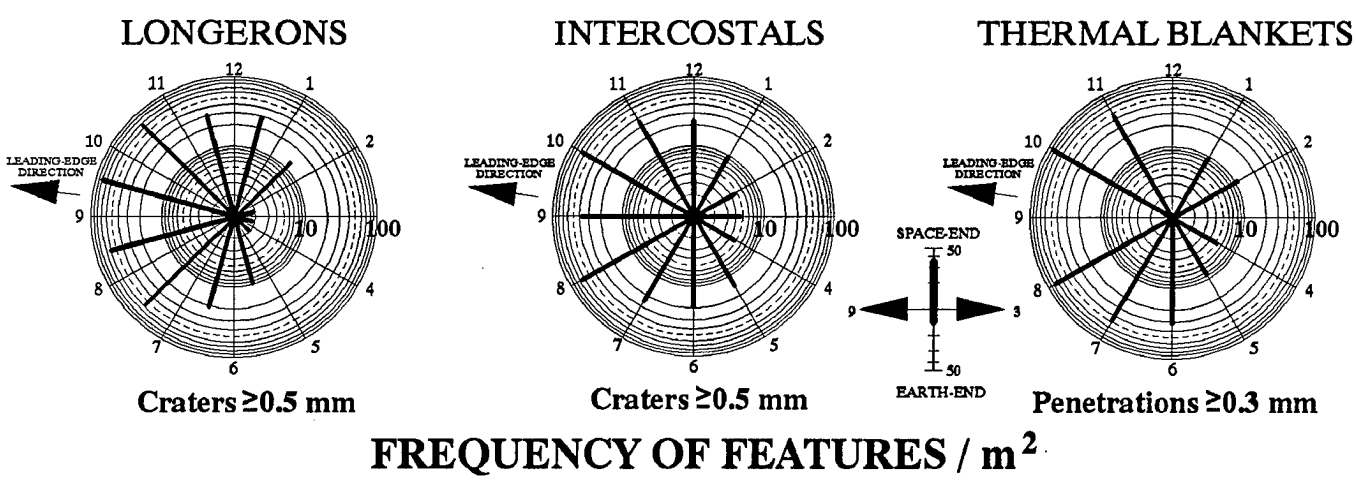

Figure 3.3.1-2. Absolute spatial density of "large" impact features on LDEF's longerons, intercostals, and the A0178 thermal blankets.

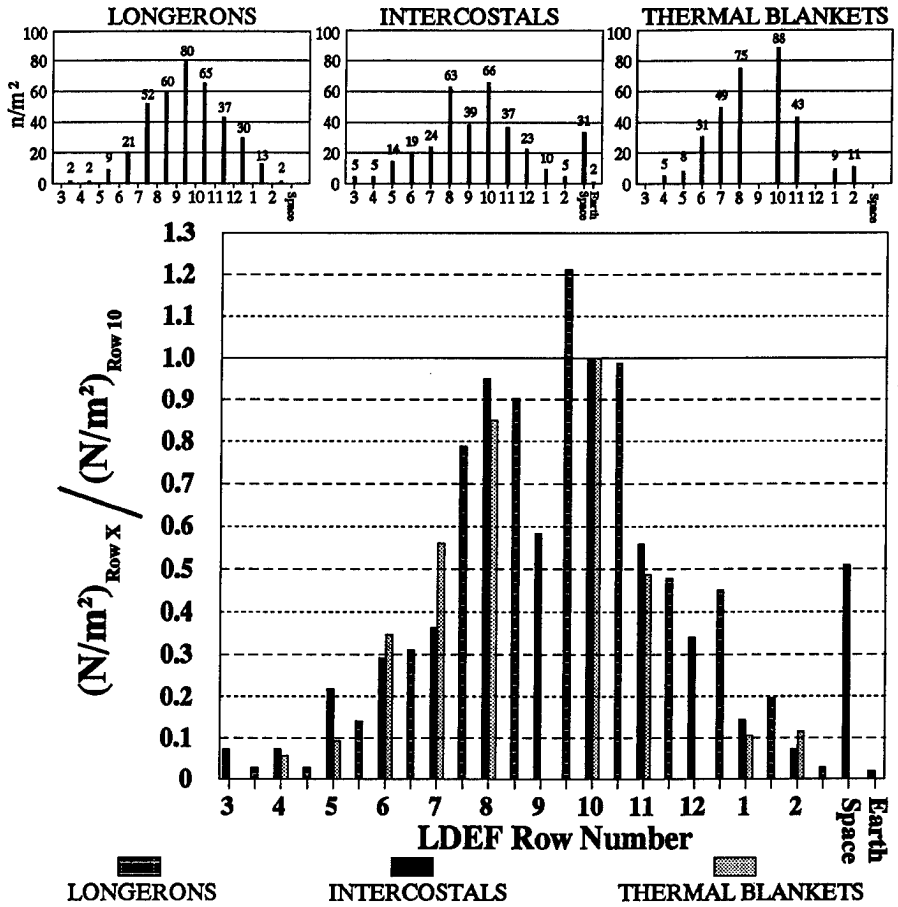

Figure 3.3.1-4. Absolute and relative frequency of impact craters ⊡ 500 μm (longerons and intercostals) and penetration holes ⊡ 300 μm (thermal blankets). Small histograms at top display absolute crater densities (n/m²) that were normalized with the Row 10 values to yield relative production rates (large histogram) for craters and penetration holes.

(penetration-hole density). It seems apparent from figures 3.1-2 through 3.1-4 that crater production has a strong dependence on pointing direction. The effective production rate of craters or penetration holes of constant size appears to differ by more than a factor of 10 between the highest and lowest frequencies.

Somewhat surprisingly, as detailed by ref. 16, the Row 9 (leading edge) intercostals display a modest crater population when compared to that of the adjacent structure. Adjacent intercostals on Rows 8 and 10, and longerons at locations 8.5 and 9.5 have consistently higher crater densities. Because of the orbital precession of the Earth (~8 deg/day), any anisotropy in particle flux would be substantially and rapidly smeared out over neighboring LDEF locations. It seems implausible from a dynamic point of view to sustain the low impact rates implied by the Row 9 intercostals and at the same time cause the apparent higher rates on adjacent surfaces that are only 15 deg and 30 deg apart, respectively. Supporting evidence for this interpretation comes from the general trends displayed by the thermal blankets as well that also yield maxima in the forward-facing directions (Rows 8 and 10).

LDEF's orbital plane was offset by ~8 deg in the Row 10 direction. Note that the highest crater densities on LDEF were obtained on the row 9.5 longeron, and that the spatial density of penetration holes is highest for Row 10. These trends differ qualitatively from those expected, which assumes bilateral symmetry about the plane of motion. It appears that LDEF received more impacts from the general direction of Rows 10 and 11 than on the symmetrically equivalent Rows 7 and 8.

If the observed minima and maxima of crater and penetration-hole densities were taken literally, the difference in calculated production rates for impact features (at constant size) between trailing- and leading-edges would be about 1:43 (longerons), 1:14 (intercostals), and 1:17 (thermal blankets). Using a statistically improved approach (i.e., averaging rearward-facing Rows 2, 3 and 4 and forward-facing Rows 8, 9 and 10), results in production rates for impact features between these principal orientations of 15 to 20 for impact features of identical sizes.

In summary, the current findings suggest highly differential bombardment histories for surfaces pointing in specific directions relative to the velocity vector of a non-spinning platform in LEO. The production rates for craters >500 μm in diameter in 6061-T6 aluminum and penetration holes >300 μm in diameter in thin foil materials differ by a factor of 10 to 20 between leading- and trailing-edge surfaces. These are substantial differences and must translate into serious engineering considerations during the design of future, large-scale, long-duration platforms in LEO.

Summary of LDEF Collisional Hazards Findings:

The first-order LDEF data indicate general agreement with existing predictions, although the latter were based on a substantial number of assumptions. This general agreement, however, does not imply that all assumptions underlying such models were correct. Indeed, modification and substantial refinement of some assumptions are suggested, resulting in a more detailed general understanding of the LEO-particle environment, particularly for non-spinning spacecraft such as the Space Station Freedom. LDEF provided the first serious test of general models and their specific derivatives for the case of non-spinning platforms.

a. The frequence of very small particles, typically <5μm in diameter, is higher than assumed in all models, leading to faster surface degradation in LEO.

b. The synergism of the combined LEO environment leads to additional surface degradation and effects that are currently not included in spacecraft design guides and that are beyond practical laboratory capabilities.

c. The small-scale particle environment exhibits highly variable fluxes, on time-scales that range from minutes to days, that are consistent with co-orbiting particle clouds, most likely associated with spacecraft operations.

d. The largest particles encountered by LDEF were approximately 1 mm in size. Most of these larger particles appear to possess natural origins (i.e., originated from comets or asteroids).

e. Statistical distribution of craters associated with these particles on all LDEF surfaces and pointing directions indicate a mean impact velocity of approximately 17 km/s. The common assumption of 20 km/s is inconsistent with LDEF observations. Even relatively small changes in mean encounter velocity will have major effects in calculating the effective energy-flux for surfaces of fixed orientations on a non-spinning spacecraft.

f. LDEF affords the opportunity to test currently accepted cratering and penetration formulas for hypervelocity impacts in space.

g. Current debris models do not include payloads in geosynchronous orbits, and especially their transfer vehicles, the most likely sources of man-made debris on LDEF's trailing edge. This mandates highly elliptical orbits.

h. Observed debris includes diverse metal particles, paint flakes and human waste products.

i. Plastic bumper sheets are very effective in protecting against impacts from small particles.

Summary of LDEF Highlights in Planetary Sciences:

a. The existence of beta-meteoroids was verified by the dynamic measurement of the IDP detectors.

b. Qualitative chemical analysis (SEM-EDX) of projectile residues in impact craters and debris sprays of penetrated thin-films reveals a substantial variety in the mineralogical composition of the impacting particles. Residues with largely chondritic melts dominate and most likely result from impacts by aggregated particles. However, melts of monomineralic composition indicate the presence of projectiles composed largely either olivine or pyroxene. The latter are occasionally associated with chondritic melts suggesting that they are clasts dislodged from a chondritic matrix. In addtion, some particles are exclusively composed of Fe-Ni rich sulfides.

c. Preliminary interpretation of residues analyzed via ion-microprobes suggests the possibility that some LEO particles differ from those available from the stratospheric collections.

d. Some impact craters contain unmelted residues of olivine or pyroxene, which are known to be most resistant to shock melting among the silicates. This demonstrates that recovery of unmelted particle fragments in LEO is feasible, especially if specialized and improved capture media are employed (e.g., the Cosmic Dust Collection Facility on Space Station).

3.2 IONIZING RADIATION

In Earth orbit the ionizing radiation environment contains a variety of primary and secondary particles. The main primary particles are trapped protons and electrons, galactic and anomalous cosmic rays, albedo protons and neutrons from the atmosphere, and occasionally solar flare particles. Some of these primary radiations will, after interacting with a spacecraft, produce secondary particles which may include protons, neutrons, low-energy recoiling nuclei, mesons, x-rays, and gamma rays. On LDEF, predictions were made of the fluences of the principal constituents (total number per unit area and solid angle), the total absorbed radiation dose, and the linear energy transfer (LET) spectra (refs. 138 & 139).

Most effects from ionizing radiation are related to either radiation dose or to "single hit" effects that can be related to the particle fluxes or LET spectra. Single event upsets in microcircuits or noise events in individual charge coupled devices (CCD) pixels are examples of "single hit" effects. Because only passive radiation detectors were carried on LDEF, the data does not directly address dose rate or flux dependent effects. However, this can be addressed using existing calculational methods.

The total exposure of LDEF was below the threshold for observable radiation effects in most materials. Confirmed radiation effects on LDEF include the radioactivity induced in the structure and genetic damage to seeds. Some degradation in the performance of uncovered solar cells and quartz crystal oscillators, possibly ascribed to radiation, are still under investigation. Ionizing radiation data gathered on LDEF, and models of the radiation environment to be validated with that data, will be extrapolated to other missions to predict radiation effects. Absorbed dose data from three LDEF experiments, shown in figure 3.2-1, indicates inaccuracies in the isotropic flux predictions for trapped protons (ref 141). A directional model of the trapped proton environment and a three-dimensional model of the LDEF structure, soon to be applied, should bring calculations and data into closer agreement.

A few dosimeters were placed on LDEF at shallow enough shielding locations to measure the dose from electrons, predicted to be ~ 300,000 rads (3,000 Gray) near the LDEF's surface. While no electron data has yet been reported, observed degradation in performance of uncovered solar cells is consistent with this value.

The Earth's magnetic field shielded LDEF from the cosmic ray protons and heavy nuclei below ~ 2 GeV. The galatic cosmic rays contributed about 10 rad (0.1 Gray) (ref. 138). However, this flux of high energy protons and heavy nuclei contributed significantly to the LET spectra via the heavy nuclei and secondary interaction products. The LET is energy transferred to a medium per unit path length of the particles. LET spectra result from a variety of particle types (electrical charge) and particle energies. LET values can be correlated with the effects on electronic devices. For example, LET values can be converted to "Q critical," the threshold for single event upsets in microcircuits. High values are associated with enhanced genetic effects in biological specimens, and LET spectra are used in determining the equivalent dose

(rem). Predicted LET spectra for LDEF are in reference 139, and measured LET spectra are reported in reference 142.

The induced radioactivity in LDEF materials is the result of nuclear transmutations caused by the interactions of protons, neutrons, and cosmic ray nuclei with the nuclei of the LDEF materials. The amount of radioactivity is small, but measurable with high-resolution gamma ray detectors. The concentrations for most LDEF materials were within the range of 1 to 100 pico curies per kilogram of material. Nevertheless, the measurements of the radioactivity in a large number of samples from experiments and structure provide an excellent dosimetric map of LDEF. Study of the spacecraft radioactivity is of interest to gamma-ray astronomers, whose observations are often limited by this type of background.

Analysis of the spectra from two trunnions, indicated gamma-ray lines due to ^{7}Be on the forward, but not the aft, trunnion (ref. 141). The ^{7}Be of concentration ~10^5 atoms/cm^2 is apparently made in the stratosphere by cosmic ray bombardment of air, and circulated up to LDEF altitudes with high efficiency. It is of interest in studying transport in the atmosphere, but is not thought to have significant effects as a surface contaminant due to its low concentration. However, the ^{7}Be discovery indicates that low concentrations of ^{7}Li, ^{10}Be, and ^{14}C should be present on the surface of LDEF, and they are being searched for by mass spectroscopy techniques.

For further information, reference 143 is a summary of the ionizing radiation measurements on LDEF made during the first year after recovery.

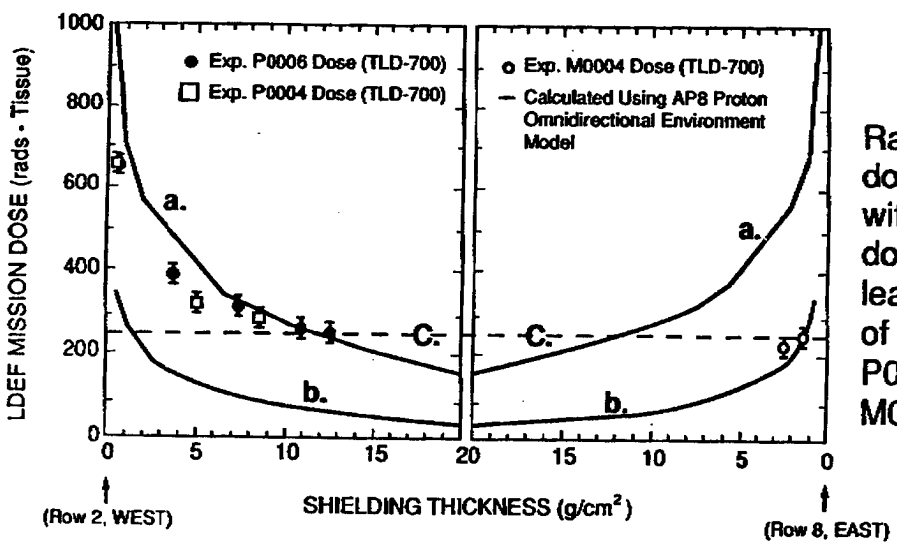

Radiation absorbed dose (RAD) measurements with thermoluminescent dosimeters (TLD) from leading and trailing sides of LDEF. Data is from P0006, P0004, and M0004.

Line 'c' in the figure indicates the annual crew dose limit (50 REM/yr). The LDEF data is influenced by its high altitude (480 km–450 km) during solar minimum.

The west side data has been used to develop the radiation dose requirements for SSF electronic parts.

3.3 ATOMIC OXYGEN

When atomic oxygen collides with a spacecraft traveling at relative velocities of 7-8 km/sec, the collision energy is 4-5 eV. At this energy, atomic oxygen may initiate a number of chemical and physical reactions with the materials of the surfaces with which it collides. These interactions contribute to material degradation, surface erosion, and contamination. Also, recent theories propose that atmospheric atomic oxygen plays a role in the production of shuttle glow.

For these reasons, atomic oxygen fluence on spacecraft surfaces is important in design consideration. LDEF flew in low Earth orbit for nearly 6 years. Because of its unique 12-sided geometry, atomic oxygen fluence varied from experiment to experiment. Knowing the atomic oxygen fluence on the materials carried by LDEF will give experimenters the ability to correlate degradation effects with exposures.

Atomic oxygen exposures were determined analytically (refs. 17 and 18) for rows, longerons, and end bays of LDEF. The analytical model used for the calculation accounts for the effects of thermal molecular velocity, atmospheric temperature, number density, spacecraft velocity, incidence angle and atmospheric rotation. Results also incorporate variations in solar activity, geomagnetic index and orbital parameters that occurred during LDEF's 69 month flight.

Charts summarizing atomic oxygen exposure, taken from reference 18, are included herein to facilitate the use of the data by LDEF experimenters. Figure 3.3-1 shows the mission total atomic oxygen exposure accumulated on each tray and longeron location of LDEF during its mission. The calculation incorporates the pitch and yaw angles for the vehicle determined by Dr. Bruce Banks, NASA LeRC (ref. 144). The yaw angle is 8.1 degrees with the spacecraft turned so that the ram direction lies between rows 9 and 10. Pitch angle is 0.8 degrees with the space end of the vehicle pitched forward. Roll angle is zero. Because of the forward pitch, trays on the space end received more atomic oxygen that did trays located on the Earth end. The calculation also incorporates the fluences of several rows during a brief attitude excursion of the Shuttle after grappling of LDEF and prior to closure of the payload doors.

The values given in figure 3.3-1 are mission total values. More extensive data has been prepared in tabular form for LDEF (ref. 18). Atomic oxygen fluxes and fluences were calculated for each week of the LDEF mission. Fluences for any period of time during the mission can be interpolated from tabulated data.

Figure 3.3-2 shows cumulative ram direction atomic oxygen fluence for LDEF expressed as a percent of total fluence for the mission. Roughly 50% of the atomic oxygen exposure accumulated during the last 6 months of the LDEF mission. The last year of the flight accounted for 75% of the exposure. The rapid increase in exposure at the end of the mission is a result of both increasing solar activity and decaying orbit altitude.

The effect of thermal molecular velocity on atomic oxygen flux is shown in figure 3.3-3. The plot compares atomic oxygen flux corrected for thermal molecular velocity with calculated values ignoring thermal molecular velocity. When thermal molecular

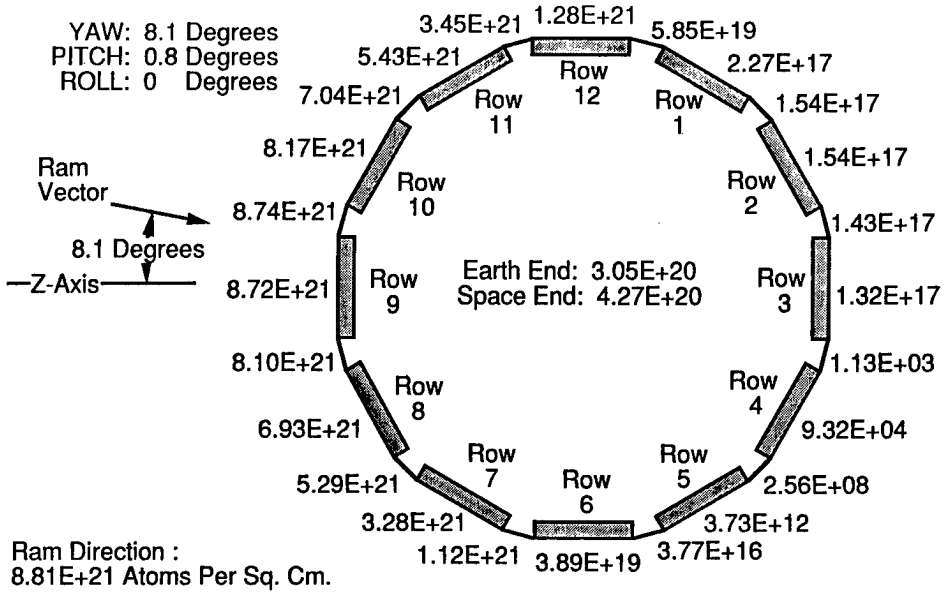

Atomic oxygen fluences at end of mission for all row, longeron, and end bay locations including the fluence received during the retrieval attitude excursion.

Figure 3.3-1. Atomic Oxygen Fluences at End of Mission for Each Tray Location

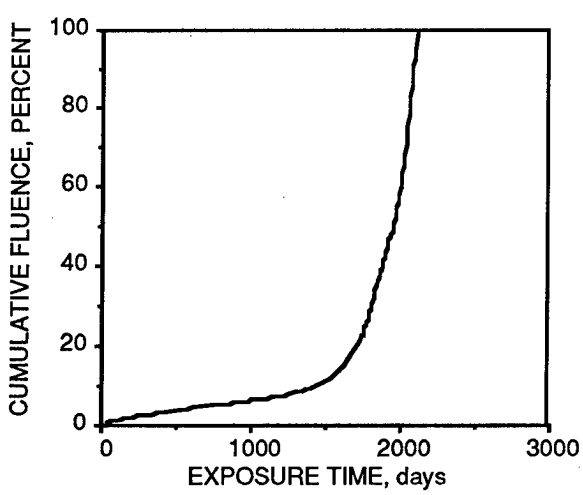

Figure 3.3-2. Atomic Oxygen Fluence as a Percent of Total Exposure

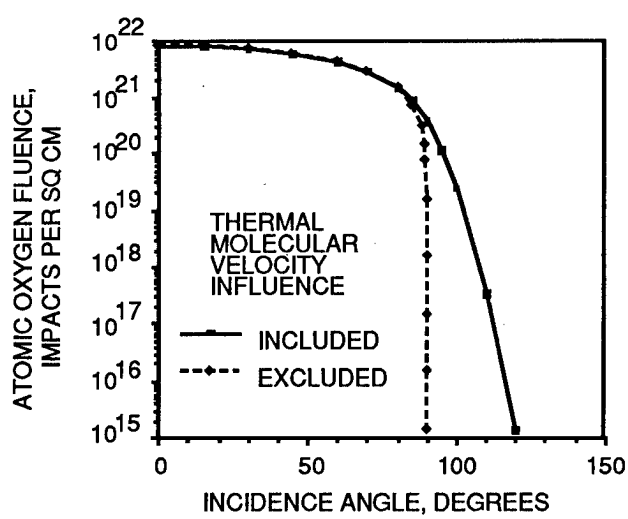

Figure 3.3-3. Effect of Thermal Molecular Velocity on Atomic Oxygen Fluence

velocity is considered, calculations show that surfaces parallel to the ram direction receive approximately 4% of the head-on flux. Surfaces at angles greater than 90 deg. from ram still receive a small atomic oxygen flux. The calculated influence of thermal molecular velocity on atomic oxygen flux is verified by results reported for exposure of photovoltaic blanket materials on Tray E6, Experiment S1003 at 98 deg. to ram (ref. 19).

The pinhole sensor also showed a ±2 deg. sinusoidal variation in ram vector direction based on the elongated exposure pattern of the silverized sensor surface. This variation is in agreement with the atomic oxygen calculation model and is caused by co-rotation of the atmosphere.

Analyses were conducted by NASA Lewis (ref. 21) on the undercutting of Kapton multilayer insulation by atomic oxygen on Tray E6, Experiment S1003. The analytical results confirm the effect of ram direction variation on insulation undercutting.

3.4 SOLAR RADIATION

The ultraviolet component of solar radiation is an important contributor to materials degradation. A summary chart for solar radiation exposure (fig. 3.4-1) is presented herein for use by LDEF experimenters. Cumulative equivalent sun hours of total direct solar and Earth reflected radiation is shown for each row and longeron and for both ends of LDEF. The data given in figure 3.4-1 may be used to calculate full spectrum solar fluence (joule/cm^2) by multiplying cumulative equivalent sun hours by 492.48 joule/cm^2-hr. This factor is based on a solar irradiance of 0.1368 W/cm^2 (ref. 22). Similarly, the solar fluence in the 0.2- to 0.4- micrometer band may be obtained by multiplying the cumulative equivalent sun hours by 39.24 joule/cm^2-hr. This factor is based on a solar irradiance of 0.0109 W/cm^2 (ref. 22) in this band. Fluences for other spectral bands may be calculated in like manner.

As shown on figure 3.4-1, the highest exposure is on the space end and the lowest is on the Earth end. Of the 12 rows, the leading and trailing rows (9 and 3, respectively) receive the highest exposure, and those nearly parallel to ram direction (rows 6 and 12) receive the lowest exposure, about 60% of the leading edge exposure.

Figure 3.4-2 shows a comparison of direct and Earth reflected radiation for the Earth end bay. The LDEF earth end bay received 72% of its exposure from Earth-reflected radiation and 28% from direct solar radiation. This is the highest proportion of Earth-reflected radiation received by any of the experiment locations. Earth reflected radiation accounted for 9% to 15% of the total solar radiation received by rows 1 through 12. The space end bays received no Earth-reflected radiation.

The solar radiation exposure calculations are based on the form factors reported in the Solar Illumination Data Package prepared by NASA Langley (ref. 23). The Earth albedo value for these calculations was based on the Nimbus 7 Earth radiation data set (ref. 24). The calculations used to derive figure 3.4-1 are discussed in references 17 and 25. Reference 25 also includes results in tabular form as a function of time. Using the tabulated information, solar exposure in equivalent Sun hours can be determined for any interval of time during the LDEF mission for any experiment.

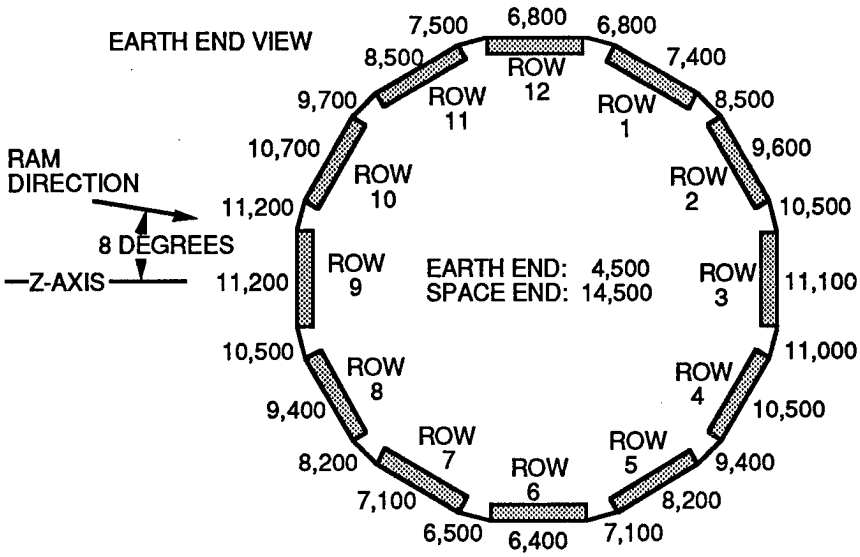

Figure 3.4-1. Cumulative Equivalent Sun Hours for Each Tray Location

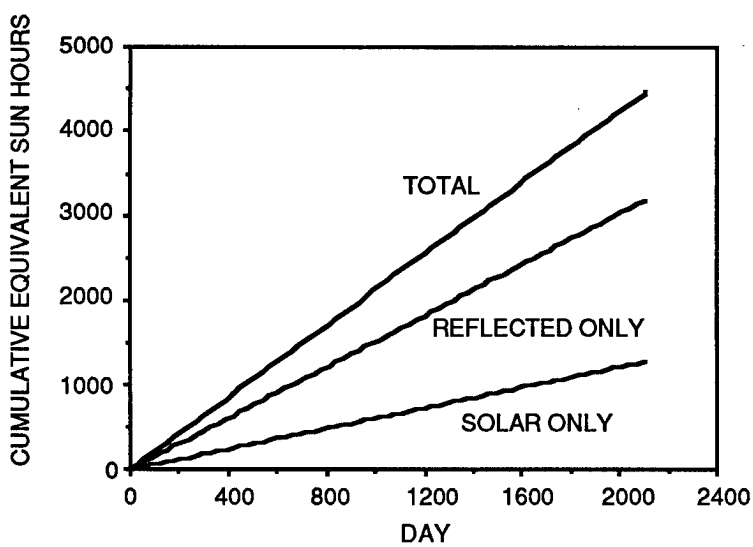

Figure 3.4-2. Earth Reflected and Direct Solar Exposures for Earth End Bays

3.5 THERMAL ENVIRONMENT (Ref. 26)

The LDEF thermal design is completely passive, relying on surface coatings and internal heat paths for temperature control and equalization. To maximize the internal radiation coupling between the spacecraft components, high-emittance coatings were used. All interior surfaces were coated with Chemglaze Z-306 flat black paint which had a pre-flight emittance of 0.90. This unexposed coating did not seem to suffer any appreciable degradation during the LDEF mission. However, because the LDEF structure was not baked out after being painted, the Chemglaze Z-306 became one of LDEF's leading sources of contamination.

Internal radiation blockage was decreased by minimizing the number of structural components inside the spacecraft. The cylindrical cavity was closed at all tray locations and at both ends to prevent solar flux from entering the interior. The tray mounting scheme minimized the contact area through which heat could be transferred between the structure and the experiments. Figure 3.5-1 shows the distribution of the exterior surface coatings. Over 50% of these surfaces were chromic-acid-anodized aluminum with a/e values ranging from 1.32 to 2.2 (ref. 27)

Actual internal flight temperatures were recorded at intervals of approximately 112 minutes for the first 390 days of LDEF's mission. Temperatures were taken using five copper-constantant thermocouples, one suspended radiometer, and two thermistors were used for reference measurements. Figure 3.5-2 shows the location of this hardware. The actual recorded temperature range for all seven locations was from a low of +39°F to the maximum of +134°F. Figure 3.5-3 shows the temperatures versus mission time for the thermocouple located on a structural member located on row six of LDEF (thermocouple #5 in figure 3.5-2). This area was parallel to the orbital plane and experienced incident thermal flux environments that varied widely, depending on the orbital beta angle (beta angle is the angle between the plane of LDEF orbit and the sun illumination vector). As can be seen in table 3.5-1, thermocouple #5 experienced the largest variations in temperatures.

Flight temperatures were compared to the predictions made using the thermal mathematical model that was used to determine pre-flight predicted temperatures. This model was unverified prior to flight. Post-flight analysis has reduced the model's uncertainty to ±18°F. As shown in table 3.5-1, design temperatures were maintained throughout the mission.

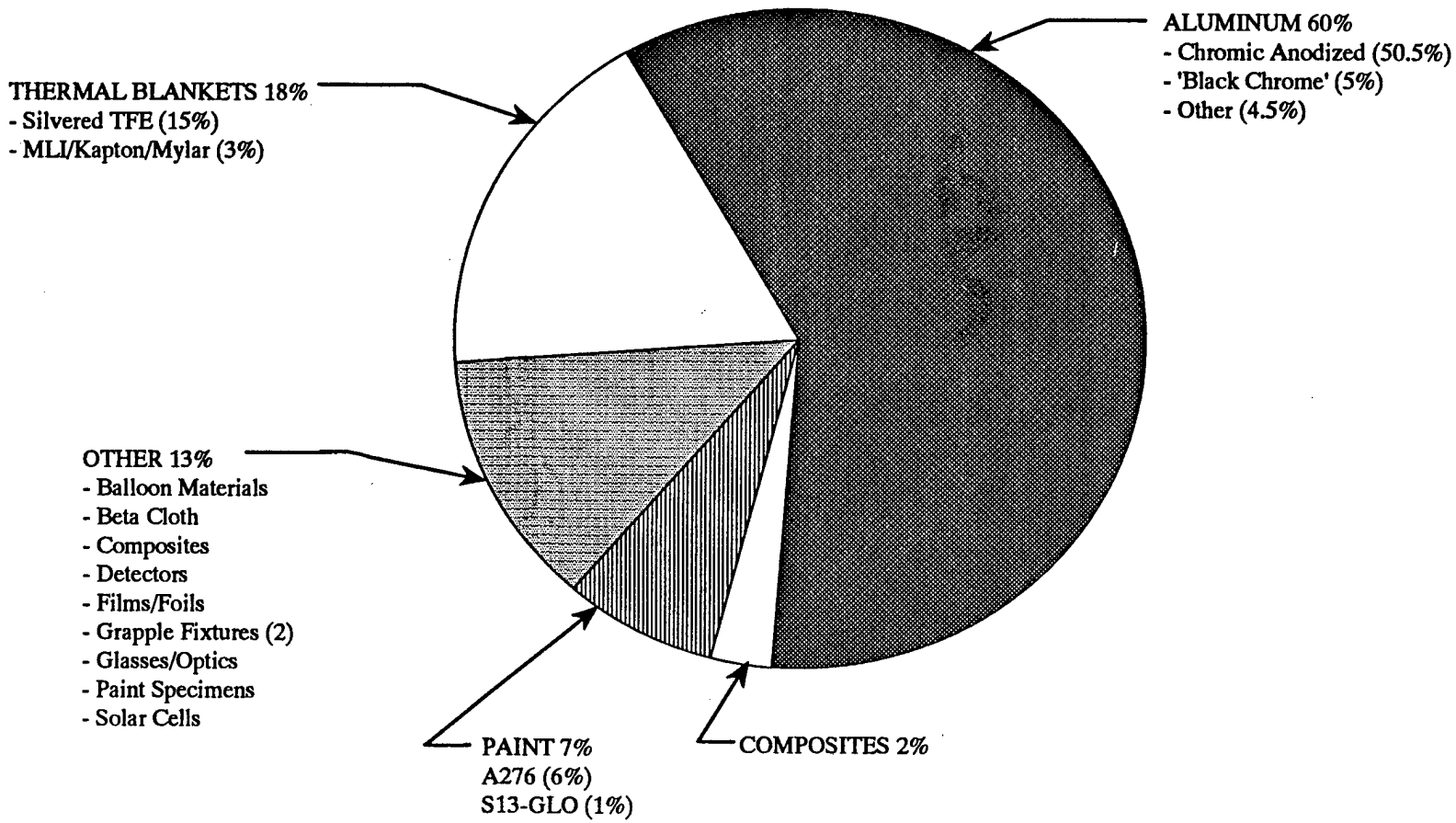

Figure 3.5-1. LDEF External Surface Coating Distribution

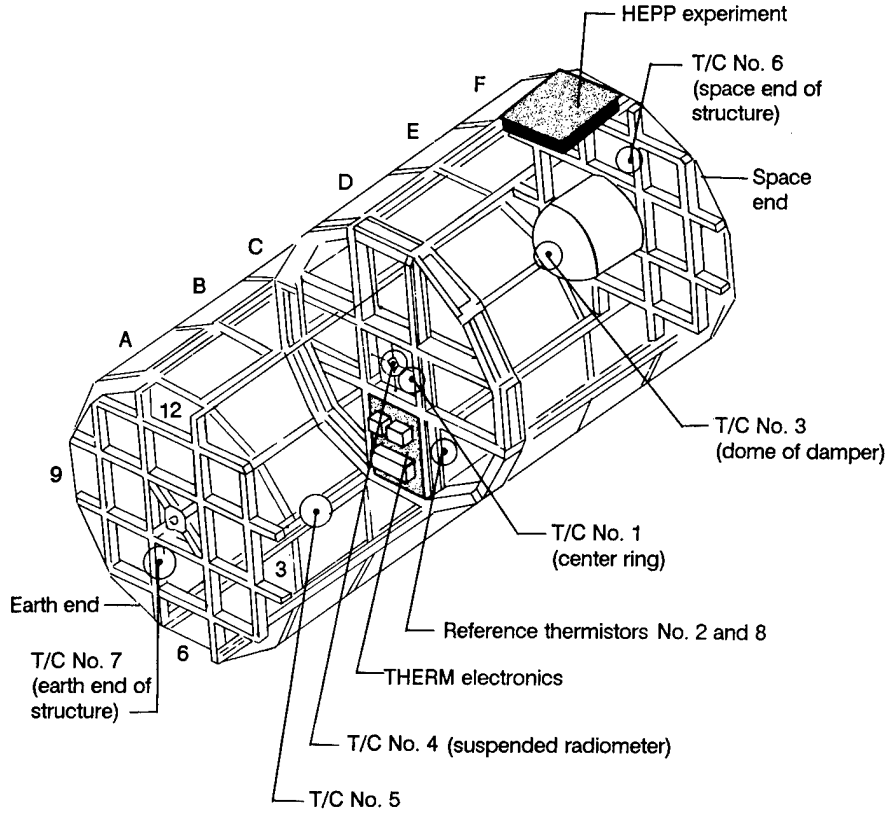

Figure 3.5-2. Location of THERM Hardware on LDEF

Table 3.5-1. Comparison of LDEF Temperature Ranges

LDEF LOCATION	TEMPERATURE DESIGN LIMITS °F	MEASURED (THERM) °F	POST FLIGHT CALCULATED °F
INTERIOR AVERAGE	10 - 120	52 - 89	58 - 89
STRUCTURE NORTH/SOUTH (ROWS 6/12)	-10-150	35 - 134	39 - 136
STRUCTURE EAST/WEST (ROWS 3/9)	-10-150	N/A	53 - 100
STRUCTURE EARTH END	10 - 135	56 - 103	57 - 104
STRUCTURE SPACE END	10 - 135	60 - 90	64 - 96

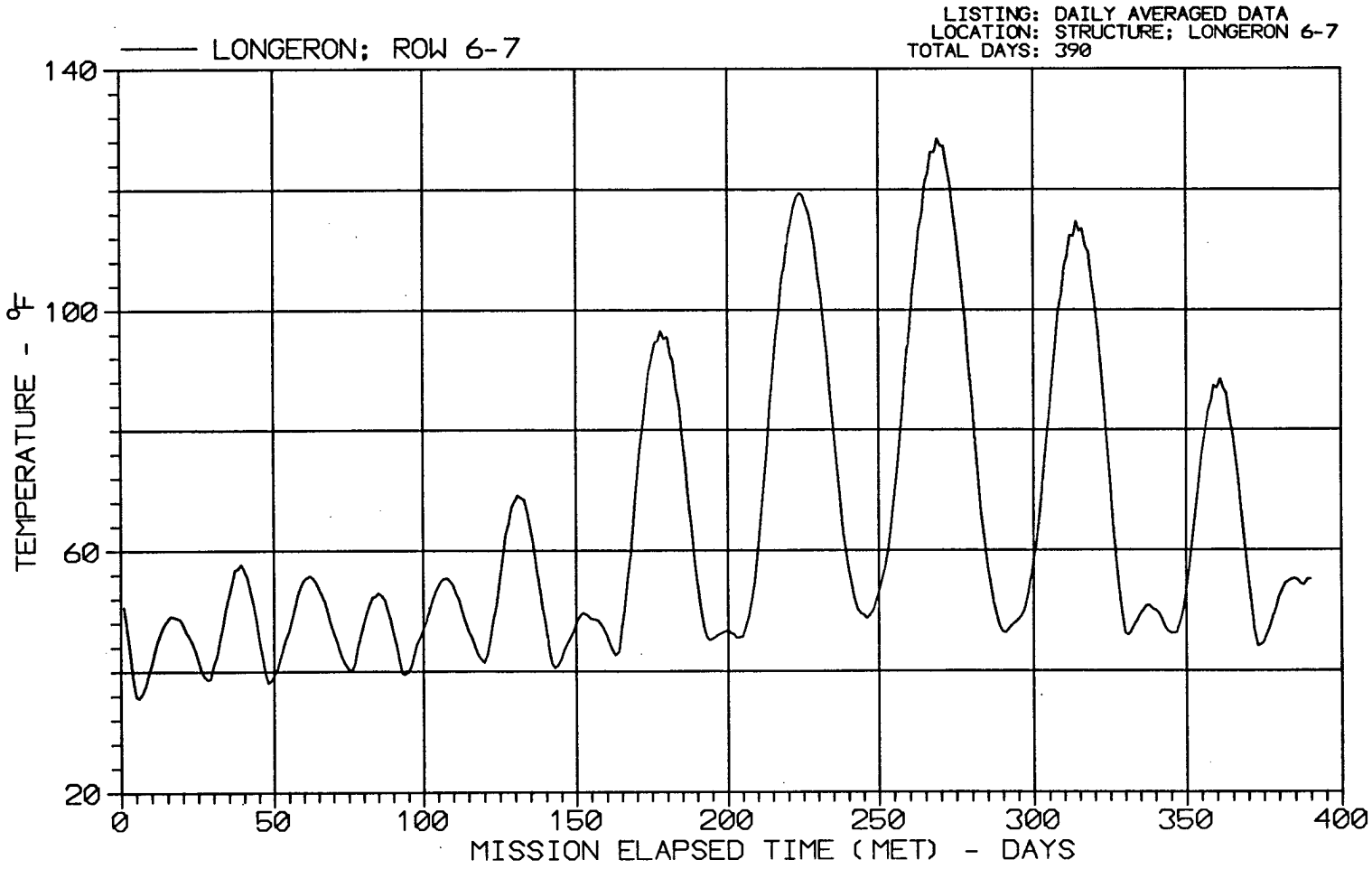

Figure 3.5-3. Long Duration Exposure Facility Thermal Measurements System

3.6 CONTAMINATION

Spacecraft systems must be considered both from the standpoint of their potential degradation due to contamination and as a source of unwanted contaminants resulting in the degradation of systems or hardware. LDEF provided examples of both. Figure 3.6-1 illustrates the contamination history of LDEF as a series of ten exposures. Ground operations prior to launch (exposure 1) and the launch environment (exposure 2) are critical to the initial performance of the systems in orbit. Early mission failures or problems may be the result of deficiencies during these phases of operation. Once in orbit (exposure 3), outgassing and redeposition of molecular films can degrade thermal control, optical, and solar energy systems. With the initiation of recovery, new sources of contamination presented themselves (exposures 4 through 10). These new contaminants and their sources were identified and backed out of the analysis in order to understand the condition of LDEF in orbit. Much of the task of identifying the post-orbit contaminants has now been accomplished and a detailed evaluation of the condition of LDEF in orbit is underway.

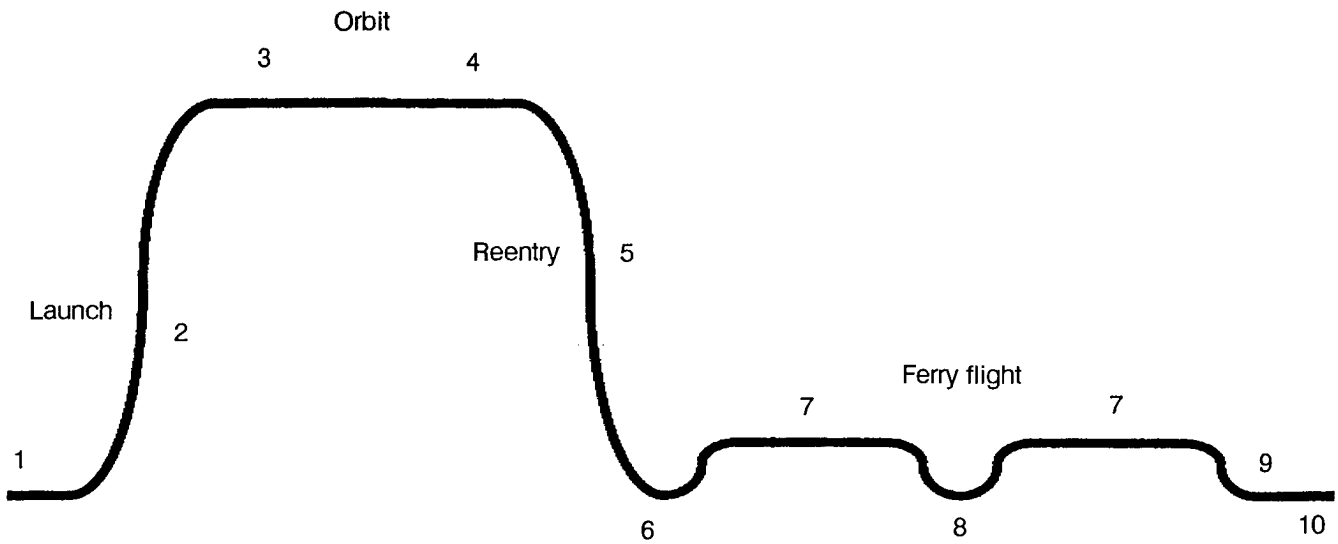

1. Condition of LDEF prior to launch: >MIL STD 1246B level 1000C for many trays.
2. During launch, many particulate contaminants are redistributed and Shuttle Bay debris is added.
3. Contaminants are modified and new contaminants are generated in the orbital environment.
4. Grappling causes some particles and films fragments to move, some may have relocated on LDEF.
5. During reentry, many particles and fragments of brittle molecular contaminant films relocate.
6. The Shuttle is exposed to the Edwards environment, accumulation of natural dusts.
7. High humidity, high gas flow velocities, thermal and pressure stresses occur.
8. HEPA filter fibers appear on tape lifts after exposure to new filters.
9. Ground operations prior to SAEF-2 include many manipulations to LDEF in complex environments.
10. SAEF-2 exposure.

Figure 3.6-1. Contamination Exposure History of LDEF

Most of the particulate contaminants present in orbit were deposited on the surface of LDEF during ground exposure or the launch environment. The particles were characteristic of fabrication, assembly, and integration activities, with some of the distributions suggesting launch redistribution or cross contamination (ref. 28). Particulate contaminants effect systems mechanically and optically. Particles optically obscure, scatter, refract, diffract, and reflect light. They may also become infrared emitters when heated by solar radiation. Scatter, refraction, diffraction, and reflection all change the path of a ray of light. The effect is to introduce unwanted energy causing a decrease in the signal-to-noise ratio in an optical system, thereby decreasing the device's sensitivity. The cleanliness level of LDEF when it entered orbit was approximately a MIL-STD 1246B Level 1000 for particles smaller than 250 micrometers or a Level 2000 for particles smaller than 750 micrometers (see ref. 29 for a more detailed discussion).

The amount of molecular contaminants in the form of non volatile residues averaged over the surface of LDEF at launch has been estimated at about 2.5 mg/ft^2 This corresponds to a MIL-STD 1246B Level C. This may have been sufficient to degrade some systems, but its effects were largely hidden by the far greater amount of outgassing materials redeposited on the surface of LDEF in orbit.

In orbit, additional particulate contaminants accumulated as a result of impacts with meteoroids and space debris. These contaminants tended to be deposited very close to the impact, with concentration dropping off with the square of the distance from the impact, as would be expected. Impacts with surfaces projecting radially from the surface of LDEF, such as tray edges or bolt heads, resulted in the greatest amount of material being deposited on the surface of LDEF. The concentration of such debris could be very detrimental to optical systems within a few inches of the impact.

The most detrimental contamination event in orbit was the outgassing and redeposition of molecular contaminants on the surface of LDEF. The brown discoloration caused by a contaminating molecular film on the surface of LDEF was evident through the windows of the Space Shuttle Columbia as it approached LDEF. This brown film was widely dispersed over the trailing rows of LDEF and at the space and Earth ends. Closer examination in SAEF-2 following recovery permitted a much more detailed analysis of the film and its distribution. Large areas of the exterior surface were covered with a film a few hundred nanometers thick. In some areas it was as much as a few hundred micrometers thick and completely opaque. Analysis of the film indicated it was a polymer consisting of a combination of silicones and hydrocarbons. The ram facing trays appeared clean but surface elemental analysis of ram surfaces indicated a silica residue remaining from atomic oxygen attack on the brown film. An infrared analysis of the film and possible sources indicated that two systems had sufficient mass to be major contributors to the film: the thermal control paints and the silicone adhesives used with both fasteners (to enable fastener assemblies to survive vibration testing without a decrease in installation torques) and the bonding of Velcro to LDEF and/or experimenter hardware.

The local thermal loading caused by the molecular film created a variety of detrimental effects. The film was a relatively effective absorber and resulted in significant heating of some surfaces. The delamination of thin films on optics and

metal-plated composite surfaces has been attributed to the combination of poor coefficient of thermal expansion matching between the delaminating surfaces and the heat cycling extremes due to the presence of this contaminating film. The film increased the thermal loading over many areas of the satellite but seemed to have relatively little effect on the anodized aluminum surfaces of the tray clamps. The ratio of absorptance to emissivity for the tray clamps was about 2.27 for both leading and trailing edge clamps. A276 thermal control paint buttons on many of the clamps did, however, experience a change. Paint buttons on the leading rows had a ratio of approximately 0.32 while those on the trailing edge were about 0.63. The brown discoloration on trailing edge buttons was largely due to the modification of the top organic layer (vehicle) of the paint as a result of ultraviolet exposure.

A decrease in the transmission through some optics was noted and has been attributed to the molecular film. A change in some of the wavelength characteristics of coated optics was noted and has been initially attributed to the effect of an added contaminant thin film (ref. 82). Elemental analysis of the surface of some of these optics on the ram side of LDEF indicated a silica residue was present from the atomic-oxygen-degraded molecular film (ref. 53). Other optical effects included selective reflection due to sub-micron droplet size, decreased signal-to-noise ratio broadband, and increased background in the infrared.

The recovery operation redistributed LDEF contaminants that were presumably stable in orbit. These contaminants included thin metal foils that remained after the organic film on which they had been vapor deposited had been removed by the atomic oxygen exposure. Fragments of partially eroded polymers were also widely distributed. Paint pigments, ash from a variety of composites, fragments of thick molecular film deposits, and both glass fibers and graphite fibers freed from atomic oxygen eroded composite materials completed the compliment of redistributed LDEF materials. Materials from the shuttle were also transported to the surface of LDEF. The materials from the Shuttle included liquid droplets containing hydrocarbons as well as solid particles, and glass from tile material and from the bay liner. This redistribution of contaminants continued through the final removal of LDEF from the Shuttle Bay (exposures 4 through 9).

The exposure to contaminants continued during the deintegration in SAEF-2. Automatic airborne particle count data indicated a controlled class 100,000 clean room environment in SAEF-2 but pollens, natural minerals, clothing fiber, paper fiber, etc. accumulated on the surface of LDEF during its exposure. Details on the types and quantities of contaminants on LDEF surfaces can be found in references 28 through 32.

In summary, the systems most susceptible to contamination were thermal control surfaces, optics, and solar cells. The systems most likely to be a source of contamination were thermal control paints, silicone adhesives, polymeric films, and carbon-based sheet materials.

4.0 SYSTEMS TEST RESULTS

The System SIG was chartered to investigate the effects of long-term exposure to the LEO environment on system-related hardware and to collate all results into a single document. This section documents the status of this investigation. The testing results were generated by either Boeing personnel, funded through the System SIG support contracts, or individual experimenters. All non-Boeing results have been referenced so that credit is given to the experimenters who performed the work and to inform the reader as to where further information can be obtained. Section 4.0 is divided into the four disciplines that the System SIG has used throughout the LDEF investigation: mechanical,electrical, thermal, and optical.

4.1 MECHANICAL SYSTEMS

This section discusses the effects of the 69-month LEO exposure on the LDEF primary structure, primary structure fasteners, experimenter fasteners, environment exposure control canisters (EECC), grapples, viscous damper, lubricants, seals, and composites. One of the most important objectives of this investigation was to evaluate the potential for space-exposure-generated coldwelding of structural materials and fasteners. Successful satellite servicing and Space Station Freedom (SSF) design depends critically upon avoidance of coldwelding because specific components, such as SSF orbital replacement units, will require periodic replacement or repair. Information obtained from this investigation will facilitate the development of proper pre-flight installation practices and thread lubrication schemes that will minimize or eliminate the subsequent risk of galling or coldwelding.

4.1.1 Primary Structure

The LDEF primary structure is a framework constructed of welded and bolted aluminum 6061-T6 rings, longerons, and intercostals. The structure is approximately 30 ft long and 14 ft in diameter. A gas metal arc (GMA) welding process developed by NASA LaRC for fusion welding of 6061 aluminum was employed to fabricate the center ring. The remainder of the structure was mechanically fastened together. The welds were inspected by dye penetrant and eddy current techniques at KSC following deintegration of the experiment trays. The welds were found to be nominal, with no evidence of any launch - or flight -related degradation.

The potential for space exposure effects on the microstructural or mechanical properties of the aluminum primary structure was investigated by metallurgical analysis of the 6061-T6 aluminum experiment tray clamps. Examination of the clamps avoided removal of any the 6061-T6 aluminum structural components for analysis. The tray clamps are representative of the primary structure and were distributed uniformly around the exterior of LDEF. Clamps from near leading edge (E10) and near trailing edge (E2) were cross-sectioned and prepared for microstructural examination by standard metallographic techniques. Microstructures from surfaces on these two clamps that were either directly exposed or protected by an overlaying shim are displayed in figure 4.1.1-1. The microstructures are normal for 6061-T6 aluminum. The lack of any differences between the samples illustrates that space exposure has no discernible effect on the bulk microstructures of

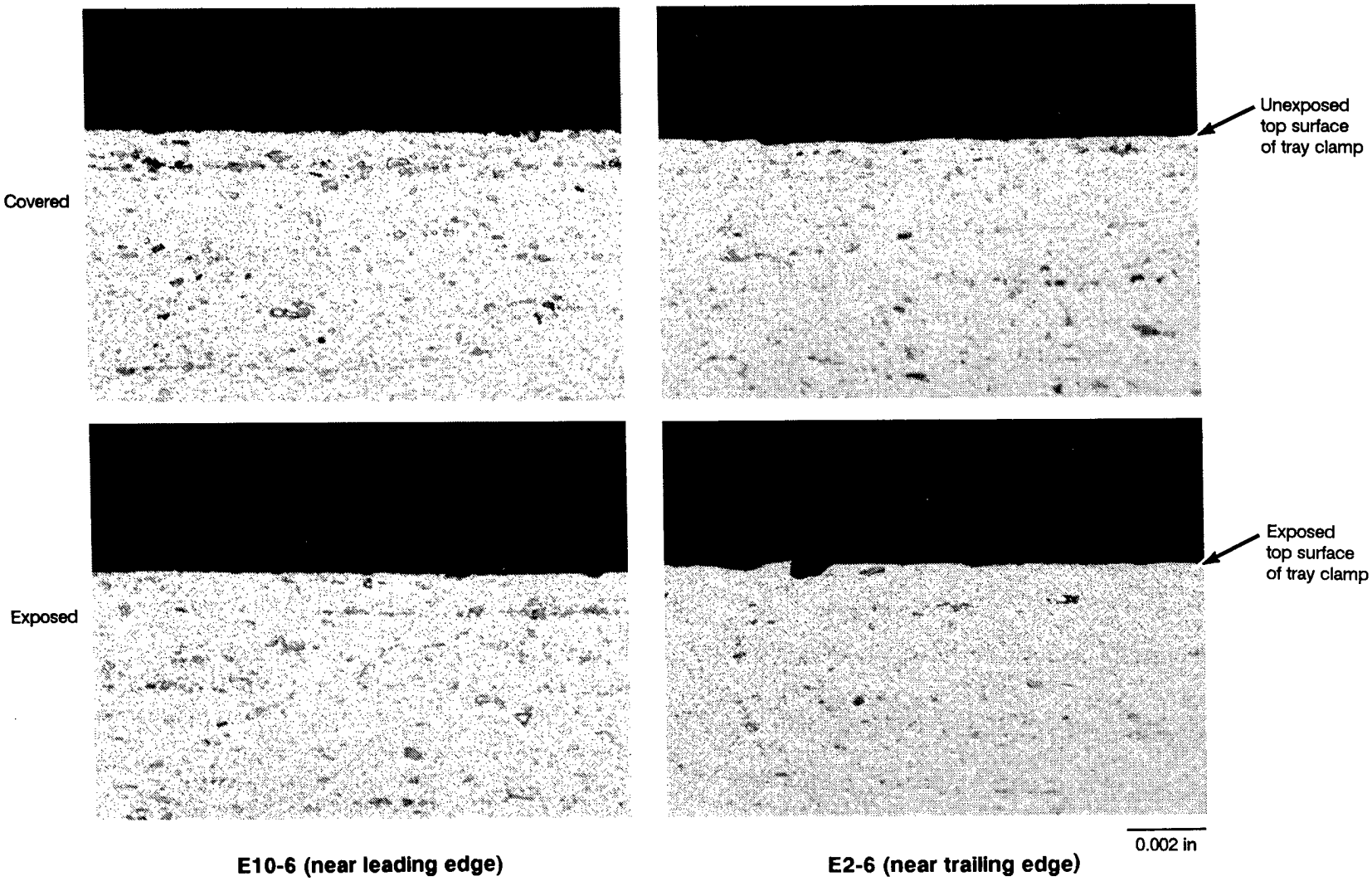

Figure 4.1.1-1. As-Etched Microstructures of 6061-T6 Aluminum Experiment Tray Clamps From Near-Leading and Near-Trailing Edge of LDEF. Covered areas of the clamps were protected by an overlying shim.

typical structural metals. Mechanical property changes are precluded in the absence of microstructural changes. Surface analysis investigations, including scanning electron microscopy of the anodized surfaces of the clamps, did, however, show some smoothing or erosion effects on exposed areas near the leading edge.

4.1.2 End Support Beam

The end support beam (ESB), shown in fig. 4.1.2-1, is an 18-ft. long welded 6061-T6 aluminum truss that held the two end trunnions that supported one end of the LDEF within the shuttle bay (two other trunnions were fixed to LDEF and provided the required additional support). The ESB was designed to allow a plus or minus 1.5 deg. rotation about a 5-in.-diameter 17-4 PH stainless steel spindle. No lubricant was used between the spindle and ESB. The purpose of the rotation was twofold: (1) during the design phase, it allowed the LDEF loads to the Shuttle to be statically determinant and (2) accommodated potential misalignment of the LDEF structure and permit reberthing into the shuttle bay. Deintegration of LDEF at KSC required that the ESB be removed. A great deal of difficulty was encountered during removal. The ESB seized on the spindle, and use of a gear puller was required to complete removal. Since no similar difficulties had been reported during pre-flight testing, there was concern that coldwelding might have occurred between the ESB and spindle during flight.

As seen in figure 4.1.2-2, the spindle bore of the ESB was damaged by severe galling and scoring. Discussions with the LDEF deintegration staff indicated that the ESB slid easily off approximately the first inch of the spindle at which time it bound onto the spindle. Review of the video documentation of the ESB removal operation confirmed this observation and revealed that the hoist used to support the ESB caused it to cock and jam on the spindle as the beam cleared the inner land of the spindle. Figure 4.1.2-3 illustrates the details of the binding. Numerous rotations of the jammed ESB about the spindle in an unsuccessful attempt to free it caused the deep circumferential scoring visible on the bore of the ESB. The separation between the two circumferential score marks is the width of the outer land of the spindle.

Examination of the spindle revealed corresponding minor galling and transfer of aluminum onto its outer land. Metallographic cross-sectioning of the spindle through the adhered aluminum (fig. 4.1.2-4) revealed a discrete interface between the aluminum and stainless steel which confirms that coldwelding did not occur during flight. Shear deformations of the adhered aluminum are consistent with the removal operations. Axial scoring of the ESB bore, figure 4.1.2-2, occurred when adhered aluminum on the spindle gouged the bore as the beam was removed with the gear puller.

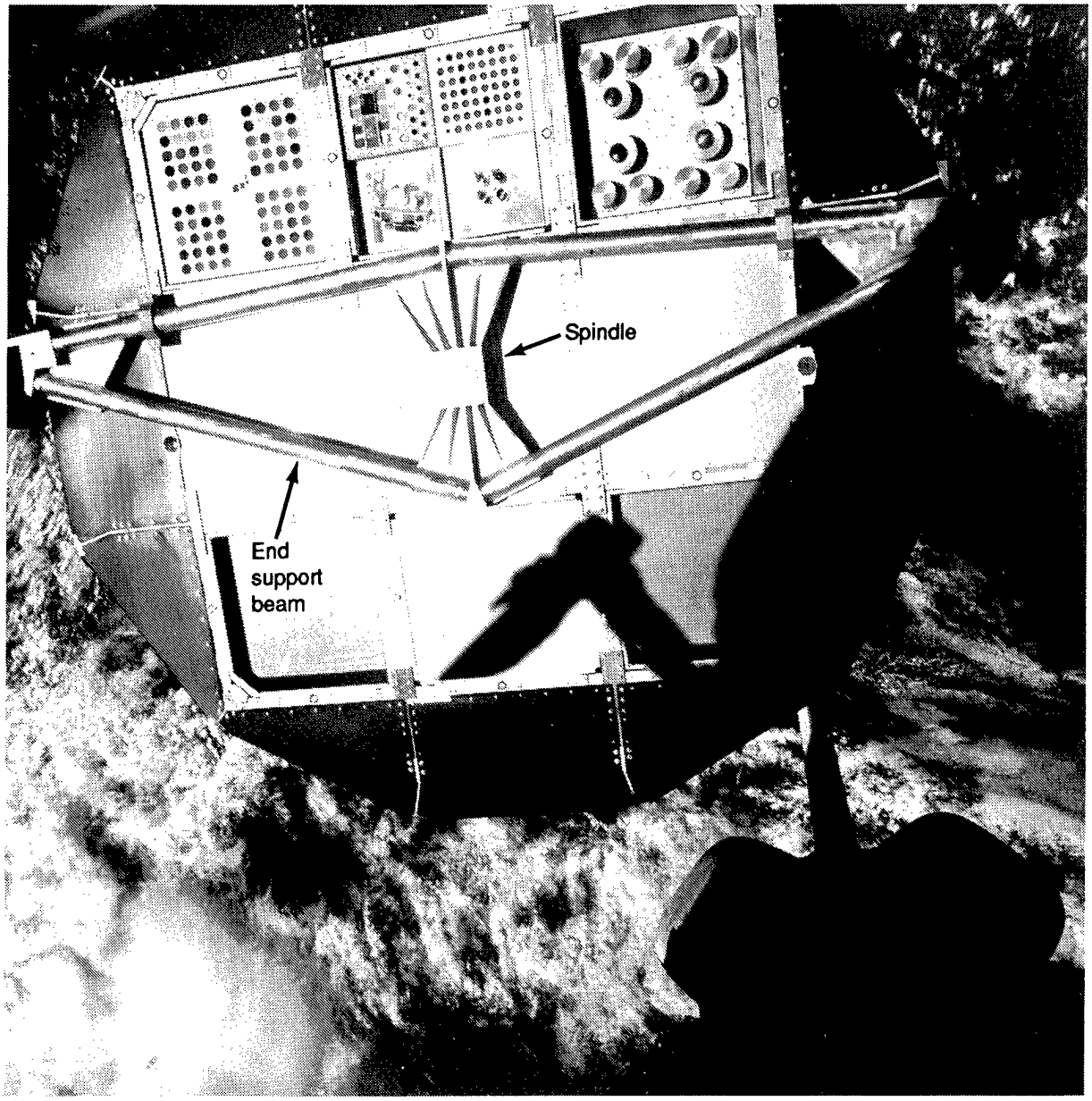

Figure 4.1.2-1. End Support Beam

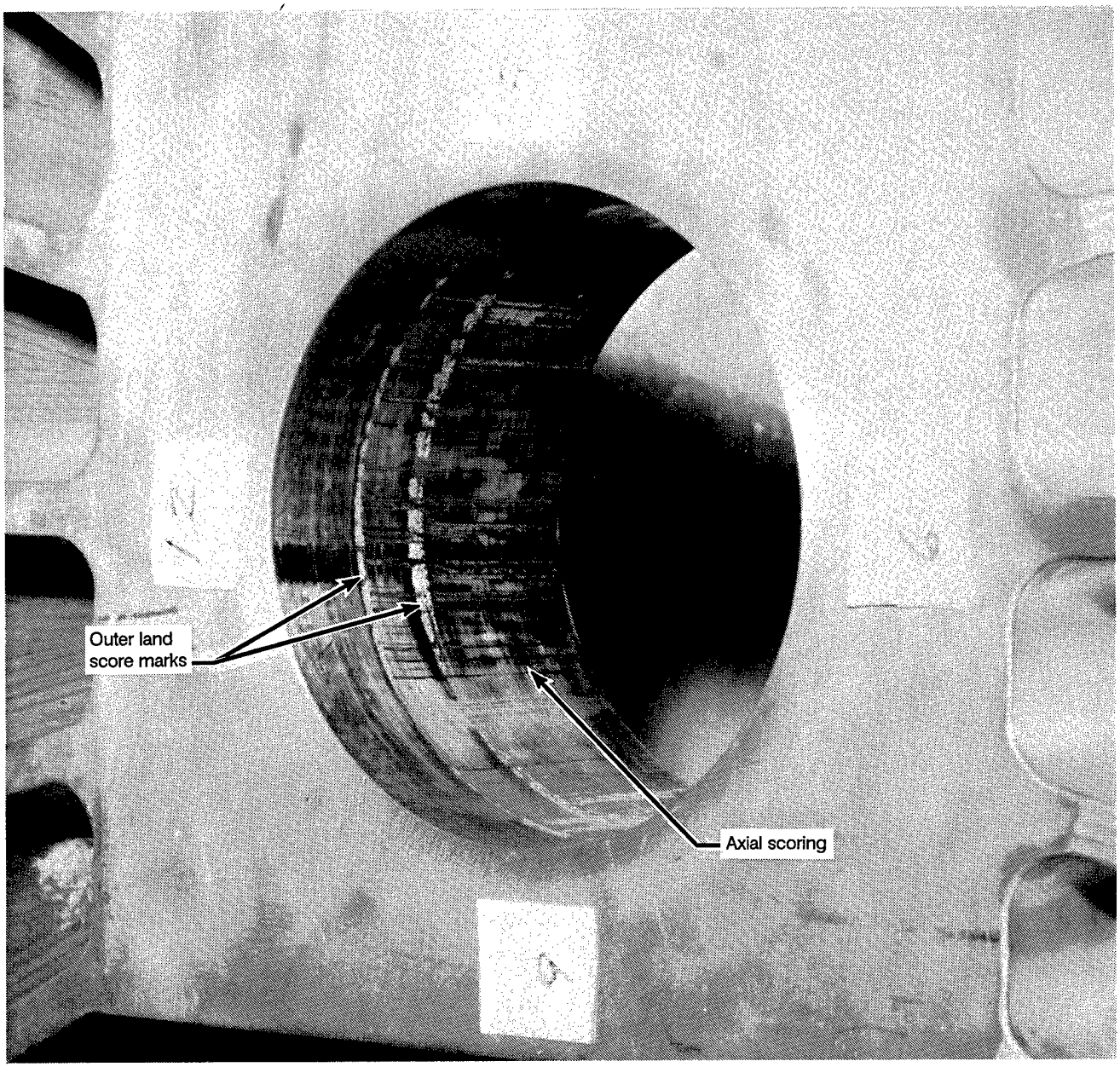

Front Surface of ESB

Figure 4.1.2-2. Closeup of ESB Spindle Bore Showing Scoring Damage Observed After Removal From Spindle During Deintegration

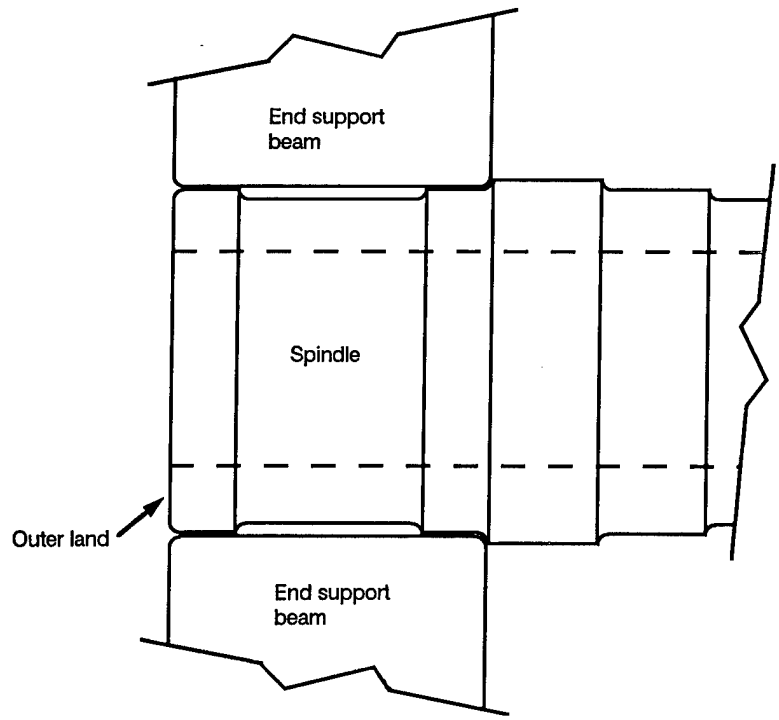

Flight Position of End Support Beam

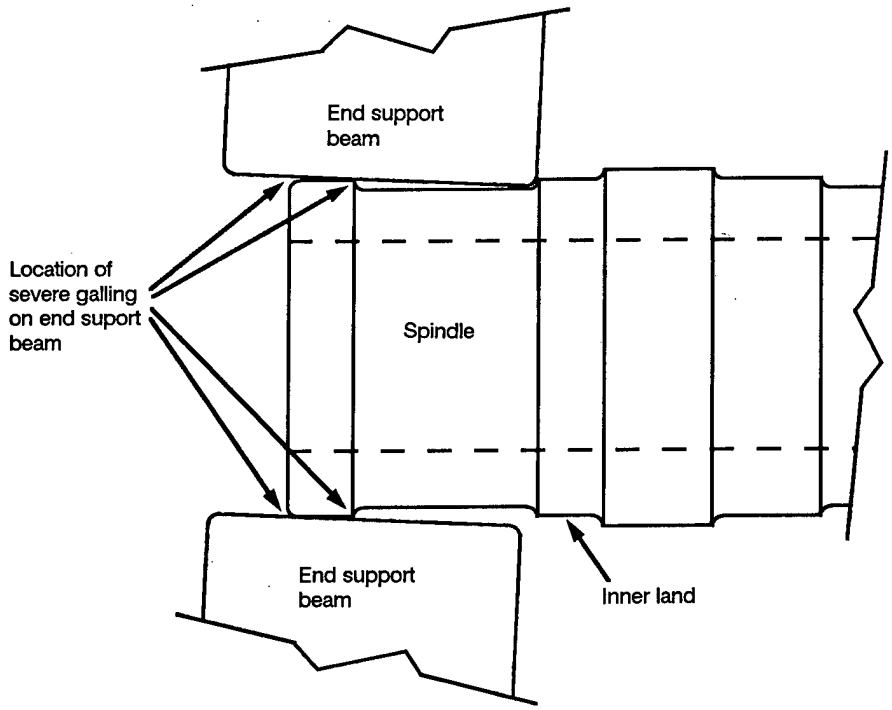

Position of End Support Beam When It Became Stuck on Spindle During Removal Attempt

Figure 4.1.2-3. Schematic Illustration of Cause of ESB Seizure During Removal

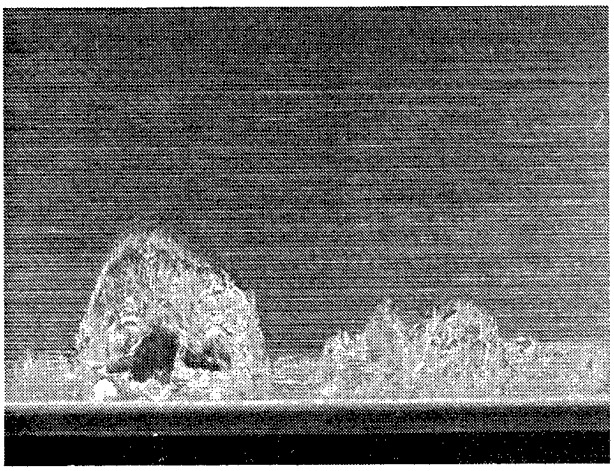

Galling and aluminum adhesion

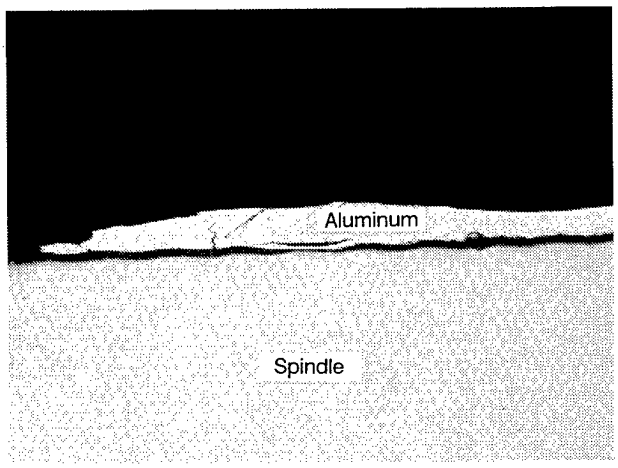

0.005 in

ESB Spindle Cross-Section

Figure 4.1.2-4. Galling and Adhesion of ESB Aluminum on Stainless Steel Spindle

4.1.3 Fasteners

4.1.3.1 Primary Structure Fasteners

Following the completion of the experiment deintegration, all primary structure fastener assemblies were re-torqued to pre-flight values. The fastener assemblies consist of stainless steel bolts ranging in diameter from 1/4 to 7/8 inch with silver-plated locking nuts (MS 21046). Only 4%, or 119 of the 2,928 assemblies, had relaxed. Nut rotations required to reestablish pre-flight torque levels for those that relaxed ranged from 5 to 120 deg. The small number of relaxed fastener assemblies indicates that the reliability of bolted joints in space applications is very high. This conclusion must be tempered by the fact that LDEF was exposed to a rather benign thermal environment with minimal thermal swings, as indicated by review of the on-board thermocouple data.

An undisturbed, as-flown intercostal fastener assembly is shown in figure 4.1.3.1-1. It was removed from the LDEF structure to investigate the possibility of coldwelding of the structure fastener assemblies during space exposure. The fastener was selected because of its availability and not because of any evidence of coldwelding of it or other similar fasteners. The stainless steel bolt/aluminum interfaces and bolt/nut faying surfaces were examined for indications of cold- (or solid state-) welding. Closeups of these areas are shown in figures 4.1.3.1-2 and 4.1.3.1-3. Examination of the bolt shank interface reveals no metallographic evidence of coldwelding. The thread faying surfaces also show no evidence of coldwelding; however, some minor galling and smearing of the silver plating on the nut is evident. The behavior of the plating is normal because it is specified to act as a lubricant during both installation and removal to prevent galling and seizure of the nut on the bolt.

Twenty-four silver plated nuts from LDEF intercostal clips were removed and analyzed. The nuts were removed from clips located on the inside of LDEF at the Earth and space ends. Two sizes of nuts were examined: 1/4 in. and 3/8 in. Analyses included FTIR, X-ray photoelectron spectroscopy, Auger electron spectroscopy, and photomicroscopy. Photographs of each nut were taken before any testing was done. A typical photograph is shown in figure 4.1.3.1-4. All exposed nut surfaces had a brown contaminant film, some more than others. The color and distribution of this film varied between nuts and over the surface of each nut. There was no apparent correlation between the location of the nuts and the amount of film. It was initially speculated that the film was caused by oxidation of the silver plating. However, the results from the analysis showed that the film was caused by deposition of molecular contamination, which was similar to other interior surfaces. The nuts had a deposition of silicone and silica/silicates from the decomposition of silicone, and of the amide material that may have originated from urethane paint. No degradation of the silver was observed. Several fasteners were cross sectioned and examined for wear. As can be seen in figure 4.1.3.1-5, all examined external surfaces appear nominal.

4.1.3.2 Tray Clamp Fasteners

The experiment trays were held in the structure openings by aluminum clamps. The clamps consisted of flat 0.25-in-thick rectangular or "L" shaped plates with three

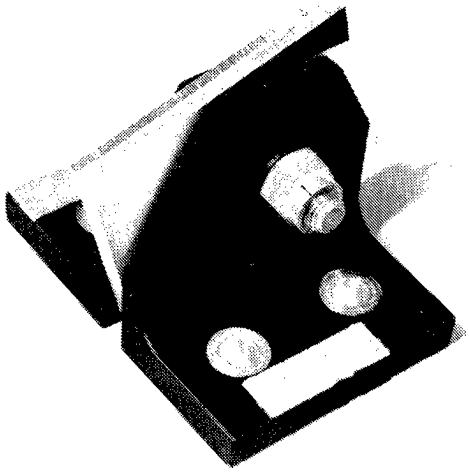

Fastener Assembly

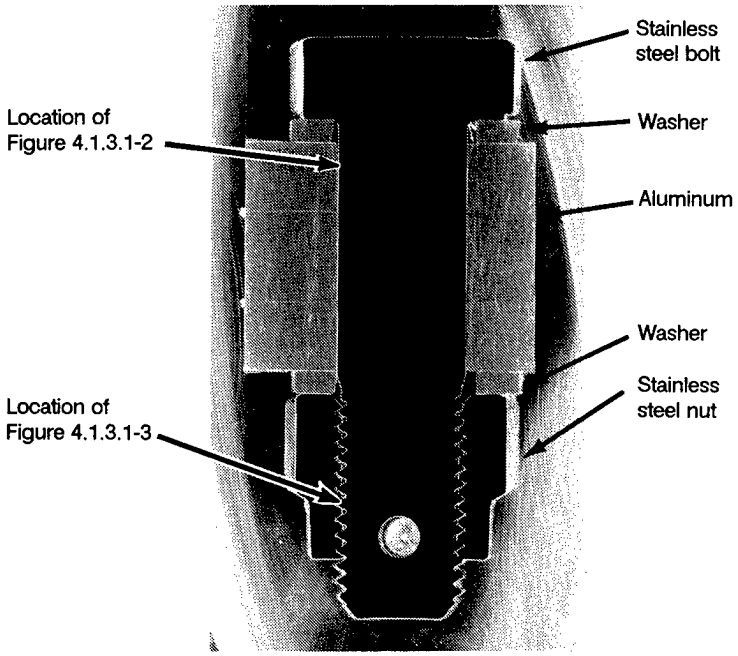

Metallographic Cross-Section

0.040 in

Figure 4.1.3.1-1. Unassembled Intercostal Fastener Assembly

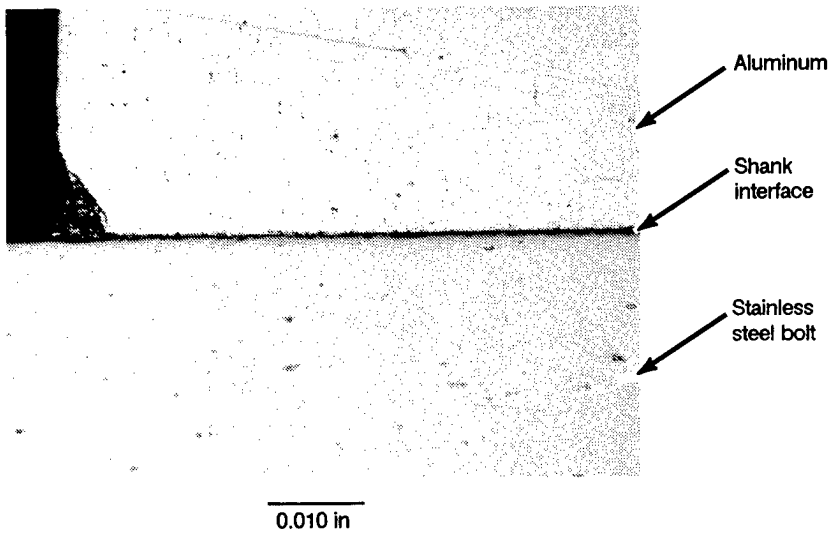

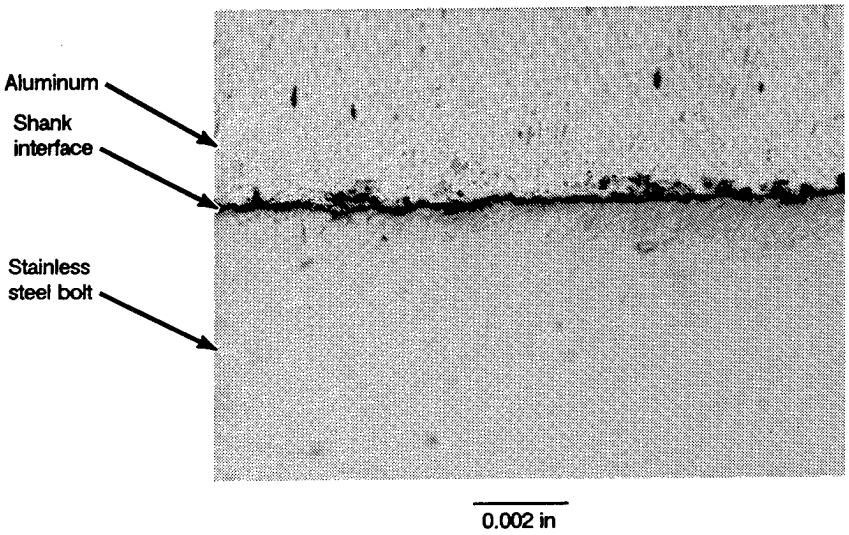

Intercostal Fastener Assembly Cross-Section

Figure 4.1.3.1-2. Closeup of Shank Interface Area Indicated in Figure 4.1.3.1-1.

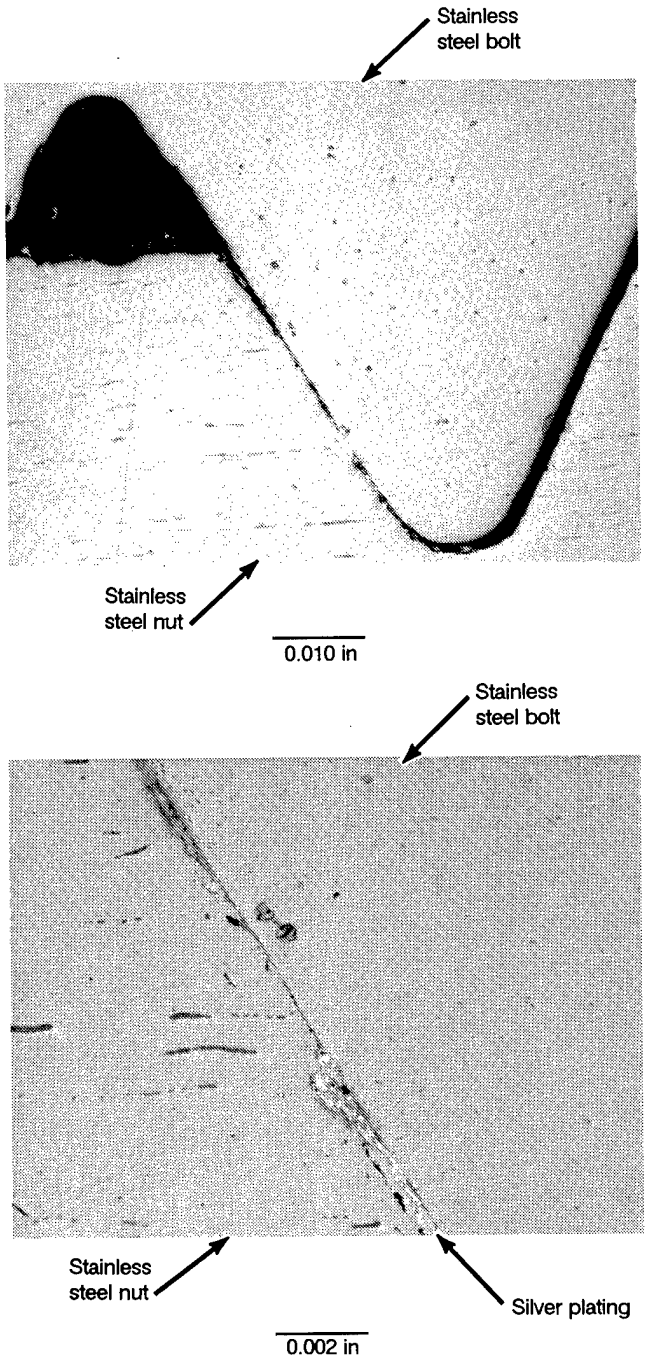

Intercostal Fastener Assembly Cross-Section

Figure 4.1.3.1-3. Closeup of Nut/Bolt Thread Faying Surfaces as Indicated in Figure 4.1.3.1-1. (Note Smearing of Ag-Plating Which Acts as a Lubricant Between the Nut and Bolt.)

(See color photograph on p. 292)

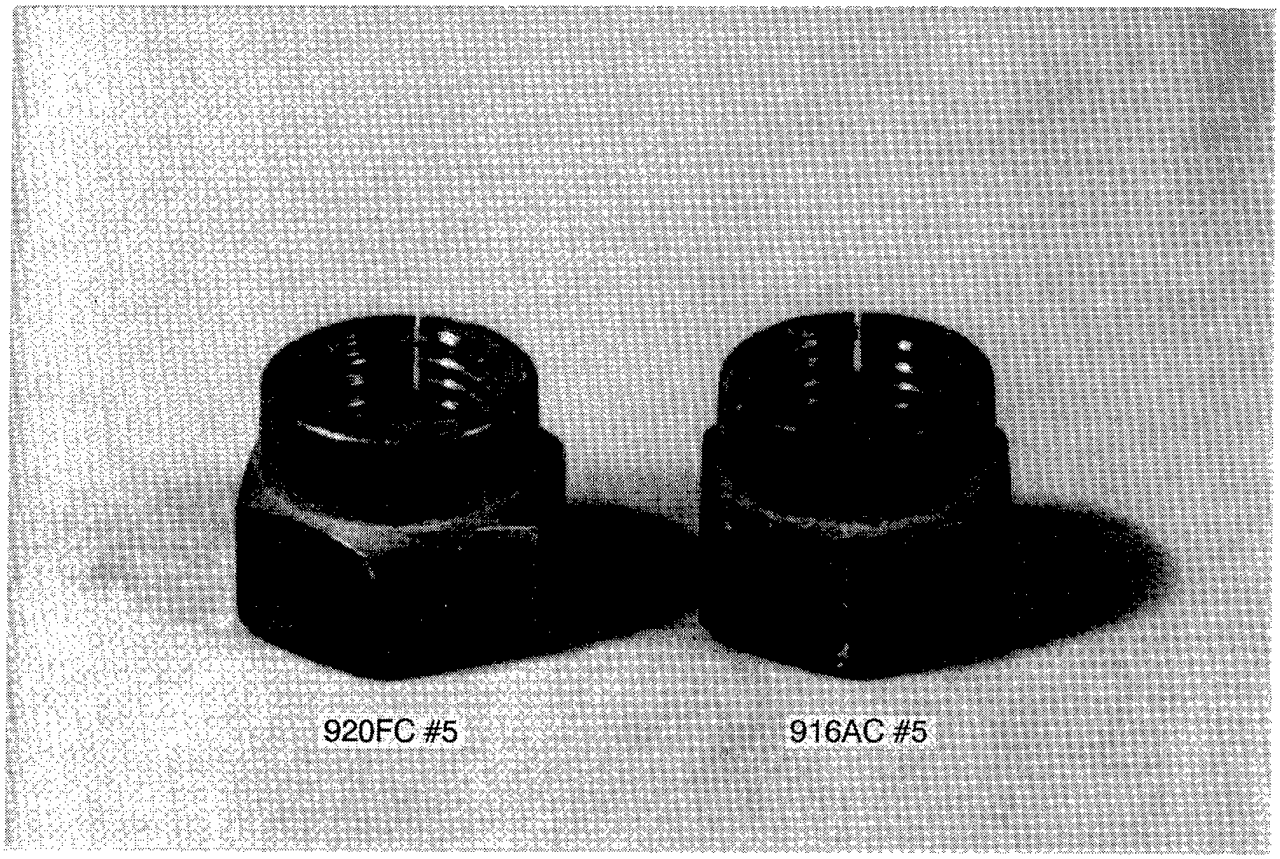

Figure 4.1.3.1-4. Photograph of silver plated nuts—All exterior nut surfaces had a brown contaminant film, some more than others. The discoloration of the nut was not atomic oxygens caused oxidation.

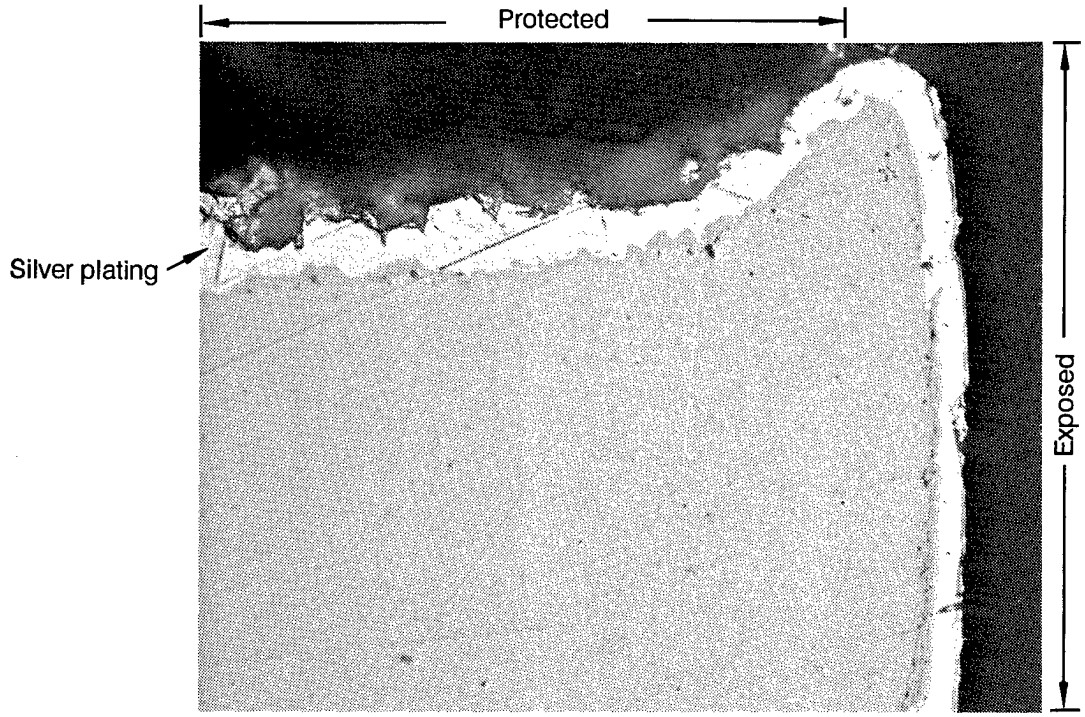

920FA #1 Loc. 2 500x

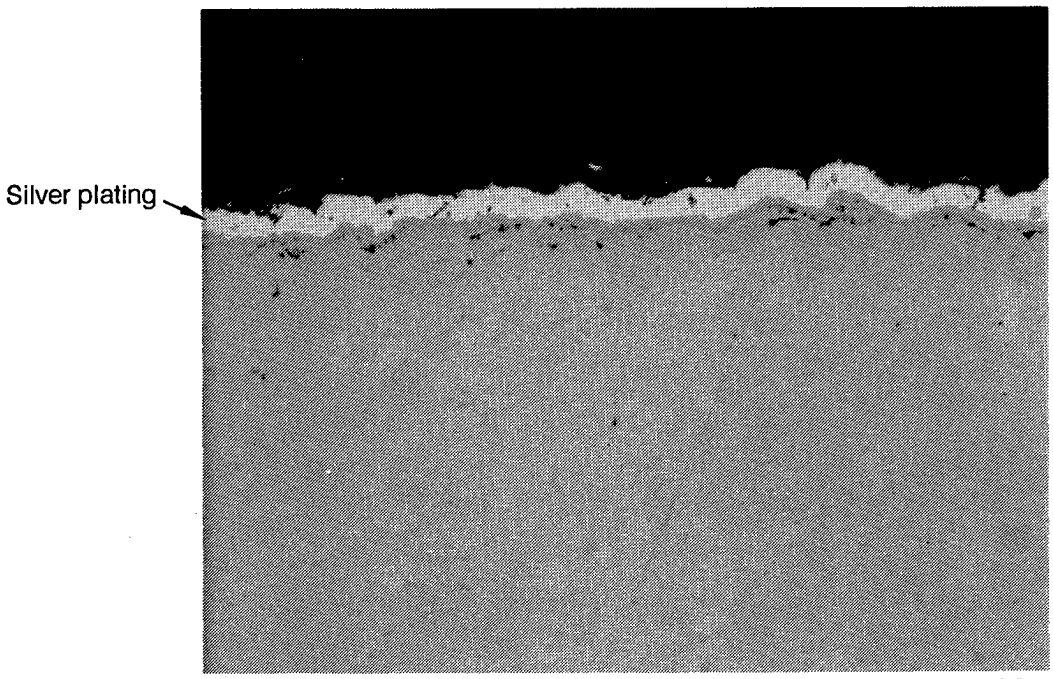

920FA #1 Loc. 3 500x

Figure 4.1.3.1-5. Cross-Section of a Silver Plated Nut

mounting holes in them. They were attached to the structure with NAS1004-4 hexagon head 0.25-28 UNJF-3A size A286 heat-resistant steel bolts, heat treated to 140,000 psi ultimate tensile strength, with a passivated finish. The bolts, with alodined aluminum washers under the head, were installed into self-locking thread inserts on the primary structure. The bolts were cleaned with alcohol and patted dry prior to installation. The bolts were installed with a preflight forque of 75 +/-5 in-lb. Note that bolts were installed into these thread inserts at least twice, and three times for some inserts. It is unknown whether the initial bolt was reinstalled into the same insert, into a different insert, or if a new (unused) bolt was installed each time.

During deintegration of LDEF, unseating (breakway) torque values were recorded for all 2,232 tray clamp fasteners using a dial-indicator-type torque wrench. Prevailing (running) torque values were obtained for every third bolt (the middle of the three bolts in each clamp). A database was created that contained all of the unseating and prevailing torques as a function of location of LDEF.

The unseating torques averaged 72 in-lb and ranged between 10 and 205 in-lb. The averages of the 20 lowest and 20 highest values were 31 and 175 in-lb. The average unseating torques were similar throughout LDEF, indicating no pronounced effect of varying space exposure conditions on bolt torque behavior. The prevailing torques averaged 17 in-lb and ranged between 2 and 132 in-lb. The average of the 20 highest prevailing torques was 58 in-lb. There was little correlation between high prevailing torques and high unseating torques. Only one bolt possessed both one of the 20 highest prevailing and one of the 20 highest unseating torques.

Bar charts showing the distribution of bolt unseating torques and bolt running torques are contained in figures 4.1.3.2-1 and 4.1.3.2-2. The threaded insert vendor stated that they were not surprised by the wide variation and range of unseating torques shown in figure 4.1.3.2-1. These values are very unpredictable due to fatigue, bolt stretching, corrosion, particles contamination, etc. However, the amount of bolts that exceeded prevailing torque specifications (not to exceed 30 in-lbs of torque) was unexpected. Almost 10% of the 720 prevailing torques that were measured during the deintegration exceeded the 30 in-lb specification. Activities to identify the cause are discussed in the following paragraphs

Eighty-nine tray clamp mounting bolts and washers were selected from the database using the parameters noted below and visually examined using a binocular microscope at 8X and higher magnification.

Highest prevailing torque
Highest unseating torque
Lowest unseating torque
Bolts with 3 - 30 in-lbs prevailing torque (within mfg spec)
Bolts having matching control bolts
Control bolts (CRES washers)
Random selection

To aid in the evaluation, each bolt and washer was given a rating code as noted below.

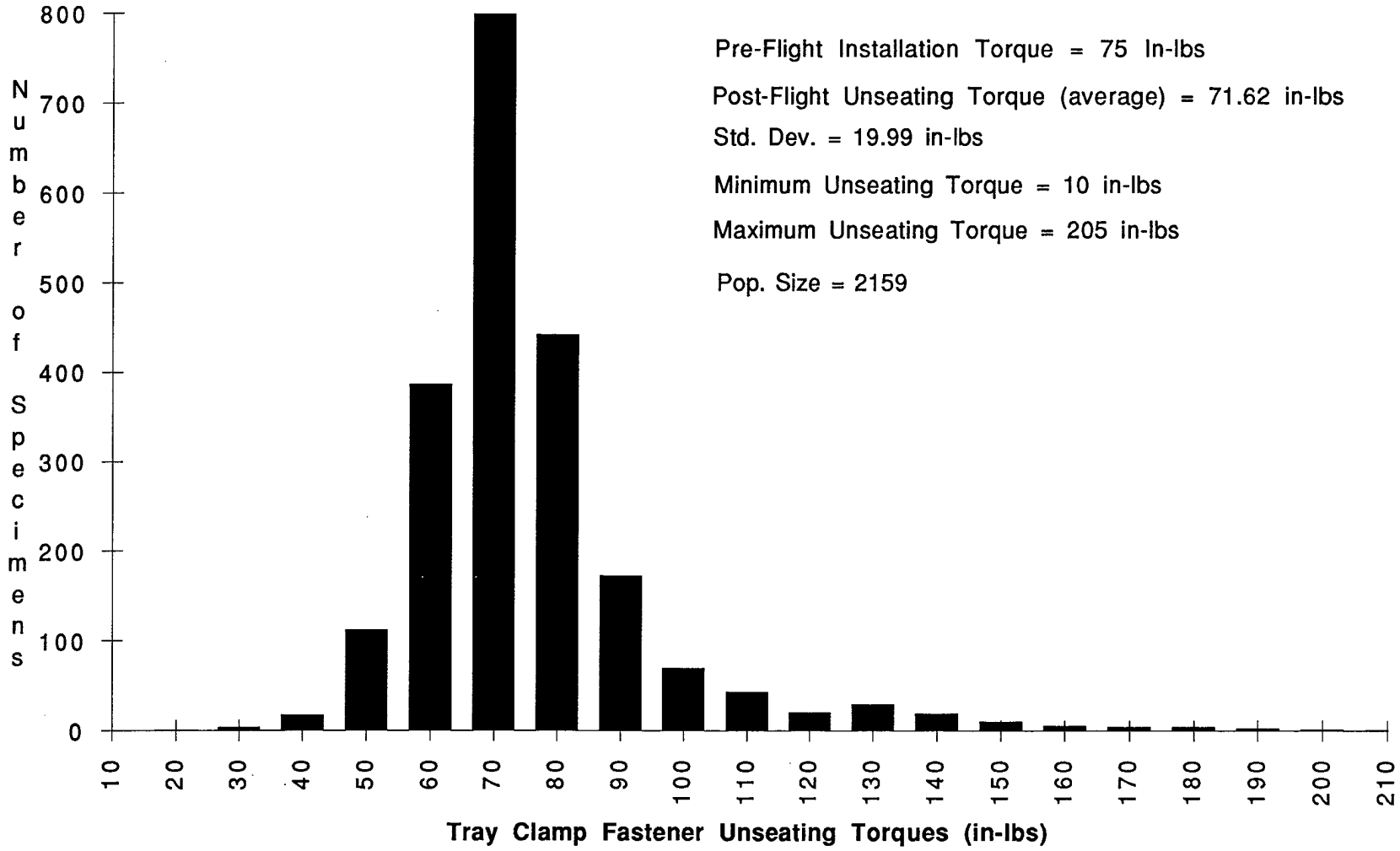

Figure 4.1.3.2-1. Tray Clamp Fastener Undeating Torques

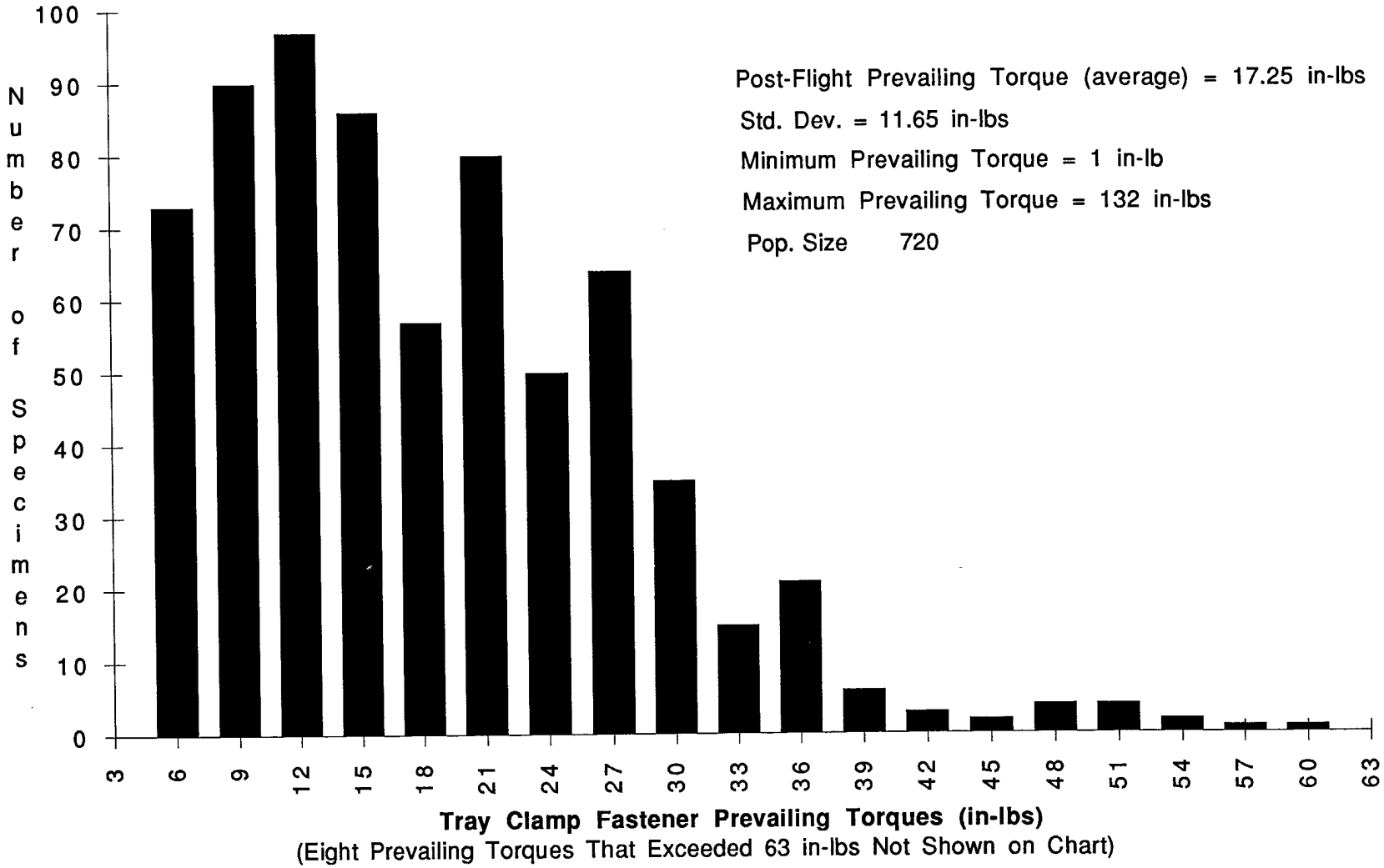

Figure 4.1.3.2-2. Tray Clamp Fastener Prevailing Torques

Bolts
- B1 = No galling, very little scoring on threads.
- B2 = Light galling or thread wear, no metal deposits, thread crests may be sharpened or rounded.
- B3 = Medium galling, threads may be sharpened or rounded, a few deposits and smears, a few areas of metal removal.
- B4 = Heavy galling, threads sharpened or rounded, several metal deposits, smears or areas of metal removal, slivers.
- B5 = Threads mostly removed, much smearing, deposits, metal removal.

Note: Some bolts were given mixed codes i.e. B2/B3, to better describe them.

Washers
- W1 = Very little smearing or scoring.
- W2 = Moderate smearing or scoring.
- W3 = Heavy smearing or scoring

These codes, along with the associated bolt torque data and the associated parameters noted above, were entered into another database. As would be expected, the threads of those bolts with higher prevailing torques generally exhibited greater damage from galling, to the extent of complete thread removal from some, but not all, of the bolts with highest prevailing torques. Figures 4.1.3.2-3 through 4.1.3.2-6, are photographs of bolts coded B1, B3 and B5, respectively. Figure 4.1.3.2-4 does not reveal the degree of galling metal smearing and metal transfer that is seen with a microscope at 8X. Figures 4.1.3.2-5 and 4.1.3.2-6 show two different fasteners with similar B5 ratings. Note that the first B5 bolt has a below average unseating torque and a high prevailing torque while the second B5 bolt has a very high unseating torque and a moderate prevailing torque.

Most of the bolts examined have varying amounts of smears or deposits of aluminum on the grip (unthreaded) portion of their shank, suggesting that there was a hole misalignment between the clamp and the structure. Visual examination of a few clamps revealed varying amounts of burnishing in most of the holes. A visual examination of 21 shims revealed varying degrees of bolt thread contact in the holes, from no contact to grooves in one side of all three holes (as shown in figure 4.1.3.2-7). It was thought that this apparent misalignment may be contributing to the high unseating torque and high prevailing torque of some bolts upon removal. However, review of visual inspection notes and the torque data are inconclusive.

Tray Clamp Fastener Summary. It is believed that an unusually high percentage of bolts exhibited prevailing torques above the 30 in-lb maximum permitted for these self-locking inserts, especially for only two or possibly three installation/removal cycles. It is unknown how much contact with the clamp and shim holes and the relative softness of these bolts (140,000 psi versus more commonly used 160,000 psi ultimate tensile strength) may have contributed to this observation.

No clear correlation has been made between thread condition, washer condition, and unseating torques. No evidence of coldwelding was observed. All thread damage was consistent with galling damage.

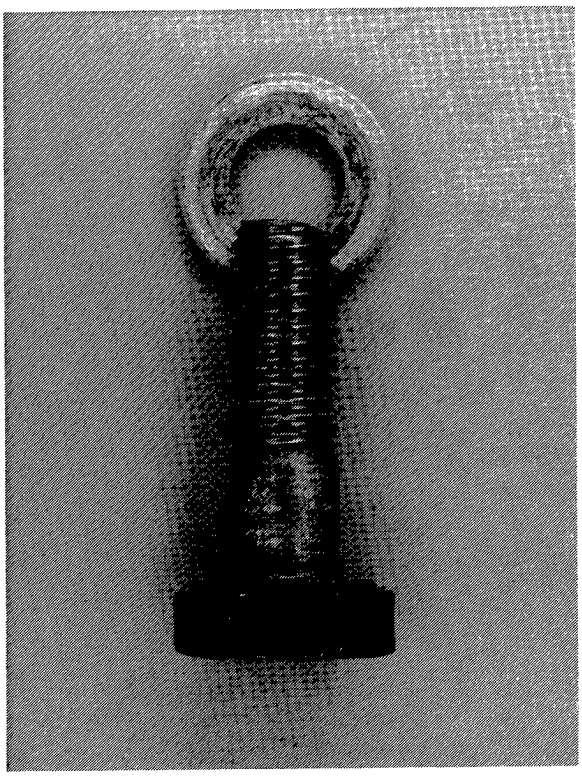

G4-6B 2.5X

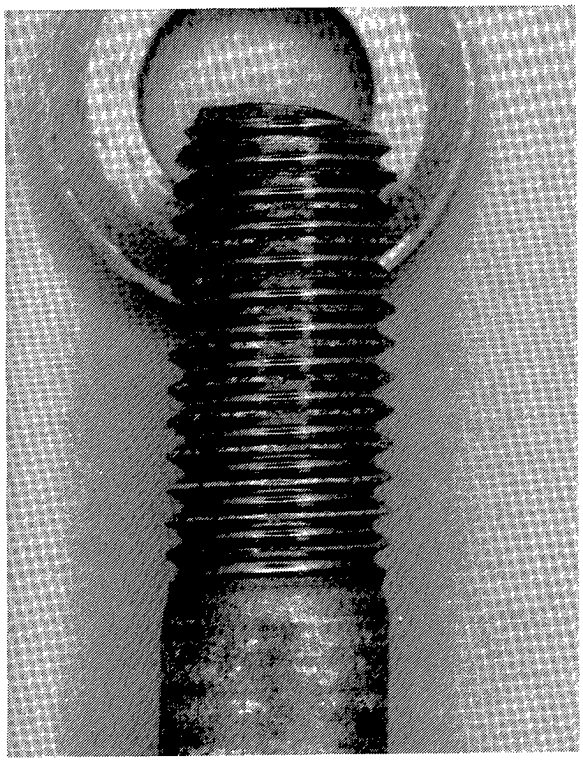

G4-6B 4.5X

Unseating torque = 70 in-lb

Prevailing torque = 15 in-lb

Figure 4.1.3.2-3. Tray Clamp Fastener With a "B1" Rating

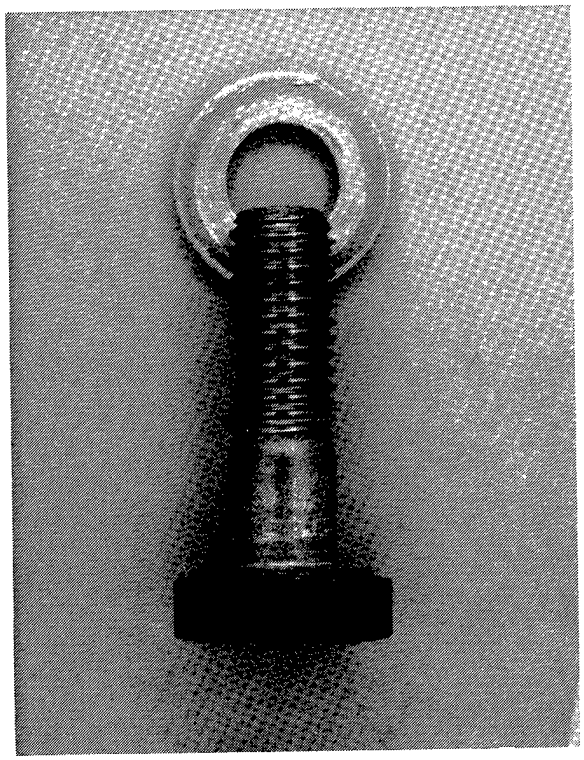

B3-8B 2.5X

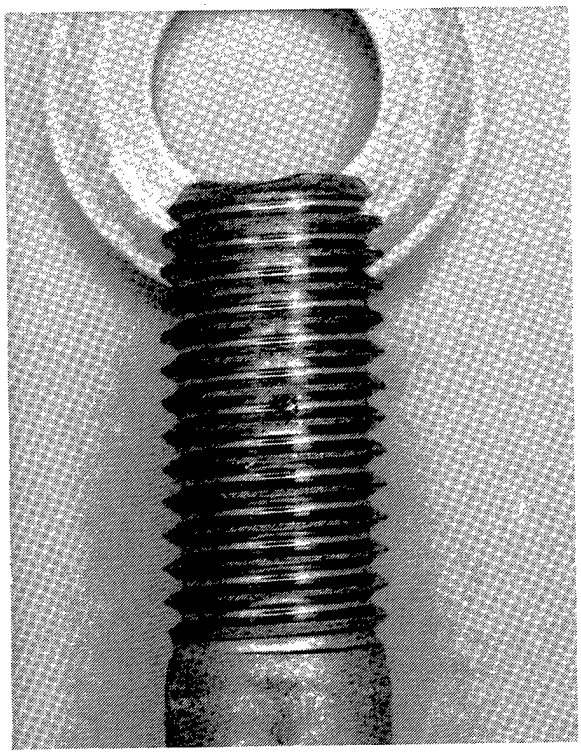

B3-8B 4.5X

Unseating torque = 74 in-lb

Prevailing torque = 7 in-lb

Figure 4.1.3.2-4. Tray Clamp Fastener With a "B3" Rating

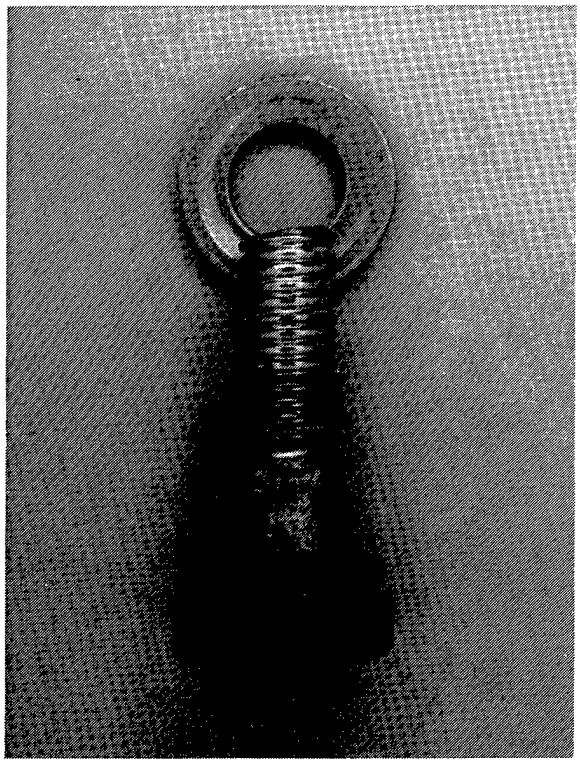

A4-1B 2.5X

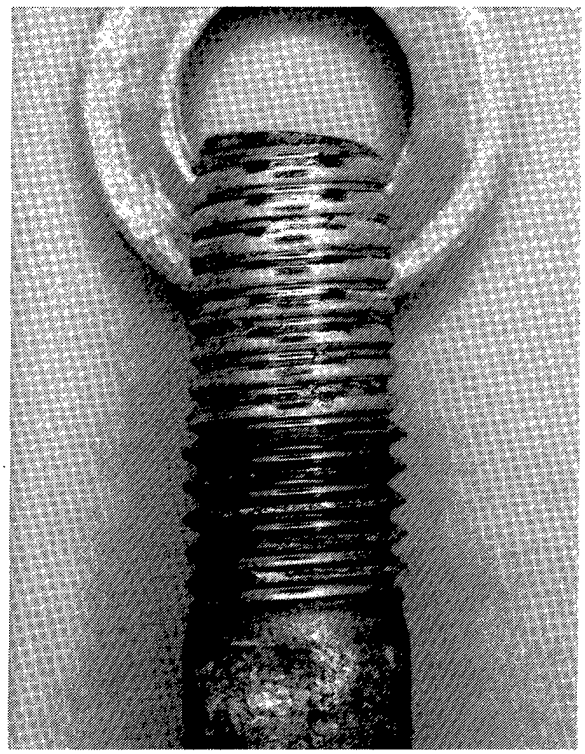

A4-1B 4.5X

Unseating torque = 57 in/lb

Prevailing torque = 60 in/lb

Figure 4.1.3.2-5. Tray Clamp Fastener With a "B5" Rating

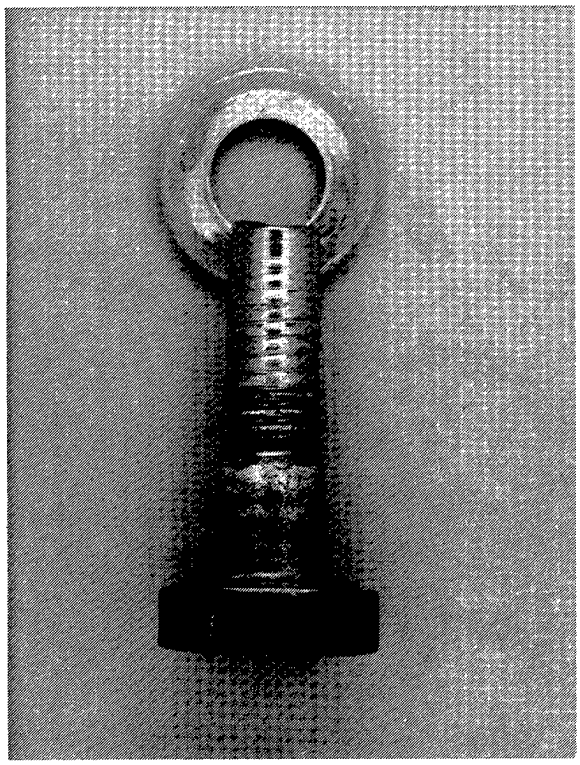

C1-8B 2.5X

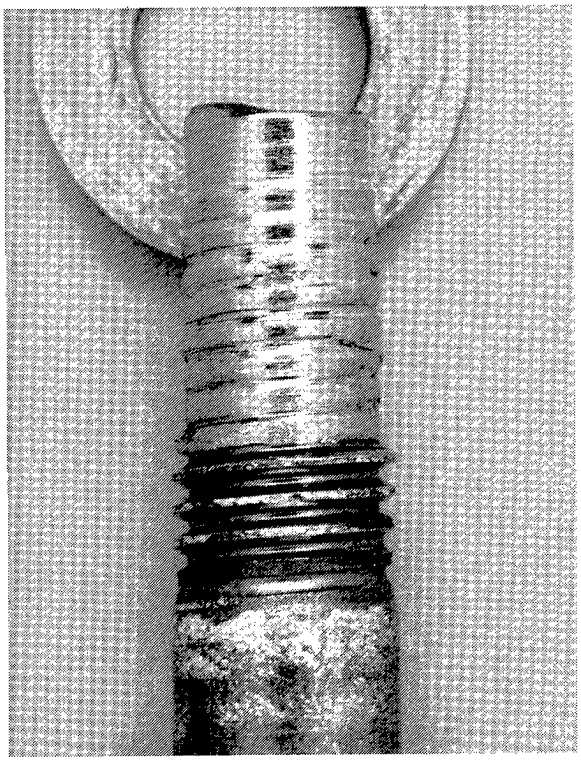

C1-8B 4.5X

Unseating torque = 190 in-lb

Prevailing torque = 35 in-lb

Figure 4.1.3.2-6. Tray Clamp Fastener With a "B5" Rating

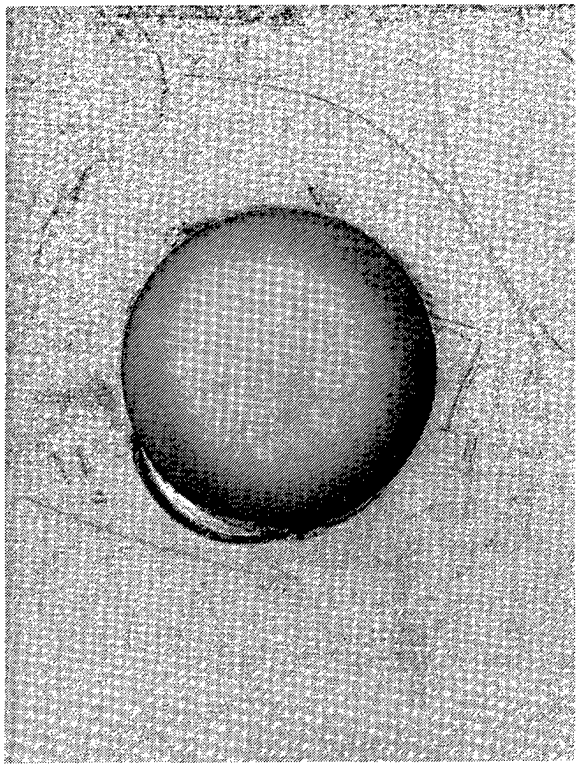

E1-3 2.5X

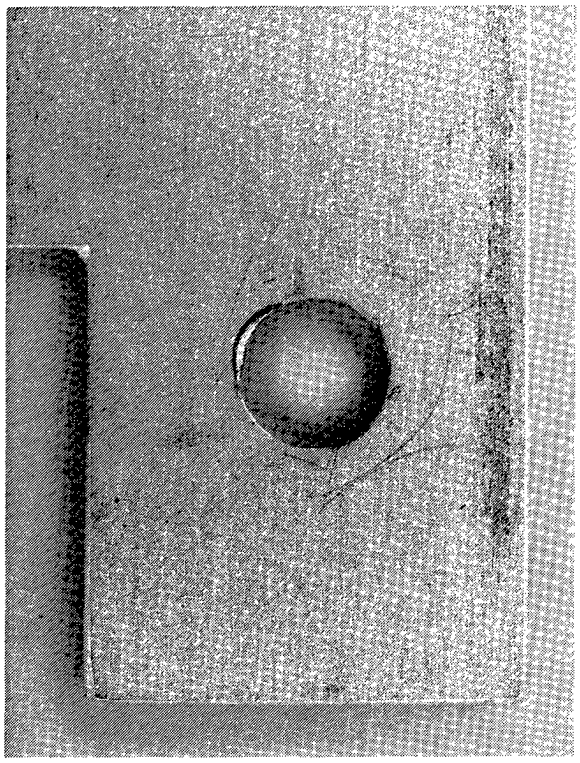

E1-3 5.5X

Unseating torque of bolt = 62 in-lb

Prevailing torque = Unknown

Figure 4.1.3.2-7. Tray Clamp Shim

4.1.3.3 Experimenter Fasteners

The LDEF Project Office suggested that experimenters use type 303 stainless steel bolts combined with self-locking nuts (AN, MS types). In fact, a wide variety of fastener assemblies and lubrication schemes were used (see appendix A for a list of fasteners flown on LDEF). This section discusses the results, to date, of the evaluation of experimenter fasteners.

Dr. Richard Vyhnal of Rockwell International, Tulsa Division reported severe difficulties with seizure and thread stripping during removal of fasteners used to locate graphite-reinforced composite test panels of the A0175 (trays A1 and A7) experiment. Typical fastener damage is shown in figure 4.1.3.3-1. This photo shows both a sheared fastener and a severely damaged nut plate. The fastener assemblies consisted of NAS1003-5A, passivated A286 CRES bolts installed into BACN10JN3CM, A286 CRES self-locking nut plates with AN960-C10L washers. It was reported that the nut plates had the original MoS_2 dri-film lubricant removed by acid stripping prior to installation because of concerns with possible volatilization and contamination while in orbit. The MoS_2 was then replaced with cetyl alcohol. Initial speculation was that the A286 fasteners may have coldwelded on orbit because of insufficient lubrication provided by the cetyl alcohol. However, testing and analysis of the fastener assemblies has shown that all removal difficulties were caused by galling which had begun during installation.

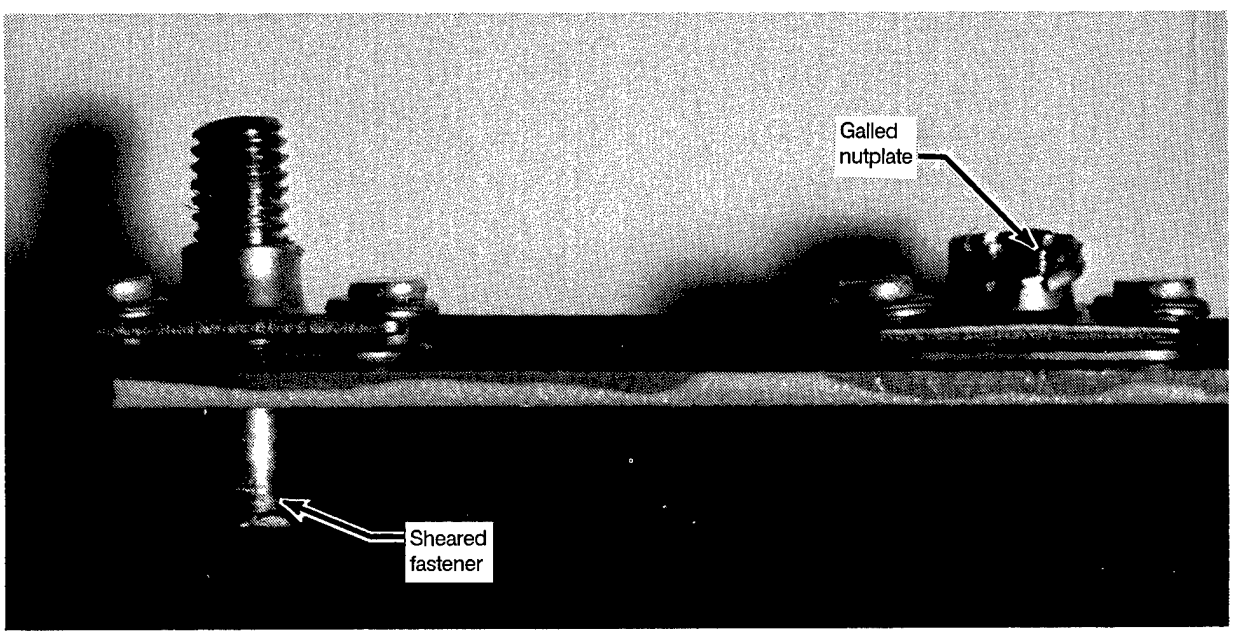

Figure 4.1.3.3-1. A0175 Sheared Fastener and Galled Nutplate

Unseating and prevailing torques were obtained for the majority of the fasteners by the Rockwell International group. Some fasteners were left undisturbed for analysis by the System SIG. Examination of tray A1 at Boeing revealed that some of the nut plates had not been stripped of their dri-film lubricant. As shown in figure 4.1.3.3-2, bolts removed (with difficulty) from acid-stripped nut plates displayed severe thread damage including stripped threads, whereas those removed from nut plates with intact lubrication were not damaged. Inspection of exposed threads on undisturbed bolts mated to acid-stripped nut plates indicated that the threads were damaged by galling during original installation. Threads on bolts inserted into nut plates with intact MoS_2 were undamaged. Cross-sections of undisturbed bolts, shown in figure 4.1.3.3-3, confirmed that thread damage occurred on installation. Fourier transform infrared spectroscopy (FTIR) found no post-flight traces of cetyl alcohol remaining in the threads of either the nutplates or the bolts.

Correlation of the Rockwell torque data with the lubrication conditions of the nut plates showed that the average prevailing torques associated with the MoS_2 nut plates was 15 in-lb as opposed to 64 in-lb for bare nut plates. The specification for these type of nutplates (with MoS_2) requires a prevailing torque range of 2 to 18 in-lbs. The average unseating torques were the same for both the MoS_2 and cetyl alcohol nut plates at 31 in-lb. If coldwelding had occurred in the cetyl alcohol nutplates, the unseating torques would have been substantially higher and there would have been a difference in unseating torque values between the MoS_2 and cetyl alcohol nutplates. The excessively high prevailing torques of the bolts using the cetyl alcohol nutplates is a result of the severe galling. Therefore, the removal difficulties are directly attributable to the lack of adequate lubrication and galling damage that occurred on original installation and the additional galling on removal. This resulted in seizure, thread stripping, and sheared bolts.

Additional Experiment Fastener Observations. Fasteners used to mount the tray cover plate on the NASA LeRC Ion Beam Textured & Coated Surfaces (Experiment S1003) were investigated by Curtis Stidham. Breaking and running torques were measured for each of 56 No.9-32, 101 deg flathead CRES screws. The screws were 1/4 in long with a nylon insert locking feature. The breaking torque mean value was 23 in-lb with a standard deviation of 3 in-lb. The minimum observed breaking torque was 11 in-lb and approximately 20% of the values were outside + one standard deviation. The prevailing torques ranged from 2 to 5 in-lb for all fasteners except one that had a prevailing torque of 10 in-lb. No anomalies were noted with the exception of one screw that had pulled down through the tray cover plate. The low prevailing torques indicate no galling had occurred. The self-lubricating behavior of the nylon locking insert apparently precluded galling damage upon installation or removal.

4.1.3.4 Velcro

Velcro was used to attach the flexible heat shields used on the FRECOPA canisters (sec. 4.1.4.2). These heat shields consisted of Teflon glass fabric and Mylar sheet aluminized on the inside surface. Velcro was stitched to the heats shield with NOMEX thread. This thread, which was directly exposed, turned yellow. Tensile testing of the thread showed a 10% reduction. The mating side of the Velcro was

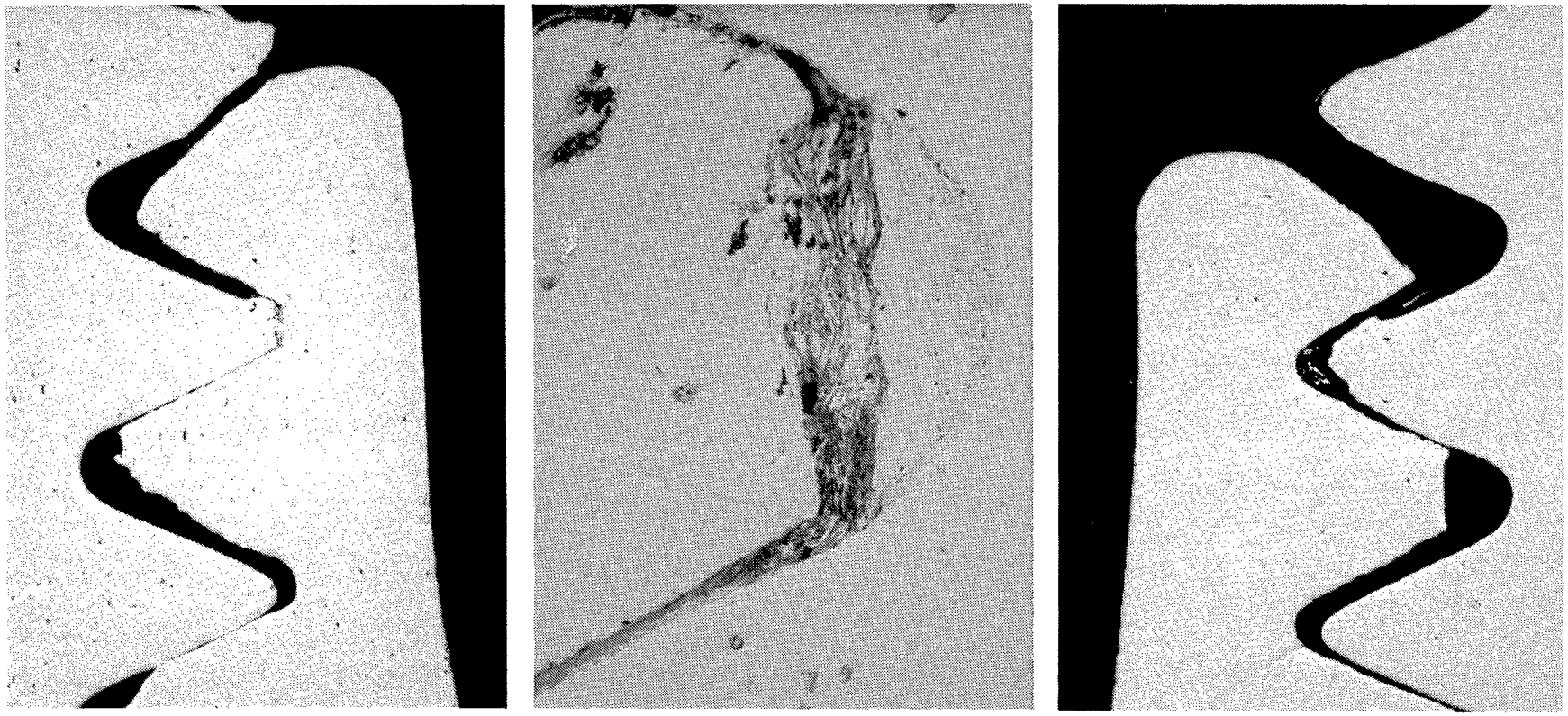

0.020 in
No MoS2

0.002 in
No MoS2

0.020 in
MoS2

Figure 4.1.3.3-3. (Left and Center) – Galling Damage of Bolt Threads in Nut Plate Without MoS2; (Right) – Normal, Undamaged Threads in Nut Plate With Intact MoS2

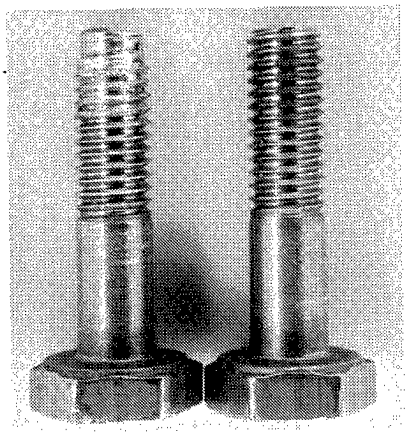

No MoS2 MoS2

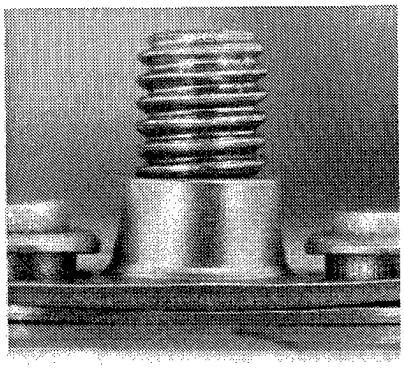

No MoS2

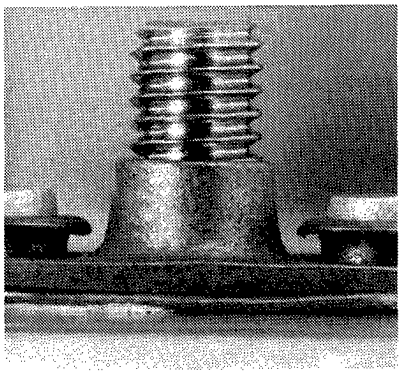

MoS2

Figure 4.1.3.3-2. (Top) – Comparison of Thread Conditions of AO175 Tray Bolts Removed from Nut Plates. Undisturbed Assemblies Were Cross-Sectioned as Shown in Figure 4.1.3.3-3. Note Thread Galling Damage on Fastener That Had MoS2 Removed (Center).

bonded to the tray structure using EC2216 adhesive. Traces of the adhesive, although cleaned during preflight assembly, appeared due to the long term UV exposure. The Velcro proved to be a successful method to fasten the heat shields. Qualitative tests carried out during disassembly showed a high level of separation resistance. Quantitative tests are currently in progress (ref. 36).

Velcro was also used to fasten the 3 ft by 4 ft silverized Teflon thermal blankets used as the exterior surface on Experiment A0178. This experiment consisted of 16 trays located throughout LDEF. Approximately 54 one-inch strips of Velcro were used for each thermal blanket. with one surface of the Velcro bonded to the backside of the blanket and the other surface bonded to aluminum surfaces on the tray. The experimenter responsible for the experiment deintegration reported that the Velcro seemed to have retained it's pre-flight disassembly parameters.

4.1.3.5 Coldwelding

Spacecraft mechanisms are required to operate in the high vacuum of space for extended periods of time. A significant concern to the designer is the possibility of metal-to-metal coldwelding or significant increases in friction. Coldwelding is defined as the solid state metallic bonding between atoms on opposing surface layers of similar or dissimilar metals. LDEF provided hardware that had been exposed to the LEO environment for 69 months and contributed greatly to our understanding of whether coldwelding is a significant design consideration. However, it is also important to note that LDEF was a "static" satellite and possessed minimal mechanical hardware that was in motion while on orbit.

4.1.3.5.1 LDEF Coldwelding Experiment

The only coldwelding-related experiment flown on LDEF was the French Experiment A0138-10 titled "Microwelding of Various Metallic Materials" (ref. 33) The materials, surface treatments, and lubricants evaluated are actually used on spacecraft for sliding electrical contacts, antennas, and deployable solar panels. Therefore, these material combinations were selected so coldwelding would not occur. The materials tested included Al alloys, Cu alloys, Ti alloys, stainless steel, Cu-Be alloy, silver alloys, and palladium. Selected combinations of materials were chromic acid anodized or sulfuric acid anodized. Other combinations used MoS_2 and Molykote Z lubricants. Specimens were 1 in-diameter washers and were alkaline cleaned and then stacked into eight columns of six pairs each. All pairs of each column were loaded together by use of Belleville disc springs. Contact pressures ranged from 25 to 135 MPa. Ground-based control specimens were kept under vacuum for the 69 months that LDEF was in orbit. The control specimens were selected for possessing high solubility and consisted of various combinations of gold, silver, and chromium deposited onto aluminum washers.

This was a rather simple experiment with no active monitoring of data and no sliding motion between specimens. All flight and control specimens have been analyzed and no coldwelding occurred. The experimenters believe that, because this was a static experiment, there was no removal of the oxide layer between the mating pairs. This oxide layer kept the pairs from coldwelding.

4.1.3.5.2 Coldwelding Summary

To date, no instances of coldwelding have been found on LDEF during the deintegration and subsequent testing and analysis of hardware. This finding indicated a need to review previous on-orbit coldwelding experiments and on-orbit spacecraft anomalies to determine whether the absence of coldwelding on LDEF was to be expected (ref. 34). Coldwelding can occur between atomically clean metal surfaces when carefully prepared in a vacuum chamber on Earth. The question is whether coldwelding will occur in on-orbit service conditions.

Coldwelding is defined as the solid state metallic bonding between atoms on opposing surface layers of similar or dissimilar metals. Contamination-free surfaces are required for bonding to occur. The presence of lubricants or naturally occurring

oxides will effectively prevent adhesion. These oxides or lubricants could be removed, pre-flight or on-orbit, by fastener installation/removal, during sliding contact, thermal expansion and contraction, or if located on the spacecraft exterior surface and directly exposed to space environment. If the oxide layer is removed on-orbit, it will reform very slowly, if at all, in the vacuum of space. The susceptibility of materials to coldweld is also dependent on compressive stresses between mating surfaces, temperature, abrasion, and time. In extreme cases, the contamination films on metal surfaces can be penetrated under unusually high contact stresses, resulting in coldwelding of asperity contacts. The susceptibility for dissimilar metals to coldweld is enhanced by like crystal structures, similar atom sizes, or mutual solubility.

Galling is defined as a wear condition whereby excessive friction between high spots (asperities) results in localized welding, with subsequent metal tearout or metal transfer and further roughing of the metal surfaces. The symptoms or results of seizure are the same independent of whether they were caused by galling or coldwelding. In both cases, photomicrographs of a cross section of the seized joint would show solid-state metallic bonding between the mating surfaces. The difference is that coldwelding is caused by contamination-free surfaces, resulting in metal adhesion where as galling is caused by excessive friction (due to poor tolerances, insufficient or improper lubrication, or improper material selection) between mating surface asperities, resulting in metal adhesion. Another important distinction is if seizure could have developed under terrestrial operating conditions, galling not coldwelding, is the cause of the seizure. An example of this is a loss of lubrication leading to a bearing failure caused by galling between mating surfaces. This failure would have also occurred in space, but not because of coldwelding.

The results of this investigation into previous on-orbit coldwelding experiences, described in detail in reference 33, shows that there have been no documented cases of a significant on-orbit spacecraft coldwelding event occurring on U.S. spacecraft. Several anomalies have been caused by seizure of mechanisms but these were due to vibration-caused fretting or galling caused by loss of lubricant. There have been a few documented cases of seizure occurring during on-orbit coldwelding experiments. However, the seized materials had been selected for the experiment because of their susceptibility to coldweld. This susceptibility was increased by effective pre-flight cleanliness procedures.

Metal surfaces exposed to only the vacuum of the space environment are not likely to become sufficiently clean enough for coldwelding to occur in a practical mission lifetime, unless the rate of removal of surface films is accelerated by some form of electrical or mechanical means. Oxide, lubricant, and contamination removal/deposition rates for metals on exterior surfaces of spacecraft are a more complex issue due to effects of atomic oxygen and/or UV radiation exposure. Many factors influence these removal/deposition rates including location on spacecraft, shadowing by adjacent hardware, spacecraft altitude, proximity to outgassing by nearby materials, and material selection.

If contact is made between two mating surfaces in a preflight environment without any coldwelding occurring and these surfaces are left undisturbed during the mission, no on-orbit coldwelding will occur. This applies, in particular, to fastener

assemblies. If the correct materials, tolerances, and lubricants are used such that galling does not develop during pre-flight fastener installation or removal, or during the launch environment, and the fastener remains undisturbed while on-orbit, no difficulty will be encountered during post-flight removal. This also applies to an on-orbit replacement. No difficulty due to coldwelding will be encountered if a non-galled fastener assembly is removed on orbit. However, repeated on-orbit removals and installations will require the use of appropriate lubrication schemes and the correct design of self-locking nuts to ensure that no thread or lubricant damage occurs. Even though there have been no documented on-orbit coldwelding related failures, precautions still should be taken to ensure that not only does coldwelding not occur in the space environment, but that seizure does not occur in the pre-launch or launch environment.

4.1.4 Mechanisms

4.1.4.1 Environment Exposure Control Canisters (EECC)

Five EECCs were flown on LDEF. These canisters were used by individual experimenters for controlled exposure studies of the effects of LEO on various structural, thermal control, and optical materials. Figure 4.1.4-1 shows the front and back side of the S0010 EECC as mounted in the B9 tray. The EECC is essentially a sealed drawer in which small samples were mounted for controlled space exposure; typically the canisters were programmed to open 10 days after deployment and close 1 week prior to the originally anticipated retrieval of LDEF (day 297). The drawer is opened by a screw drive actuator driven by an 28V dc electric motor. The drawer is sealed by a butyl rubber seal.

Systems SIG personnel participated in the opening of the M0006, S0010, and the two M0003 canisters. Technical support was provided for opening of the S1002 canister. Initial canister pressures just prior to opening, canister leak rates, internal gas samples, drawer opening times, and drive motor currents were obtained for most of the canisters. Only the drawer opening time, and motor currents were obtained for the S1002 canister. A portable gas sampling manifold with pressure gages and a sorption vacuum pump was utilized for the gas measurements. A strip chart recorder monitoring the voltage drop across a 0.25-ohm resistance in series with the motor was employed to record the drive currents supplied by the EECC ground support equipment.

Data obtained during the canister openings is summarized in table 4.1.4-I. The initial pressure of the M0006 canister was not obtained because the EECC purge valve loosened and leaked during hook up of the gas sampling manifold. However, it was noted that the canister was below atmospheric pressure, which is consistent with the measured leak rate and length of time after LDEF retrieval. The S1002 experimenters reported that a pressure differential between the canister and atmosphere was not apparent at the time of opening. The typical pre-flight leak rates for the canisters were around 1.3 torr/day. The post-flight leak rates for the M0006 and M0003/D4 canisters located at or near the trailing edge are comparable to pre-flight values. The higher leak rates for the S0010 and M0003/D8 canisters flown at or near the leading edge are suggestive of the differences between atomic oxygen exposure levels and possible corresponding damage to or contamination of the drawer seals. However, the seals only saw atomic oxygen for the first 9 months of the mission. The seal evaluation (discussed further in sec. 4.1.8) has not been completed.

Typical drawer opening time was around 17 min. which was approximately the same as preflight values. Motor currents oscillated between the limits shown in table 4.1.4-1 during each revolution of the drive screw. This behavior is illustrated in figure 4.1.4-2 where the strip chart traces corresponding to steady run opening currents are compared for the M0006 and S0010 canisters. These oscillations are caused by cyclic variations in alignment of the drive shaft and variations in the friction proprieties of the lubricant. The longer opening time of the M0006 canister and higher-than-typical current draw are consistent with noise indications of higher torque loading of the motor noted during opening. Damage to the drive screw (warping) or to its MoS_2

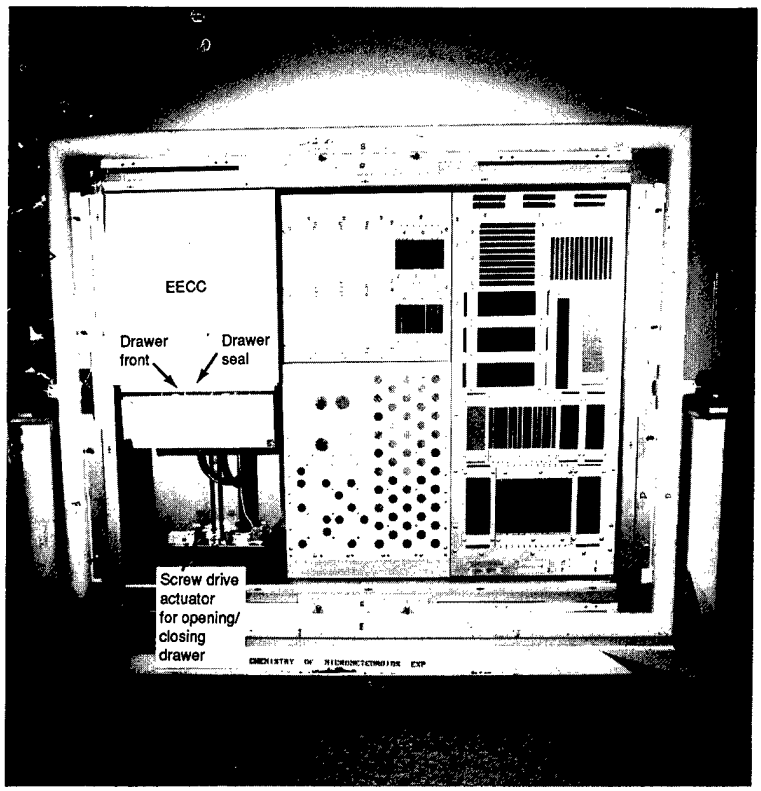

Frontside

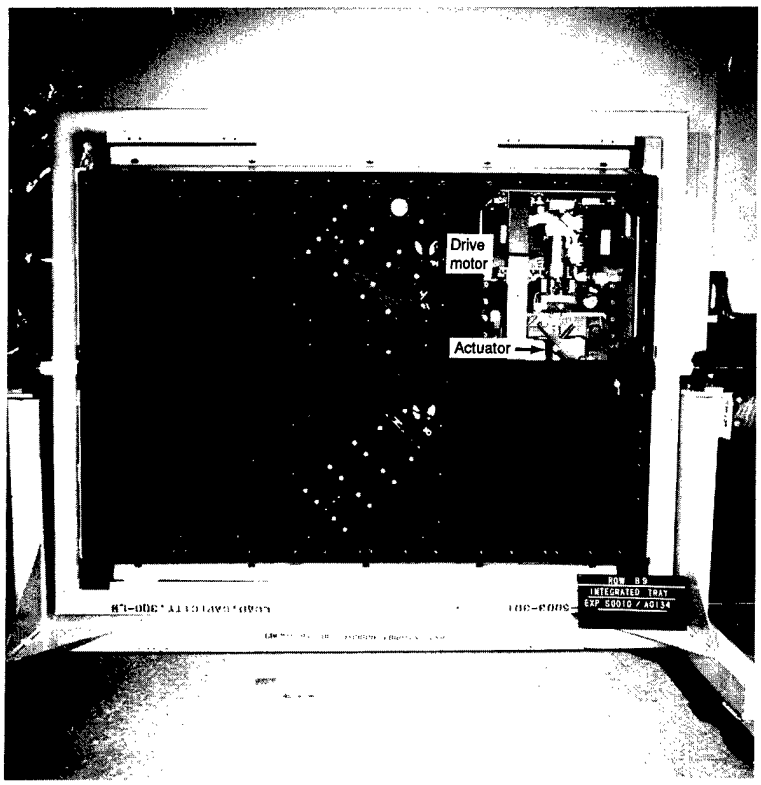

Backside

Figure 4.1.4.1-1. S0010 EECC as Mounted in Tray B9

Table 4.1.4.1-1. EECC Performance Data

Experiment number	LDEF location	Initial pressure TORR	Leak rate TORR/day	Opening time minutes	Motor run current mA	Days EECC opened after LDEF returned to earth
M0006 (Air Force) S/N 003	C3 (trailing)	<1 atm	2.7	19.5	130-230	60
S0010 (LaRC/SLEMP) S/N 001	B9 (leading)	642	12.3	16.9	110-120	102
S1002 (West German) S/N 002	E3 (trailing)	1 atm	—	16.8	150-180	122
M0003 (Aerospace) S/N 004	D8 (off-leading)	1 atm	12.6	**	**	149
M0003 (Aerospace) S/N 005	D4 (off-trailing)	282	* (1.9)	15.4	150-190	150

*: Purge valve would not reseal after initial opening. Calculated leak rate based on initial pressure is shown in parentheses

**: Opening time and motor current not obtained due to ground support equipment problem

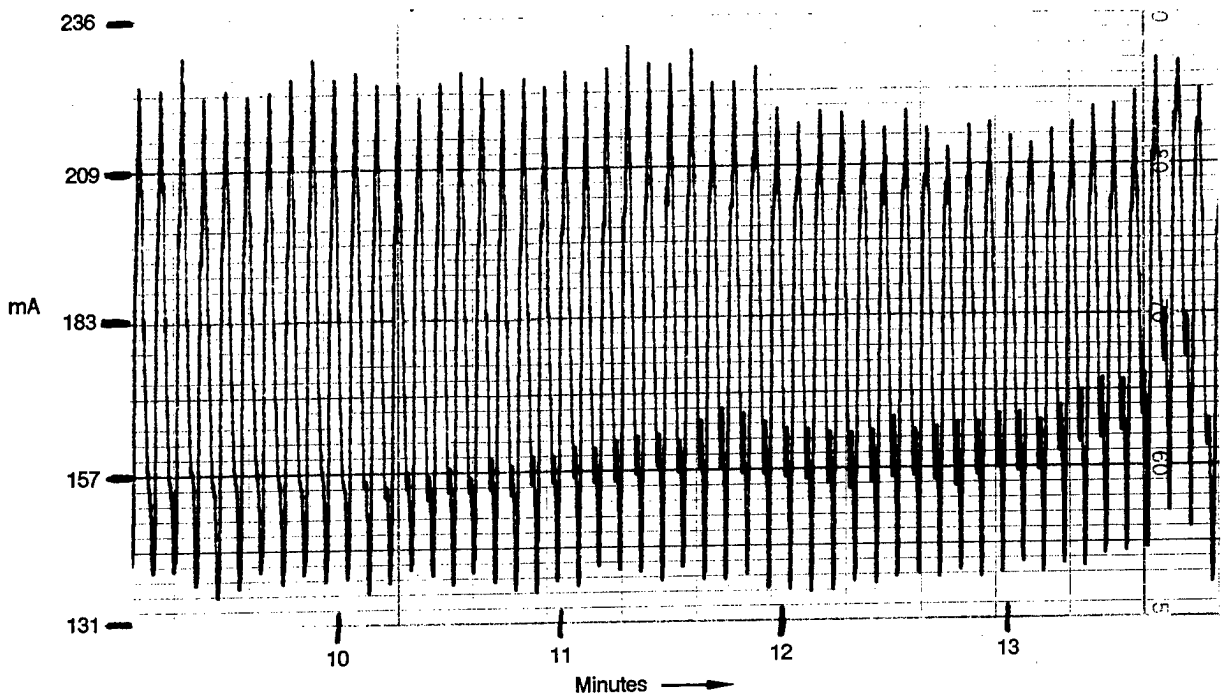

M0006 Canister

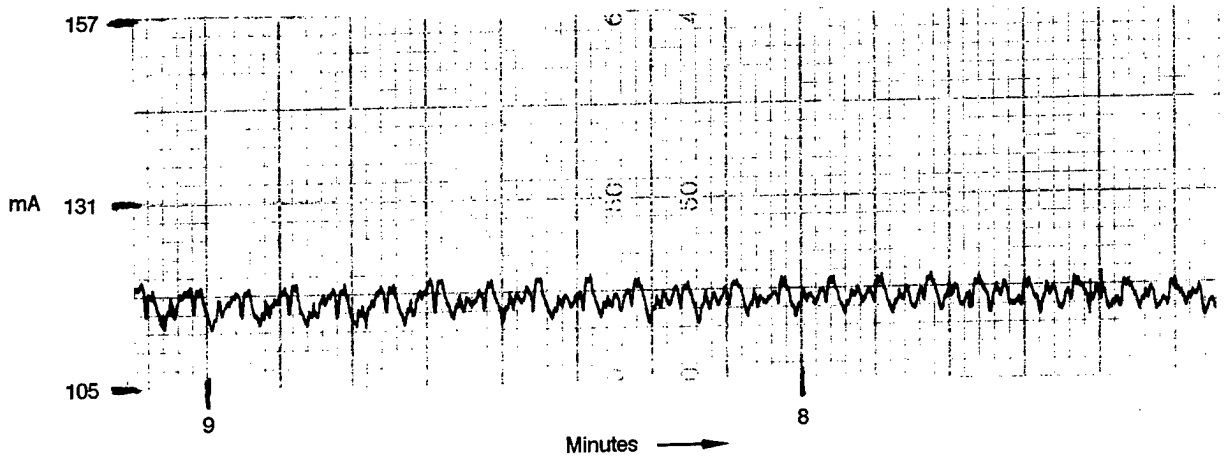

S0010 Canister

Figure 4.1.4.1-2. Motor Current Traces During Initial Opening of M0006 and S0010 EECCs

dri-film lubrication are possible causes to account for the degraded performance. The low motor current of the S0010 canister corresponded with observations of a smooth and steady drawer opening. The S0010 canister was the prototype EECC and, as such, its good performance is likely the result of "breaking in" of the mechanism during extensive operation during development testing.

The S1002 EECC, which was located on the trailing edge, was received by the System SIG for further examination. No anomalies were noted other than the peak cyclic motor current during opening had increased from 180 mA, as reported by the experimenters, to 230 mA. Possible deterioration of the MoS_2 dri-lube on the drive screw by re-exposure to atmospheric humidity could be a cause. The MoS_2-coated Belleville springs, used to maintain controlled pressure on the drawer seal, were also examined along with the drawer seal. The results are discussed in section 4.1.8.

The other four EECCs have not yet undergone component evaluation. It is hoped that a joint test program will be developed within the EECC community to maximize the amount of information learned.

4.1.4.2 French Cooperative Passive Payload (FRECOPA) Canisters

Because of the extended LDEF mission, CNES set up a team to analyse the FRECOPA canisters. Work started by developing a set of procedures for disassembling the various system components. Part of this disassembly (batteries and heat shields) took place at KSC. All remainng activites took place at the appropriate CNES departments.

The FRECOPA experiment canisters performed the same function as the EECCs but, as seen in figure 4.1.4.2-1, opened and closed like clamshells to control LEO exposure of passive experiment samples. Three FRECOPA boxes were flown on the trailing edge in Tray B3 (trailing edge). CNES formed a working group of experts to examine the box system elements in detail. Durin (ref. 36) of CNES has reported the details of their investigation. The canisters are aluminum alloy and a butyl rubber seal was bonded to one of the canister face-plates for vacuum tightness. An aluminum structure supports the canisters and the open/close mechanisms. The opening mechanism consists of one electric motor driving two screws by means of a double six-stage reduction gear chain. Four locking arms with DELRIN rollers provide the sealing force between the canister halves.

The FRECOPA boxes displayed normal behavior during observations at KSC during LDEF's deintegration. The status indicators confirmed that the boxes had opened and closed while on orbit. Later testing at CNES revealed no performance anomalies. Minor impacts and erosion effects did not cause any functional damage. The postflight motor drive currents were the same as noted during preflight testing. Further testing of the drive system is planned.

The DELRIN rollers displayed some erosion and the results of thermal effects. DELRIN is a material made from a polyacetal matrix embedded with short Teflon fibers. The area exposed on the pressure and guide rollers changed from a preflight condition of brown and shiny to white and dull. Testing and analysis determined that

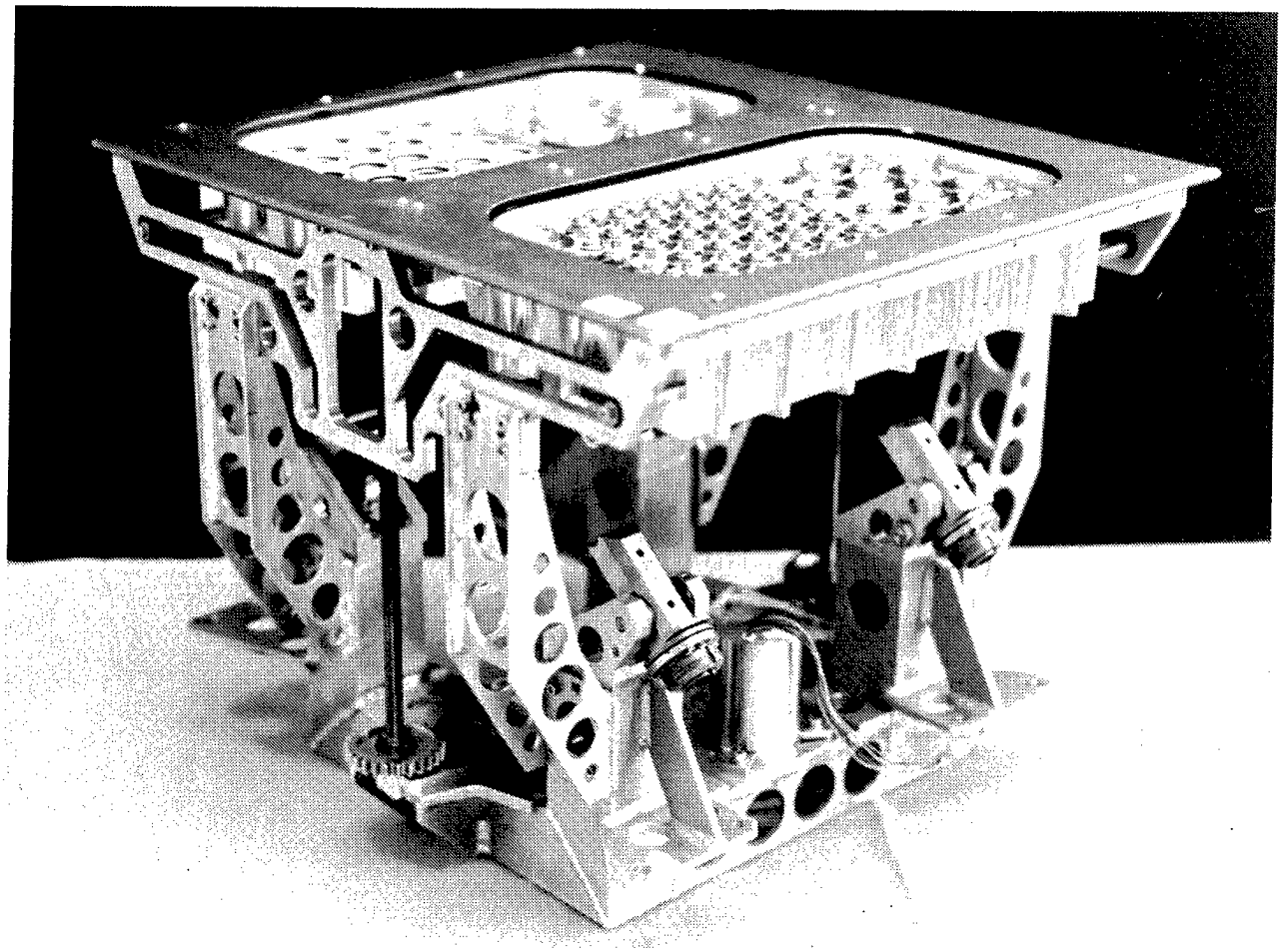

Figure 4.1.4.2-1. FRECOPA Cannister

this change was a physical change. The matrix and a portion of the Teflon fibers were exposed to thermal and vacuum conditions which led to fracture of the molecular chains and erosion. Therefore, it was determined that DELRIN is particularly sensitive to UV and its use in unprotected mechanical assemblies could pose design concerns.

All three canisters were maintaining vacuum at opening. Prior to flight, the initial internal pressure was 0.5 torr, whereas the measured postflight pressures were 1.2, 5.0, and 0.04 torr for the three canisters. Durin reported that the first two canisters contained polymeric materials and suggested that the relatively high pressures were the result of outgassing. Additional studies are required to evaluate the contribution from seal leakage but the data for the last canister indicates that its butyl rubber seals performed particularly well. Aging studies of the butyl seals are underway at CNES.

4.1.4.3 Experimenter Mechanisms

Solenoids Valves

The Variable Conductance Heat Pipe Experiment (A0076) used two latching solenoid valves to initiate the operation of the heat pipes once on orbit. Test data showed the valves successfully opened in the first few days after deployment, as programmed. During deintegration both valves were successfully energized. No additional postflight testing is planned. As a sidenote, these valves were initially installed on the second Skylab which was never used. This Skylab was being stored at the Smithsonian Air and Space Museum in Washington D.C. Arrangements were made and the valves were removed, cleaned, and integrated into the A0076 experiment.

4.1.5 Magnetically Anchored Viscous Damper

Located on the centerline of the space end internal structure, the viscous damper provided attitude stabilization of LDEF from oscillations resulting from deployment. The construction and theory of operation of the magnetically anchored viscous damper are shown schematically in figures 4.1.5-1 and -2. The damper consists of an 6061-T6 aluminum inner sphere filled with helium and containing a permanent magnet and bellows and an outer aluminum sphere having a pyrolytic graphite liner for diamagnetic centering, i.e., the graphite is repelled by the inner magnet, thus centering the outer sphere about the inner when in a zero-g environment. The space between the spheres is filled with silicone oil having a viscosity selected to provide the required damping. The bellows allows for thermal expansion and contraction of the silicone and helium gas. The mechanism of damping depends on the relative rate of rotation of the inner sphere, which is aligned with the Earth's magnetic field, and the outer sphere which is rigidly attached to the LDEF structure.

Results of postflight testing by the manufacturer, General Electric Astro Space Division, are documented in a report prepared for Lockheed Engineering and Sciences Company (ref. 35). All evidence indicates that the damper performed flawlessly over the almost 6 year flight even though the design life was 1 year. As described in the reference report, the damper appearance and performance was the same as preflight. There was no change in magnetic dipole or fluid viscosity. Infrared spectrography results showed no change in the silicone oil. However, there was a small amount of particulate matter in the oil, primarily graphite and aluminum. The amount and size of the particles was small and did not affect the performance of the damper. Inner sphere movement tests correlated well with preflight data and verified no change in damping or damage to the graphite liner. Radiographic examination revealed no voids in the fluid, no leakage into the inner sphere, nor any damage to the magnet. There was no evidence of damage to nylon spacer balls between the spheres or to either the inner or outer sphere weld joints.

It was concluded that the damper suffered no discernible degradation from long-duration space exposure and that it can be flown again after issues concerning possible limited bellows life are addressed. The original design life of 10,000 cycles for the bellows maybe increased to 100,000 based on new manufacturer ratings. The damper was refilled with silicone oil and returned, flight ready, to the LDEF Project Office at NASA LaRC.

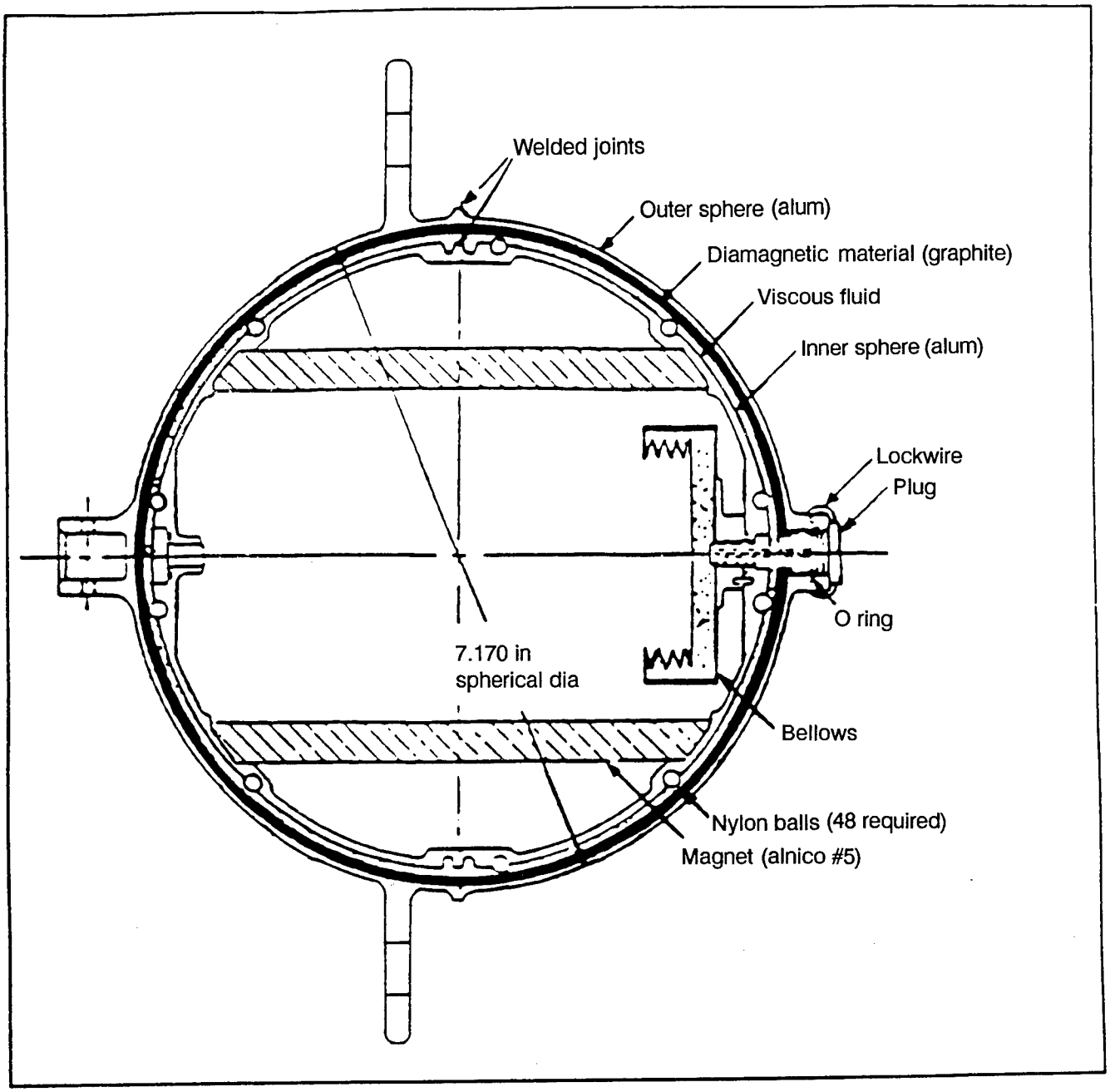

Magnetically Anchored Viscous Fluid Damper

Figure 4.1.5-1. LDEF Damper Configuration

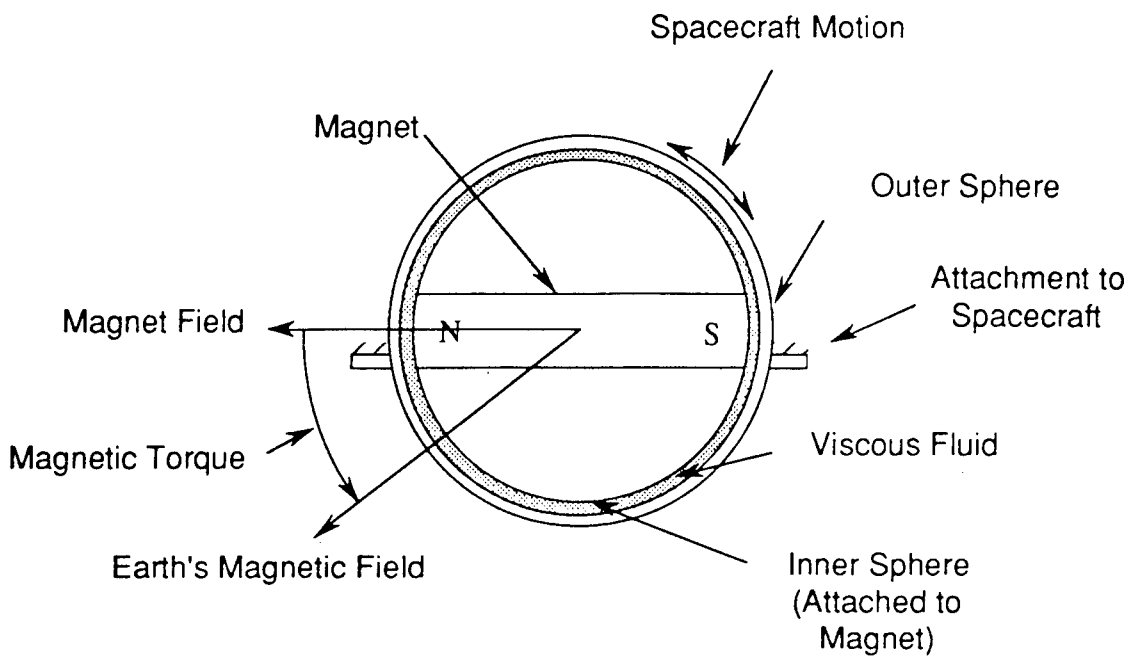

- Magnet in the inner sphere aligns with Earth's magnetic field and anchors magnet
- Spacecraft is attached to outer sphere and oscillates in gravity gradient mode
- Relative motion between spacecraft and magnet is damped by viscous fluid
- Spacecraft oscillations settle over time

Figure 4.1.5-2. Magnetically Anchored Viscous Damper—Theory of Operation

4.1.6 Grapples

Both the rigidize-sensing (active) and the flight-releasable (passive) grapple fixtures are undergoing post-flight evaluation to provide information about their on-orbit performance. The rigidize-sensing grapple, shown in figure 4.1.6-1, was designed to activate the LDEF experiment initiate system (EIS) on or off via the RMS with the LDEF still in the shuttle bay. The flight-releasable grapple was used to deploy and retrieve LDEF via the RMS. Both grapples performed as designed during deployment and the passive grapple performed as designed during the retrieval of LDEF. Due to the extended mission length and consequent uncertain state of batteries, and the desire not to disturb the final state of certain experiments, it was decided not to reset the systems. Therefore, retrieval the rigidize-sensing grapple was not used during retrieval.

Both grapple fixtures were returned to JSC for postflight examination. Tungsten-disulfide lubricant and paint samples were evaluated. Section 4.1.8 discusses the result of the testing and analysis of the tungsten-disulfide. All surfaces have been examined by the Micrometeoroid and Debris SIG. Four of the electrical/mechanical switches (used as electrical interface between the rigidize-sensing grapple and the experiment initiate system) were removed and sent to Micro Switch (original equipment manufacturer) for non-destructive testing. Comparison of post flight and pre flight results indicated insignificant changes and all four switches (part number 9HM25-REL-PGM) were still within specifications. The grapples are currently at the original equipment manufacturer, Spar Aerospace, for possible functional testing of the rigidize-sensing grapple.

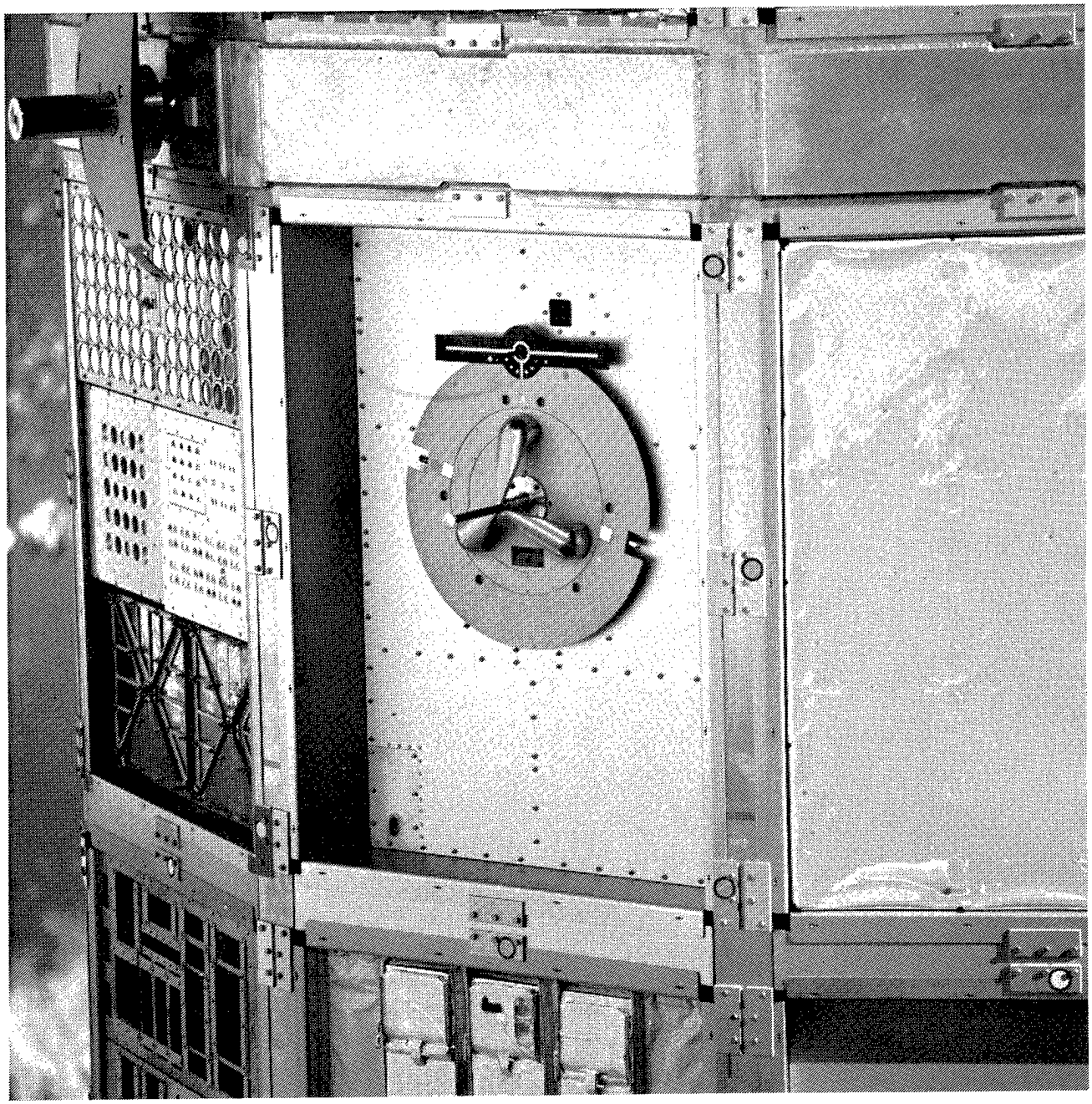

Figure 4.1.6-1. On-Orbit Photograph of the Rigidize Sensing (Active) Grapple

4.1.7 Lubricants and Greases

A variety of lubricants and greases were flown on LDEF. With the exception of the samples from experiment M0003, all lubricants were components of functioning hardware and not the principal item of the investigation. The current status and test results of all lubricants flown on LDEF, listed in table 4.1.7-1, will be discussed in this section. The majority of the lubricants were shielded from direct exposure to space and performed their design function as anticipated. However, a MoS_2 dry film lubricant exposed to the trailing edge environment completely disappeared.

Cetyl alcohol and a molybdenum disulfide (MoS_2) dry film lubricant were used on fastener assemblies on experiment A0175. Either the dry film lubricant or cetyl alcohol was used on the nutplates. Postflight inspection of the fasteners installed into nutplates with MoS_2 dry film lubricant showed no damage to the threads. Fasteners installed without the lubricant and using only cetyl alcohol sustained substantial damage to the fasteners and nutplates. Postflight FTIR examination of the nutplates found no remaining traces of cetyl alcohol. Section 4.1.3.3 discusses these results in greater detail.

MIL-L-23398 air-cured solid film lubricant was used on several places on the five EECCs. The lubricant was applied to the Belleville washers, drive shafts, and linkages. Visual examination of a EECC located on the trailing edge revealed no evidence of abnormal wear or coating degradation on the surfaces not exposed to UV. Portions of the drive shaft exposed to UV exhibited slight discoloration. Further testing is planned. We plan to compare these results with those being generated by the experimenters possessing the other four EECCs which were located in a various positions on LDEF. Section 4.1.4 contains more information on the EECCs.

Tungsten disulfide (WS_2) dry film lubricant was used as the lubricant on both the rigidize sensing and flight-releasable grapple shafts. This lubricant was used to ensure successful release of the grapple from the RMS during initiation of the active experiments, deployment, and retrieval of LDEF. The lubricant performed as designed. Because the tray was located 22 deg. to the ram, the base of the grapple saw an atomic oxygen exposure of 22E+17 atoms/cm^2. However, because the shaft extended 3 to 4 inches beyond the LDEF surface, portions of the shaft (and the teflon tip) were exposed to a much greater fluence. During postflight analysis at Johnson Space Center, samples of WS_2 were removed from both grapple shafts for SEM and EDX analysis. This analysis showed the bulk lubricant to be intact with no discernible difference between the lubricant exposed on the ram surfaces of the shafts and the lubricant exposed on the trailing edges. No surface analysis was performed. To date, the tribological properties of the WS_2 have not been determined.

Table 4.1.7-1. Lubricants and Greases Flown on LDEF

VENDOR	MATERIAL	DESCRIPTION	EXPERIMENT	TRAY
	Cetyl Alcohol		A0175	A1, A7
	MIL-L-23398	Air cured solid film lubricant	EECC'S	
	MoS_2		A0138 A0175	A1 A7
	WS_2		GRAPPLE	C1
Apiezon	H	Petroleum based thermal grease	A0076	F9
Apiezon	L	Petroleum based lubricant	A0180	D12
Apiezon	T	Petroleum based lubricant	M0001	H3, H12
Ball Aerospace Systems Group	VacKote 18.07	MoS_2 with polyimide binder	S0069	A9
Ball Aerospace Systems Group	VacKote 21207	MoS_2	S0069	A9
Ball Brothers	44177	Hydrocarbon oil with lead naphthanate and clay thickener	EECC'S	VARIOUS
Castrol	Braycote 601	PTFE filled perfluoronated polyether lubricant	A0187	A3
Dow Corning	340	Silicone heat sink compound	A0133 M0001	H7 H3, H12
Dow Corning	1102	Mineral oil filled with Bentonite and MoS_2	S1001	F12, H1
Dow Corning	Molykote Z	MoS_2 powder	A0138	
DuPont	Vespel 21	Graphite filled polyimide	M0003	D3
DuPont	Vespel	Polyimide	A0147 A0187-1 S1002	B8, G12 E3
Everlube	620	Heat cured, bonded dry film lubricant	M0003	D3
Exxon	Andok C	Channeling petroleum grease	S0069	A9
Mobil	Grease 28	Nonchanneling silicone grease	MTM'S	various
New Hampshire Ball Bearings	PTFE coated Nomex liner	Rod end bearings	M0003	D3

Apiezon H was used as a heat sink grease on experiment A0076, Cascade Variable Conductance Heat Pipe. The grease was not exposed to atomic oxygen or to UV radiation. To determine the effect of extended hard vacuum on the grease, a sample was tested for outgassing in accordance with NASA SP-R-0022A. The LDEF sample had considerably higher total mass loss than the control sample, but the volatile condensible material was similar. It was postulated that this was due to the LDEF sample picking up moisture between satellite retrieval and sample test. Therefore, a series of tests were performed to determine the propensity of Apiezon H to absorb atmospheric moisture. A thin film of the grease was exposed to 100% humidity at room temperature prior to testing. The absorbed moisture caused a total mass loss similar to the difference between the LDEF sample and the control sample. The results are shown in table 4.1.7-2. Chemical analysis of the grease indicates that both the grease and the condensible material from the volatility test match those of a control sample.

Table 4.1.7-2. Apiezon H Outgassing Data

SAMPLE	TEST DURATION	TOTAL MASS LOSS	VOLATILE CONDENSIBLE MATERIAL
LDEF	7 days	2.32%	0.66%
LDEF	1 day	1.42%	0.44%
Control	7 days	0.97%	0.58%
Control	1 day	0.53%	0.18%
Control with 2 days humidity	1 day	0.72%	0.21%
Control with 1 month humidity	1 day	1.38%	0.25%
MSFC HDBK 527	1 day	0.86%	0.16%

Apiezon L was used on experiment A0180, The Effect of Space Environment Exposure on the Properties of Polymer Matrix Composite Materials, as a lubricant during fastener installation. It was not examined after LDEF retrieval.

Apiezon T was used on experiment M0001, Heavy Ions in Space, as a lubricant for installation of a large O-ring in a flange seal. Examination of the lubricant/O-ring by optical microscopy revealed some slight separation of the oil from the filler. Infrared spectroscopy of the lubricant showed no changes from the control. The O-ring was entirely wetted with the oil and showed no evidence of attack. Postflight examination of the flange revealed migration of the Apiezon T onto the flange. This migration was not quantified.

Ball Brothers lubricant 44177 was used to lubricate a thrust washer on the EECCs. A nearby bracket was found to have a diffraction pattern due to the off-gassing of the volatile component of the lubricant as shown in figure 4.1.7-1. Although the 44177 is still used on previously designed spacecraft, Ball Brothers no longer recommends it for new design.

VacKote 18.07 and 21207 were used on experiment S0069, Thermal Control Surfaces Experiment. No postflight examination of the lubricant has been performed.

Castrol Braycote 601 was used to lubricate the four drive shafts which opened and closed the clam shells of experiment A0187-1, Chemistry of Micrometeoroids. Since these drive shafts were exposed to space when the clam shells were in their open position, the Braycote 601 was exposed to UV radiation. However, the experiment was located on the trailing edge of LDEF so the lubricant was not exposed to atomic oxygen. The lubricant had picked up a black color, as yet not identified. Castrol examined the Braycote 601 with the following results. Infrared analysis showed no new carbonyl groups, indicating that no oxidation took place. New peaks were found in the 1100 to 1400 range. These might be attributed to C-F bonds indicating some degradation of the PTFE filler, but additional investigation is warranted. Some of the LDEF sample was separated into oil and filler by filtration. The viscosity of the base oil was lower than that of a control sample. This would indicate chain sissioning of the polyether and is consistent with exposure to UV

(See color photograph on p. 293)

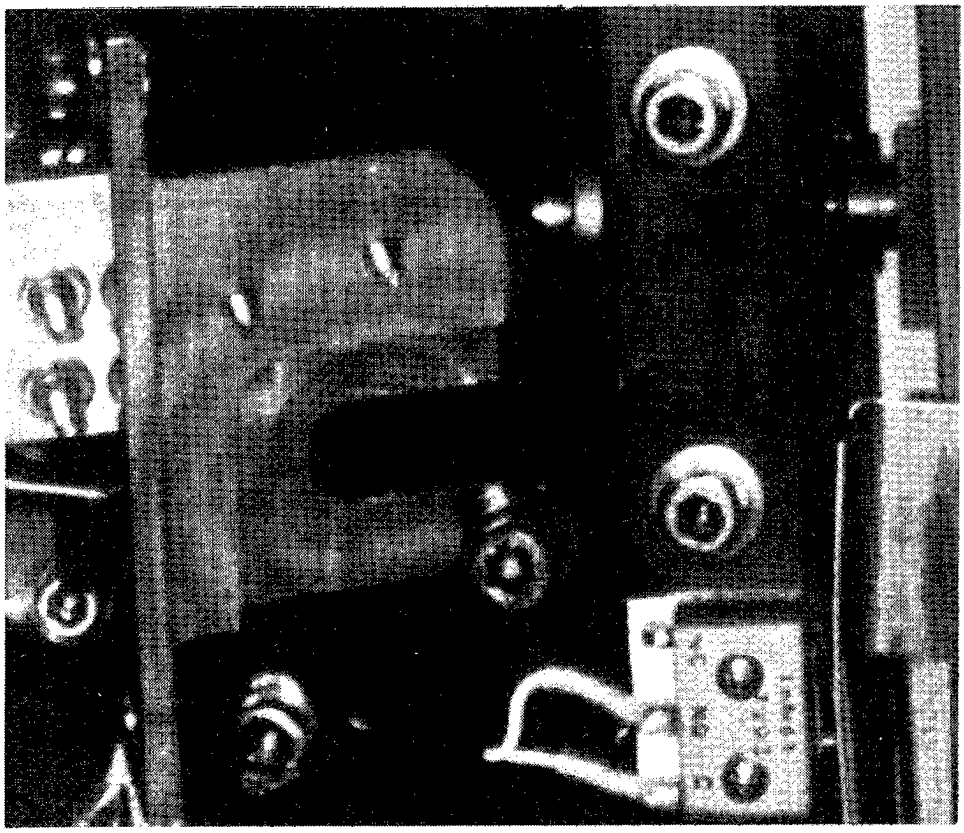

Figure 4.1.7-1. Offgassing Diffraction Pattern of Ball Brothers Lubricant 44177

radiation. Thermal analysis (differential scanning calorimetry and thermal gravimetric analysis) of the extracted oil revealed a new endotherm at approximately 106° C. This may be attributable to moisture effects. The LDEF grease also had a new endotherm at 211° C. This has not been explained at this time. Further testing is planned.

Dow Corning 340 heat sink compound was used on two experiments on LDEF; A0133, Effect of Space Environment on Space Based Radar Phased Array Antenna, and M0001, Heavy Ions in Space. The heat sink compound in both experiments performed as expected, transferring heat from one surface to another. Neither application exposed the Dow Corning 340 to U.V. radiation or to atomic oxygen, but both experiments saw hard vacuum and mild thermal cycling. The infrared spectra of a sample of Dow Corning 340 from experiment M0001 was unchanged compared to that of a control sample.

Dow Corning 1102, used on Experiment S1001, Low Temperature Heat Pipe, is an obsolete heat sink compound that was composed of 85% mineral oil, 10% Bentonite, 3% MoS_2, and 3 percent acetone. Postflight visual examination of the material showed no change from the initial condition.

Dow Corning Molykote Z was used on Experiment A0138. No results have been reported.

Exxon Andok C was used in Experiment S0069, Thermal Control Surfaces Experiment. No results have been reported.

Mobil Grease 28 was used on the magnetic tape modules (MTM) The MTMs were tested and compared to pre-flight measurements. No significant changes were noted. The MTMs were not disassembled so no grease analysis has been performed. No changes in the greases would be expected as both greases were used in sealed enclosures backfilled with inert atmospheres.

Vespel bushings were used in experiments A0147, Passive Exposure of Earth Radiation Budget Experiment Components, A0187, and S1002, Investigation of Critical Surface Degradation Effects on Coatings and Solar Cells. None of the bushings were exposed to UV radiation or to atomic oxygen. All Vespel bushings performed as expected.

The following three paragraphs describe the results from testing of experiment specimens (versus testing of lubricants that were used as functioning components of a system). DuPont Vespel 21 was tested in experiment M0003, Space Environment Effects on Spacecraft Materials. The Vespel was located on the exterior surface on the trailing edge (tray D3). Since tray D3 was on the trailing edge, the Vespel 21 was exposed to UV but no atomic oxygen. The specimens were part of a materials experiment and were not used as a component of an active experiment. Optical and EDX comparison of the surface with control specimens showed no differences. A friction test was performed (in a standard test lab environment) to determine changes in lubricity. Four specimens were tested, two flight specimens and two control specimens. The results, shown in figure 4.1.7-2, verify that the exposure did not degrade the Vespel 21.

Everlube 620 was also tested in experiment M0003 with the same exposure as the previous Vespel specimens. Post-flight visual inspection of the sample showed that none of the lubricant remained on the test specimens. EDX examination of the surface showed traces of the MoS_2 remaining in the bottom of the machining grooves of the substrate. However there was not enough remaining lubricant for testing. The binder, a proprietary organic compound, was apparently decomposed by exposure to UV and then offgassed (evaporated).

Rod end bearings were also exposed on M0003, Tray D3. The bearings were tested to the original manufacturer requirements (ref. 37). All test requirements were met including dynamic testing. One of the tests involved removing the PTFE-coated Nomex liner from the bearing body. The force required to remove the liner was similar to virgin bearings. Inspection of the Nomex/PTFE liner showed no degradation. The exterior surfaces of the bearing bodies were cadmiun plated in accordance with QQ-P-35, Class 2, Type II. The Type II designation requires that the parts receive a chromate conversion coating after plating. The conversion coating, which was an iridescent yellow brown color, exhibited signs of degradation. Post-flight visual inspection of the bearing bodies showed that the conversion coating had become more transparent. However, this change was not uniform over the the exterior surfaces of the three bearing bodies. We speculate that, as has been observed with the aluminum conversion coatings used on LDEF, the hexavalent chromium in the conversion coating has been reduced to trivalent with the associated loss of color. No changes in the cadmium plating were noted.

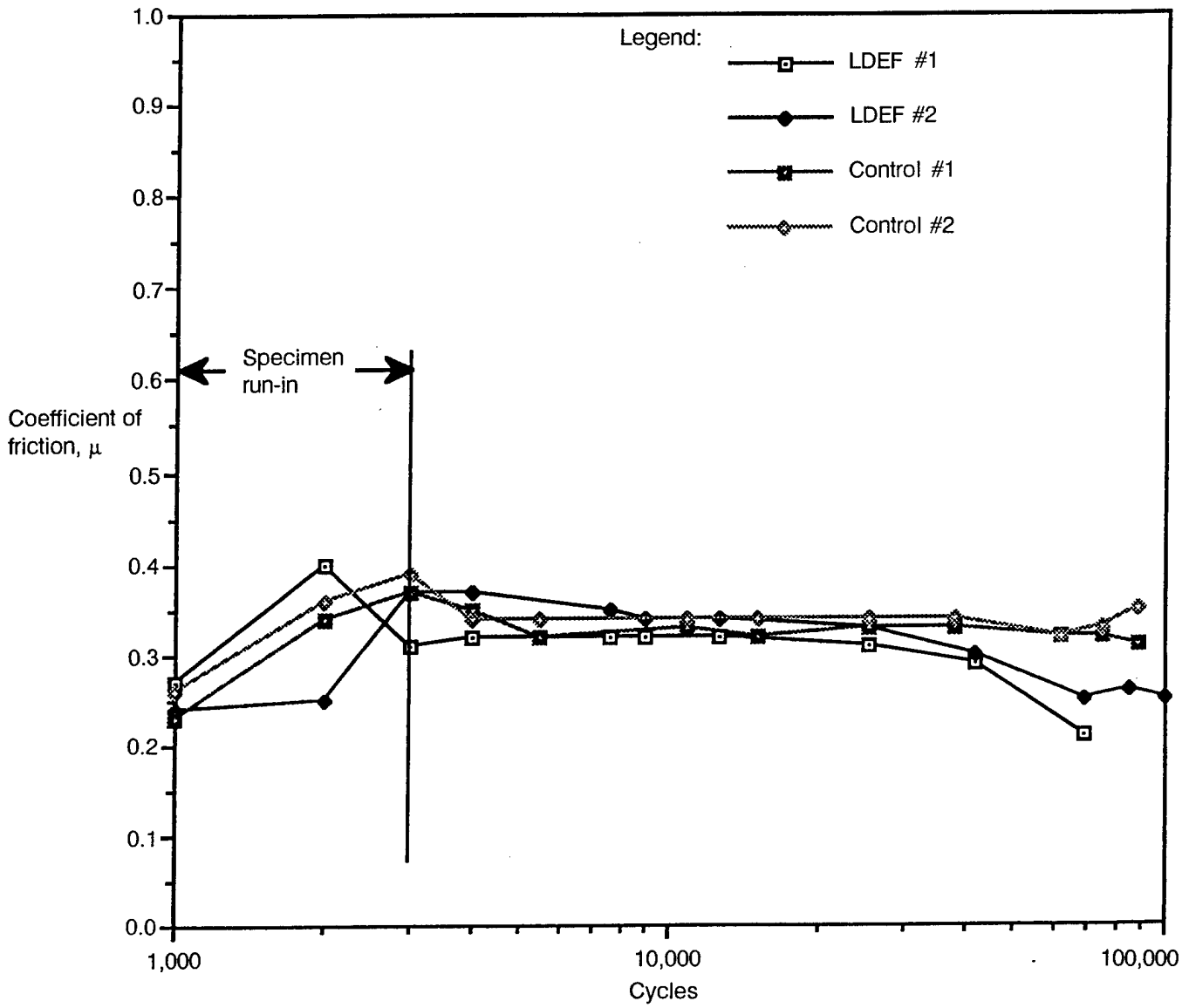

Figure 4.1.7-2. Vespel SP-21 Friction Data

4.1.8 Seals

A variety of seals were used on LDEF. These were generally O-rings, although sheet rubber was also used for seals. These materials performed as designed, sustaining little or no degradation. The exception was an ethylene propylene O-ring on Experiment S0069 which failed due to excessive compression set. In addition, materials that are commonly used for seals were used as cushioning pads. The performance of these elastomeric materials, listed in table 4.1.8-1, are discussed in this section.

Butyl O-rings were used in face seals on experiment P0004, Seeds in Space Experiment. Because the O-rings were sandwiched between metal surfaces, their exposure was limited to vacuum only. The O-rings were apparently installed without lubricant and sustained some scuff marks and pinching upon installation. Accurate post flight weights of each seed container were taken and compared to preflight values. The results showed no change in weigh. This meant that the O-rings performed as designed by preventing any desorption of moisture in space (7% of a seeds weight is moisture). There was no evidence of space-induced degradation and the performance of the O-ring seal was as predicted.

The butyl seal used to ensure vacuum inside of the FRECOPA canisters (sec. 4.1.4.3) has undergone postflight characterization (ref. 36). The seal was bonded to one of the face-plates of the canisters. In the closed position a compression force was

Table 4.1.8-1. Elastomers Used on LDEF

ELASTOMERIC PARTS	EXPERIMENT	TRAY
Butyl O-ring	P0004	F2
Butyl rubber seal	A0138	B3
EP O-ring	S0069	A9
EPDM rubber	P0005	CENTER RING
NBR rubber	P0005	CENTER RING
Neoprene gasket	A0139	G6
Nitrile O-ring	M0006	C2
Nitrile butadiene rubber	P0005	CENTER RING
Silicone gasket	S0050	E5
Silicone pad	M0004	F8
Viton O-ring	A0015	G2
	A0134	
	A0138-2	B3
	A0139	G6
	A0180	D12
	M0001	H3, H12
	M0002	LOTS?
	P0005	CENTER RING
	S0010	
	S0069	A9
Viton washer	A0189	D2
Metal "V" seal	EECC'S	

exerted on the canister to apply the necessary sealing force between canister halves. When the canisters were in the open position (10 months), the seals were protected from direct exposure to trailing edge environment by an aluminum shield. Tests reveal a slight increase in hardness (4%) but the seals were still in good working order and and efficiently adhered to the canisters.

Ethylene propylene (EP) O-rings were used to seal the lithium batteries on experiment S0069, Thermal Control Surfaces Experiment. These seals failed due to excessive compression set of the O-rings as shown in figure 4.1.8-1. The temperatures seen by the batteries, 13 to 27^0 C, were well within the limits of EP O-ring capabilities. Therefore, failure has been attributed to attack of the O-ring by the battery electrolyte, dimethyl sulfite.

Ethylene propylene diene monomer rubber (EPDM) and acrylonitrile butadiene rubber (NBR) were tested in experiment P0005, Space Aging of Solid Rocket Materials. The elastomers were not exposed to UV radiation or to atomic oxygen, but had extended exposure to hard vacuum. Both elastomers exhibited slight changes in strength, modulus and ultimate elongation as shown in figure 4.1.8-2.

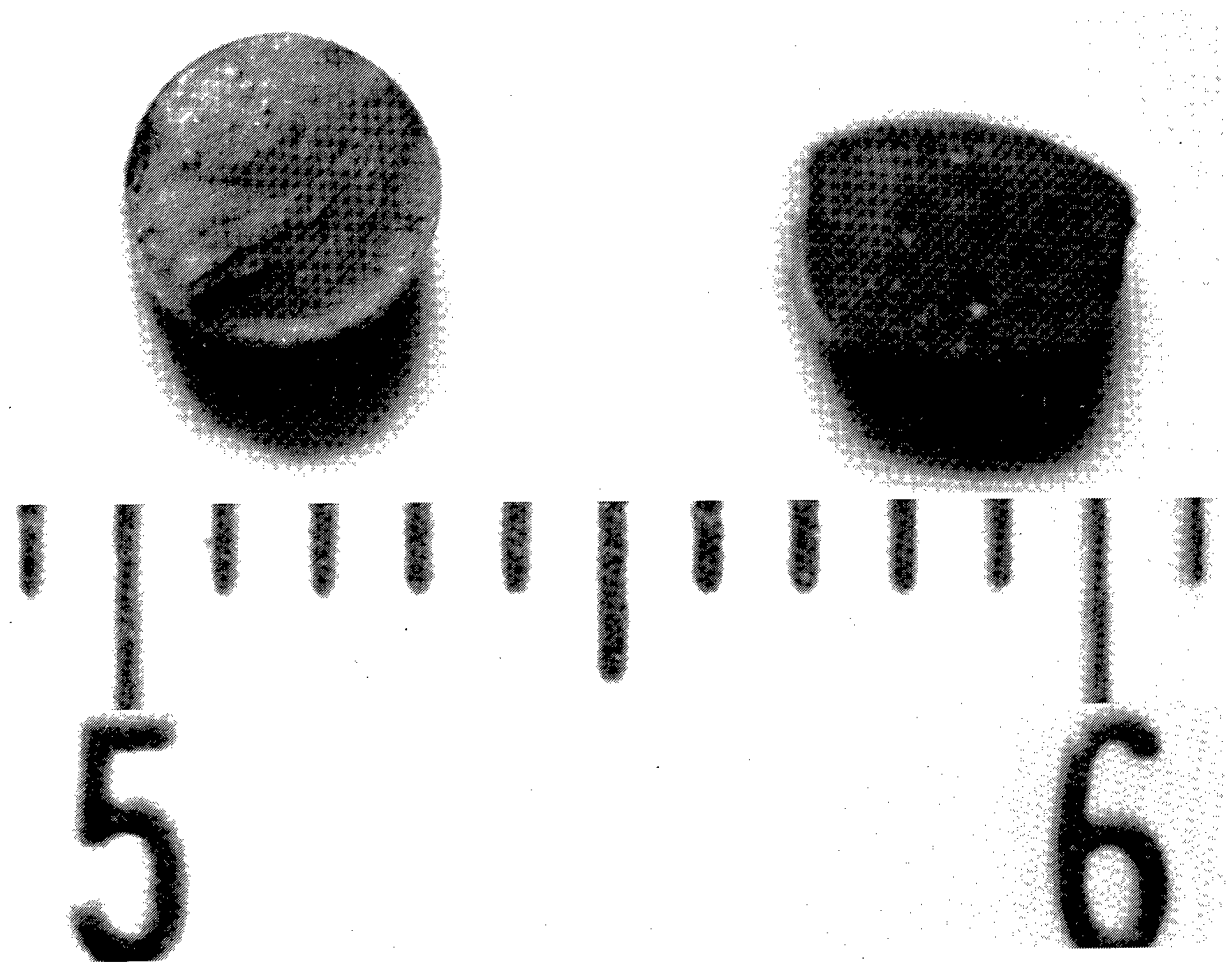

Figure 4.1.8-1. Control O-Ring Versus Flight O-Ring

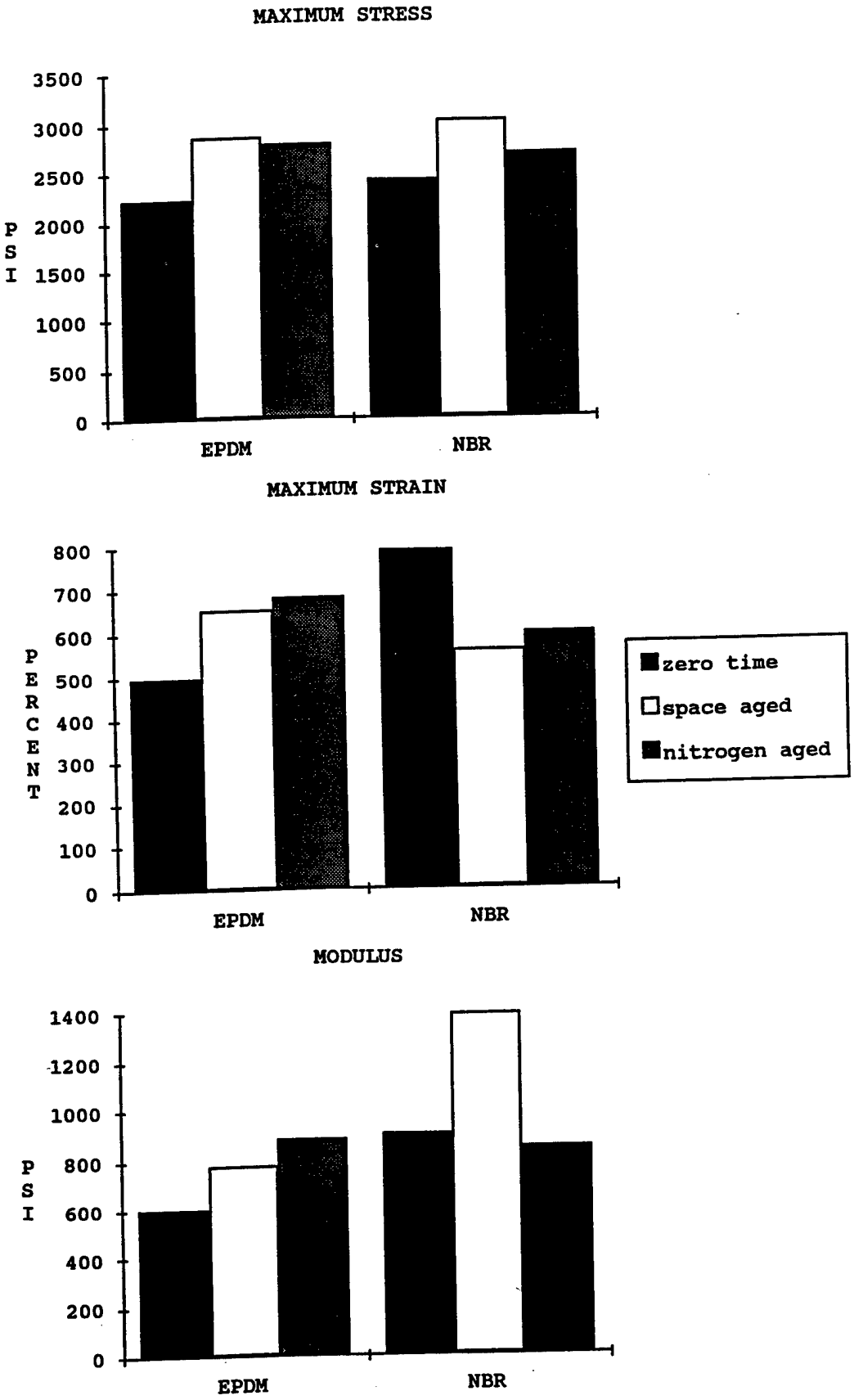

Figure 4.1.8-2. Performance of NBR and EPDM

Silicone rubber was used as a cushioning gasket between the sunscreen and the tray in experiment S0050, Investigation of the Effects on Active Optical System Components. Portions of the gasket were exposed through holes in the sunscreen. Since the experiment was on the trailing side of LDEF, the gasket saw UV radiation, but not atomic oxygen. The exposed areas of the gasket were slightly darkened but did not show any other signs of degradation. The hardness of the gasket was the same in exposed and unexposed areas, and all material was very pliable. Although control specimens were not available, tensile strength and elongation were determined and found to be within the range of other silicone elastomers.

Silicone rubber was also used as a cushioning pad between a metal clamp and some optical fibers in experiment M0004, Space Environment Effects on Fiber Optics Systems. The rubber was mostly shielded, but some edges were exposed to UV radiation and atomic oxygen. The rubber remained pliable and free of cracks. Some darkening of the rubber was observed in the exposed areas.

A large number of Viton O-rings were used on LDEF. Post flight examination of these found that they were all in pristine condition. No Viton O-ring seals failed to maintain a seal. None of the Viton O-rings were exposed to UV radiation or to atomic oxygen.

A group of Viton washers was used to pad the quartz crystal oscillators in experiment A0189, Study of the Factors Determining the Radiation Sensitivity of Quartz Crystal Oscillators. The washers were apparently dinked out of sheet stock as a fabric texture was apparent on the flat surfaces. Many of the washers had indentations on one or both of the contacting surface, indicating compression set. No further analysis is planned because the original compression is unknown.

A metal "V" seal was used to seal the pressure valve in the EECCs. The seal was made of Inconel 750 and had a currently unknown finish. It was sealing the stainless steel valve to an aluminum surface. There was no evidence of coldwelding between the valve, the seal, and the mating aluminum surface contacting an aluminum surface.

4.1.9 Composites

The most significant findings for fiber-reinforced organic composites were atomic oxygen erosion and dimensional changes. Composites directly exposed to the leading edge environment exhibited erosion of up to one ply of material along with reduction of mechanical properties. A thin protective coating of Nickel and SiO_2 was successfully used in one experiment to prevent this erosion. Composites located on the trailing edge and on the LDEF's interior exhibited no erosion and did not display any reduction in mechanical properties. In-flight monitoring of strain-gauged unidirectional tape composites revealed a period of contraction in the 90 deg. direction occurring during the first days of flight. The only reported chemistry changes to composite systems were only a few microns deep on composites mounted on exterior surfaces and had no impact on the bulk performance properties of the materials. Microcracking has been reported for several non-unidirectionally reinforced polymer matrix composites on both the leading and trailing edges.

Atomic oxygen effects: Photomicrographic results revealing atomic oxygen erosion of organic composites were reported by a number of experimenters. Leading-edge exposed specimens displayed the most recession with 3 to 7 mils of material loss reported for graphite reinforced epoxies, polyimides, and polysulfones. No recession of trailing edge exposed or shielded specimens was found. Figure 4.1.9-1 is a photomicrograph of PMR 15 located on the leading edge. This photo shows the one ply (5 mils) of erosion that occurred in the unshielded area.

Resin type (epoxy, polysulfone, and polyimide), fiber type, and resin/fiber ratio appear to be significant variables in the AO recession rates of composite materials. Resin recession rates appear to be significantly higher than those of graphite fibers. SEM observations of AO eroded surfaces revealed similar erosion patterns for epoxy, polysulfone, and polyimide composite. However, a bismaleimide/graphite composite specimen was reported (ref. 38) to have a significantly different erosion pattern than the above mentioned materials. Current activities include determining whether the actual recession rates exceed the predicted values.

Complete protection from AO attack was accomplished for one epoxy/graphite system by using a nickel/SiO_2 coating (1000 Angstroms and 600 Angstroms respectively). No erosion of the composite substrate was reported for this experiment (ref. 39). A Nomograph, shown in figure 4.1.9-2, was developed to assist in predicting survivability of uncoated composites based on altitude, AO fluence, and recession rates (ref. 40).

Strain and CTE Test Results: Reported results for on-orbit measurements of 90 deg. direction strain versus temperature of unidirectional fiber-reinforced organic composited revealed an initial period of changing CTE as the specimen shrunk in size. The CTE asymptotically approached and reached the preflight value after the dimensional shrinkage had ceased. Moisture desorption was cited as the most likely cause of the shrinkage and changing CTE. On-orbit measurement of 0 deg. CTE did not reveal any significant changes. These results verified the investigators ground-based simulation predictions.

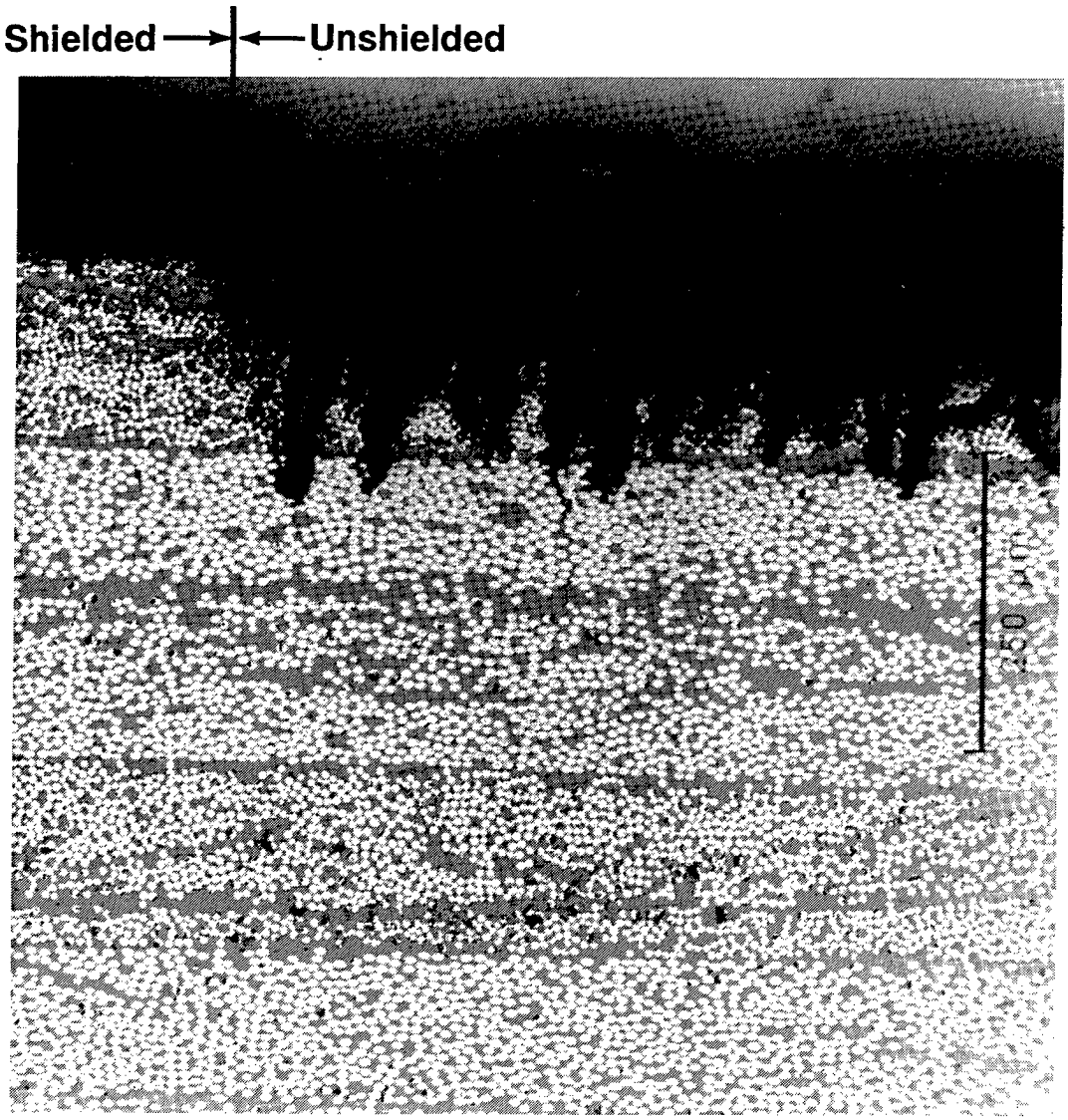

Figure 4.1.9-1. Photomicrograph of PMR 15 Located on Leading Edge

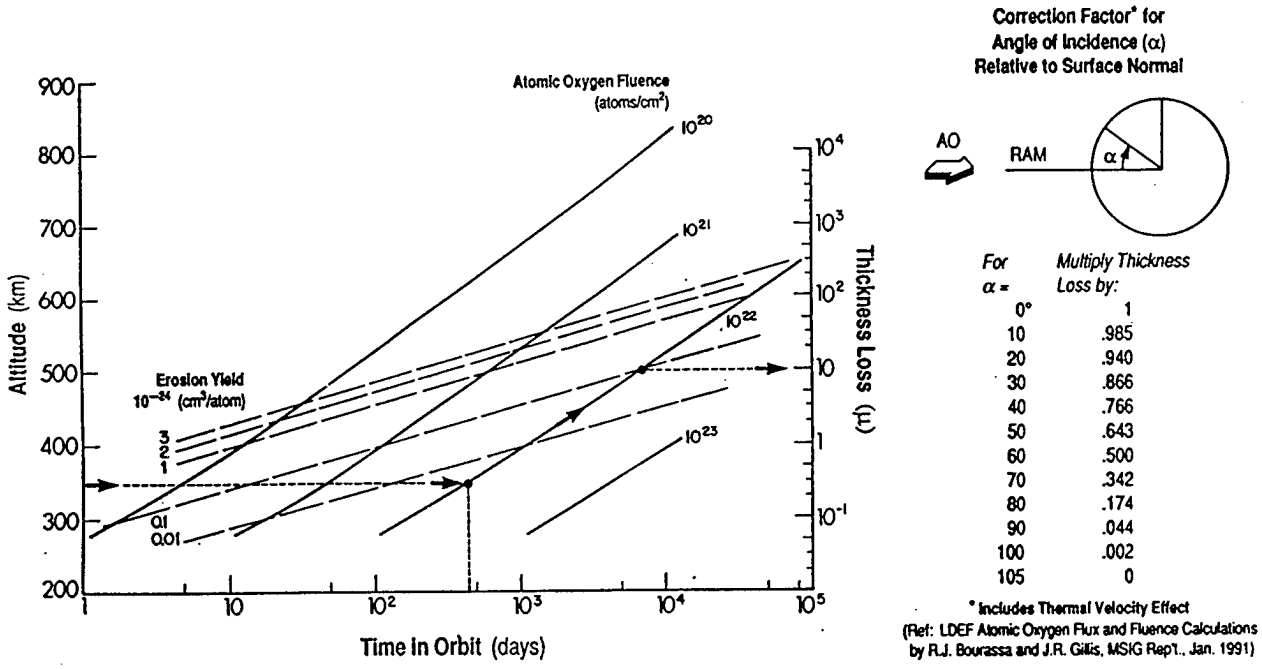

Figure 4.1.9-2. Nomogram for Calculating Atomic Oxygen (AC) Fluence and Material Thickness Loss as a Function of Orbital Altitude, Time in Orbit, and Angle of Incidence

As reported by a number of investigators, post-flight CTE measurements after equilibration with ambient conditions revealed no difference when compared to preflight values.

Resin Chemistry and Morphology: Other than the obvious oxidation of AO exposed surfaces, a number of investigators reported that changes in resin chemistry and morphology were only skin deep for the remaining composite materials. Fourier transform infrared spectroscopy (FTIR) was performed on control, leading edge exposed, shielded and freshly uncovered leading edge surfaces. The only notable difference was the absence of absorption peaks for epoxy and polysulfone leading edge surfaces. These results imply a layer of ash contamintion caused by the errosion of the composite. For unknown reasons, the polyimide specimens did not display this behavior.

Both preflight and postflight molecular weight data for polysulfone resin showed no changes. Also dynamic mechanical analysis (DMA) and thermo-mechanical analysis (TMA) test results show no change in glass transition temperatures for graphite- reinforced epoxy, polysulfone, and polyimide composites. Some evidence of UV darkening was shown for trailing edge composite surfaces using thin section microscopy.

Mechanical Properties: No significant changes in modulus and strength were reported for trailing edge and AO shielded composite materials when compared to preflight and

control specimen data. Leading edge AO exposed specimens experienced significant drops in modulus and strength. Up to 25% moduli reductions and 50% strength reductions were reported. Atomic oxygen erosion and surface roughening are the most likely causes of mechanical property degradations. Specimen gauges varied between experiments and may explain the range of mechanical property reductions reported.

Microcracking: Significant levels of microcracking occurred in some of the multidirectional reinforced polysulfone and polyimide composites. This microcracking is most likely due to the thermal cycling environment as it occurred on specimens exposed on the exterior surfaces of LDEF and not on the ground control and shielded flight specimens.

4.1.10 Mechanical Systems Lessons Learned

Fastener removal difficulties have been related to galling damage during pre-flight installation and post-flight removal. To date, no indications of any occurance of coldwelding have been found. However, it is important to remember that LDEF was a fairly "static" satellite without many mechanism or fasteners being mechanically cycled while on orbit. Because stainless steel fasteners are very susceptible to galling damage, successful application of such fasteners on orbital replacement units (ORU) will require high thread quality and effective lubrication schemes or surface modifications (such as ion implantation). Simulated space effects testing, in conjunction with tribology studies, is required to determine which solid film lubricants are optimal for use under long-term space exposure.

Coldwelding related to space exposure is apparently not of concern. No evidence of coldwelding has been observed; all suspect conditions thus far have been shown to be the result of installation or removal galling damage. Procedures need to be developed to prevent damage during assembly of ORUs.

The LDEF primary structure was unaffected, other than by micrometeroid and debris impacts. Dye penetrant and eddy current inspection of the structure revealed no anomalies. No bulk metallurgical changes occurred in the structural materials. Bolted joints appear to be a very reliable method for assembly of space structures.

The mechanical behavior of the EECCs was generally nominal. Wide swings in motor current during opening of the M0006 canister, drawer seals, and lubrication require further study. No mechanisms flown on LDEF failed to performed because of space effects.

Several different types of seals were used on LDEF. The only seal anomaly was associated with the ten LiCF batteries flown on S0069 and S1005. During the 6-year exposure, these seals degraded so that the electrolyte gas was released from the battery case. This release caused no loss degradation of the adjacent hardware. The ground-stored batteries also experienced the same seal degradation, therefore, this failure was not caused by exposure to the space environment.

A wide variety of lubricants and greases were flown on LDEF. With exception of the Vespel 21 and the air-cured MoS_2 dri film lubricants flown on M0003, all lubricants were functioning components of an experiment and all lubricants performed as designed. The air-cured dry film lubricant, exposed to the trailing edge environment, had completely disappeared during the 69-month mission.

The most significant findings for the fiber-reinforced organic composites were the atomic oxygen erosion of leading edge specimens. While these recession rates are not unexpected, the detailed comparison of ground based predictions vs actual recession rates has not been completed. A thin protective coating of nickel and SiO_2 was used on leading edge specimens to successfully prevent this erosion.

The viscous damper, rigidize-sensing grapple, and flight-releasable grapple performed as designed. The viscous damper underwent postflight evaluation and has been returned to the LDEF Program Office in flight-ready condition.

4.2 ELECTRICAL SYSTEMS

LDEF carried a remarkable variety of electrical and electronic systems, resulting from the great diversity in experiment objectives and approaches to data collection. NASA provided certain guidelines and design review requirements, but responsibility for success (or failure) rested solely with the experimenters. It is a tribute to the many individuals involved that so few problems developed. The following sections discuss observations on various systems and components which were examined by the SSIG, and concludes with a discussion of problem areas and ways to avoid them on future programs.

The LDEF design rules began with the basic requirement that all experiments should be completely independent, and that no remote command, control or communications (ground based or otherwise) would be used. The only electrical link between experiments and the LDEF spacecraft was the experiment initiate system, which provided a signal to turn active experiments on or off via NASA-supplied relays. NASA also required that all electrical circuit elements be isolated from the experiment, the tray and the LDEF structure by a minimum of 2.5 megohms, although some exceptions may have been made. A general requirement was that no failure should be capable of causing thermal runaway, burnouts, fire, etc. There was also to be protection against EMI or other interference with other experiments. Experiment designers were cautioned to use care in providing ground returns and to follow established practice on routing signal leads and utilizing shielding and other protection techniques (ref. 41). However, the NASA design review process was primarily concerned with safety and interference with other systems and experiments, rather than determining suitability of experiment designs to meet their objectives.

NASA also made available a data collection and storage system, the Experiment Power and Data System. Seven of these were used by six experiments, as an alternative to developing their own data systems. These units were of particular interest to the SSIG, as they were one of the few systems with multiple, nearly identical units located in a variety of locations on the spacecraft.

Appendix A contains a listing of most of the electrical systems and components flown. Most LDEF components were not "space rated," i.e. they had not been subjected to the rigorous testing and inspections normally required of spacecraft system components (e.g., MIL-STD-883, Class S). Some were off-the-shelf commercial quality parts, while most were MIL-STD-883, Class B or equivalent. LDEF provided a unique opportunity for evaluation of such components, with results which were both encouraging and revealing. Table 4.2-1 shows the electrical anomalies that occurred the LDEF mission and table 4.2-2 provides the details of the known component failures.

TABLE 4.2-1. Electrical Systems Anomalies

Relays and Other Electromechanical Device Anomalies:

A0038:	one tray initiate relay failed
S0069:	MTM 4-track changeover relay failed
EIS:	one unused status indicator failed

System Anomalies:

A0038:	only 1 of 35 pairs of pyro cable cutters fired
A0076:	premature shutoff
A0187-1:	clam shells not closed on retrieval
S0014:	Gulton data system failed after retrieval
MTM's:	magnetic tape took mechanical set
A0180:	magnetic tape oxide lost adhesion in dry N2

Component Anomalies:

A0038:	E-cell coulombmeters leaked (5 of 70 =7%)
A0054:	E-cell coulombmeters leaked (6 of 152 = 4%)
A0076:	transistor/resistor failed
M0004:	one fiber optic cable severed by micro-meteoroid impact
S0069:	DAC: bit 25 latched high
S1001:	NiCd battery cells bulging (may have been overcharged).

TABLE 4.2-2. Known Electrical Component Failures

PART	Part Number	MFG.	EXP.
Relay, Latching	FL11D	P&B	A0038
Capacitor, Tantalum	137D, 33uF	Sprague	A0187-1
Indicator, Miniature	BHGD21T	Minelco	EIS
Transistor	JAN2N2222A	Unknown	A0076
Microcoulombmeter	550	Pacific Electron	A0038
Microcoulombmeter	500-0002	Plessey	A0054
Relay	J422D-12WL	Teledyne	S0069 MTM

4.2.1 Experiment Initiate System

The Experiment Initiate System (EIS) was the sole "communications" link between the spacecraft and the individual experiments. Its proper operation was vital to the success of all active experiments, for it provided the initiate signal to those experiments, directing them to turn on their power and begin their operational programs. Consequently it was designed conservatively and thoroughly tested prior to installation. It was located on the spacecraft interior in a well protected location (figure 4.2.1-1), and was not exposed to extremes of temperature or other environmental hazards. The experiment initiate relays and related components (connectors and diodes) were also supplied by NASA, and were well proven, space-rated items. Complete isolation was maintained between the EIS ground return for these relays and the experiment electrical systems. Thus, the experiments only saw sets of contacts which were closed at initiation and opened when the EIS was reset.

The original EIS design included use of two parallel systems, each capable of turning on up to 40 experiments (although only one of these was used on the LDEF flight). Their only common link was their power switching relay outputs, such that either power source could drive all experiment initiate relays. Each of the two systems was to be started and stopped (set and reset) by a separate switch on the active grapple fixture shortly before the spacecraft deployment and following recapture, respectively. Each contained an internal clock and sequencer to turn on a master power source to the coil drivers, and to provide initiate signals to its assigned experiments. Thus, had this option been used, failure of either system would have affected only those experiments assigned to that half, rather than all active experiments. For the actual flight, however, only 24 initiate circuits were required, serving 20 experiments (some experiments utilized more than one initiate relay). A listing of these active experiments appears in table 4.2.1-1. Consequently, only one of the two EIS parallel systems was used (the other circuit boards were not flown). This made all experiments dependent upon a single clock and sequencer circuit.

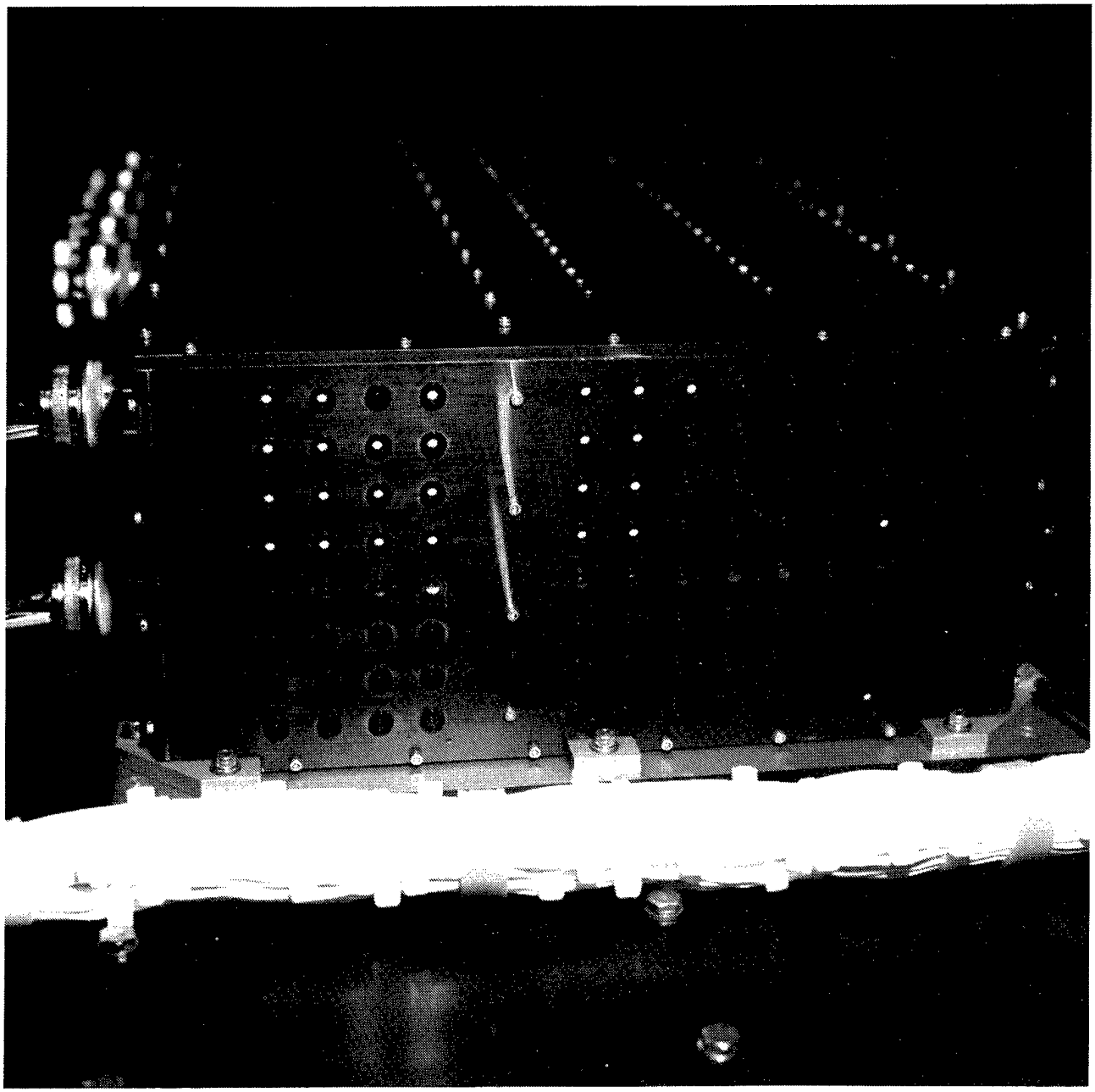

Figure 4.2.1-1. The EIS electronics box, as mounted on the interior frame of LDEF. The 24 white status indicators in the upper left portion of the array of 88 were used to record successful initiation of experiments.

TABLE 4.2.1-1. Experiments Activated by the EIS

Exp. #	Location	Major System Components
A0038	F-6	7 timer/sequencers; pyro wire cutters HVPS; master/slave relay system
A0054	B-4	HVPS; E-cells
A0054	D-10	" "
A0076	F-9	Data/control; Li battery;thermistors
A0133	H-7	Data; microprocessor; EEPROM's; HVPS
A0138	B-3	Data/control; motor-driven canisters
A0139A	G-6	Control; valves
A0180	D-12	Data; cassette tape recorder; strain guages; thermal measurements
A0187	A-3	Data/control; timer sequencer; motors
A0201	B-12 (2)	EPDS; MOS sensors
M0003	D-4 (2)	2 EPDS; 2 EECC; data/control; active
M0003	D-8 (2)	and passive components; fiber optics
M0004	F-8	EPDS; data/control; fiber optics
M0006	C-2	EECC
P0003	CENTRING	Data; thermocouples; radiometer; thermistors; used S1001 EPDS
S0010	B-9	EECC
S0014	E-9	EPDS; data; solar cells
S0069	A-9	Data/control; motor-driven carousel; lamps; chopper; detectors
S1001	F-12	EPDS; data/control; solar cells; NiCd
S1002	E-3	EECC; data/control; EAROM's
S1005	B-10	EPDS; data/control; LiF batteries

The EIS also incorporated a visual indicator system to provide a record that the experiment initiate latching relays had been activated. Six of these "status indicators" were visible to the astronauts during deployment, and were used to indicate the EIS had functioned properly (figure 4.2.1-2). As suggested by the six external status indicators, the EIS functioned flawlessly at deployment. All experiments received their initiate signal, and all the NASA-supplied experiment initiate relays functioned normally. The original LDEF flight plan called for resetting all experiments to their unpowered state when the shuttle retrieved the spacecraft, utilizing the active grapple fixture to trigger the reset operation of the EIS. Due to the extended mission length and consequent uncertain state of batteries, and the desire not to disturb the final state of certain experiments, it was decided not to reset the systems: retrieval was accomplished using the passive grapple fixture instead of the active fixture. All experiment initiate relays were therefore expected to remain in their set state throughout recovery and deintegration. This was verified prior to tray removal or any other activities which might have changed that state (including mechanical shocks associated with transportation to experimenter laboratories).

The EIS test procedure (ref. 8) also called for a thorough visual inspection of the associated cables and connectors, and measurement of disconnect torques on all connectors which were removed for access to the cable pin connections. All disconnect torques were normal, and only minor contamination particles were observed. The results are described in reference 42.

A related task conducted early in the deintegration phase was to inspect and document the state of the visual indicators on the EIS control box (figure 4.2.1-3). These small electromagnetic devices rotate a ball to display either black or white sides through a window. One was used for each of the 24 active experiment initiate relays. The signal to set the indicator to white came through a separate set of contacts on the experiment initiate relay. These could only be reset using ground support equipment (GSE), so a white indication was a reliable record that the relay had been set. These indicators were identical to those located adjacent to the active grapple fixture, and used by the astronauts to verify system operation after LDEF was placed in orbit. As expected, all the indicators associated with experiments were white at the time of this initial post-recovery inspection.

Shortly after removal of the EIS from LDEF, it was tested at KSC using the original GSE. The initial reset functional test was completely successful: all indicators which had been set (white) were observed to reset (black). However, when the system was given its first set test, it was noted that one of the previously unused visual indicators failed to shift from black to white, although its associated relay circuit functioned correctly. On two subsequent reset/set cycles, this indicator shifted properly when exercised. Power supply current traces were normal, with changes indicating correct timing of the various relay drive operations.

The faulty indicator and three other spares were removed and transported to Boeing for analysis. Two of the three extra units had not been connected and therefore had not been exercised. All units were subjected to marginal voltage testing at the minimum specified operating pulse width of 40 milliseconds. The three "spare" units all functioned consistently at 5V to 6V. The faulty unit, however, exhibited highly variable behavior, operating twice at 9.4V to10.3V, and a third time at 5.6V. This type of intermittency is characteristic of contamination, and indeed the failure was found to be caused by a small particle which could jam the magnet. Particle contamination is an all-too-common problem with small electromechanical devices, including relays.

It should be noted that the failing unit operated normally during pre-flight testing of the EIS, and under normal voltages and with long input voltage on-times. It is often necessary to subject components to testing at the limits of the manufacturer's specifications (e.g., voltage, temperature, pulse widths and timing) to detect marginal parts. These indicators did not receive such testing prior to use.

Figure 4.2.1-2. The LDEF Active Grapple Fixture. The arrow indicates the small panel with six status indicators used to verify EIS initiation during deployment.

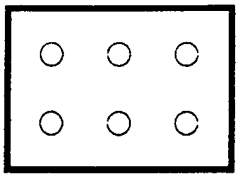

EIS BEACON INDICATORS

TEST POINT	MEASUREMENT
J413-Y TO J413-Z	
J413-Y TO J413-a	

EIS LAST STATE RELAY MEASUREMENTS

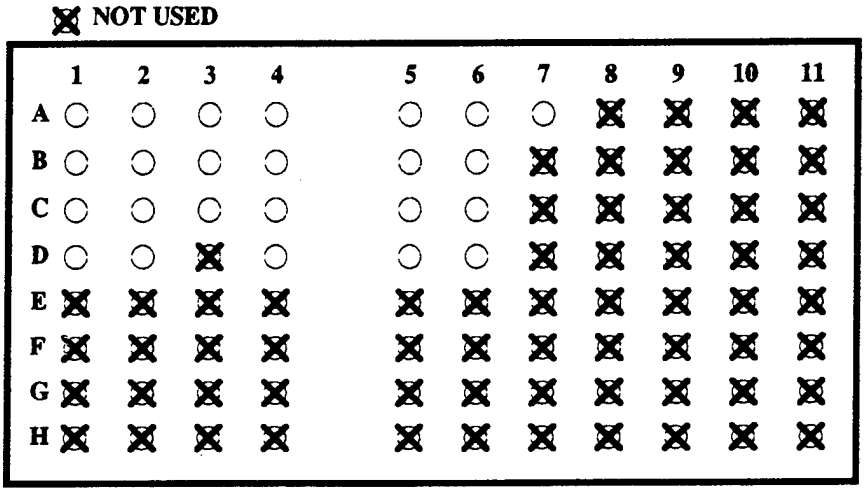

EIS BOX STATUS DISPLAY

Figure 4.2.1-3. The EIS Status Indicator Array on the Electronics Box—Those Showing White Recorded Initiation of Their Respective Experiments

4.2.2 Experiment Power and Data System

The second NASA-provided electronic system of interest was the Experiment Power and Data System (EPDS). Seven of these were flown for use on eight different experiments (P0003, A0076, and S1001 shared the same EPDS), located at various positions on the LDEF structure (see table 4.2.2-1). The EPDS components were not directly exposed to the exterior environment, being protected by their mounting plate and by external thermal shields. All the EPDS units were similar, consisting of a Data Processor and Control Assembly (DPCA), a tape recorder (the Magnetic Tape Module, MTM), and two $LiSO_2$ batteries, all of which were attached to a mounting plate designed to fit into the backside of the experiment tray. There were differences in their programming and in the mix of analog and digital data channels, but all shared a number of identical circuit cards.

Although simple compared with today's data systems, the EPDS contained many elements common to most such systems, including various control and "handshake" lines, programmable data formats and timing (via jumpers on circuit cards), and a data storage system (CMOS memory, with periodic data transfer to the MTM tape recorder). Each was furnished with a set of support equipment for ground checkout and operation with the experimenter's system, including a Data Display Box (DDB), a computer tape system for transcription of the MTM data, an MTM controller, and the various interconnecting cables. EPDS electronic components were procured to MIL-SPEC-883, Class B standards, and were not rescreened prior to installation.

Systems SIG interest in the EPDS continued through initial testing in the experimenter laboratories. Initial tests were witnessed at four facilities (in addition to the KCS tests), and technical assistance was provided in setting up and conducting some of those tests. It was concluded that all seven EPDSs functioned normally during and after the LDEF flight. Apparent anomalies proved to be due to GSE or to interactions with experiments, rather than failures of electronic systems. The only significant problems involved the MTMs. Observations are summarized below.

TABLE 4.2.2-1. EPDS Units and Locations on LDEF

Experiment No. and Title	Organization	Location
A0201 Interplanetary Dust	NASA LaRC	E9
M0003 Space Environment Effects	Aerospace	D4 & D8
M0004 Fiber Optics	AFWL	F8
S0014 Advanced Photovoltaics	NASA LeRC	E9
P0003 Thermal Measurement System	NASA LaRC	F12
A0076 Cascade Variable-Contuctance Heat Pipe	McDonnell Douglas	
S1001 Low Temp. Heat Pipe	NASA GSFC	
S1005 Transverse Heat Pipe	NASA MSFC	B10

TESTING AT KSC: Two experiments utilizing EPDS were tested at KSC (M0004 and S1001). These were the first electronic systems tested after LDEF recovery. Both experiments, including the EPDS, functioned properly. However, one system (M0004) exhibited two apparent anomalies: a higher than normal EPDS standby current (2 mA, compared with the normal 0.5 mA), and chattering in an experiment relay which was driven by the EPDS. The higher standby current was of particular interest, as it might have indicated changes in the CMOS components.

M0004 EPDS TESTS: Testing at the experimenter laboratory (Phillips Lab, Albuquerque, NM) revealed that the EPDS was functioning normally, and that the apparently high standby current was caused by a previously unrecognized experiment activation which occurred when the system was first initiated. The cause was a known characteristic of the original EPDS controller board, which provided "erroneous pulses during the initial powering up" on the four pulsed signals to the experiment (ref. 43, EPDS Manual, page 23). An optional modification to eliminate these signals had not been made. Since the first programmed data scan did not occur for some time after initialization, the early activation resulted in no loss of data. The chattering relay was also found to be due to test setup conditions (time between system tests), rather than a failure of the EPDS or experiment electronics. Both anomalies point up the fact that subtle characteristics of the interaction of different systems can cause confusion.

M0003 EPDS TESTS: This experiment utilized two EPDS. At the experimenter laboratory (Aerospace Corporation) both were set up for testing using the NASA-supplied computer tape system as well as their own computer-based tape readout system. One of the two systems performed properly during all in-lab tests. The other operated properly at the beginning of a multi-hour test. However, it was later found to be latched into a continuous data scan and tape record mode. The condition was not corrected by reinitializing the system. Examination of the tapes showed the condition to have begun at the time of the first programmed data readout. Attempts to diagnose the problem at Aerospace were not successful, and schedule commitments precluded further efforts at that time.

The unit was subsequently sent to Boeing for analysis, along with its GSE, cables, etc. Initially, it operated correctly in all modes. It was then found that one of the GSE cables had an intermittent short inside a connector, which could be activated if the cable was flexed. It was concluded that the cable had probably been moved during the test while photographers were documenting details of the experiment. The failure of the GSE cable which was completely independent of the EPDS itself, and caused no loss of recorded flight data.

MTM ANOMALIES: Two MTM anomalies have been reported, and were investigated by the manufacturer, Lockheed Corporation. Prior to LDEF recovery, it was decided to return the MTMs to Lockheed for inspection and data recovery, rather than assume they would operate normally using experimenter GSE. During these inspections it was noted that the magnetic tape on all but one unit had taken a "set" where it was wrapped around the phenolic capstan. The exception was the single unit which had operated periodically throughout the flight (S0014). The MTMs were backfilled with dry nitrogen prior to flight. During post-flight deintergration at Lockheed, the tapes were exposed to a controlled humidity, the mechanical set

gradually disappeared. Evidently some level of humidity is necessary in the sealed units to avoid this problem under long term, inactive storage. Interestingly, it has been reported that a different type of tape (a ruggedized cassette) used in the Polymer Matrix Composite Materials Experiment (A0180) did not encounter this problem even though it too had been backfilled with dry nitrogen. It has been speculated that outgassing of some other material in that tape recorder housing prevented excessive drying of the tape (ref. 44). This is supported by the observation that similar tape casettes, stored in dry nitrogen on the ground, experienced loss of oxide adhesion, unlike the flight tape. It may be concluded that additional study of the required humidity and related environmental requirements may be needed to determine optimum long-term storage conditions for each type of magnetic tape material.

One significant MTM failure resulted in loss of some experiment data on the Thermal Control Surfaces Experiment (S0069). This was the only four-track MTM used, and the experiment did not use an EPDS. The latching relay which should have switched track sets (from tracks 1 or 3 to tracks 2 or 4) failed to operate during the flight. Consequently, portions of the early flight data on track 1 were overwritten and lost. During initial inspection at Lockheed, the relay was found to have one contact set stuck in an intermediate state (neither track set selected). This prevented the track selection circuit from activating the relay because that contact set was used to sense which track set was currently selected. It was necessary to apply power directly to the relay coil pins to test it during the initial post-flight analysis. When this was done, it operated and then continued to function normally using the track selection circuit. Such behavior is not unusual for relays, in that contact contaminants may prevent one or more switching operations and yet be dislodged in subsequent activations, restoring normal operation. If anticipated, such failures may sometimes be overcome by sensing correct operation and arranging for reactivation if necessary. However, this was not a feature of the affected unit.

FOLLOW-ON EPDS TESTING: Originally, the Systems SIG planned to subject all the EPDS units to a detailed test sequence, followed by parametric testing of selected components. This was to have taken place after release of the units by the experimenters, and would have included a search for LEO-related degradation and radiation effects. However, this plan was set aside when it was realized that all original test data had been discarded by the EPDS manufacturer (Base 10 Systems, Inc., Trenton, N.J.) after the normal 7-year archive period. Thus, parametric studies of degradation would have been limited to statistical comparisons with similar populations not subjected to LEO, rather than direct comparisons with pre-flight data. The lack of non-flight reference parts from the same sources and date codes was also a factor (the only source of reference parts would have been the spare EPDS unit). It was not considered desirable or necessary to destroy one or more EPDS units for such a study, particularly since the successful performance of all EPDS units, and their well shielded construction and positioning on the tray undersides made it unlikely that major parametric changes related to LEO would have been found.

4.2.3 Batteries

Three different types of batteries were used on LDEF: lithium sulfur dioxide ($LiSO_2$), lithium carbon monofluoride (LiCF), and nickel cadmium (NiCd) batteries. This section will discuss the results and status of the post-flight testing. A summary of the batteries used on specific LDEF experiments is shown in table 4.2.3-1. The quantity, type of battery, and the pre-retrieval predicted state of charge remaining for each battery/experiment are tabulated.

4.2.3.1 Lithium Sulfur Dioxide Batteries

Six organizations are involved in studying the lithium sulfur dioxide ($LiSO_2$) batteries used to power all but three of the active experiments flown on LDEF: The Aerospace Corporation, Jet Propulsion Laboratory, NASA LeRC, NASA LaRC, Naval Weapons Support Center Test Laboratories, and SAFT America (original manufacturer of the batteries). The primary objective of the study is to identify degradation modes of the batteries, and to provide information useful to future missions. The $LiSO_2$ technology is relatively new and has had (prior to LDEF) only a short history of application to space activities. NASA selected the high-energy-density $LiSO_2$ cell as the power supply for the active LDEF experiments. Preflight concerns included the hazards associated with elemental lithium, the electrolyte, the discharge process, and all chemical degradation associated with cell aging and those which may be induced by long-term exposure to the LEO environment. The batteries were in the LEO environment for 69 months, which was a sufficient enough period of time to disclose any design inadequacies. Control batteries remained on Earth in cold storage and undischarged from time of manufacture. The analysis, to date, has shown that all $LiSO_2$ batteries performed satisfactorily for their experiment designed loads.

The 92 $LiSO_2$ battery packages were divided into three configurations, 7.5V (12 cells in 4 parallel x 3 cell series strings), 12V (10 cells in 2 parallel x 5 cell strings), and 28V (11 cell series strings). All parallel strings were diode protected to eliminate charging currents. The cells were D-size, type LO-26S SX-2, manufactured by Duracell (now SAFT America). All batteries were located on the backside of the various active trays.

During deintegration of LDEF at KSC, all batteries were checked for leaks and post-flight voltages determined. However, no remaining capacity measurements were made. Interest in the ability of these batteries to retain charge has prompted testing to understand the benefits and limitations of maintaining charge in $LiSO_2$ batteries for space applications.

Discharge data of selected experiment batteries was performed by L. Thaller of Aerospace Corporation (ref. 46). The discharges were performed by placing resistive loads across the cells and monitoring the voltage to determine capacity remaining.

SAFT received ten flight batteries and three control batteries to conduct experimental and destructive physical analysis (funded by the Systems SIG). The results are detailed in reference 45. The retained capacity testing showed that the capacity loss of the non-flight control batteries over a period of 6 years was around

Table 4.2.3-1. LDEF Lithium Batteries—State of Charge

TABLE 1. LDEF LITHIUM BATTERIES - STATE OF CHARGE					
Exp #	**Experiment Name**	**Battery**	**Voltage**	**# of Batts**	**SOC**
A 0038	Pyro Cable Cutter	Li/SO2	12	7	0%
A 0054	Space Plasma - High Voltage	Li/SO2	28	4	39%
A 0076	Variable Conduction Heat Pipes	Li/SO2	7.5	1	0%
A 0076	Variable Conduction Heat Pipes	Li/SO2	28	1	84%
A 0133	Space Based Radar	Li/SO2	7.5	3	25%
A 0133	Phased Array Antenna	Li/SO2	12	2	60%
A 0138-8	Epoxy Composite Materials	Li/SO2	7.5	3	75%
A 0138-8	Frecopa	Li/SO2	28	3	74%
A 0139-A	Crystal Growth Dewers	Li/SO2	7.5	13	49%
A 0180	Recorders for Space Exposure	Li/SO2	12	2	64%
A 0187-1	Clam Shell Elect-Micromeorites	Li/SO2	7.5	1	59%
A 0187-1	Clam Shell Elect-Micromeorites	Li/SO2	12	2	73%
A 0201	Sun Sensor-Dust Experiment	Li/SO2	7.5	2	20%
A 0201	Sun Sensor-Dust Experiment	Li/SO2	12	2	85%
A 0201	Sun Sensor-Dust Experiment	Li/SO2	28	6	88%
M 0003	Space Env. Effects on S/C Mater.	Li/SO2	7.5	2	0%
M 0003	Space Env. Effects on S/C Mater.	Li/SO2	7.5	2	76%
M 0003	Space Env. Effects on S/C Mater.	Li/SO2	12	2	0%
M 0003	Space Env. Effects on S/C Mater.	Li/SO2	12	1	46%
M 0003	Space Env. Effects on S/C Mater.	Li/SO2	12	2	76%
M 0003	Space Env. Effects on S/C Mater.	Li/SO2	12	1	88%
M 0004	Space Effects on Fiber Optics	Li/SO2	7.5	1	0%
M 0004	Space Effects on Fiber Optics	Li/SO2	12	1	71%
M 0004	Space Effects on Fiber Optics	Li/SO2	12	2	85%
M 0004	Space Effects on Fiber Optics	Li/SO2	28	6	85%
M 0006	Space Effects - Optical Surfaces	Li/SO2	7.5	1	76%
M 0006	Space Effects - Optical Surfaces	Li/SO2	28	1	77%
P 0003	LDEF Thermal Measurements	Li/SO2	7.5	1	73%
S 0010	Exposure of S/C Coatings	Li/SO2	7.5	1	76%
S 0010	Exposure of S/C Coatings	Li/SO2	28	1	77%
S 0014	Photovoltaic Cells - Sun Sensor	Li/SO2	7.5	1	0%
S 0014	Photovoltaic Cells - Sun Sensor	Li/SO2	12	1	85%
S 0014	Photovoltaic Cells - Sun Sensor	Li/SO2	28	2	0%
S 0069	Carosel, Opt sys	Li/SO2	7.5	1	0%
S 1001	Low Temp Heat Pipes	Li/SO2	7.5	1	0%
S 1001	Low Temp Heat Pipes	Li/SO2	12	1	85%
S 1002	Solar cells, QCM	Li/SO2	7.5	1	0%
S 1002	Solar cells, QCM	Li/SO2	28	2	80%
S 1005	Flat Plate Heat Pipe Experiment	Li/SO2	7.5	1	0%
S 1005	Flat Plate Heat Pipe Experiment	Li/SO2	12	1	85%
INIT	LDEF Initiation System	Li/SO2	28	2	89%
S 0069	Carosel-Thermal Cont. Surfaces	Li/CF	28	4	0%
S 1005	Flat Plate Heat Pipe Experiment	Li/CF	28	6	0%
S 1001	Low Temp Heat Pipes	NiCd	18	1	Recharge

11% (average of three batteries) versus almost 30% of the initial capacity for an unused flight battery. The difference in capacity loss is tentatively attributed to differences in ambient temperatures. The ground-stored batteries did not see temperatures above 40°F and the flight batteries were subjected to temperatures ranging from 41°F to 95°F over the 69-month mission.

Figures 4.2.3.1-1 through 4.2.3.1-7 show representative photographs of the $LiSO_2$ battery disassemblies performed by SAFT. Figure 4.2.3.1-4 shows a closeup of the glass to metal seal. The corrosion around the glass seal was expected and was also found on the control batteries. The most recent $LiSO_2$ design uses TA-23 (Sandia) glass instead of the borosilicate (Corning 7052) glass used on the LDEF batteries. This design change minimizes the possibility of lithium attack of the glass insulator. Figure 4.2.3.1-6 shows the condition of the lithium and the carbon cathode from a control battery. Figure 4.2.3.1-7 shows the lithium and carbon cathode from a flight battery which was at a 35% state of charge. Note the absence of lithium.

In general, $LiSO_2$ batteries generally exhibit good charge retention, with loss in capacity of less than 3% to 5% per year. LDEF $LiSO_2$ batteries showed charge-retention properties commensurate with that expected, based on the temperatures experienced by these batteries. The favorable performance of LDEF lithium-sulfur-dioxide batteries adds credence to the selection of lithium-sulfur-dioxide batteries of similar design for the Galileo mission.

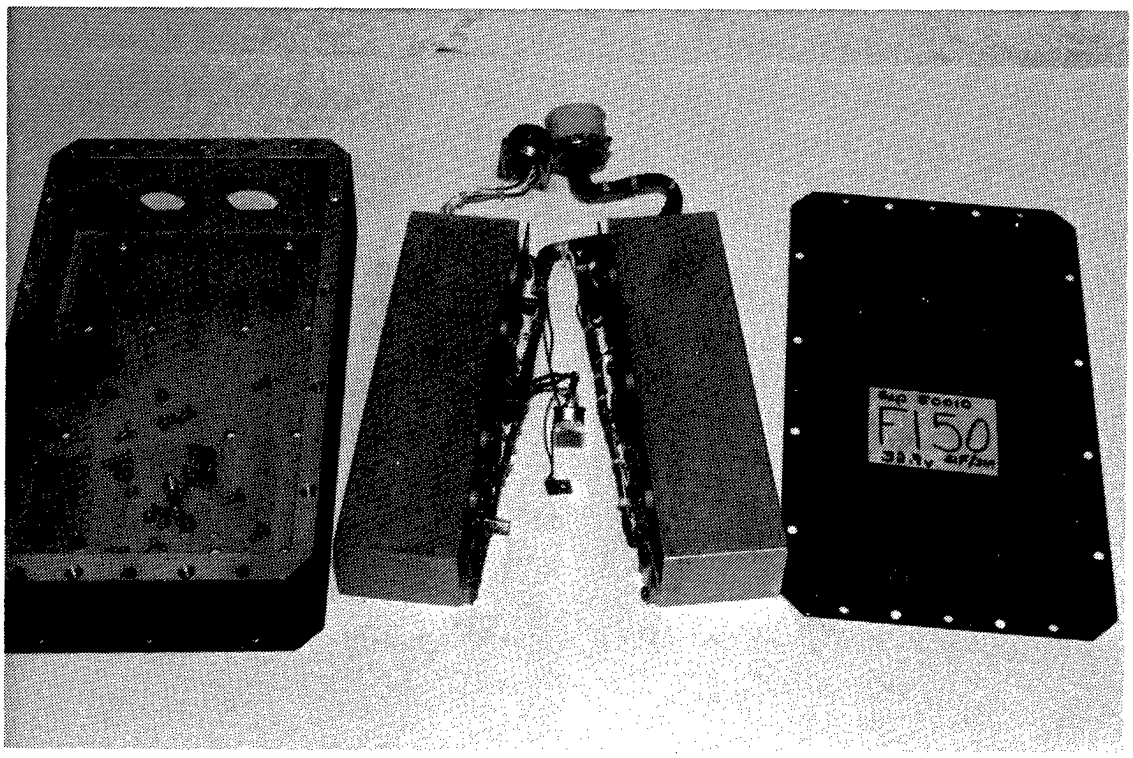

Figure 4.2.3.1-1. $LiSO_2$ Battery Case Disassembled

Figure 4.2.3.1-2. Closeup of $LiSO_2$ Cell Block

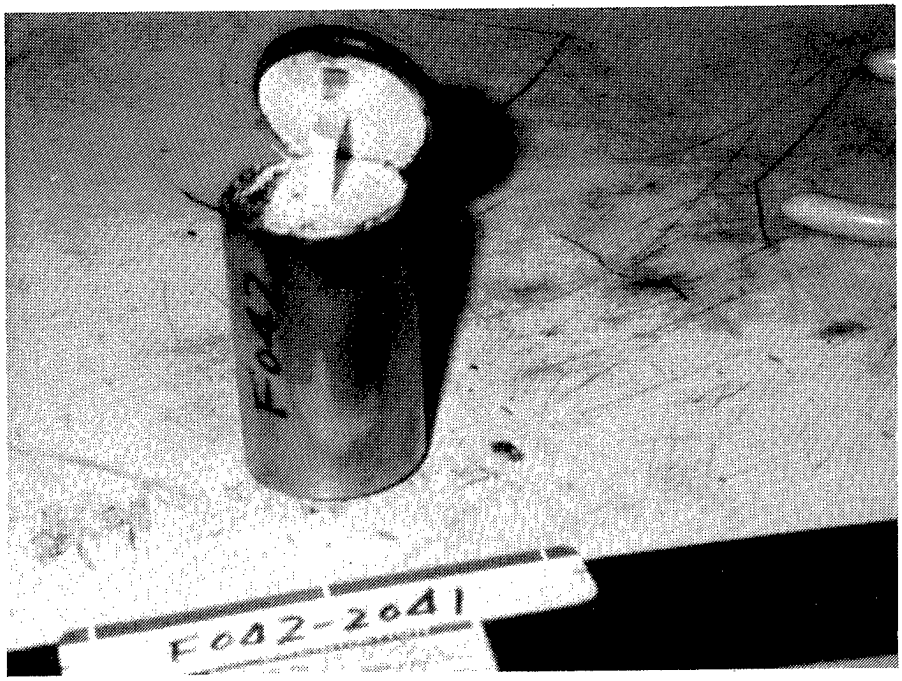

Figure 4.2.3.1-3. $LiSO_2$ Cell Opened

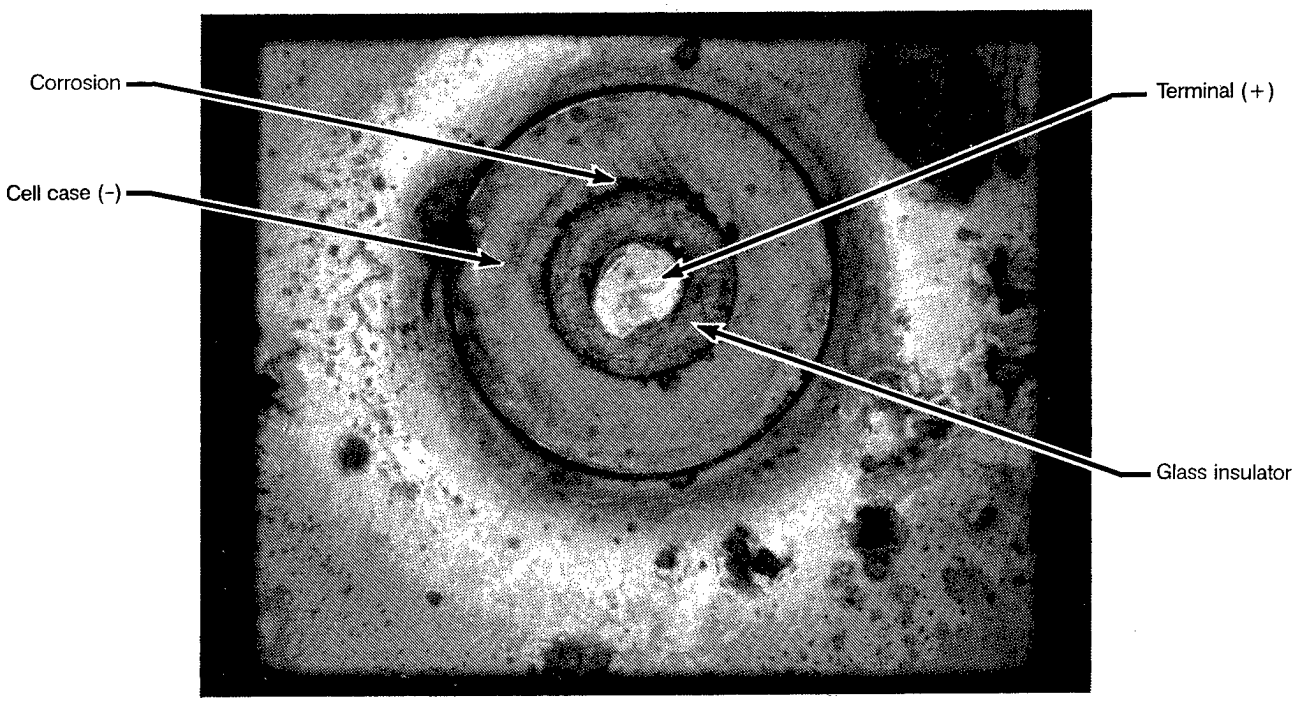

Figure 4.2.3.1-4. Closeup of Glass to Metal Seal

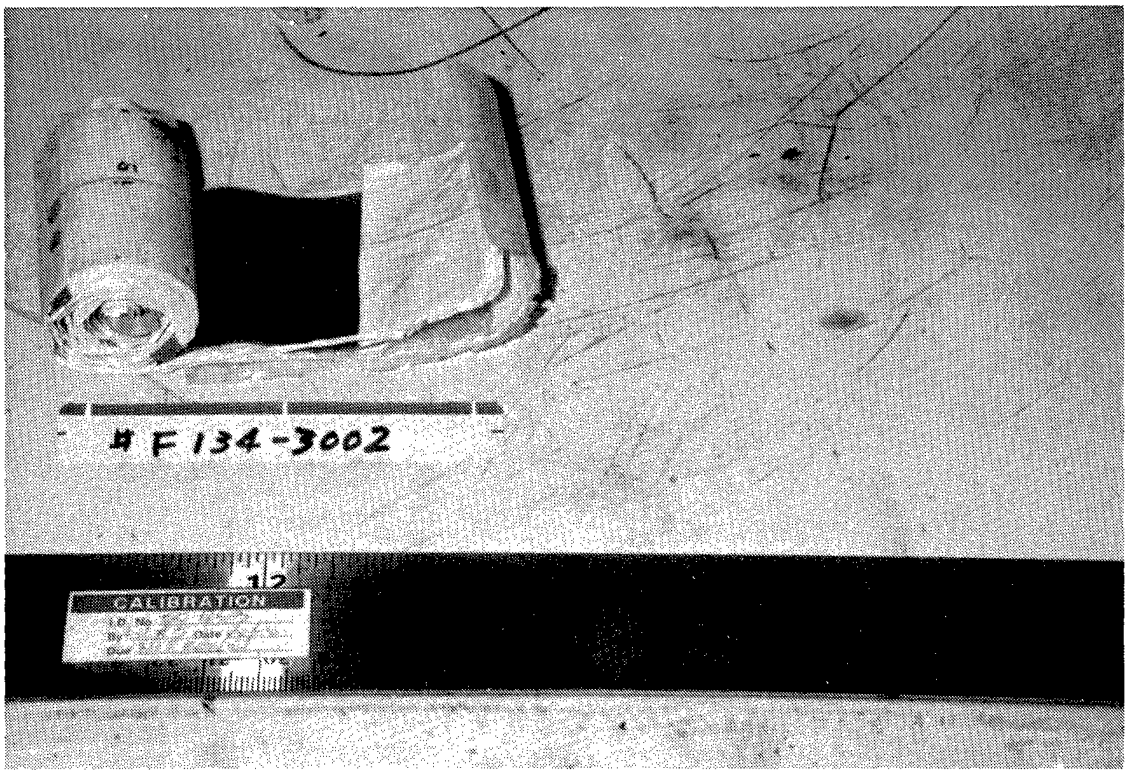

Figure 4.2.3.1-5. $LiSO_2$ Cell Electrode Materials

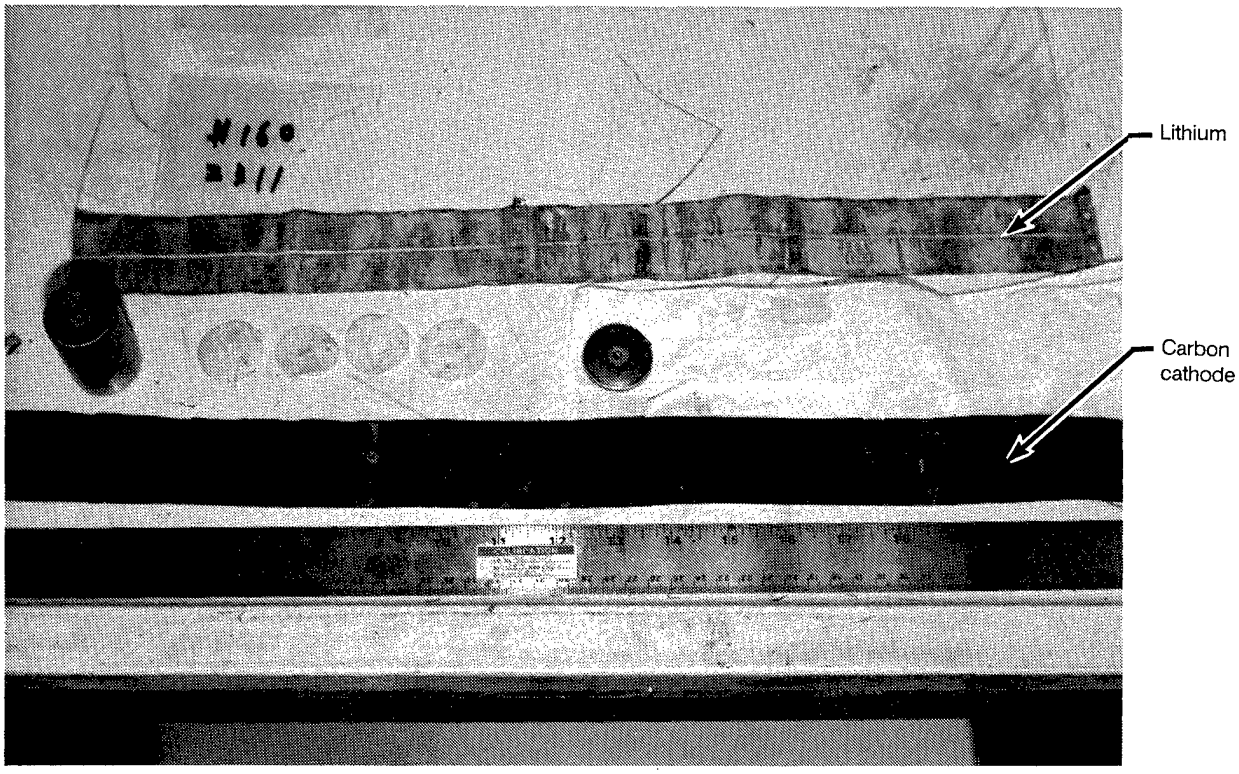

Figure 4.2.3.1-6. $LiSO_2$ Cell Components – Control Cell

Figure 4.2.3.1-7. $LiSO_2$ Cell Components—Flight Battery With a 35% State of Charge

4.2.3.2 Lithium Carbon Monofluoride Batteries

Investigation of lithium carbon monofluoride (LiCF) batteries was performed by AZ Technology, NASA MSFC, and Naval Weapons Support Center. Four LiCF batteries were flown on the Thermal Control Surface Experiment (S0069) and six batteries were used on the MSFC heat pipe experiment (S1005). As predicted, all 10 batteries were depleted on return of LDEF. Figure 4.2.3.2-1 shows the gradual degradation of battery voltage with time for one of the four batteries used on S0069 (ref. 47). The required experiment life was 12 months, with an expected life of 15 to 18 months. All batteries met or exceeded both of these.

The cells were roughly double D size, vented construction with a rated capacity of 25 Ah and a nominal voltage of 3 volts. The cells were potted into a plastic block (figure 4.2.3.2-2). The shelf life of these cells was predicted to be about seven years. They were manufactured in January 1982 by Eagle-Picher Industries (ref. 48).

All 10 LiCF batteries had a strong odor, first noticed during the deintegration of S0069 and S1005 at MSFC. The electrolyte used in the Eagle-Picher LiCF batteries is dimethyl sulfite, which contains small amounts of other sulfur compounds that can be quite odorous. AZ Technology investigated the effect of the leaked electrolyte vapors on the ethylene propylene O-ring seal of the battery containment case (ref. 49). The presence of this strong odor was determined to be the normal byproduct of the discharge process. The LiCF cell is designed with an expansion diaphragm on the top of the cell with a sharp, rigid protrusion adjacent to the diaphragm. Figure 4.2.3.2-2 shows a LiCF battery (made up of 13 individual cells) removed from the battery case. Figure 4.2.3.2-3 is a closeup of one of the LiCF cells showing the expansion diaphragm. The diaphragm expanded during the slow discharge process when internal cell pressures increased. Eventually the diaphragm was punctured, releasing the solvent vapors. The cells were in sealed battery boxes. The seal (O-ring) experienced a softening and deformation due to the extended exposure to the electrolyte vapors which resulted in leakage of the vapors. However, this created no performance problem for the battery or associated equipment. Figure 4.2.3.2-4 shows the cross section of one of the battery box seals and figure 4.2.3.2-5 shows a control O-ring and flight O-ring. Examination of the ground-stored LiCF batteries showed the same phenomena.

H.L. Lewis and V. L. Hammersley at the Naval Weapons Support Center, Crane, Indiana performed a detailed investigation in to the post-flight condition of three LiCF batteries; one flight battery provide by MSFC, one control battery discharged to 0 volts prior to dissection, and one control battery dissected as received (ref. 48). Their findings showed that no significant changes occurred in the chemistry or function of the LiCF cells as a result of operation on LDEF. The differences found in material compositions between the three batteries were either trivial, or when significant, a result of long term degradation of cell electrolyte in storage prior to discharge.

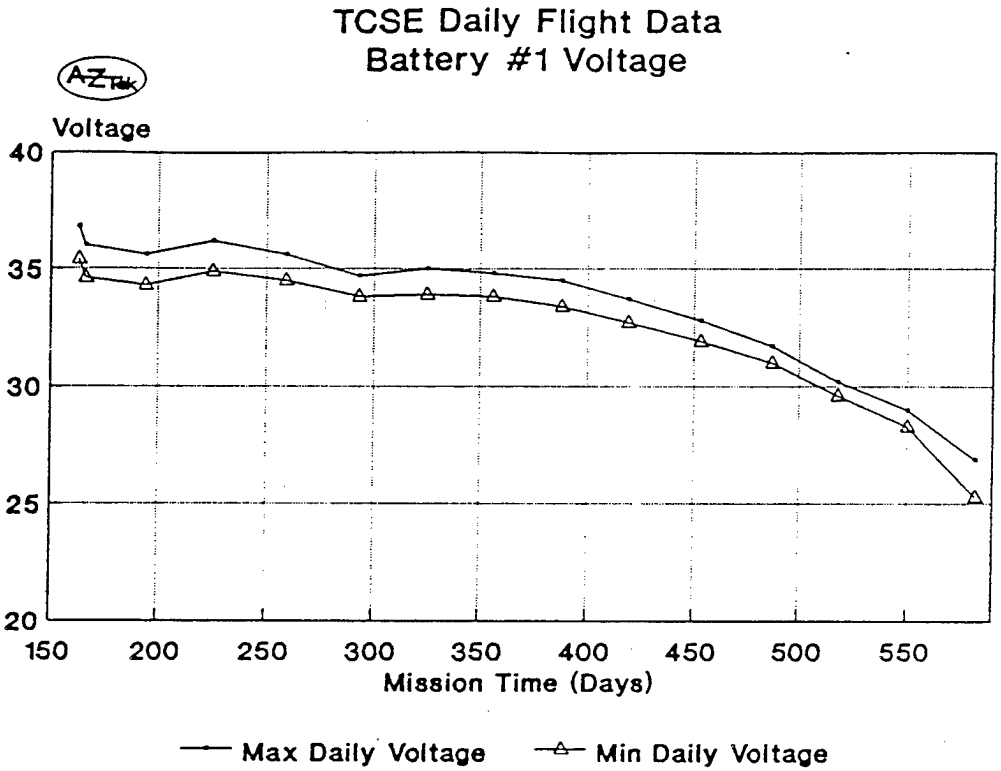

Figure 4.2.3.2-1. Gradual Voltage Decay of LiCF Battery in Flight

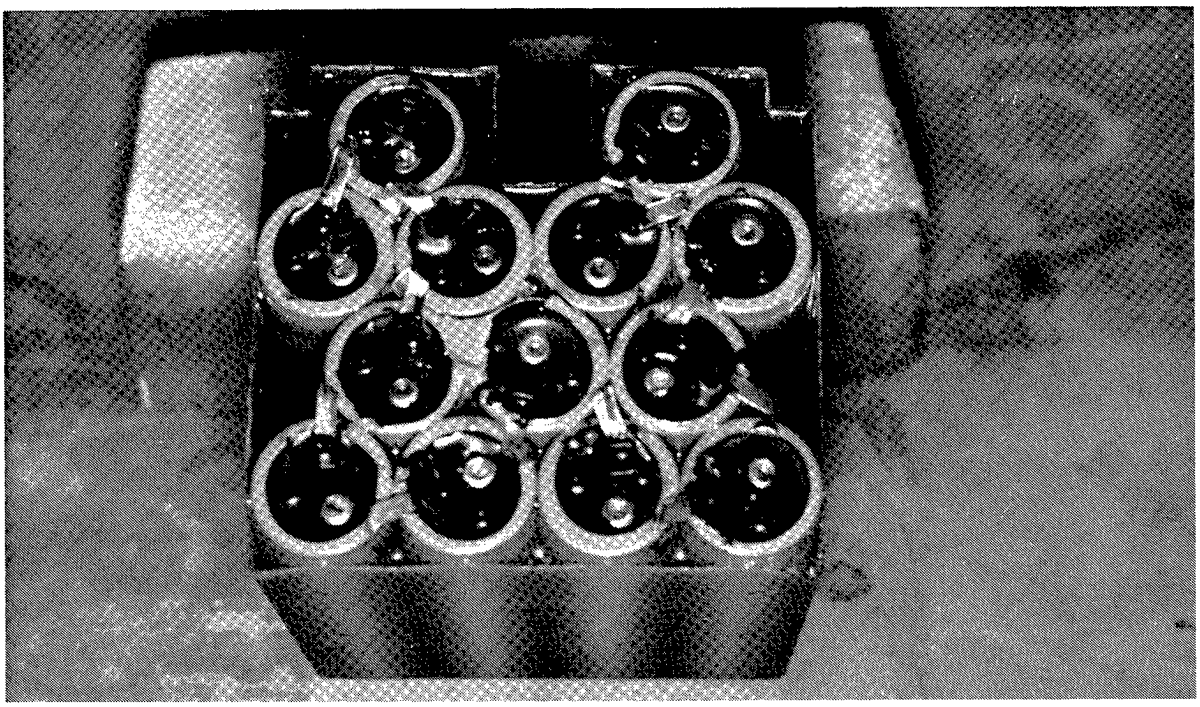

Figure 4.2.3.2-2. LiCF Cells Removed From Battery Case

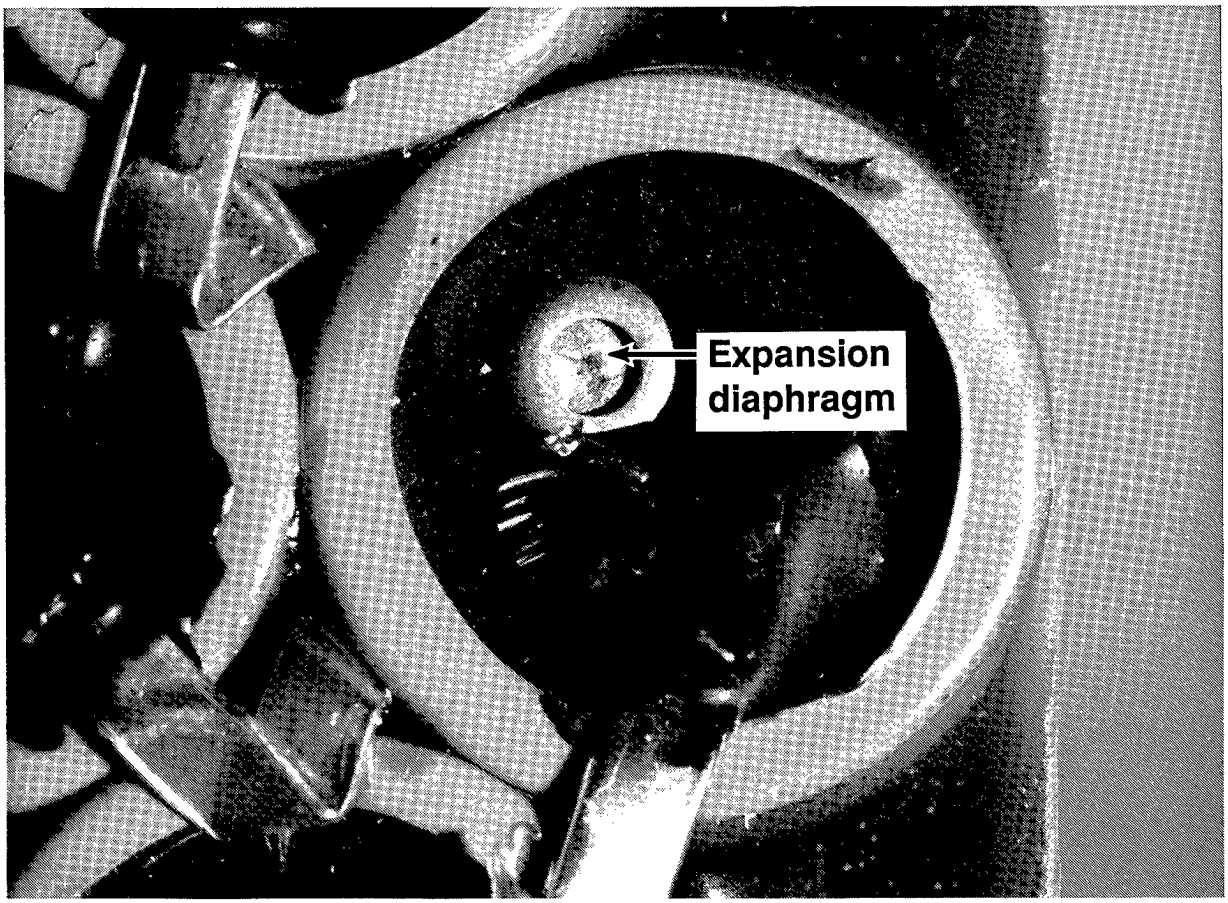

Figure 4.2.3.2-3. LiCF Cell

Figure 4.2.3.2-4. Battery Box O-Ring

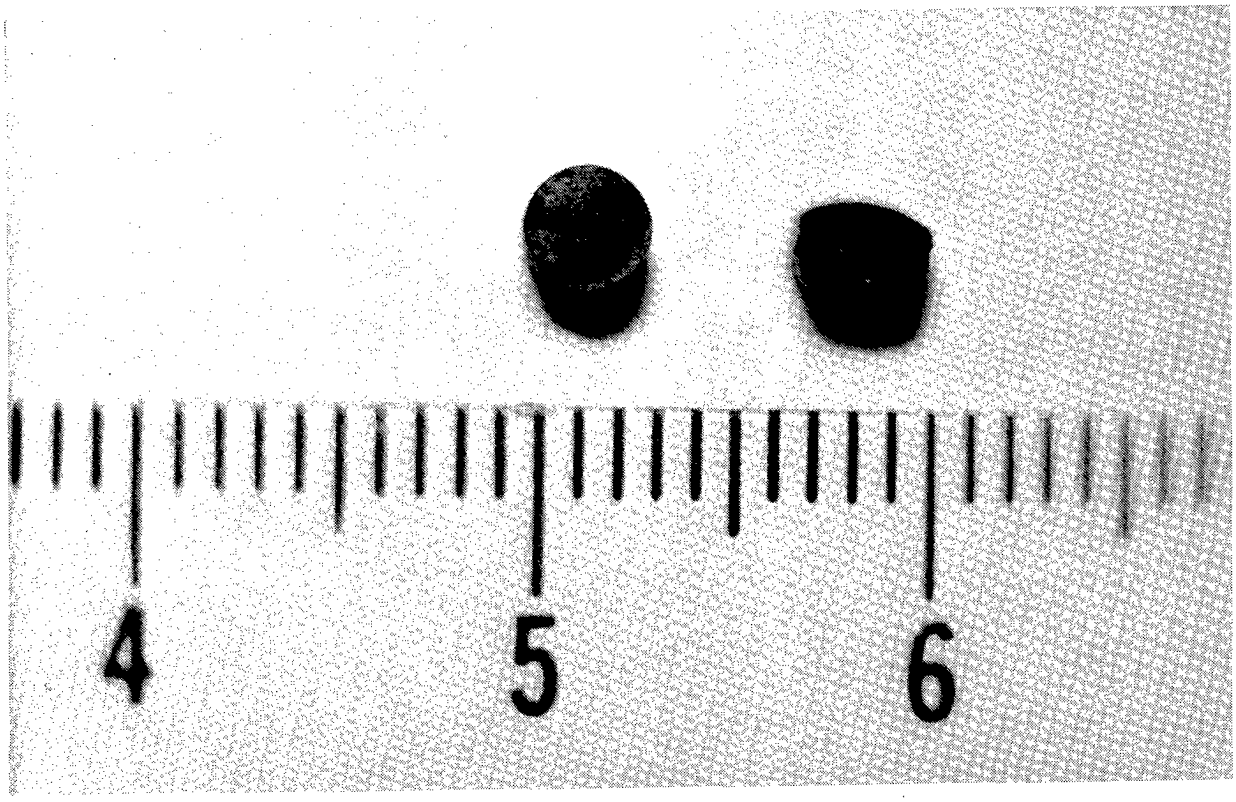

Figure 4.2.3.2-5. Control O-Ring Versus Flight O-Ring

4.2.3.3 Nickel Cadmium Batteries

One nickel cadmium battery, manufactured by General Electric, was flown on the Low Temperature Heat Pipe Experiment Package (Experiment S1001). This battery was continuously charged by a four arrays of solar cells located on the space end of LDEF (see section 4.2.7 for more details on the 4 arrays). Analysis and test of the battery has been conducted by S. Tiller and D. Sullivan of NASA Goddard Space Flight (ref. 50). The battery consisted of 18 cells, which were mounted onto a 0.75-in thick aluminum baseplate. Prior to flight, power analysis for the 12-Ah NiCd battery indicated a need for 2 to 3 amp discharge; however, reduction in the experiment current requirements during flight resulted in a much lower power demand. The resulting overcharge of the battery became a duration test for the NiCd battery. These batteries are not known for their ability to withstand excessive overcharging for long times. The battery survived the entire 6-year usage and was still functioning upon retrieval. The overcharge developed internal pressure, resulting in bulging of the cell cases, especially those cells on the end of the cell pack (see figure 4.2.3.3-1).

The loss of overcharge protection is obvious from the difference in voltage performance shown for preflight and postflight cells on constant charge, see figure 4.2.3.3-2. Preflight charge profile showed all cells were matched and reached full state of charge in 18 hours, while maintaining voltage below 1.46V. Post-flight data reflected considerable differences between cells with cell #10 (this cell bulged the most during the mission) reaching a high voltage of 1.52V which tripped the charge for the battery off at 14 hours of charge. Discharge performance (figure 4.2.3.3-3) produced similar results with preflight reaching 6.4 hours discharge at a total capacity/4.8 hour rate (2.5 amps) while postflight cells attained only 6 hours for the same conditions.

Despite the obvious bulging of some cells, loss of overcharge protection, and the failure of cell #10 during the open circuit recovery test, the battery still has the capability to provide output current in excess of the cell manufacturer's rated capacity of 12.0 ampere-hours.

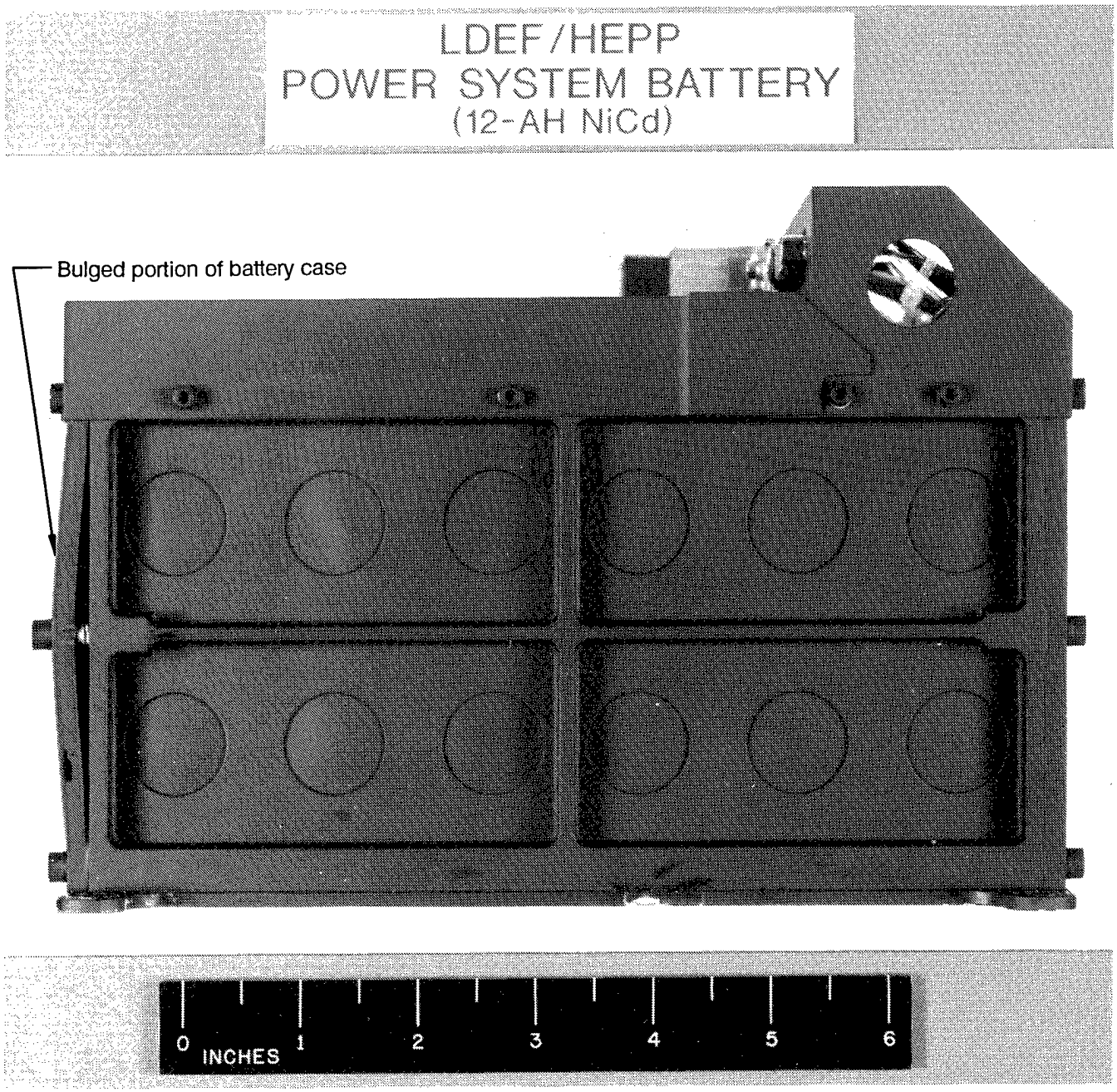

Figure 4.2.3.3-1. Bulging of NiCd Battery Case

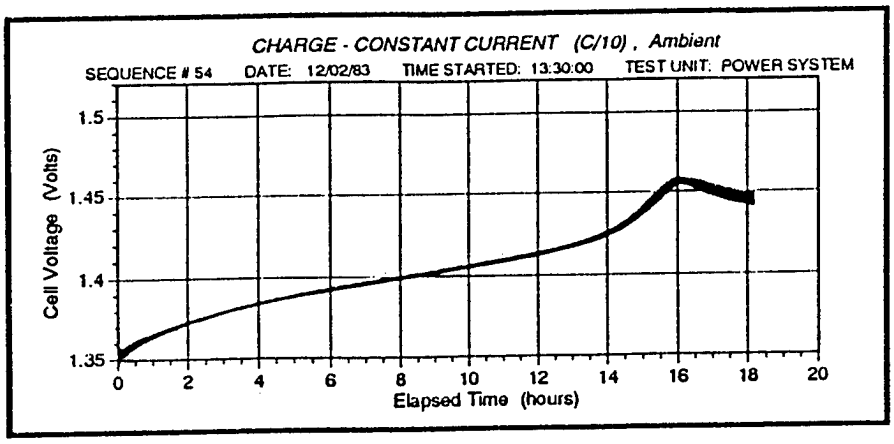

Pre-flight Capacity Charge

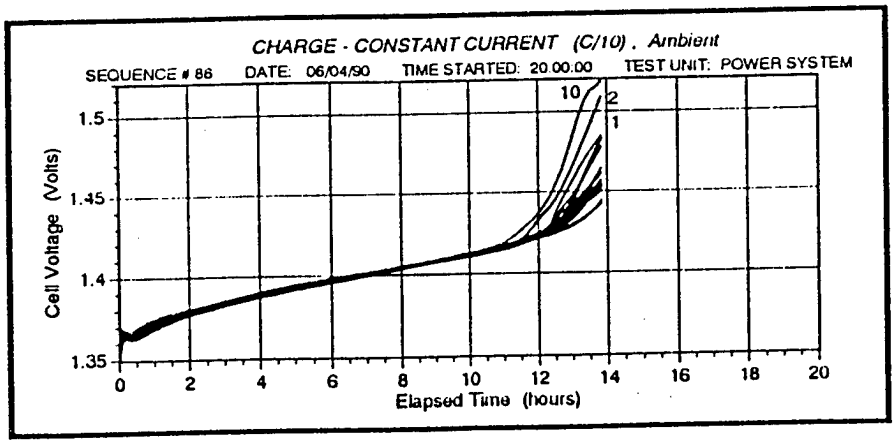

Post-flight Capacity Charge showing loss of overcharge protection

Figure 4.2.3.3-2. Pre- and Postflight Charge of NiCd Cells

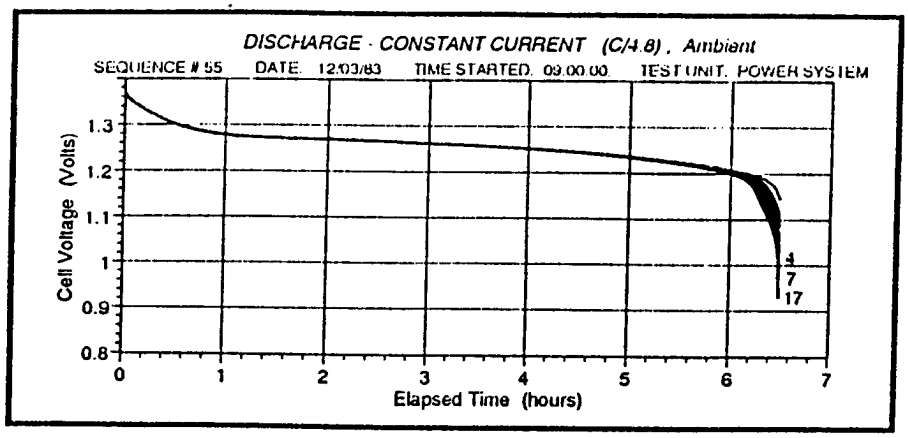

Pre-flight Capacity Discharge

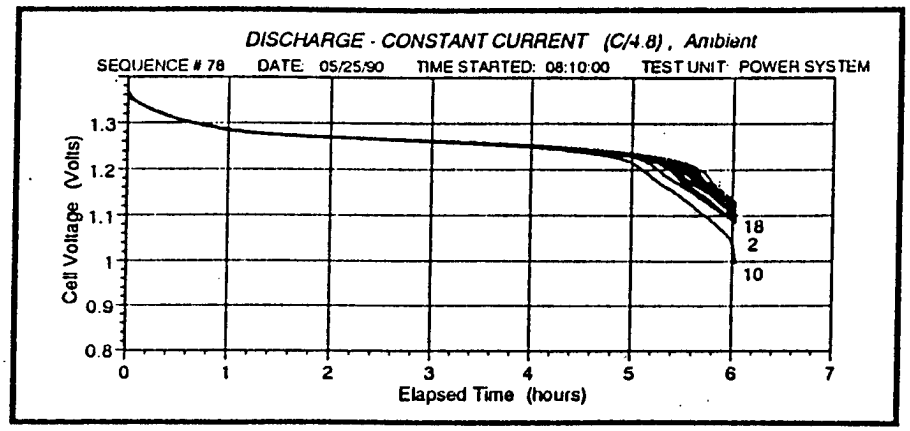

Post-flight Capacity Discharge

Figure 4.2.3.3-3. Pre- and Postflight Performance of NiCd Cells

4.2.4 Wire Harness

The LDEF wire harness was essential to the success of all active experiments, as it carried the initiate signals from the EIS. It was assembled in-place on the LDEF frame, using Teflon insulated wire and nylon cable ties. Much of the harness also was protected by shielded braid and an outer Teflon jacket. The majority of the harness was well shielded from direct exposure to the external environment. There was considerable interest in determining whether any significant deterioration had taken place.

The first objective was to perform as much inspection and testing as feasible prior to any disruption of the harness and associated connectors. This initial inspection took place during the tray removal activity. As the LDEF structure was rotated, all accessible wiring of the primary structure and of the experiment trays was visually examined with five power magnification. Later, as more of the system became accessible, continuity measurements were made. Insulation resistance measurements at 500V dc were made after all the trays were removed. Disconnect torque measurements were also made on all connectors whenever possible during their initial removal. Following deintegration of all trays, the entire wire harness was removed and examined (fig. 4.2.4-1) and portions were subjected to additional testing at Boeing.

During the in-place visual inspection, several small tears were observed in the Teflon jacket, in some cases severe enough to expose the shield braid. However, these were attributed to installation, rather than to the orbital exposure. None of these tears was caused by or led to any failure of the electrical system.

All connectors were found to be properly coupled, and disconnect torques were within specified limits. There was no degradation of dielectric components, interfacial seals or finishes on any of the connectors examined. The wiring remained flexible with no indications of insulation cracking or other degradation within the primary structure. Electrical tests (continuity and insulation resistance at 500V dc) showed the circuitry to be intact, with no observed insulation degradation.

The harness connectors supplied by the LDEF project to the experimenters were space rated, and had been subjected to vacuum bakeout. It was noted that many of the other connectors used by experimenters were Mil-Spec or equivalent commercial variants, and were not space rated. Most were not subjected to a vacuum bakeout process prior to assembly, which would have reduced outgassing in a low-pressure environment. Lack of thermal-vacuum testing was common among experiment systems.

Most wire harness connectors did not contain strain relief adaptors or cable clamping devices. A silicone encapsulating compound (thought to be Products Research Corp. PRC 1535) had been applied at the point the wiring exited the connectors. The encapsulant remained flexible. However, outgassing of silicones was found to have contributed significantly to surface contamination on the spacecraft and experiments (ref. 32).

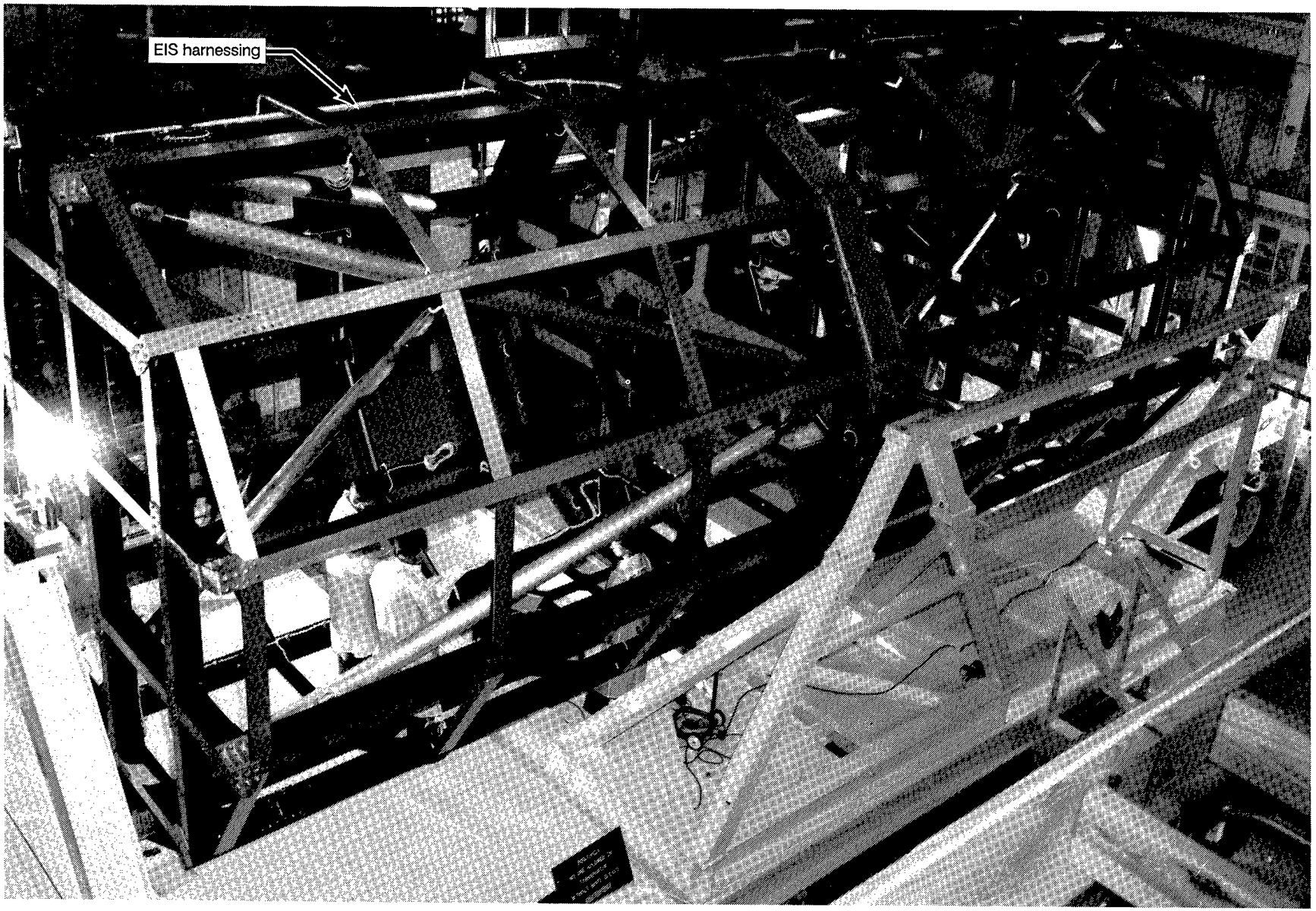

Figure 4.2.4-1. EIS Harnessing on LDEF Structure

The primary wire harness was attached to the spacecraft with glass-filled nylon cable clamps, and wire bundles were held together with nylon cable ties. The only failures occurred on the exterior of tray B9 (experiment S0010) in conjunction with a cannister (EECC). As shown in figure 4.2.4-2, some of these nylon cable ties had fractured, and many were blackened (normally they are beige or white). It is thought the failures occurred from stresses applied during the opening and closing of the canister, following damage from exposure to ultraviolet radiation.

The only evidence of connector deterioration was found on the four trays of the Interstellar Gas Experiment (A0038). The interfacial seals of uncapped circular connectors were shriveled, and the silver plating on MHV coaxial connector bodies was severely tarnished. Both of these connectors were mounted on externally surface of the trays.

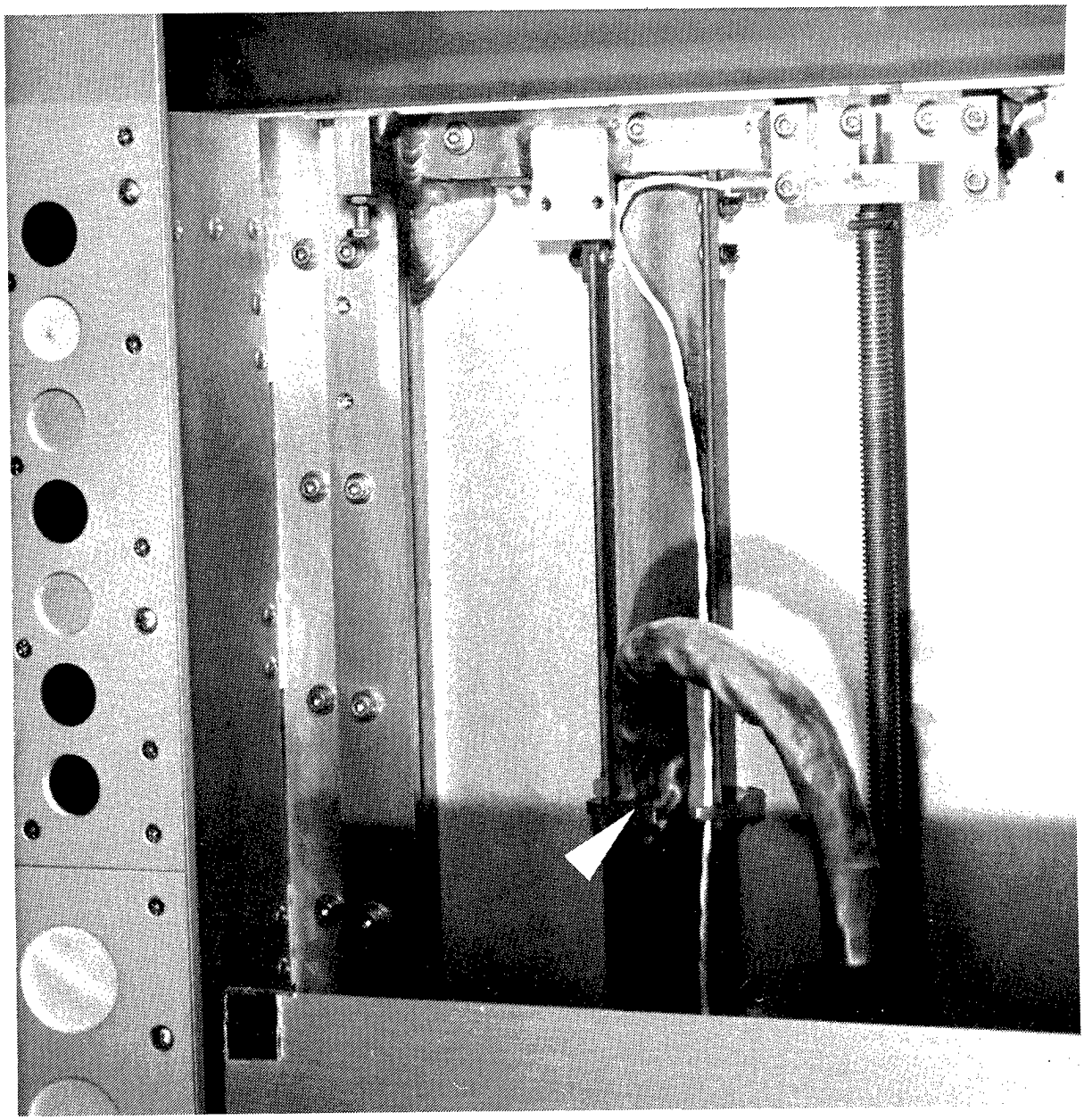

Figure 4.2.4-2. An Example of a Broken Cable Tie on the EECC

4.2.5 Failure Analysis of A0038: Interstellar Gas Experiment

The Interstellar Gas Experiment (IGE) was one of the more complex experiments on LDEF, with seven "cameras" located on four trays (fig. 4.2.5-1). Each camera contained five copper-beryllium foil plattens, which were to be sequentially rotated out of their exposed position by firing pyroelectric wire cutters when pulsed by their electronic timer/sequencer units. After return of LDEF to KSC, it was found that only one of the 35 plattens had rotated during flight (tray H9, S/N 1005). It was also noted that one tray (tray F6) containing a single camera and the master initiate relay, had apparently failed to activate: its battery was almost completely charged, while those of all the other six units were completely discharged. Most of the electronic systems were sent to Boeing for failure analysis. The results provide a good illustration of some of the pitfalls in experiment design which should be avoided in the future.

Experiment Set/Reset System. The experiment systems were activated by the LDEF EIS, which operated a single master initiate relay (standard NASA-supplied part). The experiment utilized this relay to activate separate slave relays in each of the seven camera systems. Activation of the slave relays applied power to individual timer/sequencers and high voltage power supplies (HVPS) in each camera, but timer countdown and sequencer operations could not begin until the voltage on a reset input control line was raised above a startup threshold level. The master relay was found to be activated (set), and six of the seven slave relays were set. However, one slave relay did not activate during flight, so its sequencer (tray F6) never received power. This condition was documented at KSC during the preliminary examination, and intermittent operation of the F6 slave relay was confirmed in the laboratory.

The only link between the seven cameras other than the slave relay controls was a common reset control line. Upon initiation, the voltage on this line was controlled by a resistor-capacitor network duplicated in each camera (fig. 4.2.5-2). The purpose of the network was to keep all timer/sequencers inactivated for several minutes after power was first applied. Timer operation could only begin when the reset voltage rose above the switching threshold of the input CMOS microcircuit (approximately 5V when the batteries were fully charged). However, failure of the slave relay on the F6 camera prevented power from being applied to the F6 circuitry. Therefore, its input diodes (part of the CMOS ESD input protection circuit) became forward biased by the reset voltage, and the circuit acted as a current sink, drawing enough current to hold the reset voltage down to about 2V (due to the high impedance of the RC network charging resistors). Thus, the reset voltage remained below the switching threshold of the powered circuits, and all should have been prevented from operating and firing any of the wire cutters. Even though held in the reset state, current drain through the HVPS was sufficient to fully discharge the 6 powered unit batteries in about six months.

The principal failure mode is thus explained by the relay failure in tray F6. This should have prevented firing of all 35 platten sets. It does not explain why the first wire cutter set fired on one of the six powered cameras. It was noted that shortly prior to launch, all four IGE trays plus the CME tray (A0187-2) were removed from LDEF to

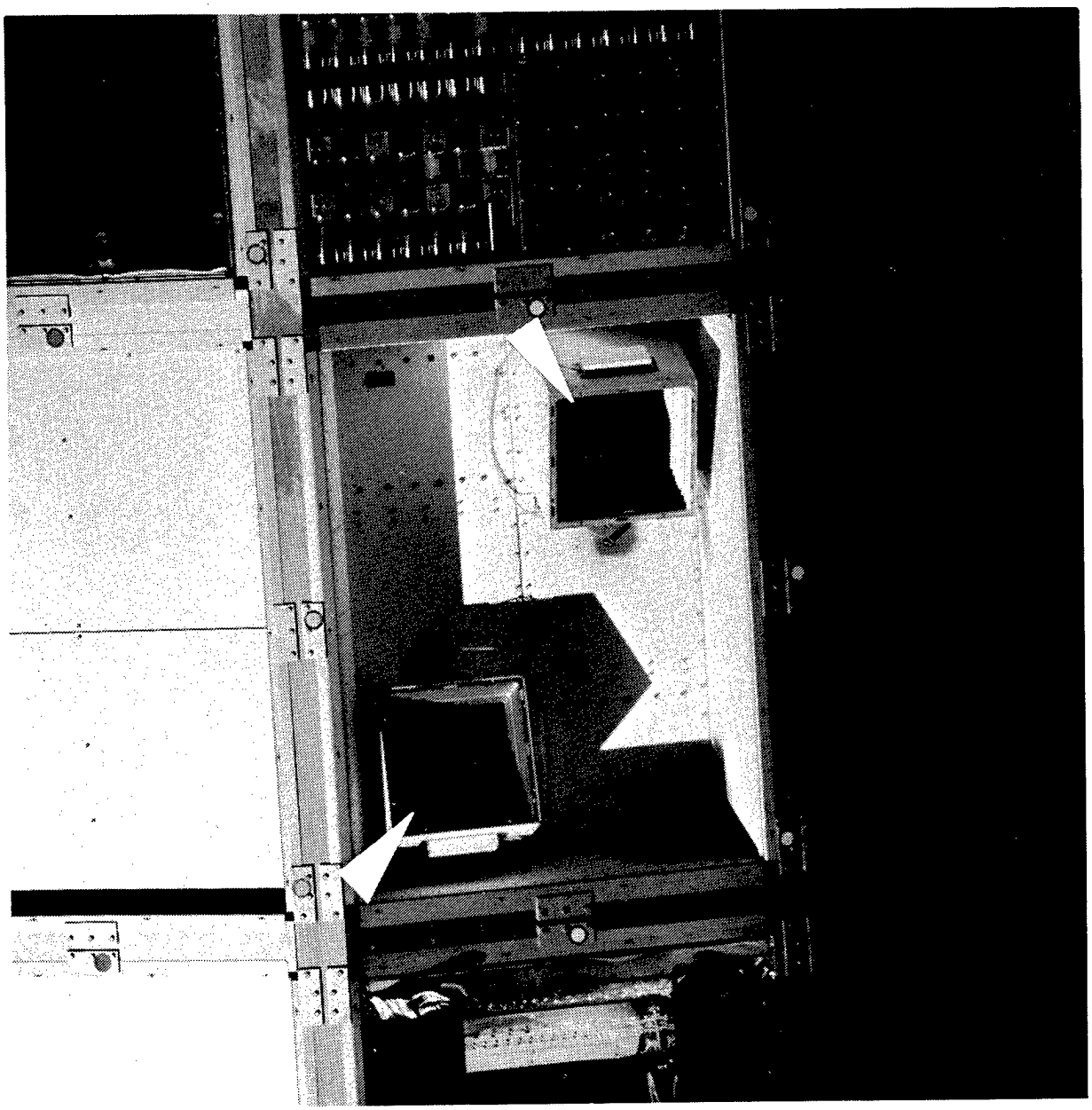

Figure 4.2.5-1. Tray E-12, Showing Two of the IGE Cameras (Arrows)

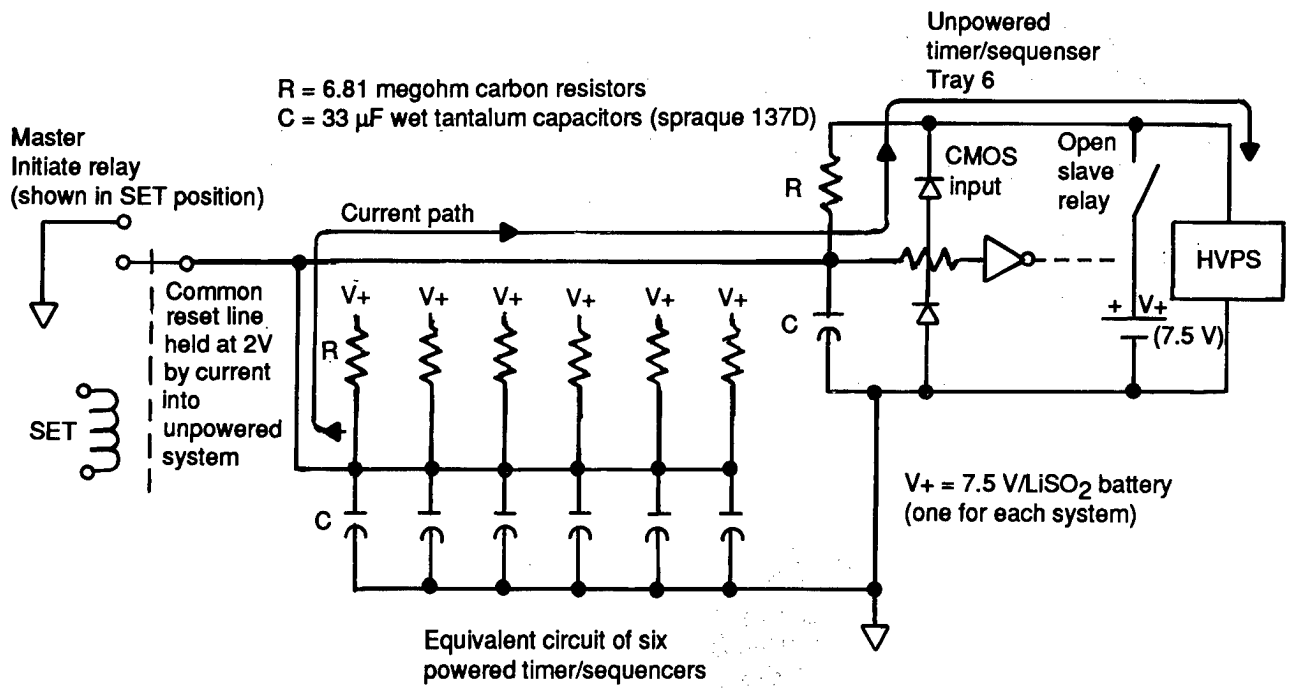

Figure 4.2.5-2. The Reset Circuit of the IGE Systems, With the Failure Current Path Indicated. Due to the high value resistors (R), the voltage on the common reset line was held below the startup threshold level for the systems.

check cable integrity, due to observed open plug connections. All the tray cables were apparently removed and tested, the open connections repaired, and the systems reassembled, reset, and reinstalled. The pyroelectric wire cutters are known to be very static sensitive. It is conceivable that the set which fired was activated by ESD during the repair operation. Since the cameras were kept covered until the just before flight, such a firing might not have been noticed (very little noise occurs during firing).

The flight wire cutters and other spare units were tested at the Pyrotechnic Test Facility at Johnson Space Center. This was the same test lab that had performed the pre-flight testing in 1979. Testing at JSC included bridgewire resistance, X-rays and N-rays (used to determine status of propellant), and firing of four of the wire cutters. All those tests indicate the wire cutters were in good condition and fired normally. Wire cutters were also successfully fired at Boeing, using two different timer/sequencers. There was no indication that the system would not have fired the cutters if the timers were operating normally.

The reset input design relied upon a high impedance circuit, charging a high-value capacitor through a high resistance to obtain a long time delay. The capacitor chosen was a silver case, wet tantalum unit known to develop silver dendrites which can cause shorting (this type of capacitor is not recommended in current spacecraft designs). Due to the high charging resistance, insufficient energy was available to clear such shorts. This failure mode was responsible for the failure of the similar timer/sequencer in another experiment (A0187-1, Chemistry of Micrometeoroids, discussed in sec.4.2.6). The required leakage current to prevent operation of a single

timer/sequencer is less than one microamp. Also, use of a common reset line would make such a short in one unit affect all seven systems.

E-Cell Observations. These small microcoulombmeters were used by two experiments to record the time of certain events. On both experiments (IGE and A0054, the Space Plasma High-Voltage Drainage Experiment), several of these cells leaked electrolyte into the vacuum environment. The resultant emission of acidic electrolyte destroyed the Teflon sockets on the IGE units (fig. 4.2.5-3). Leakage affected roughly 5% of the E-cells in both experiments, even though they were from two different manufacturers (Plessey and Pacific Electron Corporation). It appears that none of the E-cells had been subjected to thermal vacuum testing, so a 5% failure rate may not be unreasonable. The IGE E-cell failures occurred in high-voltage power supply boxes which received direct solar exposure, so heating may have been a factor.

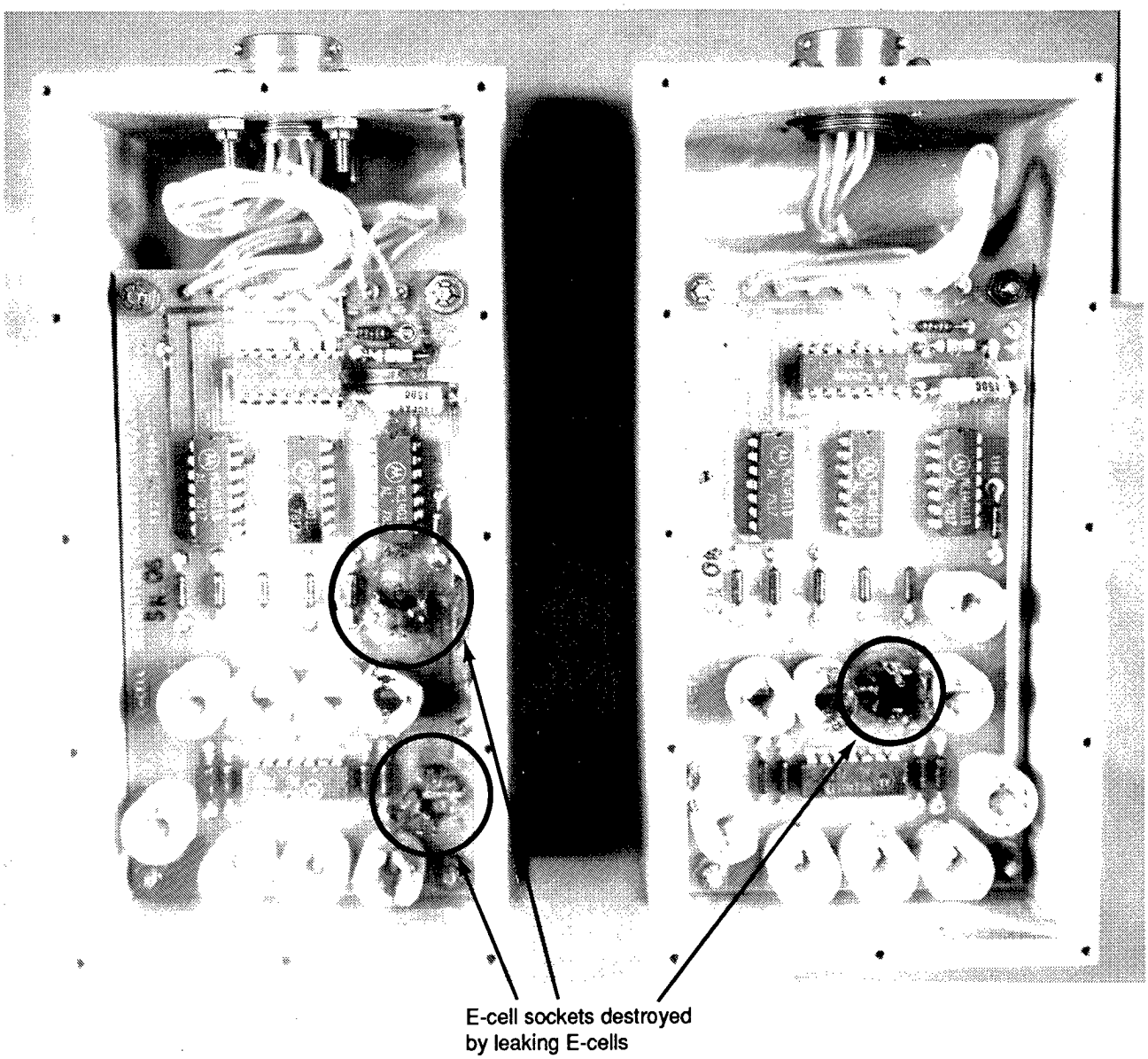

Figure 4.2.5-3. Two of the IGE High Voltage Power Supplies Showing Effects of E-Cell Electrolyte Leakage

4.2.6 Failure Analysis of A0187-1: Chemistry of Micrometeroids Experiment

This experiment utilized sets of foil collector plates hinged along one side and controlled to open or close in a clamshell fashion. They were launched in the closed position. During flight they were to open for approximately 300 days, and then close. On recovery they were found to be open. Preliminary analysis showed there was no stop designed into the timer/sequencer program, because the original LDEF mission was to have only lasted 10 to 12 months. There was sufficient battery life to cycle the clamshells throughout the 69-month mission and they happened to be open at the time of recovery due to the programmed open-close time periods.

A second anomaly was observed during initial attempts to close the clamshell doors at KSC. It was necessary to bypass the timer/sequencer to close the doors, since its external clock input did not seem to be working. Subsequent failure analysis at Boeing showed the entire timer/sequencer was being held in a reset state due to leakage in the reset input capacitor (C in fig. 4.2.5-2). This timer/sequencer is the same design as used in the IGE experiment, although only one system was used rather than seven in parallel. It is not possible to determine when the leakage condition occurred. The system worked during the initial startup period, opening the clamshell doors. If the capacitor leakage developed prior to the programmed door closure, the doors would have remained open, rather than going through multiple open-close cycles.

4.2.7 Solar Cells

This section presents the results obtained by the photovoltaic community on technologies and materials used to fabricate space solar arrays. An opportunity such as this, to generally experiment with technologies in an environment that is technically unfeasible to reproduce on the Earth's surface, does not come without risks nor guarantees of success. However, given the opportunity, the technology, and the participants, the LDEF experiment has provided valuable data pertaining to the use of solar arrays in a space environment, parts of which are presented here.

This section will focus on those experiments that were designed specifically for studying the effects of a LEO space environment on actual solar cell technologies. A brief description will be presented of the experiments, followed by a brief summary of the results obtained from the particular experiment. The information contained here are only the highlights and results that each experimenter has reached given the data from their particular experiment. Following the discussion of the individual experimenters results will be a cumulative summary of the results presented along with fabrication methods and techniques to use when building solar arrays to avoid similar degradation mechanisms. Table 4.2.7-1 lists the experiments that are covered by this section, the number and types of solar cells, and a brief description of the experiment.

Table 4.2.7-1. List of LDEF Photovoltaic Experiments

Principal Investigator	Type of Cells	Number of Cells	Experiment/Description
NASA LeRC - D. Brinker	Si, GaAs	155	S0014 - Advanced Photovoltaic Experiment
NASA MSFC - A. Whitaker	Si	4 modules & 5 cells	A0171 - Solar Array Materials Passive LDEF Experiment
NASA LeRC - D Brinker	Si	20	A0171 - Solar Array Materials Passive LDEF Experiment
JPL - P. Stella	Si	30	A0171 - Solar Array Materials Passive LDEF Experiment
NASA GSFC - E. Gaddy	Si	45	A0171 - Solar Array Materials Passive LDEF Experiment
Wright Pat AFB - T. Trumble	Si, GaAs	70	M0003-4 - Advanced Solar Cell and Coverglass Analysis
NASA GSFC - S. Tiller	Si	4 arrays	S1001 - LDEF Heat Pipe Power System
MBB - L. Preuss	Si	3	S1002 - Evaluation of Thermal Control Coatings and Solar Cells
TRW - J. Yaung	Si	12	A0054 - Space Plasma High Voltage Experiment

S0014 - Advanced Photovoltaic Experiment

The Advanced Photovoltaic Experiment, located on the leading edge, was designed to provide reference solar cell standards for laboratory measurements. This was to be accomplished by placing individual solar cells in orbit, measuring their current-voltage characteristics or short circuit current values while in orbit, and returning the solar cells to the respective organizations for use as reference standards for space (air mass zero) calibrated measurements (ref. 51). The data acquisition for the cells in orbit was to take place once per day throughout the mission lifetime of 325 days. Short circuit current measurements of 120 cells were obtained whenever the Sun angle was optimum by measuring the analog voltage across a 1-ohm precision resistor. Current-voltage characteristics on 16 cells were measured using the open circuit voltage value and six different load resistors.

The solar cells were permanently mounted onto removable aluminum plates using RTV 511 and primer. Temperature measurements were obtained by Springs Instruments type 16429 thermistors at 128 different locations. Data were transferred to a flight recorder using a tape format. The majority of the photovoltaic devices flown were Si type obtained from industrial and government institutions and represent silicon state-of-the-art space photovoltaics as of the mid-1982 flight hardware integration. In addition, three LPE GaAs solar cells were flown which were provided by JPL, LaRC, and USAF. A short summary of the cell types flown is in table 4.2.7-2 , but because of space limitations a complete listing of >150 types is not possible. A preflight photograph of the tray containing all the solar cells flown is shown in figure 4.2.7-1.

From a visual inspection of this panel upon retrieval, the following physical changes were observed:

a) Much of the black paint was removed from the upper surface of the field-of-view plates.

Table 4.2.7-2. Summary of Solar Cells Aboard S0014, "Advanced Photovoltaic Experiment"

Si:	BSR/BSF
	Violet
	Vertical Junction
	Textured
	5.9X5.9 cm PEP
	2 mil thick
GaAs:	LPE
Coverglasses:	Fused Silica
	Ceria Doped Microsheet
	V- and U-Grooved

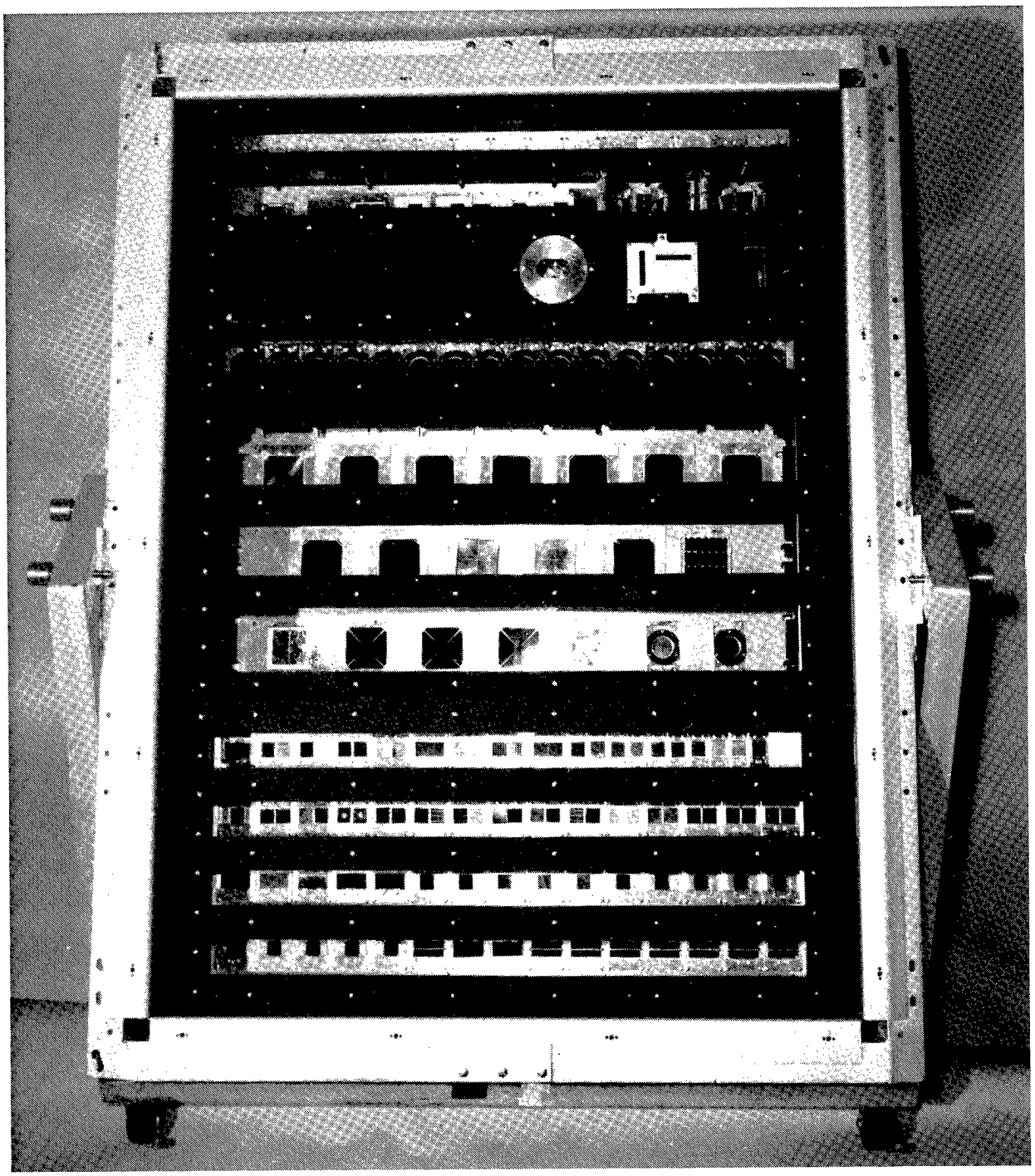

Figure 4.2.7-1. Preflight Photo of S0014

b) A contamination film is evident on cells and mounting plates in the two rows nearest the space end of the tray. The location of the deposits reaffirms the report that LDEF was rotated along its long axis toward Row 10. Analysis of the contaminating film shows its major constituents are silicon, oxygen, and carbon.

c) Impacts from meteorites and debris has been characterized at the SAEF-2 facility at the KSC with the result that this experiment had 632 impacts, 569 of which were 0.5 mm in diameter or smaller. The largest was 1.8 mm in diameter.

The on-orbit IV (current/voltage) curve analysis has not, to date, been analyzed. These data will determine the degradation of the solar cells as a function of time in orbit. The post flight I-V curves have been taken using a laboratory solar simulator and comparisons to pre-flight data have been performed. The contamination film found on much of the surface of the cells, in no way degraded the solar cells performance nor were there observed changes in coverglass or antireflection coatings. Some discoloration in the RTV used to bond the cell wiring harness was observed. Degradation in I-V curves from individual cells was found to be mainly attributable to the severity of damage from micrometeorite impact damage. Figure 4.2.7-2 show post-flight I-V curves of three cells that had been impacted by micrometeoroid or space debris. The first cell, M-3, has a small impact crater in the coverglass, but not penetrating the cell itself. From the curve it is apparent that there is little change. The second cell, NA-9, has a large (about 1.8- mm diameter) impact crater which penetrated into the silicon cell. The cell was apparently shunted by this damage, resulting in a decrease in a Voc of approximately 100 millivolts. The third cell, M-9, has an impact crater in the coverglass which cracked the coverglass and the cell. The cell crack does not go all the way across the cell, but the resulting discontinuity in many of the current collection busbars on the front has caused an increase in series resistance and a drop in fill factor.

A0171 - Solar Array Materials Passive LDEF Experiment

This passive experiment, contained in Tray A8, was subdivided into four individual solar cell experiments. Figure 4.2.7-3 is an on-orbit photograph of Tray A8 and shows the four solar cell experiments. Because no published results are yet available for the LeRC and GSFC experiments on A0171, only the MSFC and JPL experiments will be discussed.

MSFC Portion of A0171

This part of A0171 contained over 100 specimens of which seven photovoltaic test articles were retrieved (ref. 52). In addition to the photovoltaic test specimens, many metals, dielectrics, and composites were flown, including aluminum, titanium, silver (disk and cold rolled ribbon), niobium, magnesium, copper (disk and cold rolled ribbon), molybdenum, tantalum, and Tophet-30, HOS-875, and Ni-Cr alloys in the as-received and pre-oxidized condition. Materials including RTV-511, Halar, PEEK resin, TFE Teflon, carbon fiber, and glass fiber composites were included in the test specimens. The general results from a visual inspection of this panel are as follows:

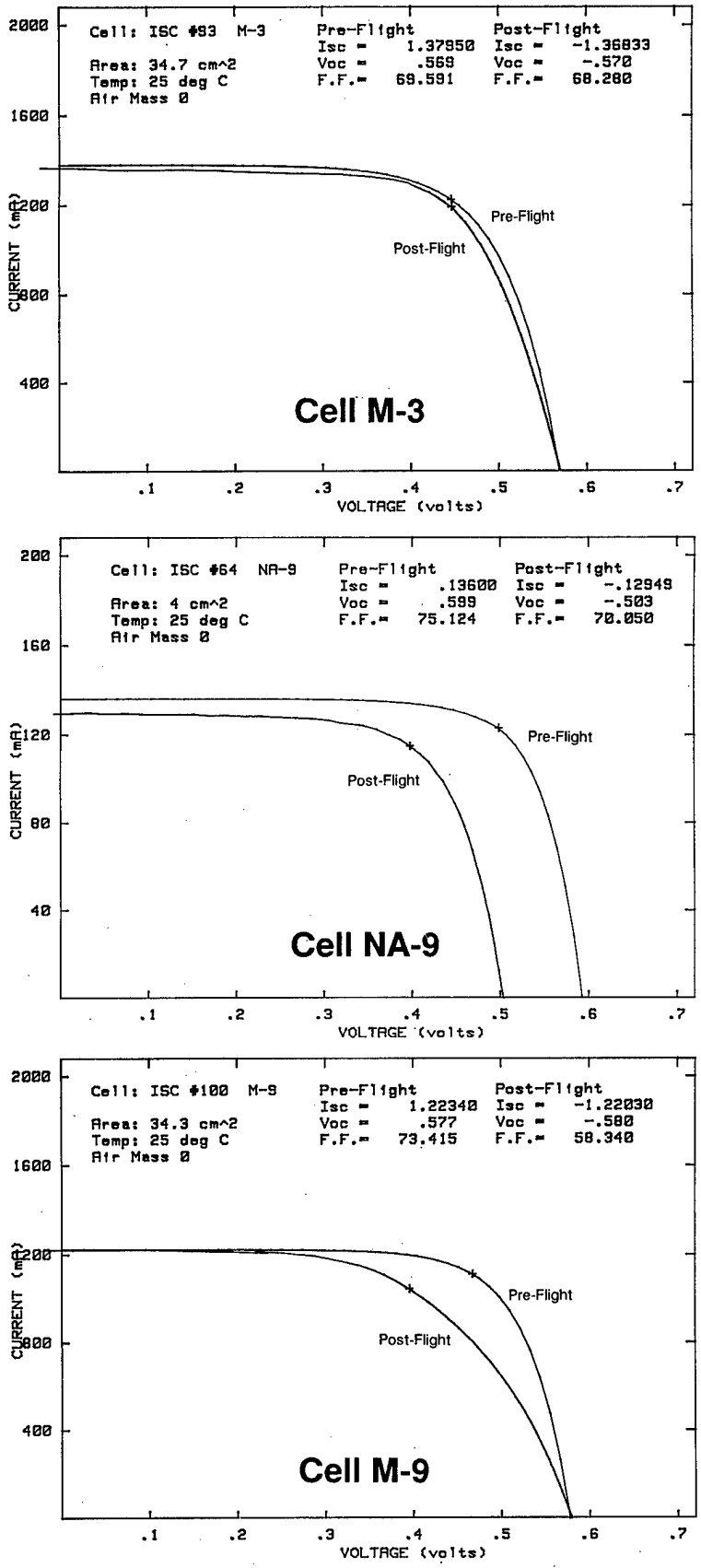

Figure 4.2.7-2. I-V Curves of S0014 Cells Impacted by Micrometeoroide or Space Debris

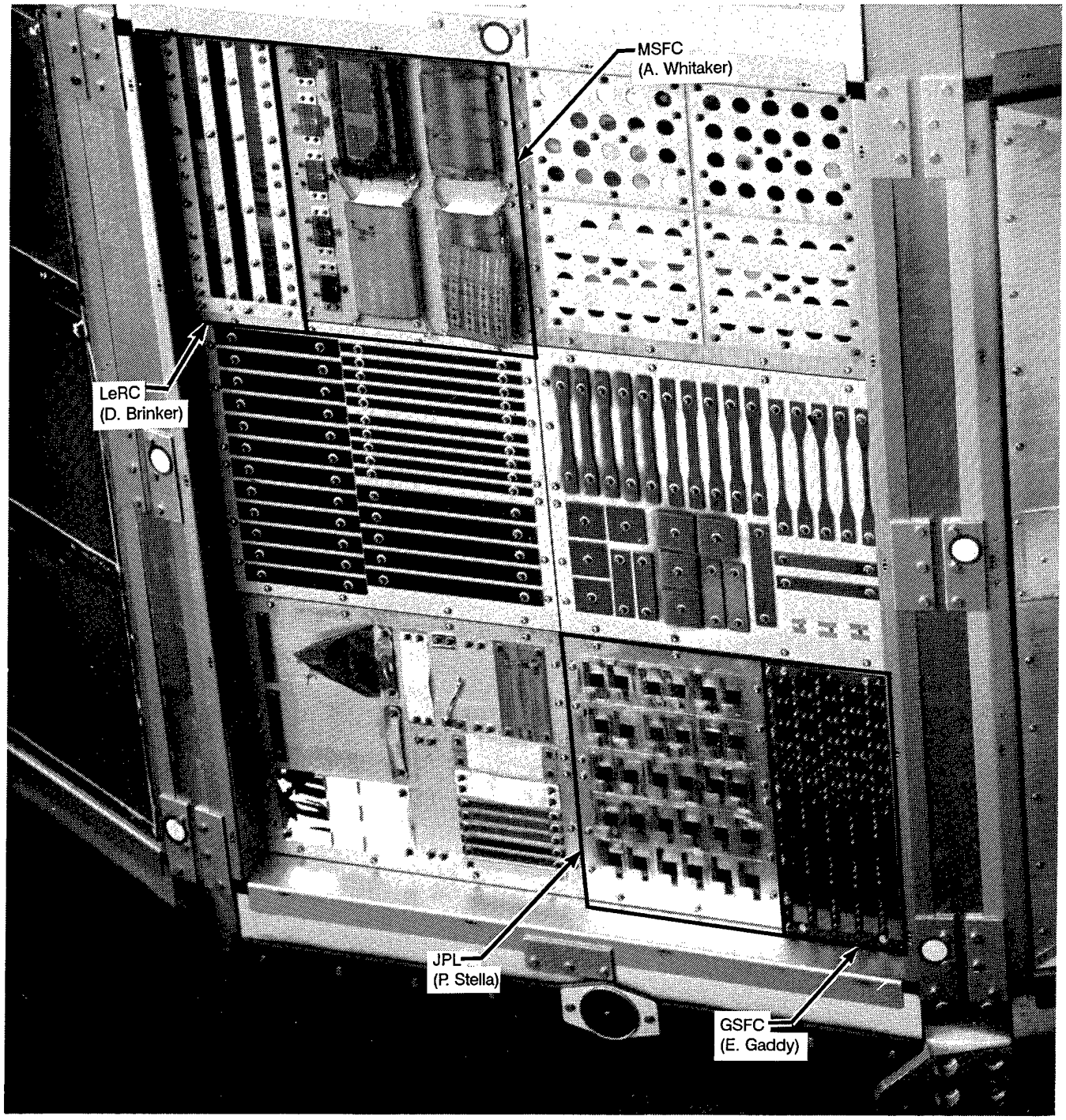

Figure 4.2.7-3. On-Orbit photograph of Tray A8 which contained four different solar cell experiments

a) Organic materials such as the polyimides, silicones, and polyurethanes were observed to luminesce after the mission when excited by UV light.

b) Fiberous "ash" material was observed on carbon-fiber-based composite materials.

c) New synergistic effects were noted where atomic oxygen and copious amount of contamination were interactive.

d) Considerable darkening of all polymers occurred as a result of exposure.

e) All metals gained weight from interaction with atomic oxygen except the pre-oxidized alloys which showed a slight mass loss.

f) Specular paints became diffuse and diffuse paints became more diffuse.

The photovoltaic test articles were fabricated by Lockheed Missiles and Space Company for MSFC; Lockhead also provided the pre-flight electrical characterizations. The solar cells used for the four modules were of two different cell types, ASEC 200 micron 2x4 cm, n/p 2 ohm-cm BSR solar cells and ASEC 50 micron 2x4 cm n/p 10 ohm-cm BSF. In addition, five indivdual solar cells were flown. These five were encapsulated with various types of coverglass (spraylon, Teflon, microsheet, or fused silica), with different thicknesses (150 micron or 50 micron), or were unencapsulated (i.e., no coverglass). Various interconnect techniques (aluminum or copper) were utilized and the modules were mounted on LDEF with either the solar cell top surface facing the space environment or the module rear- surface facing space.

As a result of the longer-than-planned flight duration, an increased amount of atomic oxygen erosion of some of the polyimide substrates caused significant problems to several of the solar cell modules. One module was lost prior to shuttle rendezvous with LDEF, one module was drifting away as LDEF was grappled (fig. 4.2.7-4), and one module (M3) was attached by only one corner (this module can be seen in figure 4.2.7-3) during the retrieval and was later found on the floor of the cargo bay when LDEF was removed from the Shuttle. The fourth module (M4) remained attached to the tray. Post-flight visual inspection M3 showed that 5 of the 12 cells had sustained cracks in either the solar cell or the cell cover. All of the returned test articles showed atomic oxygen degradation in the polyimide substrates of the cells.

The solar cell and solar module maximum power point (Pmp) degradation ranged from 4.3% to 80%. However, over 75% of the 18 cells (includes the 12 cells on M3) had less than a 10% degradation. Of the cells with the largest degradation, three of the four were cells from M3 and the fourth was an unencapsulated solar cell. DIscounting these four cells, the average Pmp degradation of the other 14 cells was 6.5 %. Exact degradation mechanisms have not been determined for each individual cell but are consistent with increased series resistance and/or decreased shunt resistance. Other degradations are consistent with cracks in the cell either due to the handling of the cells/modules on retrieval or damage due to micrometeorite impacts.

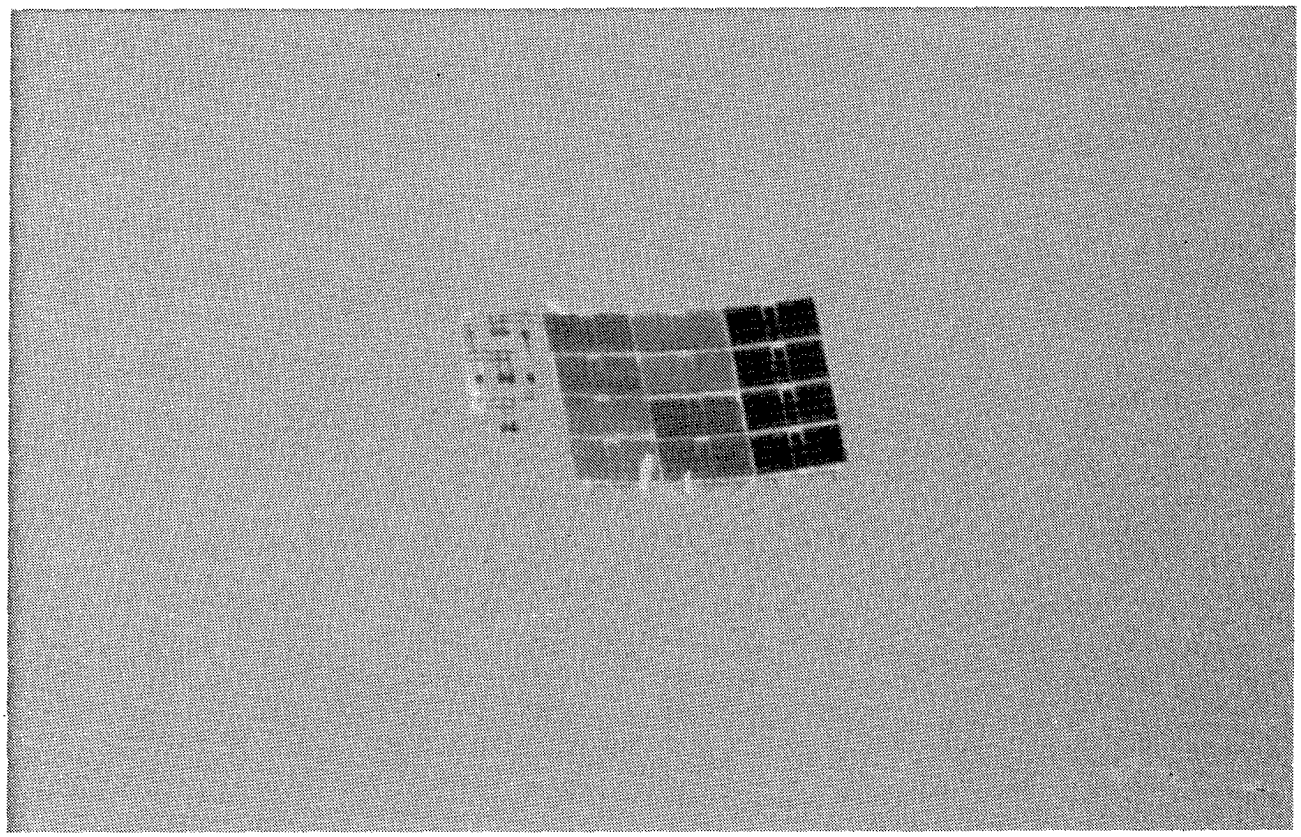

Figure 4.2.7-4. On-Orbit photograph of the AO171 Solar Module that had separated from LDEF prior to retrieval.

JPL Portion of A0171 - LEO Effects on Conventional and Unconventional Solar Cell Cover Materials

The LEO effects on conventional and unconventional solar cell cover materials LDEF experiment is one portion of the A0171 SAMPLE outlined above (ref. 56)]. This subplate, was designed by JPL and fabricated by G.E. Company, is 11 in. x 16.3 in. and consisted of 30 different combinations of cells/covers (table 4.2.7-3). The solar cell material for the 30 experiments were Solarex Corporation 50-micron-thick 2x2 cm^2 silicon with silver-plated Invar tabs welded to the N and P contacts. All electrical measurements were performed by Spectrolab, Inc. with JPL assistance. From the initial visual survey of the retrieved subplate, the following results were obtained;

a) The test plate and samples exhibited brownish-orange stains, which are residues of adhesives and/or encapsulates that had reacted with the LDEF space environment.

b) Large numbers of micrometeorite and debris impacts are apparent, ranging in size from 0.05 mm to 1.0 mm in diameter with >157 total impacts over the subplate surface. While most impacts appeared to be generated from a normally incident micrometeorite, a small number of elongated craters were observed.

Table 4.2.7-3. Experimental List of the Materials Aboard JPL Portion of A0171.

Number of Cells	Coverglass Thickness	Coverglass Material	Adhesive
6	100 micron	microsheet	5 different incl 93500
10	50 micron	FEP Teflon	5 different silicone
10	--	--	6 different adhesives only
2	--	--	GE X-76 polyimide
2	--	--	Bergstron and Assoc. GE BE225HUP

c) Impact damage show visual differences between the observed craters on Invar interconnects, the aluminum plate, polymer cell covers and the silicone and microsheet covers.

No micrometeorite damage was found to cause significant electrical degradation to the solar cells. The degradation in cell performance for all samples was due to a loss of cell current due to a darkening of the adhesive and/or coverglass due to exposure to UV, charged particles, and mainly atomic oxygen. The amount of cell current loss was directly dependent upon the type of material used in the particular cell. Table 4.2.7-4 lists the overall degradation values obtained in the short-circuit current (Isc) of the cells as a function of the encapsulant and a general description of the degradation observed. From the electrical measurements the following conclusions are obtained:

a) The smallest Isc loss and least visual damage was found with the cerium-doped microsheet samples.
b) The BE-225HUP copolymer samples showed similar Isc loss as the cerium-doped microsheet samples, but also exhibited areas on the solar cell completely void of the encapsulant.

Table 4.2.7-4. Solar Cell Isc Degradation for Devices on the JPL Portion of A0171

	Isc (mA)			Comments
Cover/Encapsulant	Pre-	Post-	Isc loss	Cover/Encapsulant
Microsheet (Cerium doped)	136.5	132.4	3	
FEP Teflon	136.8	106	22	Darkened top surface loss varies from -10 to -43%
Silicone (soft)	132	115	13	Crazing, some loss near cell edges
Silicone (hard coat)	135	112	17	Crazing, flaking, close to complete removal
BE-225HUP Polyimide Silicon Copolymer	125	121	3	Partially removed--Voids
GE-76 Polyimide	129.5	119	8	Encapsulant significantly removed

c) The next lowest loss in Isc was found with the samples covered with X-76 polyimide (8% loss), soft silicone (13% loss), and the hard coat silicone (17% loss). However, the X-76 polyimide sample also exhibited areas void of encapsulant.

4) The largest current loss was found with the Teflon-covered samples. In one case the Teflon cover was completely missing with only a layer of RTV remaining. With other Teflon samples, the surface of the Teflon was soft and somewhat tacky.

M0003-4 - Advanced Solar Cell and Coverglass Analysis

The advanced solar cell and coverglass analysis experiment consisted of 63 coverglass samples and 12 solar cell strings (5 cells each string) (ref. 53). Of the 63 samples, 16 were on the leading edge, 16 were on the trailing edge, 16 on the backside of a tray protected from direct exposure to the LEO environment, and 15 were used as control samples and were not flown. Coverglass samples were characterized by optical transmission, reflectance, and absorbance in their as-returned "dirty" condition. The surface contamination found on all samples did not interfere to a significant degree with the optical characteristics, but the contamination film does increase the absorption by moving the short wavelength transmission of the top surface to longer wavelengths. This was observed to be more pronounced with the trailing edge samples of LDEF and less with the leading edge samples (it is suspected that atomic oxygen provides a "scrubbing effect"). Details of the chemical composition of the contaminants follows:

a) Leading-edge MgF_2 samples indicate the presence of fluorinated organic contaminants, and the oxygen has replaced fluorine in the materials.

b) Leading edge ThF_4 samples indicated that all fluorine has been removed, but no thick layer of oxide was observed.

c) Leading edge SiO_2 samples showed no change.

d) Trailing edge samples show a contamination layer some 100 Angstroms thick over all surfaces composed of high levels of Si, C, and O and half the samples showing trace amounts of N, F, and Sn.

e) Trailing edge samples also showed a contamination of a silicone-based material.

Solar cell analysis was initiated with a photographic survey. Visual comparisons of cell strings indicated that the metallization process will have a large effect on the lifetime of arrays in this orbit. Metal migration and contamination between the coverglass and the cell are two of the main concerns. Oxidation of silver, contamination, and discoloration on the cell contacts and interconnects were observed. Electrical characterization of these cell strings have not, to date, been examined.

S1001 - LDEF Heat Pipe Power System Results

The LDEF heat pipe power system experiment consisted of a self-contained direct-energy transfer power system which functioned properly during the entire mission lifetime to provide power to a Low-Temperature Heat Pipe Experimental Package (ref. 54). This power system, located on the space end of LDEF, consisted of four solar array panels, one 18-cell, 12 ampere-hour, nickel-cadmium battery, and a Power System Electronic unit. A photograph of the four solar panels as mounted on the LDEF structure is shown in figure 4.2.7-5. A detailed visual inspection of the four solar panels found that most cell damage could be attributed to the 99 micrometeorite hits recorded, of which 29 hits caused cover glass cracks. In addition, burned residue and a small area of debris were found on one panel with all panels showing adhesive spread on the edges. These solar cells, however, were manufactured during 1971 and 1972 and were already showing some affects of aging prior to launch.

Postflight IV analysis made 5 months after the LDEF retrieval indicated that the solar panels' current and voltage performance had degraded an average of 1.5% and 3.3%, respectively. IV analysis of a monitor panel which remained on Earth during the entire mission showed degradation of current and voltage of only 0.27% and 0.6%, respectively. Flight degradation of the solar panels was concluded to be due to a combination of charged particle radiation, darkening of the cover adhesive, and micrometeorite damage. The extent of damage due to any one of the mechanisms was not discussed.

S1002 - Evaluation of Thermal Control Coatings and Solar Cells

The purpose of the evaluation of thermal control coatings and solar cells experiment was to determine the effects of the LDEF orbit space environment on these materials and to collect micrometeorites and debris (ref. 55). This experiment was mounted in a trailing edge EECC (sec. 4.1.4 describes the EECCs) and was only exposed to the LEO environment for the first 297 days of the mission. The thermal control coating experiment was comprised of 7 different configurations of optical coatings deposited and/or laminated to glass, aluminum, and/or Teflon. The different configurations were functionally equivalent to different optical hardware currently in use on spacecraft. The configurations included, second surface mirrors (SSM), optical solar reflectors (OSR), interference filters (IF), and conductive thin film layers (LS). The results of these experiments and the results from the solar cell configurations on this panel are presented.

The analysis of the optical coatings portion of the experiment spanned several different characterization techniques. The coatings that were deposited in the configurations of the SSM/IF and SSM/IF/LS were characterized by analyzing the change in the coating's solar absorptivity and emissivity. All the space exposed anodized surfaces turned yellowish due to a contamination layer and showed a corresponding increase of solar absorptivity. The magnitude of the solar absorptivity change varied from sample to sample but spanned the values of negligible change to 0.12 dependent upon the amount of contamination deposited. In another portion of the experiment, 150 Angstroms of ZnS and In_2O_3 were deposited on separate quartz crystal monitors (QCM) prior to the flight, and by measuring the difference in QCM

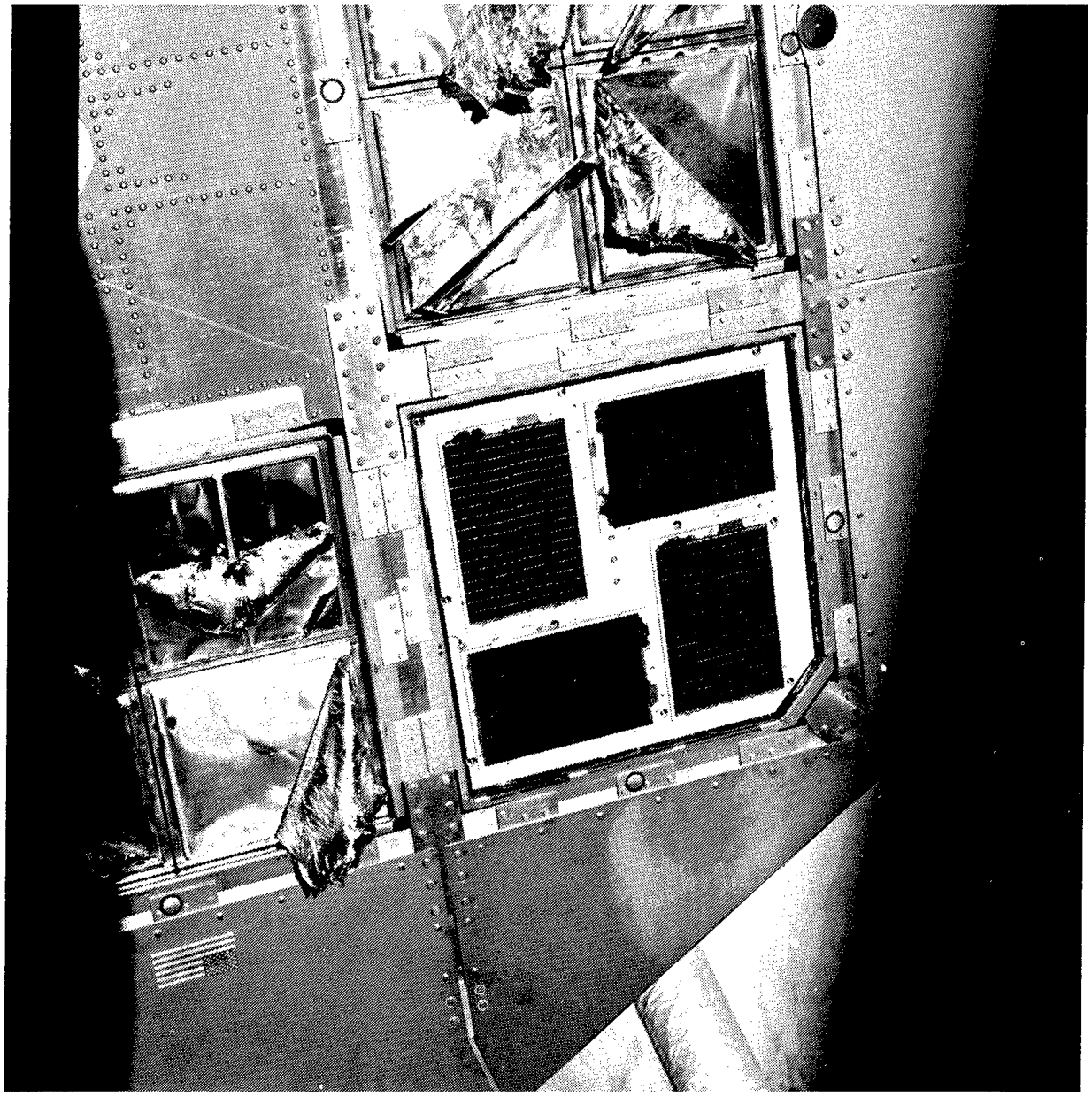

Figure 4.2.7-5. On-Orbit Photo of S1001 Solar Arrays

frequencies between the pre- and post-flight, it was determined that approximately 8 nanometers of contamination were deposited during the flight.

The solar cell portion of this experiment consisted of three cells. The performance of these cells was actively monitored during their exposure to the LEO environment. The electrical resistance of the ITO layers of the GEOS cells and the short circuit current of both the GEOS and OTS cells was monitored. Figure 4.2.7-6 shows the three cells mounted on the EECC mounting plate (other hardware on the mounting plate includes the two QCMs and the thermal control coatings).

The solar cell material used in this experiment consisted of 1-ohm-cm Si cells, fabricated by floating molten zone recrystallization method, and were of the type used in the OTS and GEOS satellites. The exact configuration for these cells is shown in table 4.7.2-5. The experimental design indicated that on-orbit short circuit currents would be measured; the analysis of these data has not been received. On each of the GEOS solar cells, three of the four interconnects (located between ITO layers) had visual cracks, but still maintained electrical integrity. All silver interconnects changed to a dark color and were later characterized to be silver sulfide. Of the three solar cells, short-circuit currents showed degradations ranging from 3% to 5%. Open-circuit voltages showed degradations of 1.0% to 1.5%. Fill factor values showed little to no degradation for each of the cells.

A0054 - Space Plasma High Voltage Experiment

Twelve Si solar cells were flown on LDEF with six cells on the Row 10 (near leading edge) experiment and and six cells used on an identical experiment but located on Row 4 (near trailing edge). In addition, six cells were control specimens which were kept in the experimenter's lab for comparative purposes. The two six-cell modules flown on LDEF were a functioning component of the experiments. To date minimal test results have been reported.

Table 4.7.2-5 Configuration of Solar Cells Flown on LDEF Experiment S1002.

OTS Solar Cell	GEOS Solar Cell
CMS; 300 um	In_2O_3; 200 A
DC 93500; 30 um	OCLI Fused Silica; 300 um
OTS Si solar cell; 200 um	XR6 3489; 30 um
RTV 566/DC 1200; 80 um	GEOS Si solar cell; 200 um
DP 46971; 5 um	RTV 566/DC 1200; 80 um
Kapton; 25 um	DP 46971; 5 um
DP 46971; 5 um	Kapton; 25 um
Al Honeycomb	DP 46971; 5 um
	Al Honeycomb

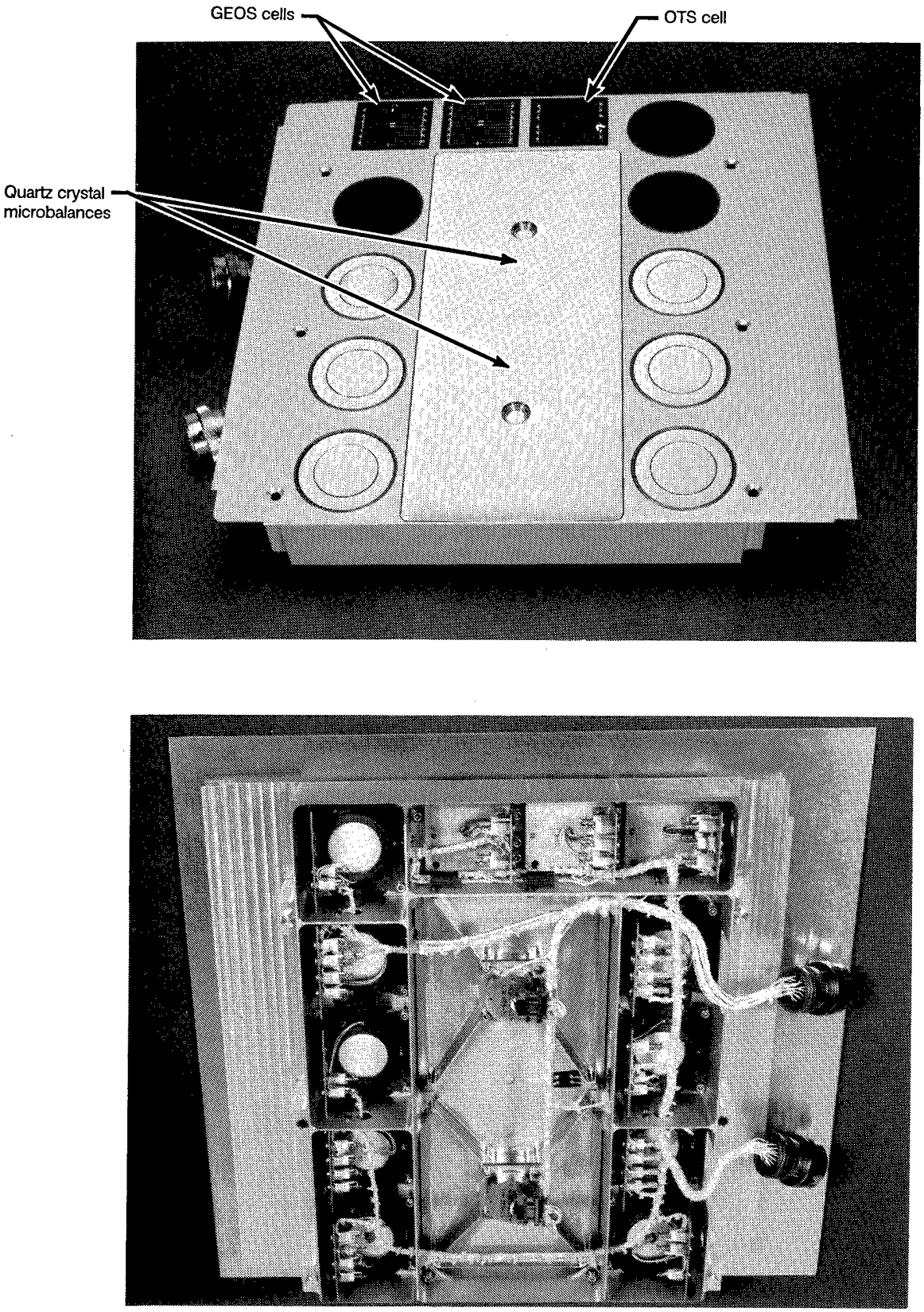

Figure 4.2.7-6. S1002 Solar Cells—Front and Back of EECC Mounting Plate

Summary of LDEF Solar Cell Findings

The data presented thus far include the observations and conclusions reached by the individual scientists given the set of data gathered using their particular panels and modules. From these individual conclusions, a pattern emerges regarding the performance of the solar cells and solar array materials in the LEO environment. The following discussion looks into the overall observations and an assessment is made as to how one can avoid the same degradation mechanisms as found on this flight. The discussion is broken down into four sections which have been identified as to have caused the largest performance loss for these photovoltaic devices and are presented in order of importance to the LEO solar array designer:

1) Meteoroid and space debris.
2) Atomic oxygen.
3) UV radiation.
4) Charged particle radiation.

Meteoroid and Space Debris. From the results presented on the solar cells aboard LDEF, the most extensive degradation of the solar cells came from meteoroid and debris impacts and the resulting cratering. The extent of the damage to the solar cells was largely dependent upon the size and energy of the micrometeorites. The timeframe which one could expect measurable damage was from an instantaneous performance loss due to cracking of the coverglass, interconnect, and/or solar cell, to a gradual performance loss caused by small cracks that eventually propagate through the solar cell active area or interconnect due to thermal cycling. The extent of the performance degradations attributed to impacts of micrometeorites and debris with the solar cells are from a small power loss of cell current due to the reflective nature of coverglass cracks to a significant power loss in current and/or voltage due to increases in series resistance, decreases in shunt resistance, or open circuits due to a loss of electrical continuity.

To eliminate the power output decrease due to the micrometeorites and debris impacts on a solar array is one area that is only loosely addressed when designing a solar power system for a space application. Currently deployed solar cell designs, however, have much thicker coverglass and adhesive layers which does offer a great degree of protection from impacts of this type. The new ultra-lightweight designs now being proposed that decrease the array weight by decreasing the coverglass and adhesive thicknesses will require modeling of solar cell damage due to micrometeorite impacts (i.e. the thinner the glass and adhesive the less protection). Towards this end, this flight has provided valuable information of the expected spectrum of micrometeorite size and energies in LEO which will be needed for the modeling tests.

Atomic Oxygen. The performance degradation of solar cell assemblies due to atomic oxygen manifested itself in several ways. The actual semiconductor materials themselves are typically inert to the chemical reactivity of the atomic oxygen due to the normal encapsulation techniques used for solar modules and arrays used in a space environment. The major degradation of solar cell output due to the reactive nature of atomic oxygen is a loss in cell current because of a loss in the amount of light reaching the semiconductor material. The light loss is due to either increased absorption or

increased reflection in the normally transparent surfaces above the active region of the solar cell. Atomic oxygen was shown to erode materials from the array structure and redeposit films on all the surfaces of the structure and from line-of-site redepositing of the eroded material was shown to be dark in color. The loss of cell current in this case was caused by the contamination absorbing the light. In other tests, atomic oxygen was found to degrade the antireflection coating of coverglass by replacing the fluorine contained in the antireflection coatings with oxygen. Because antireflection coatings, materials, and thicknesses are optimized to maximize the amount of light reaching the active layers of the solar cells, any change in the refractive indices of the layers will presumably increase the amount of reflected light and thereby decrease the output of the solar array. Erosion of materials due to the reaction of atomic oxygen with Kapton is thought to have been the prime reason of the delamination of three of the four panels on the SAMPLE tests. The undercutting of surface layers by the reaction of atomic oxygen with Kapton from any unencapsulated edges is a well documented array degradation method.

UV Radiation. Degradation of solar cell performance due to the exposure of solar arrays to extensive UV radiation has been well documented and is one of the tests required to space qualify any new material. Reported results from many of the materials aboard the LDEF test structure indicated that the extent of UV degradation of these materials are still of interest. The UV degradation of many of the different adhesives, Teflon, or other coverglass materials has been well documented from Earth studies and has been confirmed from the materials returned aboard LDEF. However, one report eluded to synergistic effects of the atomic oxygen and copious amounts of contamination and also reported on various types of materials which were found to luminesce after returning from space. While extensive UV radiation will increase the absorption of materials by creating additional color centers, whether it plays a role in these additional processes has not been explored.

Currently, the most widely used method to eliminate UV degradation in adhesives is to simply eliminate the amount of UV reaching the adhesives. This is accomplished in two ways: (1) by reflection mode in which UV rejection interference filters reflect the UV such as those obtained from OCLI's fused silica coverglass or (2) by absorption, in which the ceria doping of the glass in Pilkington's CMX and CMZ coverglass simply moves the absorption band edge of the glass toward the red. The drawback to the ceria doping is that the cuton wavelength is directly proportional to the thickness and, as the weight of solar arrays becomes increasingly important as a cost saving measure, the thickness of the solar cells and the coverglass materials becomes a dominant weight issue. Toward this end, LDEF was again important in the testing of new coverglass materials, with the BE-225HUP polyimide/silicon copolymer looking as a clear leader with little to no degradation. However, the delamination/erosion problem clearly shows that the newer coverglass materials still must undergo addtional evaluation before deployment on a solar array in a space environment.

Particle Radiation. Particle radiation is one area of solar array design that must constantly be adjusted for changes in every aspect of the array design and mission orbit. In the case of LDEF, the particle radiation was low enough that it was not discernible from the other degradation factors. One reason for this was that the original mission precluded inclusion of a radiation degradation model in the test matrix

because radiation degradation was not expected to be measurable at this orbit. The fluence levels for particle radiation were reported to be 109p+/cm^2 (0.05 - 200 MeV) for protons and (1012 - 108) e-/cm^2 (0.05 - 3.0 MeV) for electrons (ref. 52). Using these values for the total fluence of 1.0 MeV electrons and 10.0 MeV protons, the expected degradation for Si and GaAs solar cells using reported damage coefficients (ref. 57) is calculated to be less than 1% of the initial Pmax values. While it is true that different particle energies will degrade the solar cells at different rates, the assumption that all the particle energy is summed into one energy is usually valid as long as the damage incurred by the particular energy is evenly distributed throughout the cell structure. In any case, any reasonably protected cell structure (i.e., encapsulated with a 2.0-mil cover glass and adhesive) would certainly be more than adequately protected for the radiation doses incurred at this altitude for the duration of this flight. However, any cell structure with no encapsulation may show some degradation due to particle radiation. To precisely determine this degradation would certainly require an indepth look at the precision of the pre-flight data and the standard references used in the postflight analysis.

4.2.8 Experiment Electronic Systems

Many experiments carried electronic components or systems, generally for data and control purposes, including but some components to be exposed as part of experiment objectives. This section includes brief comments on those known to have carried electronics. An overview of all experiments appears in reference 5. A list of all active experiments is given in table 4.2.1-1, along with their major system components. The active experiments used a wide variety of components and materials, many of which are listed in Appendix A.

It should be noted that very few electronic components were directly exposed to the external environment. Most electronic systems were shielded by metal enclosures and/or thermal control materials, and experienced only moderate temperature excursions above or below the nominal 0° to 25° C range. Most systems had power applied only during short periods for control or data collection periods, not during the entire mission. This, plus the shielding, may explain the absence of any observed radiation effects. Generally, ionizing radiation effects require power to be applied, to redistribute and trap charge prior to recombination.

A0038: INTERSTELLAR GAS EXPERIMENT. This system was discussed earlier in section 4.2.5. The only known failure in the electronics was the relay failure in tray F6, which unfortunately prevented operation of all seven electronic timer/sequencers. All seven timer/sequencers and high-voltage power supplies were still functional in spite of the destruction resulting from electrolyte leakage in some E-cells. The pyroelectric wire cutters (Atlas Aerospace ISE192C, manufactured in 1978) were also functional, even though they were more than 7 years older than their recommended shelf life when tested.

A0054: SPACE PLASMA HIGH-VOLTAGE DRAINAGE EXPERIMENT. This system used a number of off-the-shelf Technetics power supplies, operating at 300V, 500V and 1000V. It also used E-cells as time and leakage current measurement devices, thus eliminating the need for more elaborate data recording systems. The E-

cells were not tested or rated for use in space, and experienced some failures (roughly 5%). Most survived and performed their function, however. The HVPS's and other electronics evidently functioned normally, including the timer circuit to turn the HV on and off. Some static discharge effects were reported, possibly induced by micrometeoroid impact effects, including ejection of conductive silver adhesive material which shorted some materials with HV applied.

A0076: CASCADE VARIABLE-CONDUCTANCE HEAT PIPE EXPERIMENT. The data/control system successfully started and data were collected for about 45 days instead of the expected 6 months. The 28V LiSO2 battery that controlled the two valves was completely discharged, apparently due to excessive current drain resulting from failure of a commercial quality 2N2222A transistor. Failure analysis at Boeing showed the transistor had poor quality die attach, which may have resulted in inadequate heat sinking capability (although other factors may have been involved). This transistor failure explains the why the valve battery was discharged, but not why data was only taken for the first 45 days. Data collection utilized the EPDS carried in S1001.

A0133: SPACE-BASED RADAR PHASED-ARRAY ANTENNA EXPERIMENT. A unique data collection system utilizing EEPROMs operated successfully, and data was recovered. The controller-sequencer functioned perfectly, and no evidence of data changes in the unused data memory cells was found.

A0138: FRECOPA. The electronics package for this experiment was developed in 1978, utilizing non-space rated, low-cost components. It reportedly operated perfectly during flight, and all systems, including motor drive units, were fully functional after recovery.

A0139A: GROWTH OF CRYSTALS FROM SOLUTIONS IN LOW GRAVITY. An electronic control system operated valves after deployment to initiate crystal growth activities.

A0180: SPACE EXPOSURE OF POLYMER MATRIX COMPOSITE MATERIALS. A unique data collection system was utilized, recording readings from thermal and strain gauges every 16 hours for 371 days. Data were recorded on a ruggedized magnetic tape cassette, backfilled with dry nitrogen. The flight system performed flawlessly. However, similar tapes stored in dry nitrogen in the laboratory experienced a loss of oxide adhesion.

A0187: CHEMISTRY OF MICROMETEROIDS EXPERIMENT. As discussed in section 4.2.6, failure of a wet slug tantalum capacitor in the timer/sequencer (same design as for A0038) reset the system and prevented further activities. This may have been responsible for the clamshell doors being open at the time of recovery.

A0201. INTERPLANETARY DUST EXPERIMENT. An EPDS was used to record the time history of micron-size particle impacts on 459 MOS capacitor detectors over a period of 348 days. Evidently the data collection system performed perfectly. Initial confusion resulted from periods of false impact indications, which may have

been due to spacecraft plasma effects. Some detector failures resulted from particle impacts.

M0003. SPACE ENVIRONMENT EFFECTS ON SPACECRAFT MATERIALS EXPERIMENT. This complex experiment contained material and components from a number of different sources. It utilized four trays, two EPDSs, two EECCs and a data and control system. One of the sample packages was a variety of electronic components prepared by Boeing. These included many non-space-rated, plastic-package microcircuits and discrete components, as well as a fiber optic system/optical cable experiment The Plastic Encapsulated Devices portion of the Boeing experiment consisted of -

20	CD4068BE 8-input NAND gate (CMOS)
20	DM54LS30N 8-input NAND gate (low power Schottky)
100	1 uf, 50V ceramic capacitors
100	10MegOhm, 1/4 watt, 1% resistors
50	2N2222A-type transistors
100	1N4005 diodes

The Hybrid Integrated Circuits portion of the Boeing experiment contained 63 miscellaneous hybrids, including assorted circuits, resistor test patterns (CrSi, NiCr, thick films), and assorted substrates (Al203, BeO, etc.). Both portions of these experiment are shown in figure 4.2.8-1. All the components were protected from direct exposure to the external environment (except vacuum), and many were powered up periodically during data collection periods. No failures or significant degradation were observed. The entire data and control system also performed properly, with no reported failures.

M0004: SPACE ENVIRONMENT EFFECTS ON FIBER OPTICS SYSTEMS. The data system, including an EPDS, performed properly during the flight. Initial post-flight confusion resulted from some previously unrecognized interactions between the EPDS and the data system (see sec. 4.2.2), but caused no problems or loss of data. One fiber optic cable was severed by a micrometeroid impact.

M0006: SPACE ENVIRONMENT EFFECTS. An EECC was programmed to open 2 weeks after deployment, and close prior to the initial planned recovery. No electronic anomalies have been reported.

P0003. LDEF THERMAL MEASUREMENTS SYSTEM. This system successfully provided a thermal history of the spacecraft interior, using thermocouples, thermistors, a radiometer, and the EPDS located in S1001. Since these were located throughout the spacecraft, substantial wire harnessing was also required. No anomalies have been reported.

S0010: EXPOSURE OF SPACECRAFT COATINGS. An EECC was used successfully to expose and then cover samples during the flight. During post-flight testing, problems were experienced with the system which were similar to some preflight experiences. These were not repeated during subsequent analysis, and did not affect the flight data.

BOEING ELECTRONIC COMPONENT EXPERIMENT: PARTS FLOWN

A. Plastic Encapsulated Devices Experiment

20	CD4068BE 8-input NAND gate (CMOS)
20	DM54LS30N 8-input NAND gate (low power Schottky)
100	1 uf, 50V ceramic capacitors
100	10MegOhm, 1/4 watt, 1% resistors
50	2N2222A-type transistors
100	1N4005 diodes

B. Hybrid Integrated Circuits Experiment

This contained 63 miscellaneous hybrids, including assorted circuits, resistor test patterns (CrSi, NiCr, thick films), and assorted substrates (A1203, Be0, etc.)

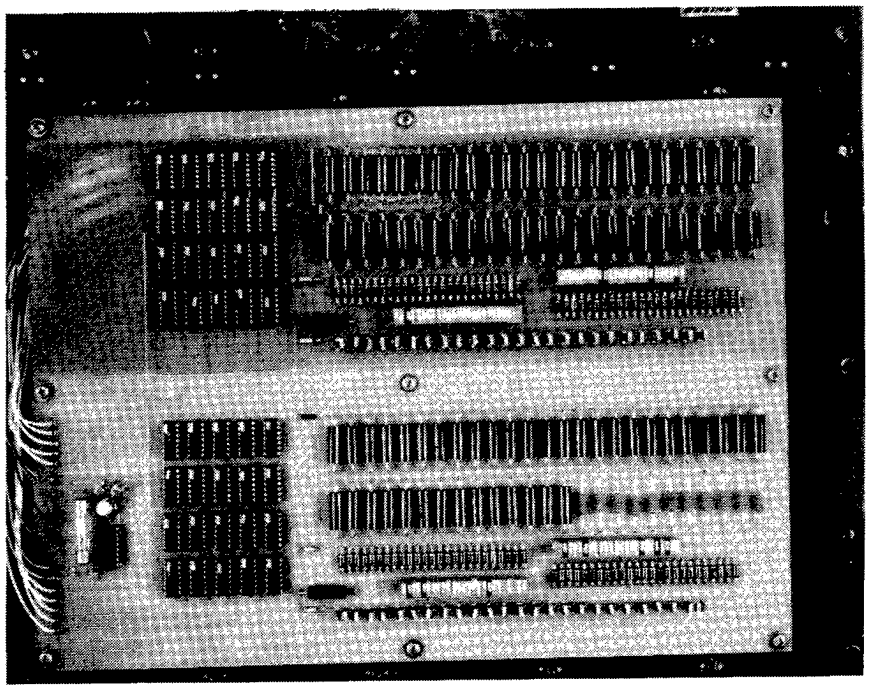

Figure 4.2.8-1. Boeing LDEF Circuit Board After Flight and Recovery

(See color photograph on p. 294)

S0014: ADVANCED PHOTOVOLTAIC EXPERIMENT. This experiment utilized an EPDS to store data collected by a custom design Gulton PCM data system. Both systems functioned normally during the LDEF flight. The Gulton system battery ran down after almost 1 year, but the EPDS continued to operate in its programmed data collection mode periodically during the entire flight. This resulted in periodic exercising of its MTM. This was the only MTM that did not develop a mechanical set in the magnetic tape. During initial testing in the experimenter laboratory after recovery, the data and control system appeared to be shorted. This was not verified in later testing at the manufacturer. The "short" characteristic, similar to a latchup condition, had apparently been experienced during preflight testing as well, and thus may have been a design and/or component problem not related to the flight. The flight data appeared to be normal, and no further analysis results have been reported.

S0069: THERMAL CONTROL SURFACES EXPERIMENT. This complex system incorporated a rotating carousel to sequentially expose samples and then perform surface measurements on them, repeating the sequence every 24 hours. It used the only 4-track tape recorder, and a variety of detectors, a motor-driven chopper, and both UV and IR lamps. A relay failure in the tape recorder resulted in some loss of data (see sec. 4.2.2). Also reported were a single-bit latchup of a DAC, and erratic output from a deuterium lamp. All four LiCF batteries developed leakage of the electrolyte (see sec. 4.2.3.2).

S1001: LOW-TEMPERATURE HEAT PIPE EXPERIMENT. The electronic data and control systems performed as planned, including the EPDS, and were still within specification limits after recovery. A NiCd battery system, charged by a solar panel, reportedly developed bulging in some cells, but remained functional. This may have been the result of overcharging by the solar panel because there was no shunt or other overcharging protection incorporated in the system.

S1002: SURFACE DEGRADATION EFFECTS ON COATINGS AND SOLAR CELLS. The experiment utilized an EECC to expose samples, and a unique EAROM-based data storage memory. No anomalies have been reported.

S1005: TRANSVERSE FLAT-PLATE HEAT PIPE EXPERIMENT. The EPDS used by the experiment worked properly, recording temperature from a number of thermocouples. The experiment also used 28V LiCF batteries to supply heat to its flatplate heat pipes. All six LiCF batteries developed a leakage of the electrolyte.

4.2.9 Electrical Systems Lessons Learned

The following conclusions are presented to suggest areas for possible improvement, and to serve as reminders of certain well known design principles. In spite of the few notable problems, most systems performed well. Actual failures were few, and these appear to be caused by traditional culprits: design oversights, testing limitations, and component or assembly problems.

a. No anomalies occurred which indicate any new, fundamental limitations to extended mission lifetimes in LEO. Protection from the effects of atomic oxygen, micrometeoroids, and ultraviolet radiation must be provided, however.

b. The longer-than-expected mission length was a bonus for some experiments, but caused problems for others. Such delays need to be anticipated, and designs should incorporate programmed shutdowns if long delays would result in problems.

c. In considering the impact of unexpected mission extensions, designers should examine circuit behavior as batteries approach their discharge state. Some circuits may continue to function (perhaps with changing characteristics) at much lower voltages than their normal limits, particularly when interfaced with other systems operating at higher voltages.

d. A key requirement (in addition to following good design practices) is a well planned component and system test plan. Testing of components at temperature, voltage and timing limits, and extensive testing of systems (including thermal-vacuum and noise tolerance testing) is essential. This must include thorough evaluation of the interfaces between systems, and special efforts to detect unanticipated noise or spurious signals which can affect system timing or operation.

e. Extensive UV, and atomic oxygen effects were observed on many experiments and on the LDEF structure. Use of metallized Teflon and other films resulted in quantities of loose, conductive material which could cause problems. This area requires considerably more investigation, including long-term degradation studies and controls on allowable materials for long mission lifetimes.

f. Electromechanical relays are a continuing problem area, well known in many production situations. Efforts have been made in some systems to eliminate them entirely, substituting solid state switches, or utilizing other design approaches (e.g. redundancy, error detection and provision for reset). There is no simple solution, but part of the answer is to use well-qualified vendors with a proven track record of supplying high-reliability parts. In addition, testing at the component and the system level is essential.

g. In a standalone system such as LDEF, with no monitoring of system performance during the mission, attention needs to be given to backup systems. On-board sensing of some critical activities, with provision for detecting failures and recycling those functions, may prevent loss of data. This requires a very

thorough design review (e.g., Failure Modes and Effects Analysis) to anticipate possible failures and look for ways to minimize their effects. Designers should seak to avoid single-point failures which can shut down major portions or entire operating systems.

h. New developments in imaging and data storage technology would make it possible to document the external appearance of a spacecraft such as LDEF but these were several failures on a periodic basis, rather than be forced to rely on initial and final appearance. Such monitoring might detect deterioration prior to major problems, or document the time history of changes in future long life missions.

i. Many low cost, non-space-qualified components performed quite well on LDEF, but there were several failures. The question of whether to permit use of commercial or MIL-STD parts in space applications is complex and involves many considerations. However, it is evident that such components can survive in some space applications, and that their use may be justified for low-cost systems when failures would not result in safety concerns or loss of mission objectives. Key to use of such components is conservative design and testing.

j. Long-term storage of materials such as magnetic tape in a sealed enclosure filled with a low humidity gas can result in changes in mechanical properties, including adhesion and flexibility. Optimum storage conditions, including upper and lower limits on humidity, and considering effects of other volatile materials in the same enclosure may have to be determined for such materials on an individual basis.

k. Lithium-sulfate batteries exhibited excellent long-term charge retention if not drained by their experiment loads. Lithium-carbon monofluoride batteries also met their lifetime objectives, but electrolyte venting might have caused problems if not confined. Electrolyte leakage from E-cells did cause damage to their sockets and adjacent circuit board areas. This phenomenom needs further study to develop improved seals and to prevent damage on missions which may experience delays and extended mission life.

l. Rechargeable batteries (e.g. nickel-cadmium) should be provided with protection against overcharging, even if anticipated loads would normally prevent this from occurring. Changes in system loads can occur due to failures or degradation.

m. Micrometeroid and debris effects on solar cells should not be overlooked, particularly as attempts are made to reduce size and weight. Impact-resistant designs (e.g., multiple or wrap around contacts to minimize effects of cracks) should be considered.

4.3 THERMAL SYSTEMS

This section includes the results obtained during the first 2 years of the LDEF investigation into the spaceflight environment effects on thermal systems, components, and materials.

The thermal investigation has been conducted under the auspices of the Systems SIG. A portion of the investigation into thermal effects has been performed by Boeing under contract to NASA Langley Research Center for systems and materials analysis, but a significant part of the investigative activity has been performed by experimenters; their contributions are acknowledged in the body of this document.

The material for this summary report is drawn primarily from research leading up to, and documentation stemming from, the First LDEF Post-Retrieval Symposium, Orlando, FL, and the LDEF Materials Workshop '91, Hampton, VA.

4.3.1 Hardware Flown

Thermal control hardware flown on the LDEF included a wide array of materials, both experiment samples and support hardware flown for functional purposes. Also flown were three heat pipe experiments that used four different types of heat pipes. Listed below are representative thermal materials and components for several categories of thermal hardware; a complete list would incorporate all experiment specimens, and for this information the reader is referred to specific experiments as listed in the references.

Instrumentation
- thermocouples
- thermistors
- passive temperature indicators (liquid crystal)
- adhesives (RTV 560, EC57, Y966)
- heaters
- platinum resistance thermometers
- thermostats
- radiometers, reflectometers, and calorimeters

Insulation
- MLI (aluminized Mylar or Kapton) with and without Dacron separators
- Betacloth
- ceramic insulators
- phenolic thermal panel insulators

Heat Pipes
- low temperature fixed conductance (ethane)
- low temperature thermal diode (ethane)
- cascade variable conductance (ammonia)
- transverse flat plate (ammonia)

Thermal Control

Surface Coatings
- Chromic Acid Anodize
- Magnesium Fluoride layers
- Conductive ITO and VDA layers
- Thermal Grease

Metallized Polymeric Films
- Silver Teflon
- Aluminized Teflon
- Aluminized, SnO_2/In_2O_3, and SiOx Kapton
- Silver Inconel

Conductive and Non-conductive Pigmented Coatings
- White Paints - Z93, S13, S13G/LO, YB71, A276, RTV615
- Black Paints - Z306, D111, Z302
- Goddard Green (sodium/potassium-silicate binder coatings)

Phase Change Material (PCM)
- n-heptane

4.3.2 Thermal Systems Lessons Learned

4.3.2.1 Thermal System Observations

Consistency of Thermal-Optical Property Measurements:

The results of thermal-optical measurements on different samples of the same materials made at different laboratories have proven to be remarkably consistent and in agreement, lending additional credibility to the results. Confidence in designers' thermal margins for longer flight missions has been increased.

Table 4.3.2.1-1 is the result of the LDEF Thermal Control Property Group Round Robin (specimen set #1). The objective of this effort was to provide validated data on the optical property measurements being conducted on LDEF materials at various laboratories. The sample from Tray F2 was specular in appearance and was mounted 150 degrees from the ram direction. The Tray C8 specimen possessed a diffuse ("milky") appearance and was mounted 30 degrees to ram. The control specimen was kept in laboratory environment during the LDEF mission.

Table 4.3.2.1-1
Interlaboratory Evaluation of LDEF Ag/Teflon Blankets
Absorptance/Emittance

Laboratory	Tray F2	Tray C8	Control
NASA-MSFC	0.08/0.81	0.07/0.78	0.07/0.81
NASA-LaRC	0.06/0.80	0.06/0.77	0.06/0.80
NASA-GSFC	0.08/0.80	0.07/0.78	0.07/0.80
Boeing	0.07/0.81	0.07/0.78	0.06/0.81
NASA-MSFC (retest)	0.09/0.80	0.08/0.78	0.08/0.81
NASA-JSC	0.11/0.81	0.17/0.78	0.11/0.81
NASA-LeRC	0.08/0.81	0.06/0.78	0.07/0.81

Discrepancies in measurements of several specimens on Experiment A0034 point to material batch variations as a significant factor in thermal design and coating selection (ref. 58).

LDEF Temperatures:

Measured temperatures within the interior of the LDEF were well within design specifications. External thermal profiles varied greatly, depending on orientation, a/e, and material mounting and shielding. The thermal stability of the LDEF adds to the accuracy of existing thermal models and enhances our ability to model the LDEF thermal history, as well as other spacecraft.

The THERM Experiment, P0003, recorded temperatures at eight locations throughout the interior of the LDEF, which was painted flat black with Z306 polyurethane paint (ref. 59). Interior temperatures throughout the mission were very moderate in the LDEF interior (typically in the 60-to-90 °F range) and never reached specified extremes. The thermal model has been verified, and temperature uncertainties have been reduced from preflight ±40 °F to post-flight ±18 °F.

Surface temperatures varied considerably among the experiments which recorded thermal data or evidenced thermal effects. A large area of discoloration on the solar collector of Experiment A0076 has been attributed to very high temperatures resulting from the erosion of a Kapton film and the resulting unfavorable thermal properties of the remaining aluminum layer (ref. 63).

The silver Teflon radiator on Experiment S1001 dropped to temperatures close to -118 °F (ref. 61).

Temperatures recorded on the stainless steel calibration tube on Experiment A0180 ranged from -30 to +140 °F, over a 400 day span at the beginning of the LDEF mission (ref. 62).

Contamination:

The thermal performance (absorptance/emittance) of many surfaces was degraded by both line-of-sight and secondary contamination. The specific contamination morphology in various locations was affected by ultraviolet radiation and atomic oxygen impingement. Overall, the macroscopic changes in thermal performance from contamination appear to be moderate at worst. Limited measurements on surfaces from which the contamination was removed post flight suggest that the surfaces beneath the contamination layers have undergone minimal thermal degradation.

An inquiry was performed on silver Teflon foils from Experiment S1005 to determine the net thermal performance of a surface from which the widespread LDEF contamination had been removed (ref. 64). The surface was repeatedly wiped with rubbing alcohol with measurements taken each time. The results show net thermal changes to be diminished by the removal of contaminants, as shown in table 4.3.2.1-2.

The results observed (ref. 66) in tests on one vapor deposited aluminum coated Kapton sample from Experiment S1001, also shown in table 4.3.2.1-2.

Table 4.3.2.1-2
Thermal Effect of Contamination Removal

	Ag/Teflon from S1005	
	alpha	epsilon
preflight	0.08	0.81
ground spare	0.08	0.79
post flight	0.16	0.75
cleaned post flight	0.11	0.75

	Aluminum coated Kapton from S1001
	alpha
LDEF Ground Sample	0.09
Post flight aluminum	0.14
Post flight wiped Aluminum	0.12

Atomic Oxygen Flux Geometry:

Atomic oxygen (AO) erosion was observed on thermal (and other) surfaces at up to 100 degrees from the ram direction, because of the thermal component of the oxygen molecular velocity plus the effects of co-rotation of the atmosphere.

This observation was confirmed by examination of the LDEF tray clamps by the Materials SIG and recession of thin polymeric films located at angles >90 degrees to the ram (ref. 65). The clamps provided a complete spectrum of orientations and environmental exposures on the LDEF.

4.3.2.2 Thermal Control Coatings

The change in performance of a wide variety of thermal control coatings and surfaces was moderate, with a few exceptions. A significant amount of these changes has been attributed to contamination effects.

Certain metals (esp. chromic acid anodize aluminum alloy), ceramics, coatings (YB-71, Z-93, PCB-Z), coated composites, aluminum coated stainless steel reflectors, and polymers with inorganic coatings (Ni/SiO_2) and siloxane-containing polymers exhibited spaceflight environment resistance that is promising for longer missions.

Other thermal control and silicone based conformal coatings, uncoated polymers and polymer matrix composites, metals (Ag, Cu) and silver Teflon thermal control blankets and second surface mirrors displayed significant environmental degradation. Ground measurements may be optimistic because of rapid bleaching effects from the ambient environment.

Ultraviolet radiation had a darkening effect on the binder in Chemglaze A276 polyurethane white paint, resulting in a degradation in thermal performance of these surfaces. The darkening of the binder far exceeded the darkening of the surface associated with silicon contamination deposits.

Many of the tray clamps on the LDEF contained discs coated with the A276 paint. The discs were to be used to visually monitor LDEF motions when it was initially placed in orbit, and a thermal control paint was used because it was flight qualified and readily available. Because of their wide distribution around the LDEF and representation of a complete spectrum of spaceflight environmental exposures, these white discs became the focus of investigation for several issues, including thermal effects. An extensive study of these discs (ref. 72) was performed by the Materials SIG. The profile of the effects of the 69 month exposure on the solar absorptance of the A276 white paint discs is shown in figure 4.3.2.2-1.

S13G and S13G/LO white coatings on Experiment A0034 darkened significantly with UV exposure (ref. 58), but were only partially "scrubbed" by AO to less than original reflectance due to silicate (oxidized silicone) buildup on the silicone surfaces. A 25% increase in absorptivity was measured despite AO erosion and ground bleaching effects (from molecular oxygen and moisture). Specimens of Z93 and YB71 white coatings were significantly less affected. The silicate-based coatings, even those containing carbon black pigments, indicate excellent stability in the atomic oxygen (AO) environment. Silicone-based materials were also observed to be resistant to AO, through reaction to silicate in a manner somewhat like the passivation of aluminum metal in air. Unlike the aluminum analogy, however, the formation of silicate from silicone is accompanied by an increase in density, resulting in surface cracking that is extremely damaging to thin silicone films.

A wide variety of thermal control coatings were flown as specimens (ref. 60) on Experiment S0069. The effects of exposure encompassed many descriptions, including cracking, speckling, chipping, texturing, and discoloration. Measured changes in solar absorptivity were generally low, with the majority of the samples increasing by less than 0.03. A few specimens changes as much as 0.33, particularly samples of A276 white paint with a clear overcoat. Materials such as YB71 and Z93 were examples of good candidates for future long duration space flight missions.

No significant degradation in performance was observed in the optical solar reflectors and second surface mirrors flown on Experiment A0138. Properties measured include absorptivity, emissivity, and specularity coefficient (ref. 74).

Degradation of samples in a canister (ref. 73) on Experiment A0138, in some cases, was worse than for similar samples mounted directly on the surface of their tray. This effect was determined not to be related to contamination, and it is attributed to higher temperatures experienced inside the canister.

A broad survey of thermal surface performance was performed by NASA Langley Research Center at KSC during the LDEF deintegration process (ref. 75).

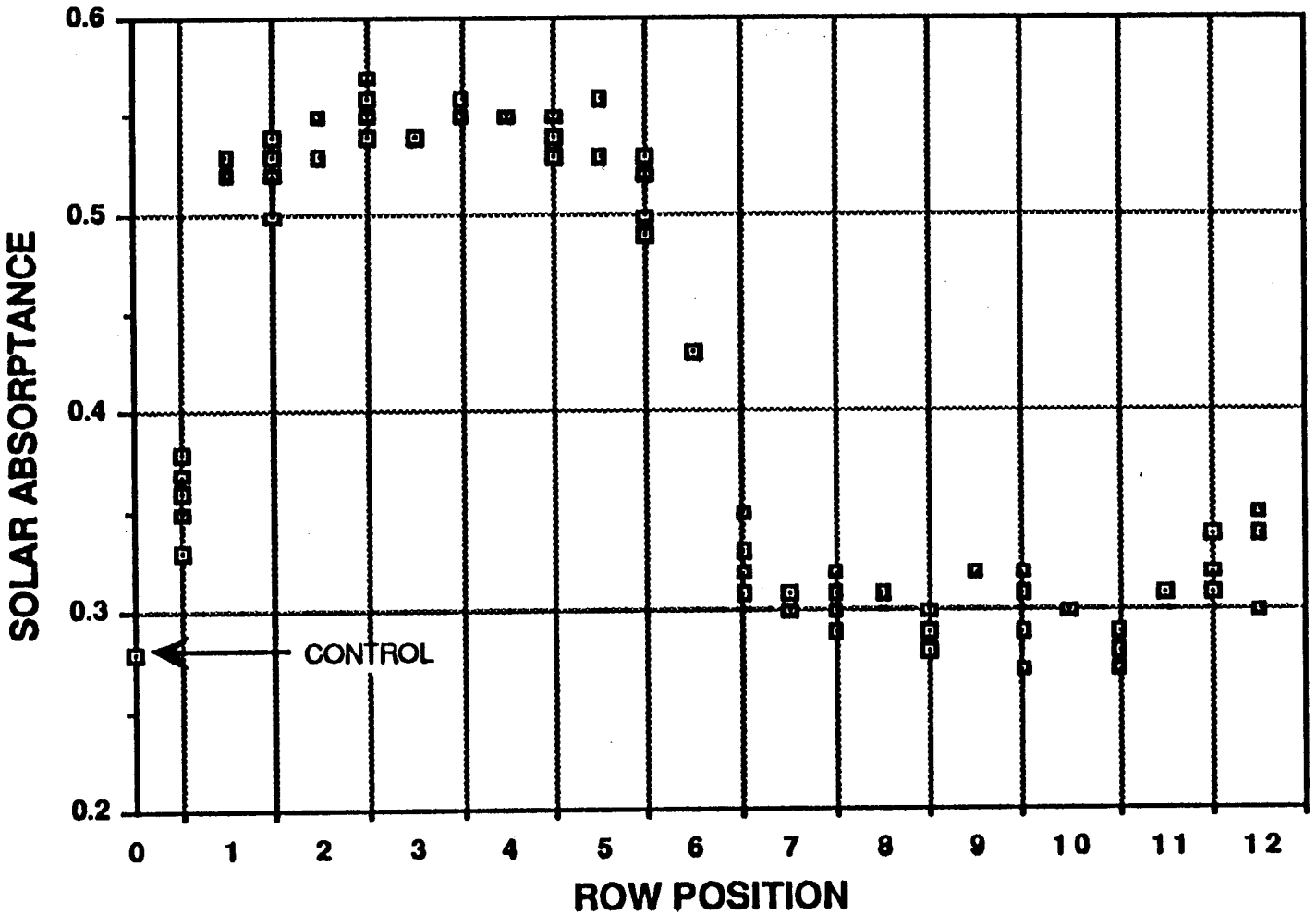

Absorptance Versus Side Tray Position For A276 White Paint Disks

Figure 4.3.2.2-1. Solar Absorptance of LDEF White Paint Discs

Their results showed the S13GLO pigment binder to be more resistant than the A276 binder to atomic oxygen and ultraviolet light effects.

All of the white paints flown on Experiment A0138-6 showed an unexpected slight increase in infrared reflectance (ref. 73). Reflectance in the visible and ultraviolet part of the spectrum decreased as expected, with changes correlating well with ground test samples subjected to ultraviolet light in the laboratory.

Comparison of thermal control coatings from Experiment S1001 with ground control samples showed increases in absorptance from 0.16 to 0.47 (white paints); from 0.33 to 0.40 (SiOx); from 0.09 to 0.55 (silver Teflon); decreases from 0.97 to 0.94 (black paints). It has not yet been determined how much, if any, of these changes are due to contamination and how much is inherent in the coatings themselves. Changes in emittance were generally an order of magnitude smaller (ref. 66).

Chromic Acid Anodize:

Slight changes in the optical properties were observed for chromic acid anodized aluminum surfaces but these changes are not perceived as a design concern. These slight changes were a within both the manufacturing variations and measurement variations. Several minor anomalous characteristics were discovered but they did not correlate with the thermal properties of the anodized surfaces.

The tray clamps on the LDEF were protected with chromic acid anodize. Because of their wide distribution around the LDEF and representation of a complete spectrum of spaceflight environmental exposures, these clamps provide a complete picture of the spaceflight environmental effects on this surface treatment.

An extensive study of these clamps was performed by the Materials SIG. The study concluded that spectroscopic anomalies were random and unrelated to exposure or position on the LDEF. Surface analysis indicated no trends in thickness changes as a function of location on the LDEF. There was an observation of an increase in the porosity of the aluminum on the leading edge of the LDEF, but no environmental component has been associated with this effect as yet. Independent of these specific observations, a slight decrease in thermal performance was measured (a/e increased 5% on average) (ref. 77).

Measurements taken in a general thermal surface survey conducted at KSC during the LDEF deintegration determined a maximum of 16% absorptivity degradation of chromic acid anodize over the LDEF mission lifetime. These measurements include the effects of contamination (ref. 75).

The variations in absorptance and emittance observed for CAA surfaces on the LDEF have been attributed to the inherent variability in anodizing, to variations in measurements, and to the effects of on-orbit contamination deposited on surfaces not subject to atomic oxygen impingement.

Silicone Coatings:

Silicones, long known to provide excellent atomic oxygen protection for vulnerable surfaces, have been confirmed to degrade and contribute indirectly to contamination and subsequent darkening of surfaces.

Silicones of many morphological configurations will form a hard silicon dioxide surface when exposed to atomic oxygen. Investigations at NASA LeRC (ref. 79) found that high levels of atomic oxygen combined with ultraviolet light exposure resulted in crazing of this surface. This was also accompanied by a release of polymerics which subsequently have deposited on other LDEF surfaces. Continued atomic oxygen and ultraviolet light exposure has resulted in a darkening of these contaminants, resulting in degraded thermal performance.

Black Chrome Discoloration:

Residual aluminum layers from eroded aluminized polymer films can significantly change the thermal environment, because of its high absorptance/ emittance ratio.

A large area of discoloration (ref. 63) was observed on the solar collector of Experiment A0076. This black chrome surface was examined for residues but none were found. The "stained" area is the same shape as a Kapton MLI flap, and it has been hypothesized that the Kapton eroded completely leaving a thin aluminum layer characterized by a very high absorptance/ emittance ratio; it is suspected that, in direct sunlight, this surface then reached very high temperatures and may have changed the oxidation state of the black chrome. Figure 4.3.2.2-2 shows an on-orbit photograph of A0076 and a close up of the solar collector showing the area of discoloration.

Atomic Oxygen Effects:

The atomic oxygen flux has been observed to have both degrading and restorative effects on thermal control coatings, depending on the location, orientation, and nature of the surface.

The atomic oxygen flux on the leading edge of the LDEF had the effect of eroding degraded materials, or effectively scrubbing some surfaces clean. In some instances, this activity countered the loss of thermal performance from contamination or darkened paint binders, including the Chemglaze A276 white paint used on the visual reference discs on LDEF tray clamps. The surface materials or coatings were mechanically weakened or degraded as a result. Increased diffusivity accompanied the atomic oxygen scrubbing (ref. 76).

Investigators for Experiment A0138 have suggested that there may also be a free oxygen chemical replacement reaction in the painted coatings, in addition to the scrubbing action, resulting in a partial restoration of the surface (ref. 73).

(See color photograph on p. 295)

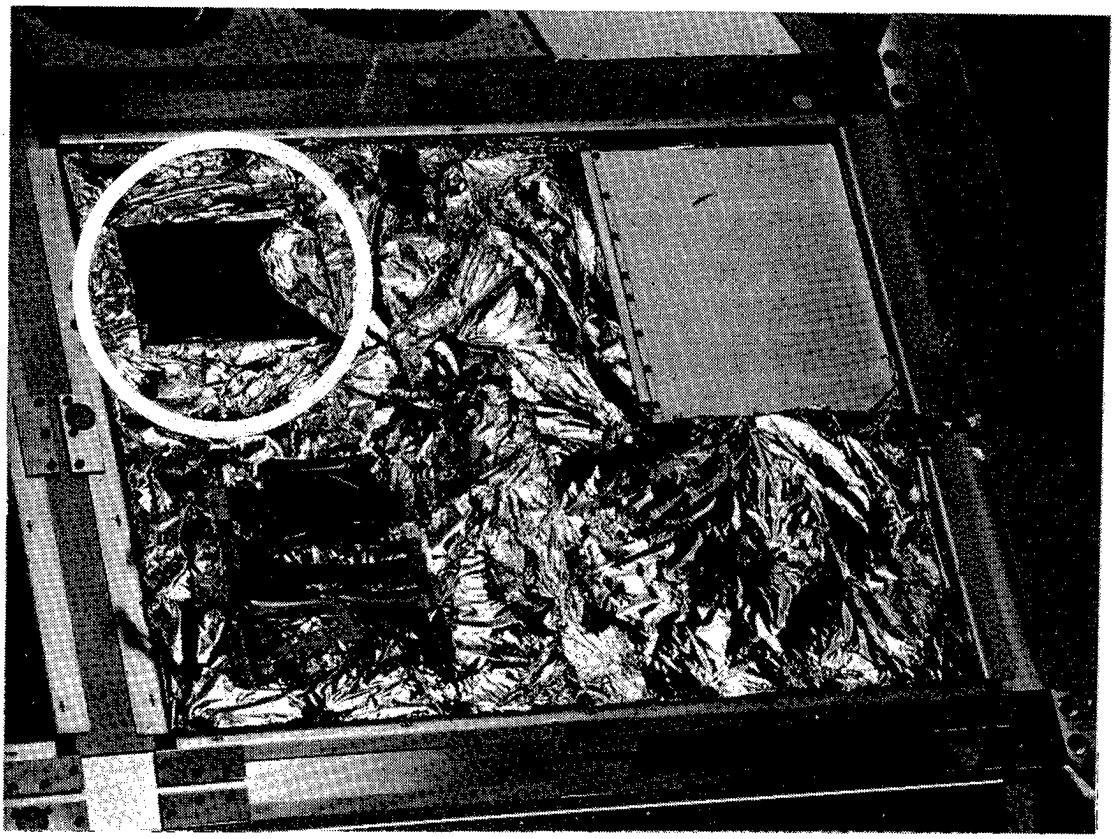

Figure 4.3.2.2-2. On-Orbit Photograph of Experiment A0076

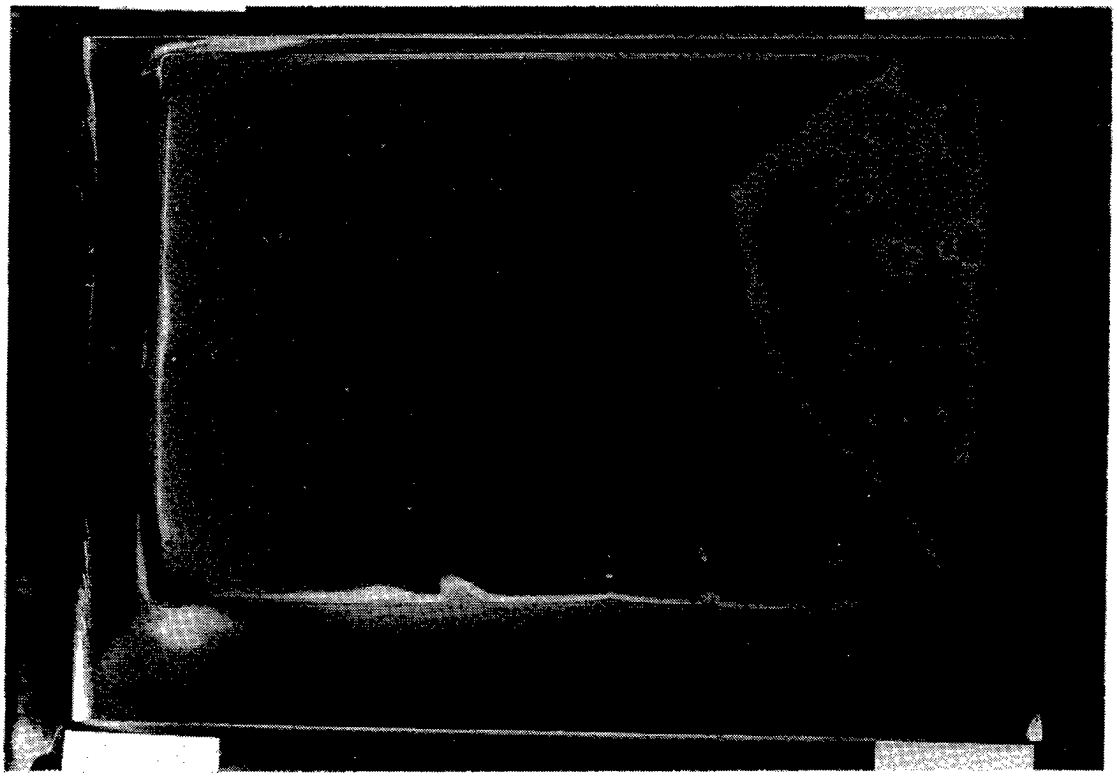

Figure 4.3.2.2-3. Close-Up of Solar Collector After Removed From the Experiment

4.3.2.3 Thermal Control Blankets

One of the most notable observations made during the on-orbit photo survey was the loose silverized Teflon thermal blankets located on Experiment M0001 located on the space end of LDEF (as shown in figure 4.3.2.3-3). 3M Y966 tape was used to hold the edges of the thermal blankets to the experiment tray frame. The blankets apparently shrunk in flight causing the blankets to detach from the frame. Portions of the tape were attached to both the blanket and frame, indicating that the tape had failed in tension. Both the blanket and Y966 remained pliable. Attempts to fail the tape to frame joint in shear were unsuccessful even though a load of approximately 100 pounds was applied to a piece of tape less than a 1/4" wide. The tape was then tested in peel. The Y966 bonded to the aluminum and to the silver on the film well enough to cause delamination of the silver from the film

Thermal Surface Specularity:

The loss of specularity of silver Teflon thermal blankets, one of the earliest observations noted at the time of retrieval, was determined to have had no significant effect on the thermal performance of those materials (figure 4.3.2.3-2). This loss of specularity is the result of first surface erosion and roughening by atomic oxygen.

The increase in diffuse reflectance is greater for materials closer to the leading edge, as shown in the accompanying chart (figure 4.3.2.3-3) of bidirectional reflectance distribution function for five specimens from varied locations on the LDEF (ref. 65). The asymmetry of the curves may be due to anisotropy of the eroded surfaces or may reflect the 8 degree yaw offset of the LDEF.

Eroded silver Teflon foil on Experiment S1005 also appeared diffuse (ref. 64), but a very light touching of the surface was sufficient to wipe away the eroded surface and return most of the material specularity.

The eroded silver Teflon surface on the radiator of Experiment A0076 showed an increase in solar absorptivity from 0.09 to 0.11; a decrease in emissivity from 0.81 to 0.79 is attributed primarily to a loss of over 20% of the original Teflon thickness (ref. 63). A significant decrease of emissivity (of 0.20) was measured on 2 mil silver Teflon which had experienced 1 mil of erosion.

Studies at the Jet Propulsion Laboratory have found a thin, highly embrittled layer on the surfaces of Teflon films located near the trailing edge of the LDEF (ref. 68). This layer was notably absent from films located near the leading edge where they were subjected to atomic oxygen erosion. This layer has been generated on Teflon films in the laboratory using ultraviolet light in vacuum.

Table 4.3.2.1-1 showed that while specimens visually appeared to have undergone significant optical changes, the differences between the hemispherical optical properties of near leading edge, near trailing edge, and control specimens of the silverized Teflon are statistically insignificant.

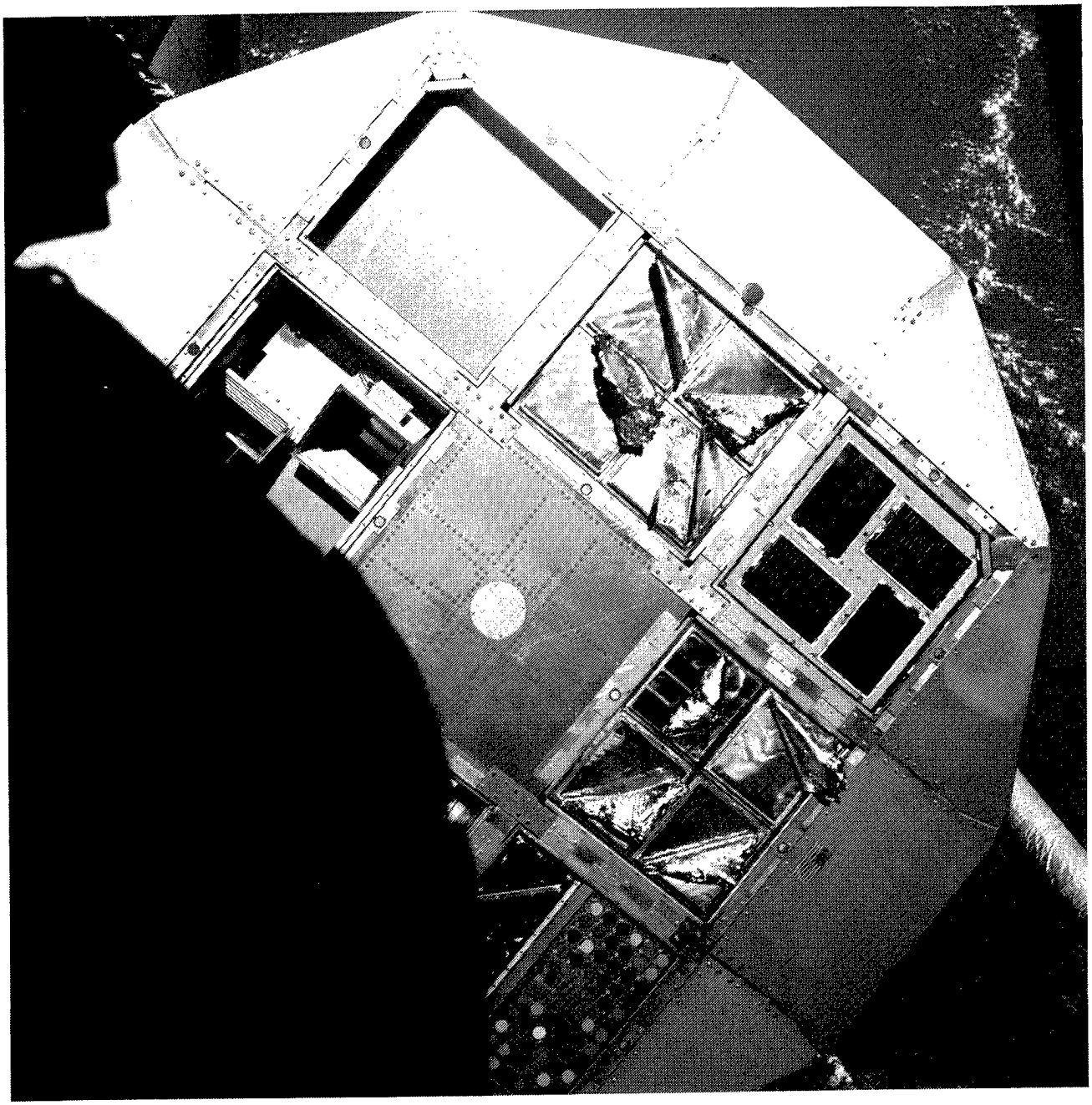

Figure 4.3.2.3-1. On-Orbit Photograph of M0001 Thermal Blanket

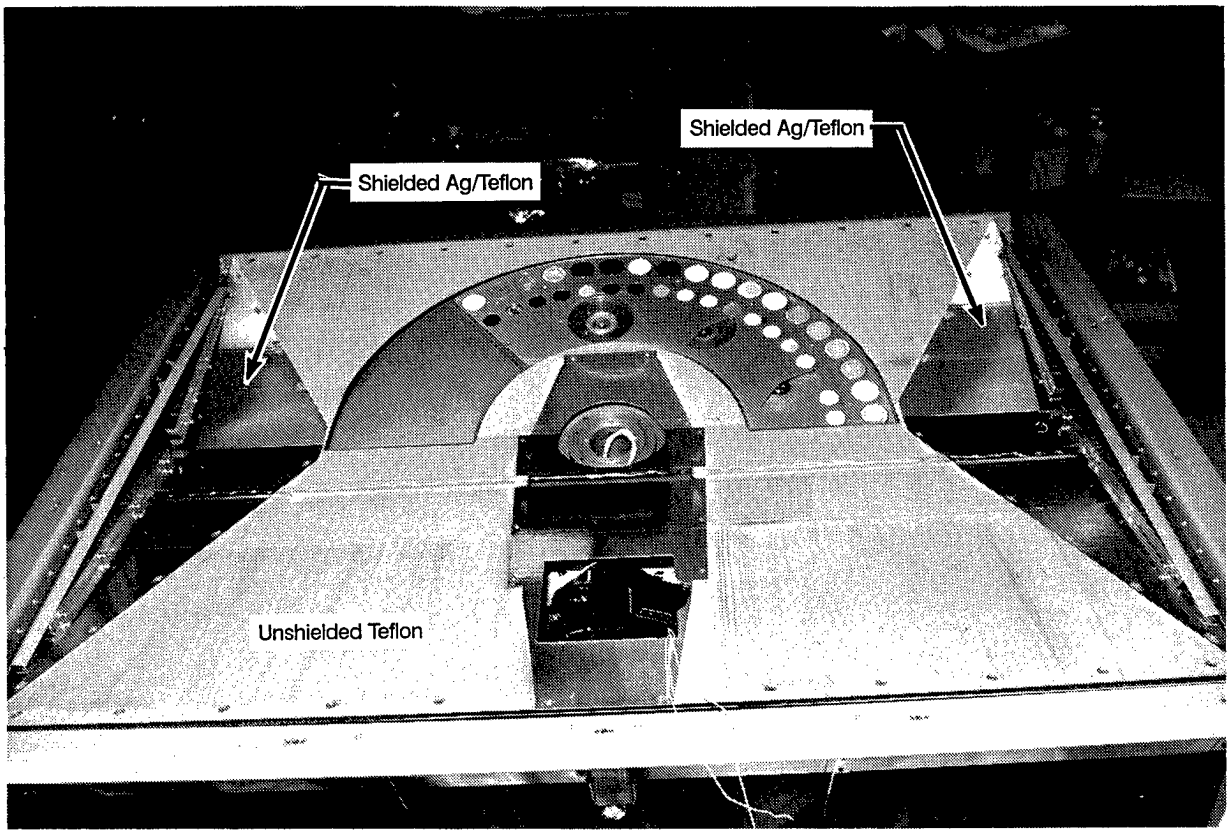

Figure 4.3.2.3-2. Bonded Silverized Teflon on S0069

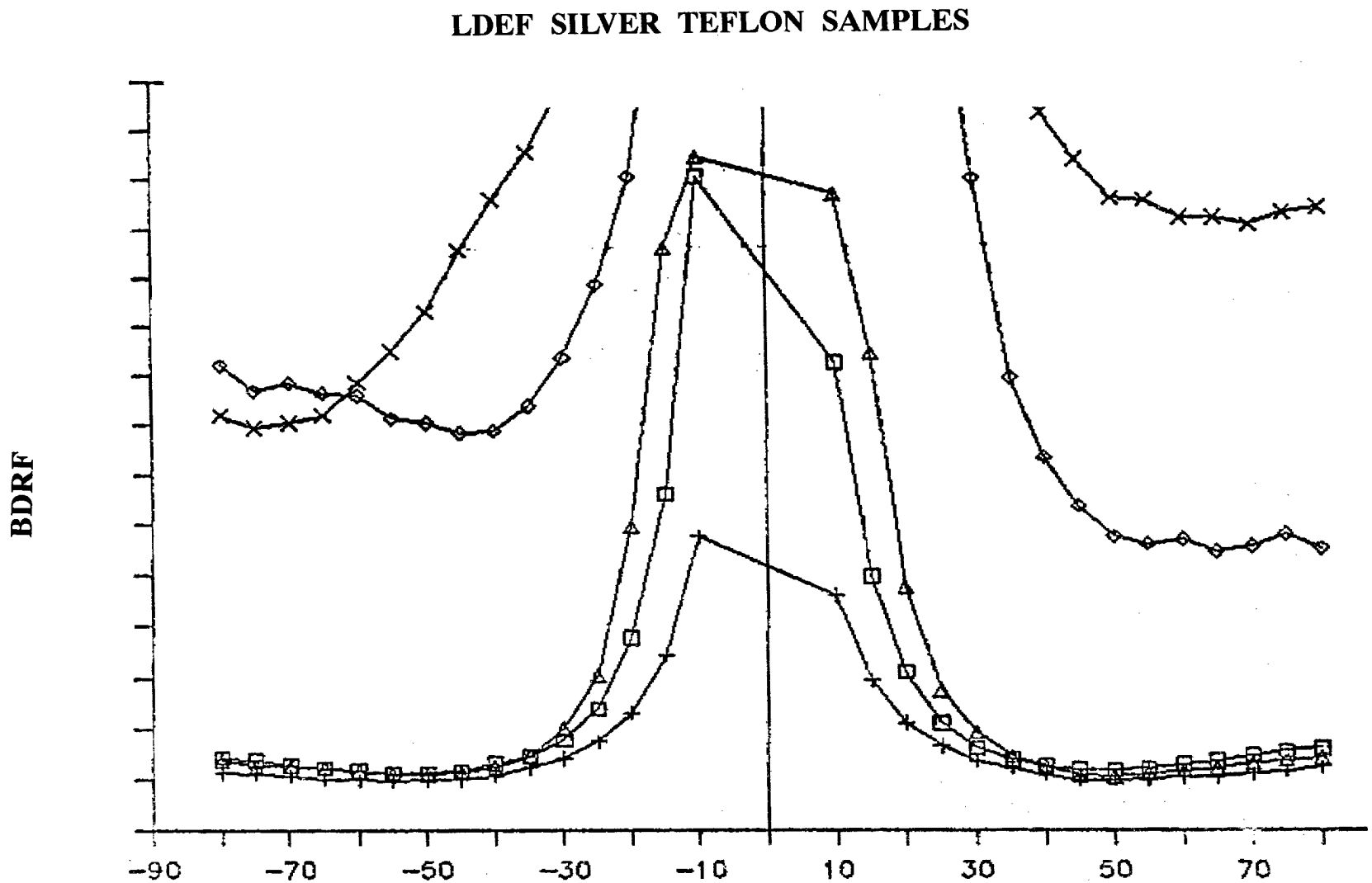

Figure 4.3.2.3-3. Diffuse Reflectance (BDRF) of Silver Teflon

Film Delamination:

The delamination and darkening of coated films, such as silver Teflon, in areas around high velocity impact sites was observed to result in a significant thermal lag in the heat transfer and radiation process. The net total lost area due to this degradation is modest and would not be a design consideration except in cases of highly limited margins.

This delamination is speculated to be a result of atomic oxygen expanding into the area surrounding the impact site and reacting chemically with a coating, such as silver which is highly reactive.

Undercutting of aluminized Kapton was studied at NASA LeRC, and undercutting profiles were compared to Monte Carlo models of atomic oxygen attack in the ram direction (ref. 69). Wide undercut cavities were observed despite the stability of the LDEF in its orbit. Undercutting cavities can develop around any surface breach, including manufacturing imperfections, installation damage, and particle impact damage sites.

Bonded Teflon:

Bonded silver Teflon films were subject to microcracking in the application process, resulting in the migration of the adhesive above the reflective silver deposit and a subsequent darkening under extended exposure to ultraviolet radiation.

In selected areas of the cover on Experiment S0069, this thermal degradation was severe, with measured changes in absorptivity from 0.1 to 0.5 (ref. 76).

This effect was also observed on Experiment S1005, in which the foil was stretched taut on the heat pipe surface, resulting in small cracks in the silver surface; the adhesive then seeped into the cracks. The subsequently exposed adhesive then turned brown, resembling the widespread silicon contamination (ref. 64).

Teflon Heat Capacity:

A significant loss of heat capacity in silver Teflon was measured, although this would only affect a bulk material application.

Samples of silver Teflon from Experiment S1005 were tested for specific heat value (heat capacity) on a Differential Scanning Calorimeter (ref. 64). The drop in specific heat for the exposed samples, compared to control samples, ranges from 25% to 40% at any given temperature; the total energy absorbed by the material dropped from 67 calories per gram to 26 calories per gram.

In a thin film application, the temperature of the film would be driven by the surface on which it was mounted and thus this loss of heat capacity would normally not be a design factor.

Kapton:

The erosion of Kapton films was as expected. No significant changes in thermal properties were observed.

Post flight measurements of interior Kapton insulation from Experiment S1005 produced characteristics (alpha =0.31 and epsilon =0.79) that were not significantly changed from published stock data (ref. 64). No preflight measurements had been made.

One set of coated Kapton specimens was lost on orbit from the Goddard Experiment S1001 because of atomic oxygen erosion of the Kapton tape which had held them in place.

Mylar:

The erosion of Mylar films was greater than expected. The degradation of Mylar film from exposure to ultraviolet radiation also exceeded expectations.

The embrittlement of Mylar films aboard Experiment A0138 from ultraviolet radiation alone was so severe that it was not possible to perform mechanical testing (ref 36).

Betacloth:

Betacloth which was exposed to the atomic oxygen flux was seen to have been cleansed of the many minute fibers that normally adorn its surface. This has been observed to have no measurable effect on the thermal performance of the betacloth, although some associated contamination issues are raised.

Exposed betacloth blankets on Experiment S1005 had acquired a diffuse white appearance, similar to the eroded silver Teflon thermal blanket materials, but there were no visible penetrations from high velocity impacts. Post flight measurements of the betacloth (unwiped) produced characteristics (alpha =0.24 and epsilon =0.89) that were not significantly changed from published stock data. No preflight measurements had been made (ref. 64).

Adhesives:

The performance of the frequently used RTV adhesive was generally good, although darkening was observed in some instances.

The RTV 560 +12% graphite adhesive bonds on Experiment M0003-5 failed in all applications, although their EC57 and Y966 bonds remained intact (ref. 78).

4.3.2.4 Heat Pipes:

Initial functional tests were performed for each of the three heat pipe experiments flown on the LDEF, and the heat pipe systems were found to be intact and

fully operational. No heat pipe penetration occurred due to micrometeoroid or debris impact.

Each of the experimenters reported anomalies in their overall experiment history. In Experiment A0076, an electronics component failed leading to a loss of control of non-condensable gases (ref. 63). In Experiment S1001, the radiator failed to cool the system to as low a temperature as expected (refs. 61 & 67). In Experiment S1005, an unexpected conductive leak was observed in the data, and an unusual "discolored" area was observed on an unheated shield (ref. 64). None of these anomalies prevented the accomplishment of the experiments' primary objectives.

Experiment S1005 was comprised of three independent variable conductance transverse flat plate heat pipes, designed to serve as both an electronics mounting plate and as a thermal control system. The heat pipes are a proprietary Grumman design and operate nominally at room temperature while transporting up to 50 watts. Data from preflight testing and flight operations were found to be consistent; two minor data variations are under investigation but are understood not to be related to the function of the heat pipes. Post flight testing is planned for late 1991 or early 1992.

Experiment A0076 was comprised of two variable conductance heat pipes connected in series (cascaded). The pipes used ammonia as a working fluid and nitrogen as the dry reservoir control gas. The flight data showed successful temperature control to within ± 0.5 °F, with only one heat pipe required to be used. There was a slight increase in both systems set points in post flight tests; this effect is typically the result of diffusion of liquid working fluid into the dry reservoir, but the actual cause of this effect in these pipes has not yet been determined. As a possible environmental effect, it represents an average drift rate of less than 2 °F per year, and control is still maintained about the shifted set point to within ± 0.5 °F.

At NASA JSC, 388 micrometeorite or debris impact sites were identified on the A0076 experiment. Of these, 167 craters were greater than 0.5 mm in diameter; one impact of 2.8 mm diameter on the silver Teflon coated radiator was accompanied by shock waves in an area exceeding 50 mm in diameter. Testing for delamination in this area remains to be performed. Despite these impacts there was no evident loss of integrity of the heat pipes as pressure vessels.

Experiment S1001- Low Temperature Heat Pipe Experiment Package (HEPP) included two ethane heat pipes for operation in the range of -190 to +10 °F. The transporter heat pipe (THP) is a constant conductance aluminum axially grooved type. The second pipe utilizes a stainless steel axially grooved extrusion and a liquid trap reservoir for diode operation. Also included is a n-heptane phase change material (PCM) canister which provides temperature stability at its -132 °F melt point by melting and freezing. More than 388 days of data were obtained with the pipes operating continuously with 1.2 watts on the THP and 1.0 watts on the diode heat pipe. The heat pipes and the radiator system experienced nine cycles which varied between -118 and +55 °F during this period. Post flight ambient tests showed that both heat pipes are still operating.

The one problem that HEPP experienced was its failure to cool below -118 °F. This prevented the freezing and subsequent melting of the n-heptane PCM canister. Also, since the HEPP electronics had a preprogrammed test sequence that was set for activation when the PCM cooled below -100 °F, transport tests with the THP and diode could not be conducted and the diode reverse mode shutdown could not be demonstrated. The reason for the inability to cool below -118 °F should be determined during subsequent thermal vacuum testing.

4.3.2.5 Radiometers, Calorimeters, Reflectometers

Flight support equipment on the LDEF included radiometers, a calorimeter, and a reflectometer for the measurement of solar and thermal parameters. In all reported instances the performance of these subsystems has been excellent, both during the mission and in post flight evaluations.

Experiment A0147 carried numerous Earth Radiation Budget (ERB) components (ref. 70). A cavity radiometer on S0014 showed only slight visible changes in the painted surface of its cavity receiver. Intercomparison tests in direct sunlight have shown changes of less than 0.05%, significantly improving confidence in solar irradiance measurements from the NIMBUS 7 satellite, on which a similar radiometer was incorporated. Thermopile sensors, including the painted receivers of directly exposed units, were virtually unaffected by the spaceflight environment.

Experiment S0069 included the most complete thermal and optical measurement system (ref. 71) flown on the LDEF. This system included three radiometers using flat black thermopile detectors and domed collection optics. Quartz lenses were used on the solar and Earth albedo radiometers, and a germanium lens was used on the Earth infrared radiometer. This experiment also contained a calorimeter of a design similar to that developed by Goddard Space Flight Center for the ATS/1, ATS/2 and OAO/C satellites. Finally, this experiment also included a reflectometer containing tungsten and deuterium lamps, a scanning prism monochrometer,and a 4.5 inch diameter integrating sphere coated with barium sulfate.

The flight data indicates that all of these systems performed well, with a repeatability of less than 2%. Anomalous noise in the reflectometer ultraviolet data occurred late in the mission but resolution of this effect has not yet been completed.

4.3.3 Unresolved Issues

In the course of the LDEF investigation numerous unanswered thermal issues have arisen, and these are documented herein to ensure that these are not omitted in any future efforts in support of the thermal investigation. These issues have their origins in the thinking of both LDEF investigators and interested applications engineers outside of the LDEF investigation proper.

Issue:

The quantification of the diffusivity of various eroded material surfaces.

Issue:

The applicability of chromic acid anodize results to alternative processes being considered for the Space Station, specifically sulfuric acid anodize; there were no sulfuric acid anodize surfaces on the LDEF.

There was contradictory data reported concerning the stability of optical characteristics for chromic acid anodize. This inconsistency remains to be resolved and, in addition, there is concern over the chromic acid anodize stability for optical characteristics beyond the range of those flown on the LDEF. Further, the data from the LDEF cannot be extrapolated to cover the Space Station life span.

Issue:

The development of many small squares of thermal blanket material, in a pattern similar to that of the "bridal veil" separating material.

Issue:

Quantification of the contamination environment dynamics.

The general contamination observed on the LDEF has been noted as a significant issue and a determination of the contamination history for the LDEF as a function of time is seen as important. Contamination analysis of the Environment Exposure Control Canisters (EECC) used on LDEF has potential to provide this history, but as yet this work has not been performed. Minimal data is available at this time to indicate how much of the thermal surface performance degradation is attributable explicitly to contamination, but the selected data available indicates that, in some cases, it is a substantial portion.

Combined effects of AO, contamination, and UV radiation require further study. The loss of electrical conductivity in carbon pigment paints is of particular concern to designers, and similar loss of thermal conductivity may become an issue. Generally observed effects which may be AO related are darkening of coatings, polymerization of contaminants resulting in increased contaminant adhesion, and stimulation of material outgassing.

Issue:

Mechanical properties of thermal films and substrates.

Issue:

Quantification of the adhesion of thermal paints and other coatings.

Issue:

Heat transfer measurements, including mechanical insulators and standoffs.

Issue:

Calculation of the net lost equivalent radiator surface from the combined effects of contamination, ultraviolet radiation, and microparticle impacts accompanied by atomic oxygen induced delamination.

A specific remaining issue is determination of the actual performance of thermal blankets damaged by micrometeoroid or debris impacts. Delamination areas many times larger than the immediate impact damage area were observed on silvered Teflon blankets. Thermography measurements have shown a significant thermal lag in conducting heat across these delaminated areas.

Issue:

The possibility of increased effects on films and other surfaces under stress.

Issue:

Tabulation of the net thermal degradation for a wide variety of materials. Most of the attention thus far has been to silver Teflon, chromic acid anodize, and A276 white paint.

Issue:

Calibration of ground testing and simulation facilities, particularly including a careful assessment of the true impact of time compression in accelerated testing.

Issue:

Resolution of all remaining thermal anomalies in heat pipe experiment functions, including

radiator shortfall;
internal conductive leak;
heat pipe set point increase;
shield surface degradation.

Issue:

Assessment of the impact of 32,422 thermal cycles on material properties.

At present, the role of thermal cycling in observed effects has not been evaluated in the LDEF analysis. Some coating degradation and possibly delamination of silver Teflon at impact sites may be due to thermal cycling.

4.4. OPTICAL SYSTEMS

Unlike the Electrical and Mechanical disciplines, the Systems SIG Optics effort has relied on the testing of hardware by the principal investigators since all space-exposed optics hardware is part of individual experiments. Thus, the main objectives of the Systems SIG have been to develop a database of experimental findings on LDEF optical systems and elements hardware, and provide an optical system overview. Minimal optical testing has been performed by the Systems SIG.

At this time, optical systems and elements testing by principal investigators teams is not complete, and in some cases has hardly begun. Most experimenters have provided observations and measurements to "show what happened." Still to come from many principal investigators is a critical analysis to explain "why it happened" and future design implications.

Throughout the LDEF research process, a requirement has existed to collate results into a database, and to make this information available to the space community. Provided within Appendix D is a paper copy of the Systems SIG LDEF Optical Experiments Database, as well as a database users guide (Appendix C). The database identifies, among other things, the optical hardware flown, the space environmental conditions the materials were exposed to, experiment objectives, results, conclusions, and future design considerations.

This section summarizes the original optical systems-related concerns, and the "lessons learned" at this preliminary stage in the LDEF Optical Systems investigation. It also describes the LDEF Optical Experiments Database which provides reference to currently available experimenter's findings, and includes a survey of current research in optical systems contamination control.

4.4.1 Optical Systems-Related Concerns

From a systems point of view, the degradation of an individual optical element can easily affect the overall system performance. For instance, surface degradation of a space-exposed transparent optical element, combined with particulate deposition, may cause an increase in diffuse scatter and a resulting loss of light transmission. In certain types of imaging systems, this could significantly degrade the final image resolution. The following outline identifies some of the original systems-related concerns:

Degradation of transparent elements (darkening, contamination, impacts):
- Reduce the throughput of available light for radiometric, photometric and imaging systems
- Degrade image resolution

Degradation of optical coatings (erosion, discoloration, delamination, pitting, contamination):
- Holes in coating may alter wavelength dependent transmission and reflection properties
- Surface contamination on coatings may decrease throughput of light

- Degraded or damaged coating may encourage initiation of other types of damage
- Redeposition of contaminants, including damaged coating materials, on other system optics (loss of resolution, reduced throughput, wavelength dependence)

Degradation of diffuse paints or diffuse metal coatings in optical systems (erosion, discoloration):

- Baffling efficiency may decrease due to increase in specular reflection; or may increase due to an increase in roughness of baffle surface topography
- Redeposition on other materials
- Contamination of system optics (loss of resolution, reduced throughput, altered wavelength dependence)

Degradation of fiber optics (radiation darkening, impacts, contamination):

- Reduced transmission
- Complete loss of signal
- Increase in system bit error rate (digital)
- Decrease signal to noise ratio (analog)

Detector changes:

- Responsivity
- Detectivity
- Rise time (system bandwidth)

4.4.2. LDEF Optical Hardware and Systems Lessons Learned

Optical materials did demonstrate a variety of effects as a result of their space environmental exposure to LEO. The significant environmental parameters which affected the LDEF optical materials are summarized briefly below.

- Contaminant films and residue were widespread in their migration over LDEF and onto optical experiment surfaces, especially due to the decomposition and outgassing of several materials; at least two possible sources being identified as those from the vehicle itself, as well as those materials used in some of the experiments.(ref. 80) .

- Micrometeroid and debris impacts caused localized pitting, punctures, cracking, crazing, and delaminations.

- Spectral radiation was indicated both in the modifications of surface coating materials (chemical decomposition caused by ultraviolet radiation), and changes to coating interfaces as a result of infrared (IR) absorption which contributed to mechanical stress and failures from thermal cycling:

- Atomic oxygen had a major effect in the oxidation degradation of many physically "soft" materials, including those for optical coatings and thin

films, as well as straight oxidation of uncoated, metallic reflective coatings (copper and silver).

- The combination of any of the individual environmental factors such as UV, AO, thermal cycling, meteoroid/debris impacts and contamination can produce "synergistic conditions" that may accelerate the onset and rate of degradation of space exposed materials and systems (ref. 81).

In order to investigate the space environmental effects in detail, the optical materials and systems are divided into seven groups by material type for categorizing the "lessons learned": Uncoated Optical Materials, Coated Optical Materials, Solar Cells, Fiber Optics, Detectors, Reflectometers and Radiometers, and Optical Sources. Discussions in each of these areas will consist of a summary paragraph followed by an experiment-by-experiment synopsis of results as reported up to this time for each individual experiment.

Please note that a detailed list of optical materials flown on LDEF can be found in the Optical Systems Database under each experiment record. In addition, a summary list of optical hardware is available in Appendix A.

4.4.2.1. Uncoated Optical Materials

Five LDEF experiments investigated space environmental effects on uncoated optical materials. In general, hard uncoated optical materials were found to be quite resistant to the space environment. Even micrometeoroid and debris impacts tended to have only localized damage without degradation of the optical performance. The impacts appeared as craters surrounded by an expanded area of damage caused by melting, cratering, spallation, or small fracture patterns as illustrated in figure 4.4.2.1-1. However, when the uncoated optical materials were contaminated, the spectral transmission on these same materials could vary from no detectable change to catastrophic loss in transmission. This emphasizes the need for contamination prevention throughout any future mission duration. Exposed, physically soft, uncoated optical materials like thallium bromide-iodide (KRS-5 and KRS-6) experienced gross physical degradation of the substrate material as a result of excess space exposure, especially due to the effects of atomic oxygen bombardment. The status of the results from each individual experiment follows:

S0050-1: Investigation of the Effects of Long Duration Exposure on Active Optical System Components Experiment. The S0050-1 experiment was composed of optical windows CaF_2, MgF_2, LiF, Al_2O_3, SiO_2 on the E6 tray as shown in figure 4.4.2.1-2 from which the S0050-1 windows were taken. Surface contamination was the only deterioration noted on the S0050-1 optical windows as shown in figure 4.4.2.1-3. A faint brown stain is visible on the front surface of the six windows and a brittle film is also present on the back surface of the three UV transmitting fluoride windows. The region of the spectrum from 100 to 300 nanometers was the principal region of interest and defines the ultraviolet (UV) as used in this experiment. The loss in the vacuum ultraviolet transmission was catastrophic. The UV absorptions were almost 100 % at 200 nm and about 50% at 300 nm due to the contaminating film. (ref. 82)

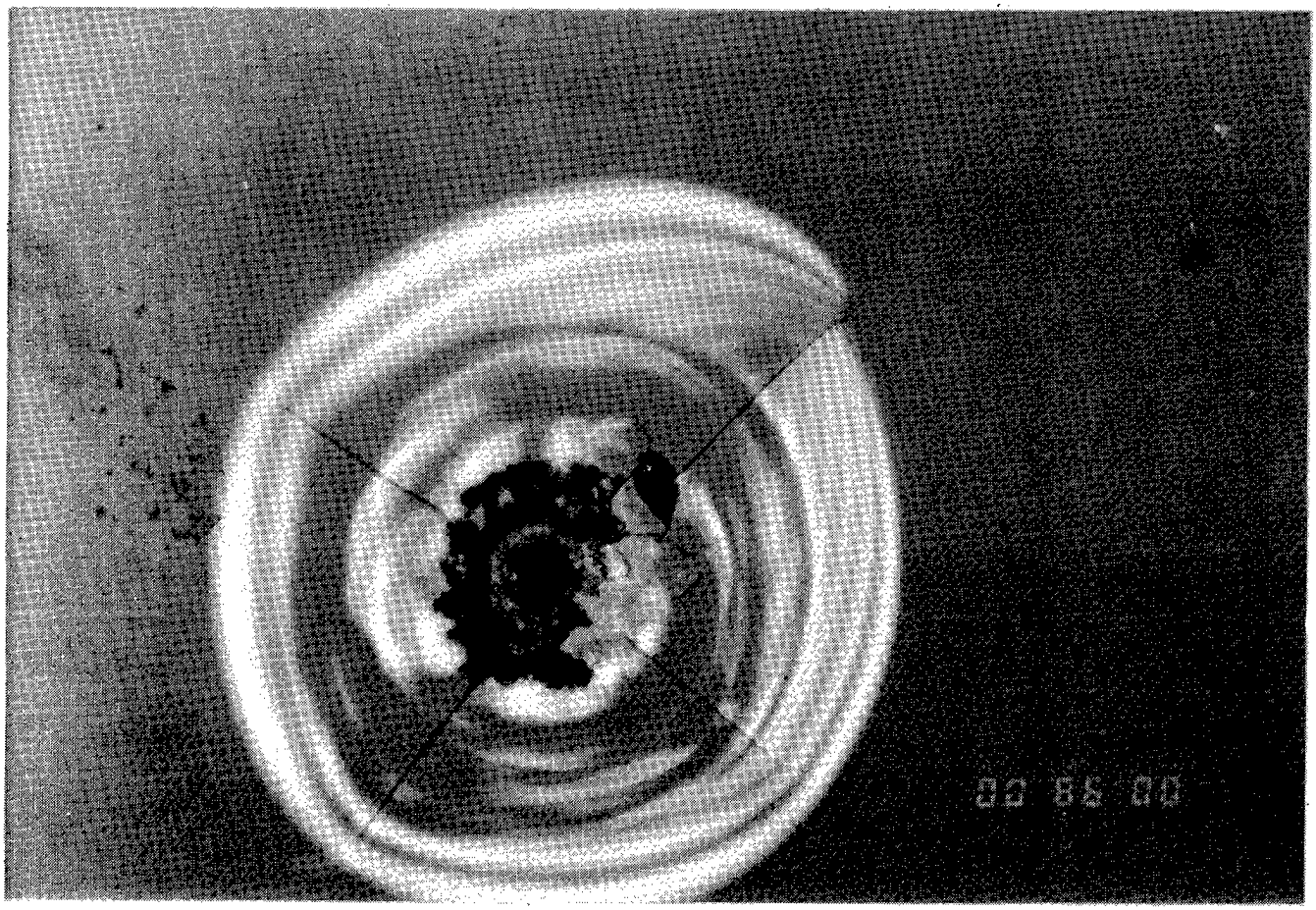

Figure 4.4.2.1-1. Impact Crater With Surrounding Localized Damage on a Transparent Dielectric-Fused SiO_2 Glass Substrate (Photograph Courtesy of The Aerospace Corporation)

(See color photograph on p. 296)

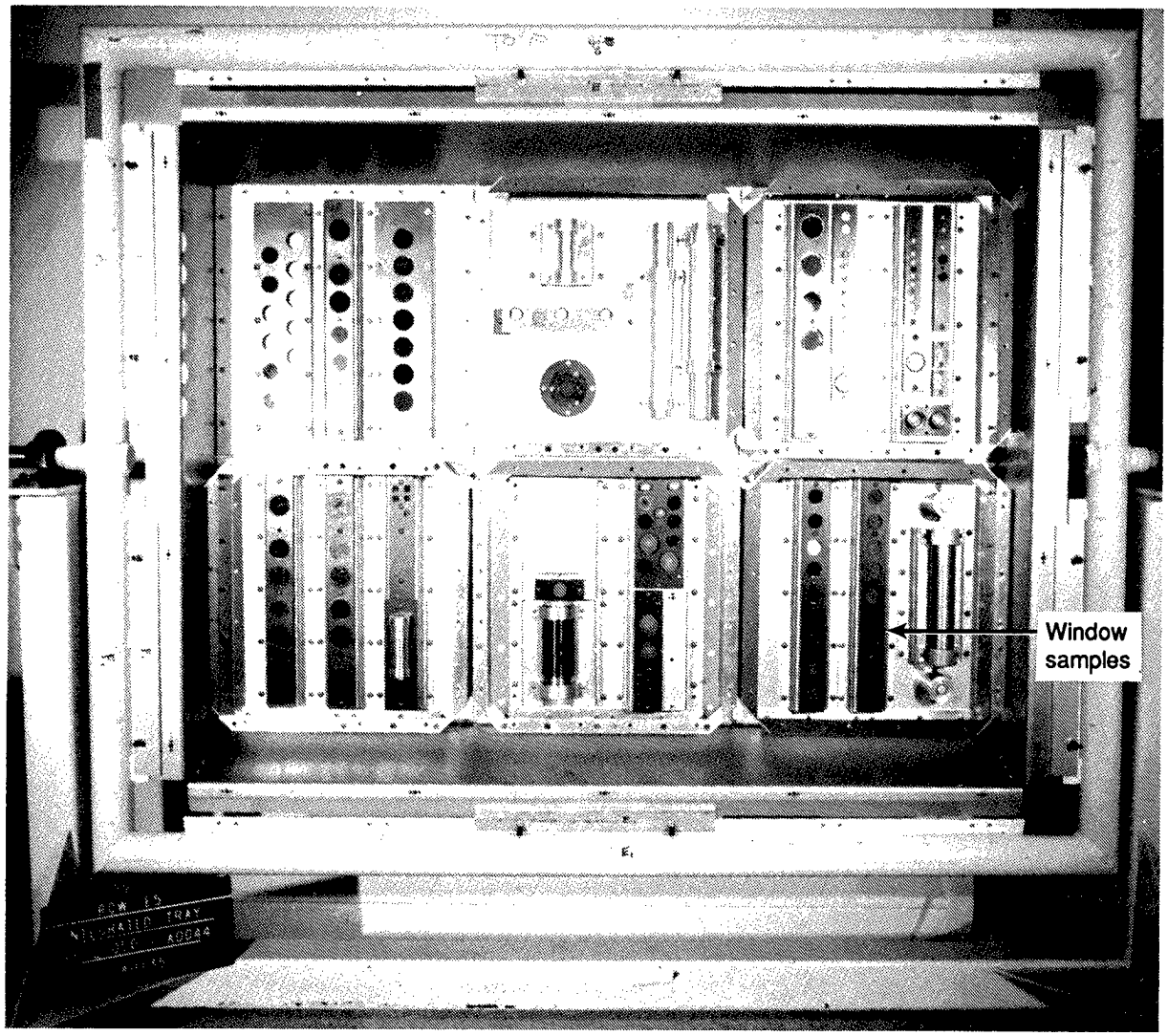

Figure 4.4.2.1-2. Active Optical System Components Experiment (S0050)

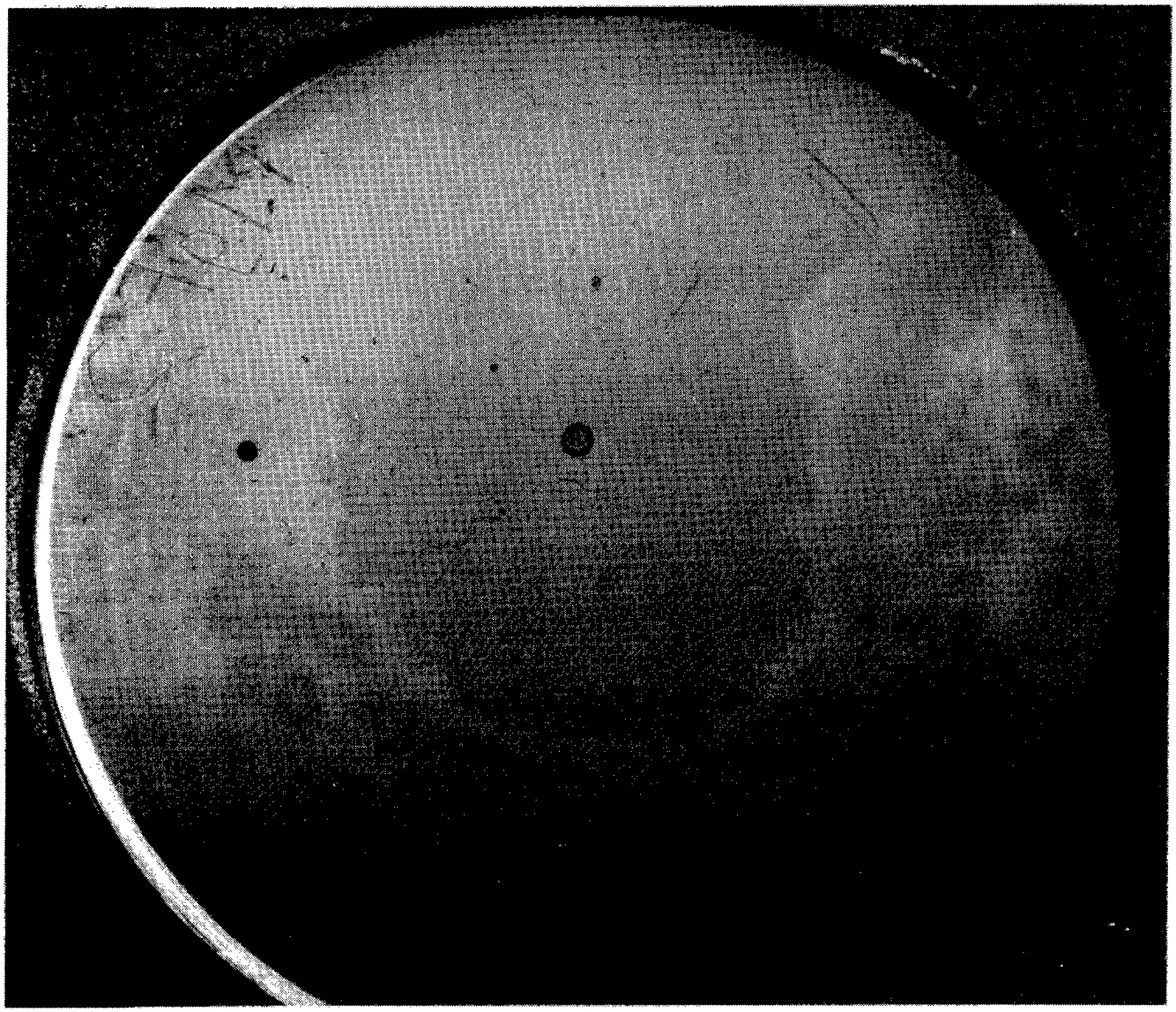

Figure 4.4.2.1-3. Effects of Long Exposure on Optical Systems Components (S0050-1) Contaminated MgF_2 Optical Window

(See color photograph on p. 297)

S0050-2: Investigation of the Effects of Long Duration Exposure on Active Optical System Components Experiment. Three fused silica and three ultra-low expansion (ULE) uncoated glasses were included with this experiment's samples. The uncoated substrates were shown to be covered with a thin layer of polymeric material which contained silicon. After cleaning with a toluene wash and methanol rinse, the optical performance of the uncoated samples returned to pre-flight levels. Micrometeroid damage was localized. No radiation darkening occurred on the ULE (though it was expected to) or on the fused silica (ref. 83).

A0147: Passive Exposure of Earth Radiation Budget Components Experiment. Fused silica windows comprised the uncoated samples in this experiment. The window materials did experience changes in spectral transmittance. Those showing the heaviest visual contamination also showed the most degradation over the whole UV region. It should be noted that no attempt was made to clean the windows at this time, however transmittance measurements are scheduled to be redone after cleaning. Cleaning was postponed awaiting further information on other LDEF results (ref. 84).

A0056: Exposure to Space Radiation of High Performance Infrared Multilayer Filters and Materials Technology Experiments. Experiment samples included MgF_2, CaF_2, KRS-5, KRS-6, CdTe, Si, Ge, Al_2O_3, Y-cut quartz, and Z-cut quartz. No significant changes were found in transmission or spectral position in the hard uncoated crystal substrates. The softer materials like thallium bromide-iodide (KRS-5 and KRS-6) were adversely affected in their physical and optical properties by long exposure in space, resulting in reduced transmission to a complete opacity. Although micrometeroid impacts damaged some hard samples, these did not detract from their function and performance as an optical component. Most impacts produced only localized damage around the periphery of the impact site (large spallation diameters and small fractures), except the calcium fluoride substrate. The CaF_2 cleaved in two directions outward, verifying the fragile and brittle nature of calcium fluoride as a substrate material. Atomic oxygen and space radiation caused no spectral effects that the investigators could detect on the hard uncoated samples (ref. 85).

A0172: Effects of Solar Radiation on Glass Experiment. The glass and glass ceramic samples exposed on LDEF were found to display limited degradation in optical transmission. Specifically, fused silica displayed decreases in transmission in the 200 to 400-nm wavelength region, and this degradation appears to be a consequence of surface contamination, primarily carbon and another species with an atomic mass near 64 on the interior surface of the samples. No detectable contamination was seen on the exterior surfaces (ref. 86). Mechanical testing and optical microscopy suggested that radiation components of the Earth orbit did not degrade the mechanical strength of the sample. In addition, the upper bound of strength degradation for the meteoroid impacted samples was 50%, using calculated values of stress corresponding to the actual stress present on the impact site during testing (ref. 87). Note that the exact number of samples tested post-flight was not described in the reference, however 120 samples were flown on this experiment (ref. 88).

4.4.2.2 Coated Optical Materials

Several important observations were made on the coated optical materials. They include:

a) Copper and silver coated optics showed oxidation due to atomic oxygen bombardment as shown in figure 4.4.2.2-1.
b) Thermal cycling or thermal excursions were implicated in the delamination of dielectric and metallic-coated optics.
c) Contamination was shown to degrade transmission or reflection in many coated optical materials as documented in figure 4.4.2.2-2; and when the contaminant was cleaned, optical results would often return to pre-flight measurements.
d) Micrometeroid and debris impacts showed localized impact damage effects, but their actual damage potential was often dependent on the impact density on the coated optical material; see figure 4.4.2.2-3.
e) Certain substances, notably ZnS and to a lesser degree MgF_2, show susceptibility to contamination and material degradation in exposed areas as shown in figure 4.4.2.2-4.
f) Other sources/causes of material degradation must be assessed (e.g. shelf life, sample handling, manufacturing defects) prior to making final conclusions about the extent of LEO exposure on LDEF coated optical materials.

Following are highlights from the individual experiments that involved coated optical materials.

A0147: Passive Exposure of Earth Radiation Budget (ERB) Experiment Components. This experiment utilized a set of interference filters, comprised of both metal and dielectric multilayer coatings (for the UV and visible/NIR region), which were exposed to the space environment, as illustrated in figure 4.4.2.2-5. The experimenter describes the coatings as having survived well, with the exception of the following:

- Increase in transmission due to pinholes in some of the metal-dielectric coatings
- Slight increase in transmission due to an apparent reduction in the extinction coefficient of ZnS
- Decrease in transmission due to increased absorption in the lead compounds (ref. 89).

S0050-2: Investigation of the Effects of Long Duration Exposure on Active Optical System Components Experiment. This experiment contained the following coated samples: (1) ULE substrates with high reflectance silver coating, (2) fused silica with an AR coating, and (3) fused silica with solar rejection coatings. Preliminary results showed the samples were covered with a thin layer of polymeric material, which contained silicon. Except for the AR-coated samples, the optical performance of the coatings returned to preflight measurements after cleaning. AR coatings are still under investigation (ref. 90).

(See color photograph on p. 298)

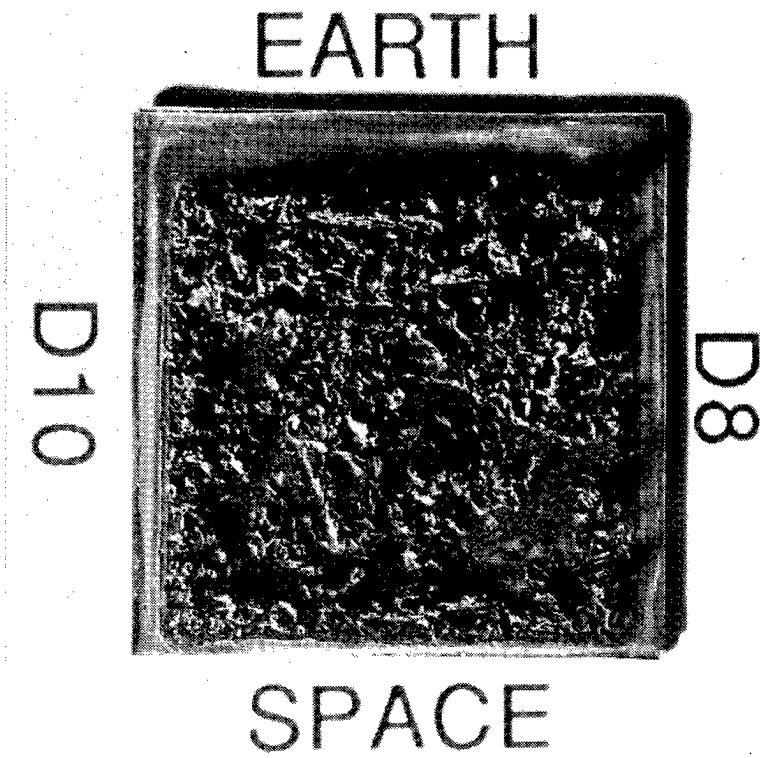

Figure 4.4.2.2 -1. Severely Corroded and Peeling Optical Solar Reflector Silver Mirror (Photograph Courtesy of The Aerospace Corporation)

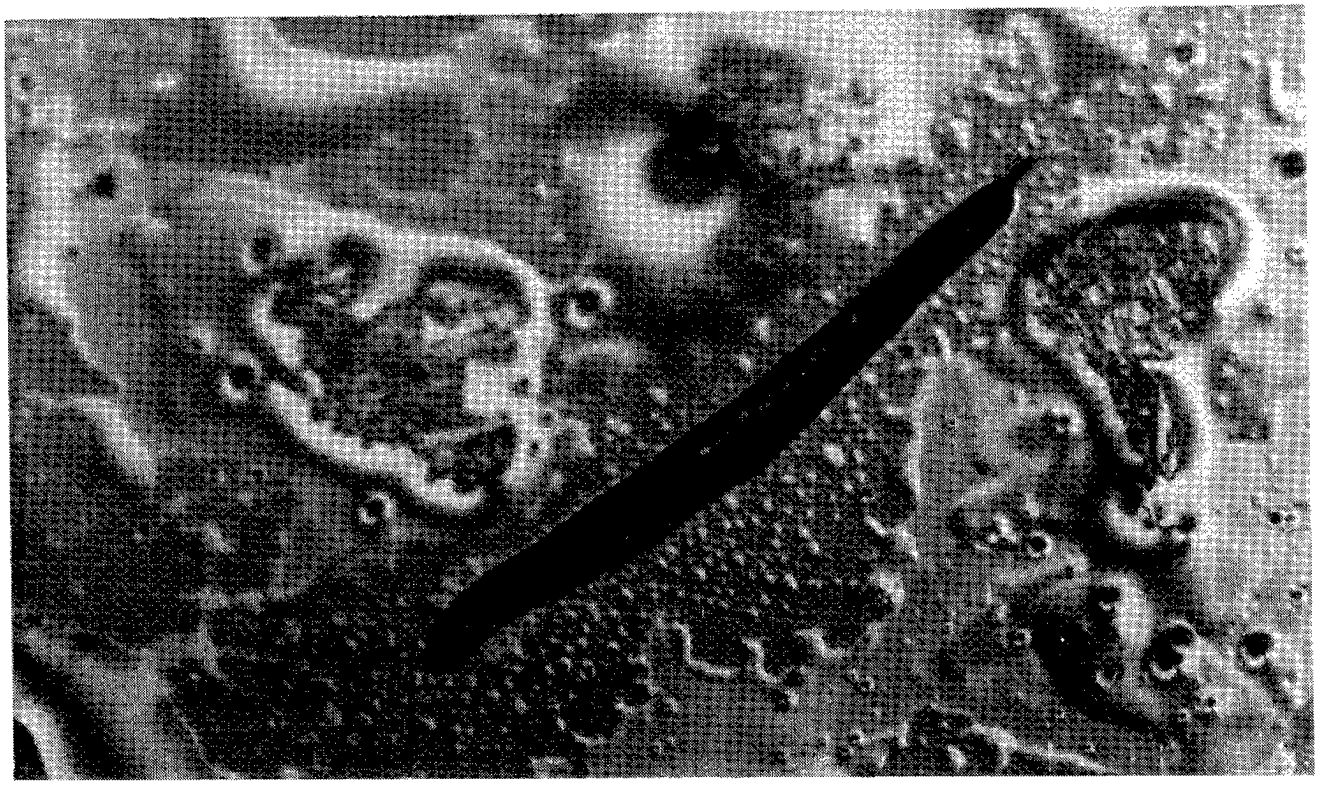

Figure 4.4.2.2-2. Contamination on Laser Mirror Photographed at SAEF-2 at the Nomarski Microscope Workstation. (Courtesy of E. R. Crutcher)

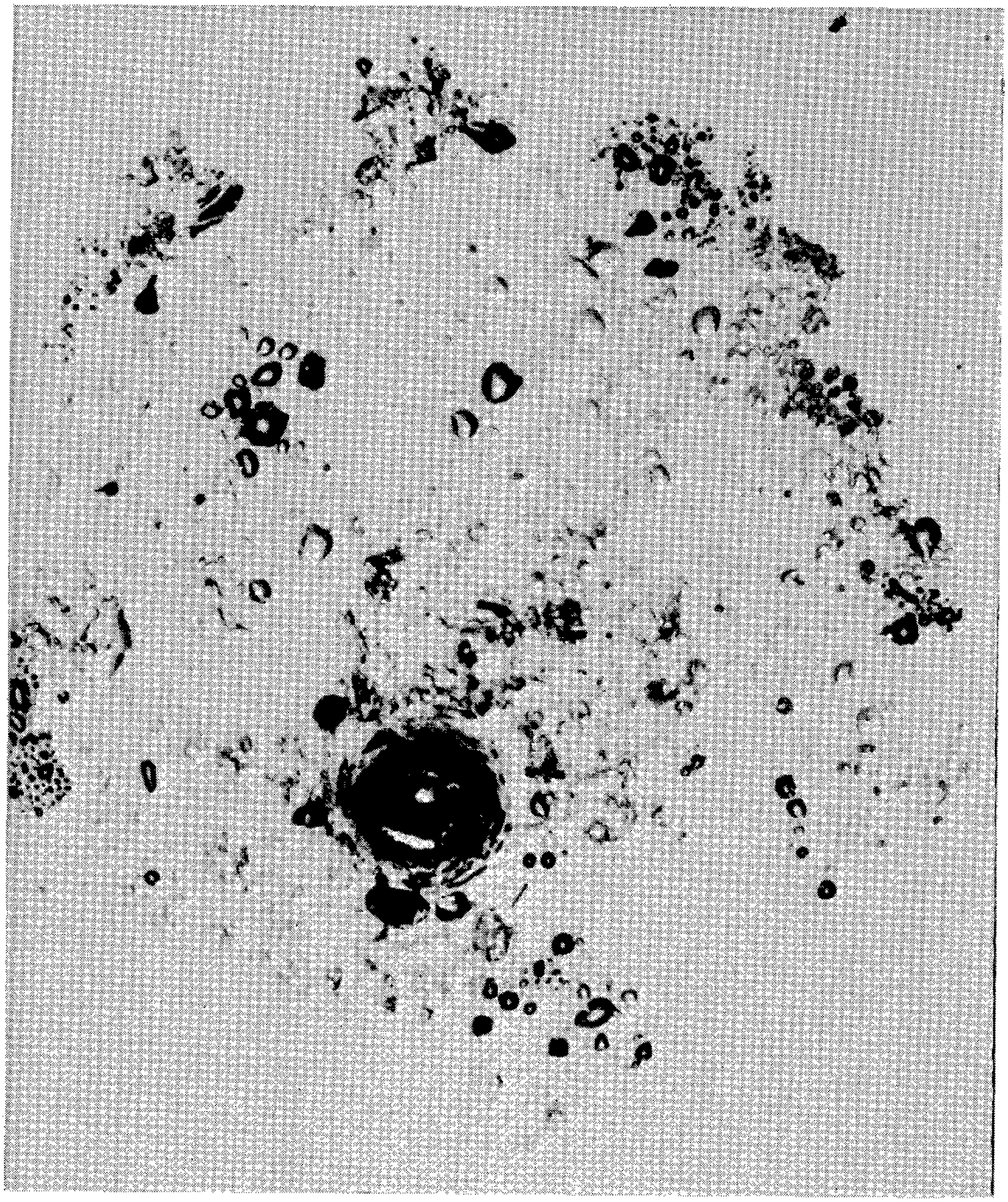

Figure 4.4.2.2 -3. An Impact Crater With an Expanded, Asymetric Area of Damage. The substrate is molybdenum with a Cr/Ag/ThF_4 coating. (Photograph courtesy of The Aerospace Corporation)

(See color photograph on p. 299)

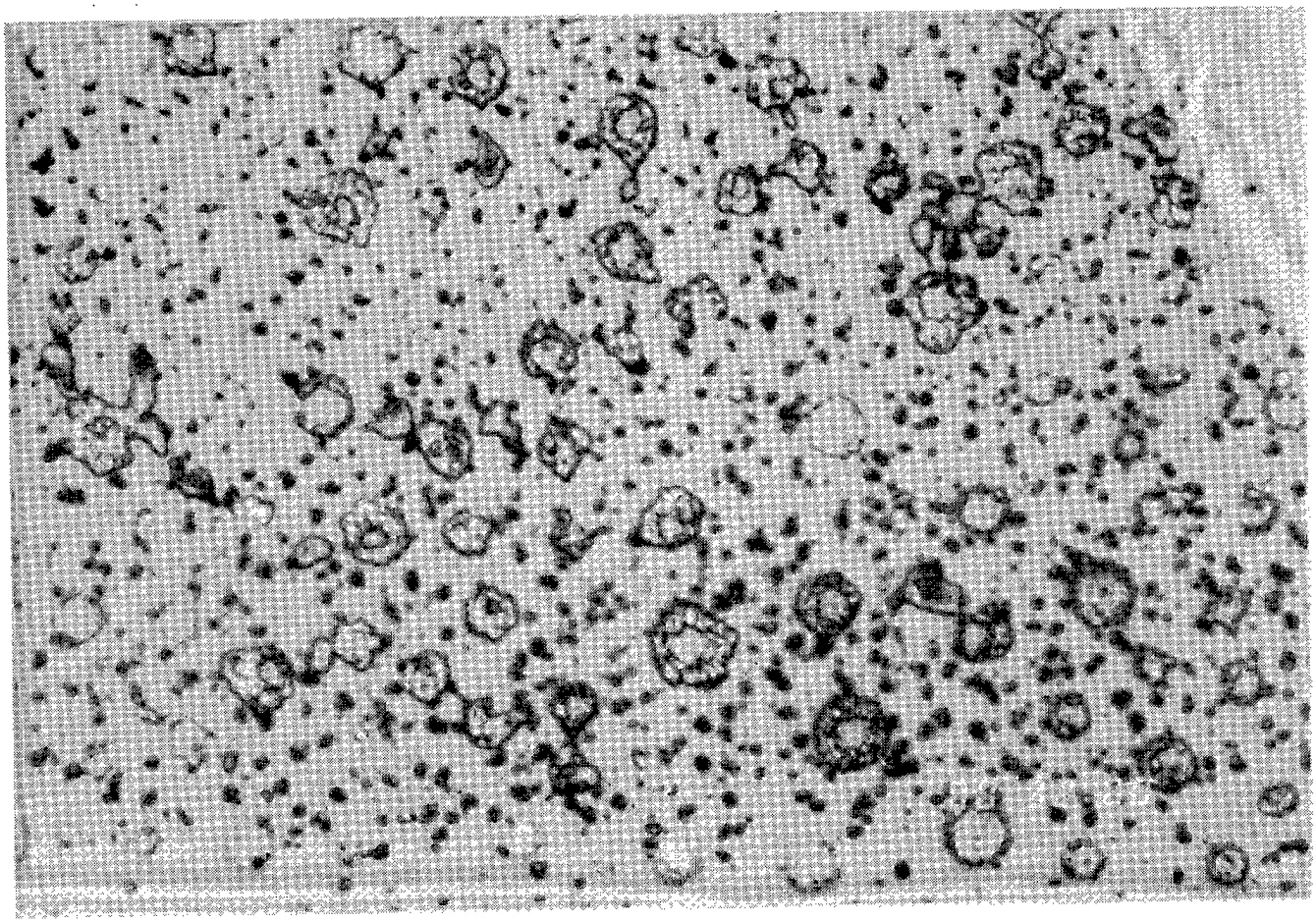

Figure 4.4.2.2-4. Degraded ZnS Coating on a SiO_2 Substrate (Courtesy of The Aerospace Corporation)

(See color photograph on p. 300)

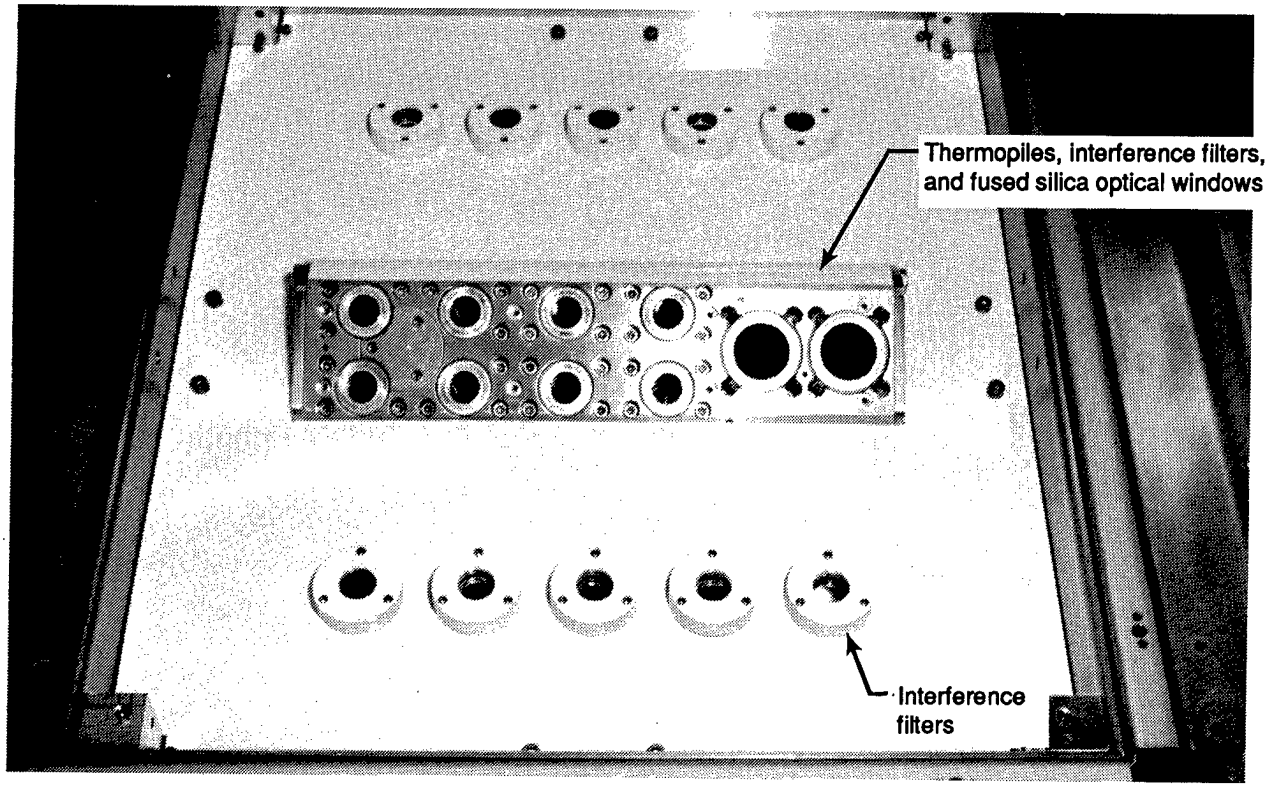

Figure 4.4.2.2-5. Passive Exposure of Earth Radiation Budget Experiment (A0147) Solar-Channel Components

A0056: Exposure to Space Radiation of High-Performance Infrared Multilayer Filters and Materials Technology Experiment. This experiment contained IR optical-multilayer filters, which the principal investigator further divided into physically soft and hard coatings. The hard multilayer coatings had a small but consistent loss in transmission, but within the uncertainties envelope. These samples were considered stable and showed no degradation from the space exposure. The soft-coated samples containing thallium bromide-iodide (KRS-5 and KRS-6) showed gross physical degradation from space exposure, including delamination of coatings and substrate material (ref. 91).

S1002: Investigation of Critical Surface Degradation Effects on Coatings and Solar Cells Developed in Germany Experiment. The S1002 coated samples were comprised of interference filters. The filters were found to contain an irregular distribution of brown areas formed in the interface between the In_2O_3 and ZnS layer, with a shift of interference filter reflection maximum to longer wavelengths. Because of this, transmission of the Sun's maximum radiance is increased and as a consequence, the polymethyl methacrylate (PMMA) intermediate layer, the fluorinated ethylene propylene (FEP) foil, and the silver reflector could not be sufficiently protected. This induced degradation will lead to further increased absorption and degradation (ref. 92).

A0138-4: Vacuum Deposited Optical Coatings Experiment. This experiment contained metallic and dielectric mirrors, UV filters, and AR coatings. The optical performance of components and coatings for visible and infrared applications showed little or no affect from space exposure. The UV filters and mirrors were sensitive to space exposure; the MgF_2 material was suggested as the main factor for the weakness. Some coatings, including many high-stressed layers (oxides and fluorides), did show an evident risk of mechanical degradation from vacuum cycling and thermal cycling tests (ref. 93).

M0003-7: Space Environment Effects on Spacecraft Materials Experiment. Several high-reflectance mirrors and a coated calcium-fluoride window were flown with this experiment. Results suggested that one mirror, a silicon/aluminum oxide design showed expected excellent stability in orbit and a long shelf life. An aluminum oxide-coated calcium-fluoride window also showed good stability. Less stable but more interesting behavior was observed on the zinc-sulfide-based mirrors that showed contamination effects and related dendritic formation (ref. 94).

4.4.2.3 Solar Cells

Overall, the solar cell experiments revealed a variety of effects from the space exposure including micrometeoroid impacts (which ranged from small nicks in cover glass to penetration of the cell), broken interconnects, silver oxidation or loss, scattered contamination, and a loss of fluorine in the antireflection coatings. Some power degradation was also noted. A great deal of information is still forthcoming from the principal investigators on optical properties of the surfaces of the cells, electrical characteristics, semiconductors properties, and radiation damage assessment. Following is a synopsis of the experimenter's preliminary observations (additional details are presented in sec. 4.2.7):

Experiment M0003-4: Space Environmental Effects on Spacecraft Materials. In this experiment, solar cell and coverglass materials were situated both on the leading edge and trailing edge of LDEF. Coverglass samples were characterized post flight without cleaning. Existing surface contamination did not interfere significantly with optical properties measurements, except to increase the absorption where the shorter wavelength cutoff of cover glass samples had moved noticeably toward longer wavelengths. This was most pronounced on the trailing edge rather than the leading edge samples. This was suggested as being due to cleansing by atomic oxygen. Besides contamination, other environmental effects were noted including micrometeroid damage on both the cover glass and solar cell samples as shown in figure 4.4.2.3-1. Further, thermal cycling stress on the cover glass and a loss of fluorine from the ThF_4 and MgF_2 were noted, as well as the oxidation of unprotected silver. Metal migration and contamination was described between the coverglass and cell proper. Finally, the principal investigators describe the solar cell fabrication process as having a large effect on the lifetime of the cells (ref. 95).

Experiment A0171: Solar Array Materials Passive LDEF Experiment. This experiment evaluated the synergistic effects of the space environment on solar array materials. The experimental findings include:

- Substantial atomic oxygen erosion of polyimide substrate structures
- Solar cell to solar cell interconnect bonds appear to have withstood thermal cycling well (no debonding found at the parallel-gap weld of the copper interconnect to the cell contacts pads)
- Micrometeroid and space debris impacts were evident on all test articles (small nicks on solar cell cover to breakage and rather deep penetration within cell)
- Power degradation in the experimental solar cells was noted, ranging from 4.3% to 80% of maximum; but the majority of the single cells tested (76%) had less than 10% degradation (ref. 96).

Experiment S0014: Advanced Photovoltaic Experiment. The solar cells on this experiment were provided by a number of industrial and Government institutions for calibration and return for use as reference standards. These samples showed:

- A contaminating film was present over most of the experiment surface; however the film did not degrade the performance of the solar cell as

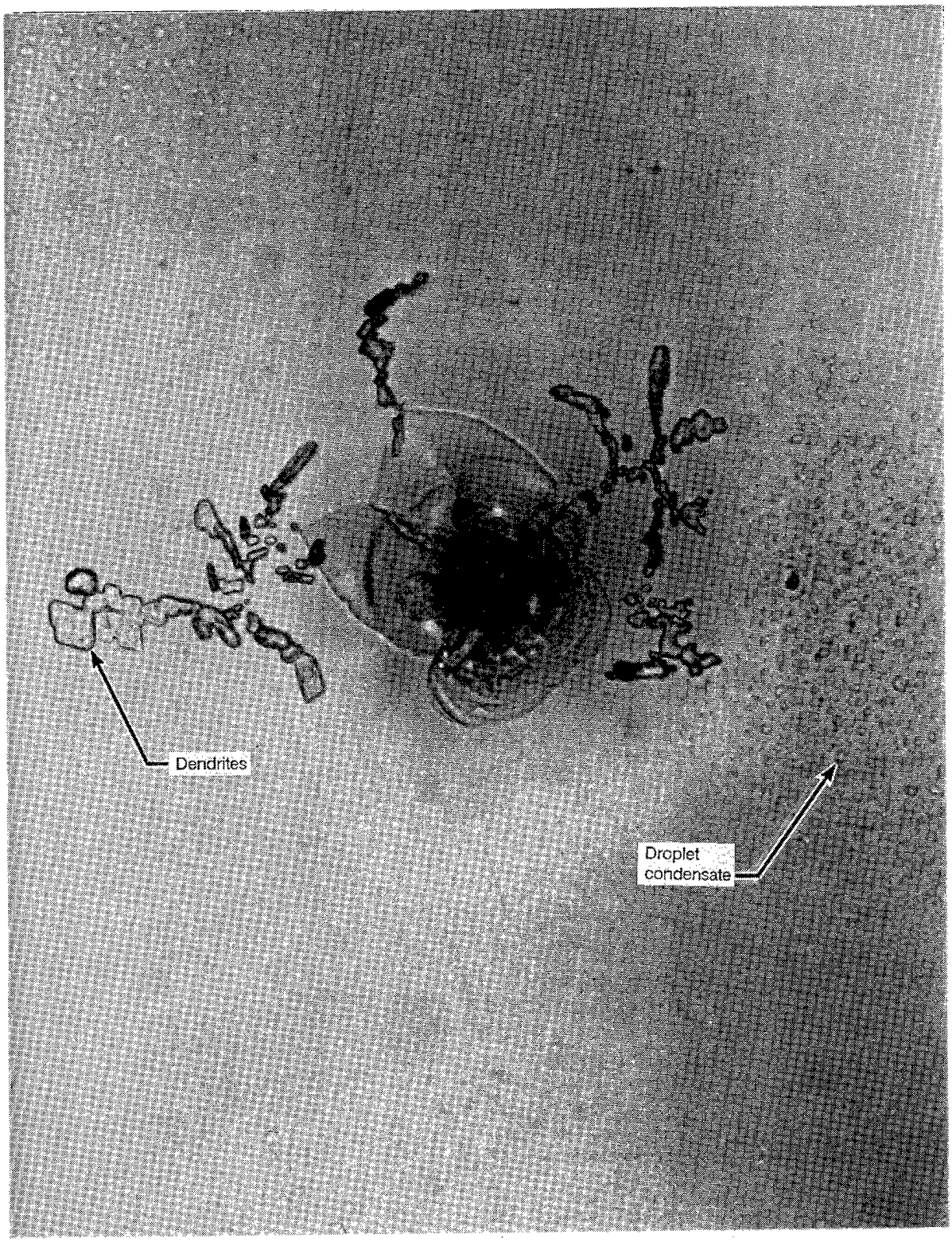

Figure 4.4.2.3-1. Damaged Area of a Coated Solar Cell Coverglass on a Silicon Wafer, Surrounded by What Appears to Be Dendrites and a Droplet Condensate (Courtesy of The Aerospace Corporation)

(See color photograph on p. 301)

indicated by post-flight solar simulation measurements and comparison to preflight data.

- A large number of impacts from micrometeroids and space debris were noted; degradation was dependent on the severity of damage to the coverglass or underlying solar cell; from minimal degradation to a drop in cell fill factor (ref. 97)

4.4.2.4 Fiber Optics

Four experiments (S0109, A0138-7, M0006, and M0004) flew fiber optics and a fifth experiment (M0003-8) evaluated fiber optic connectors. For example, the experimental test configurations for the on-orbit M0004 Fiber Optic tray is shown in figure 4.4.2.4-1. To date, the following three experimental results are available for review:

S0109 LDEF Fiber Optic Exposure Experiment (ref. 98)
M0004 Space Environment Effects on Operating Fiber Optic Systems (ref. 99)
M0003-8 Fiber Optics Experiment (ref. 100)

Overall, fiber optics performed well in the low Earth orbit space environments during the LDEF mission, with little or no degradation to the optical performance from temperature cycling extremes, radiation flux, atomic oxygen, and ultraviolet radiation. In general, environmental effects were confined to the protective sheathing, suggesting that fiber optic systems can be successfully used in low Earth orbit. However, if struck with a direct hit by a micrometeroid impact or debris that reaches the optical fibers, then catastrophic damage can result as was observed on a single link (ref. 101). Additional studies into contamination protection schemes and temperature effects on optical performance were suggested. For instance, contamination was recorded on internal and external surfaces on two experiments (S0109, M0004). Experiment results suggest only a slight to no degradation in optical performance due to contaminants. Never the less, both experimenters indicate the importance of understanding the sources and mechanisms for the observed contamination in order to eliminate any possibility of contaminant introduction because contaminating films/particles over the optically important core would contribute to degradation in optical performance. As a result, recommendations were made to mate or cover connectors in a manner that protects the core from contamination.

Preliminary data from all three experiments indicated that additional study was necessary of the temperature effects on fiber optical performance. For example, post-flight experiments performed on space-exposed fibers in the S0109 experiment showed an increase in loss with decreasing temperature, becoming much steeper near the lower end of their temperature range. This was observed in most (but not all) fiber cables. The largest change was seen in the C-6 sample, which had an attenuation increase about 3.5 dB at the low temperature extreme. The principal investigator describes this behavior as due to the specific cable structure (rather than the fiber), and would preclude its use in a severe space environment (ref. 102).

Further, the investigator details how temperature, especially colder temperatures, can affect cable performance in two ways: (1) by acting on the polymer

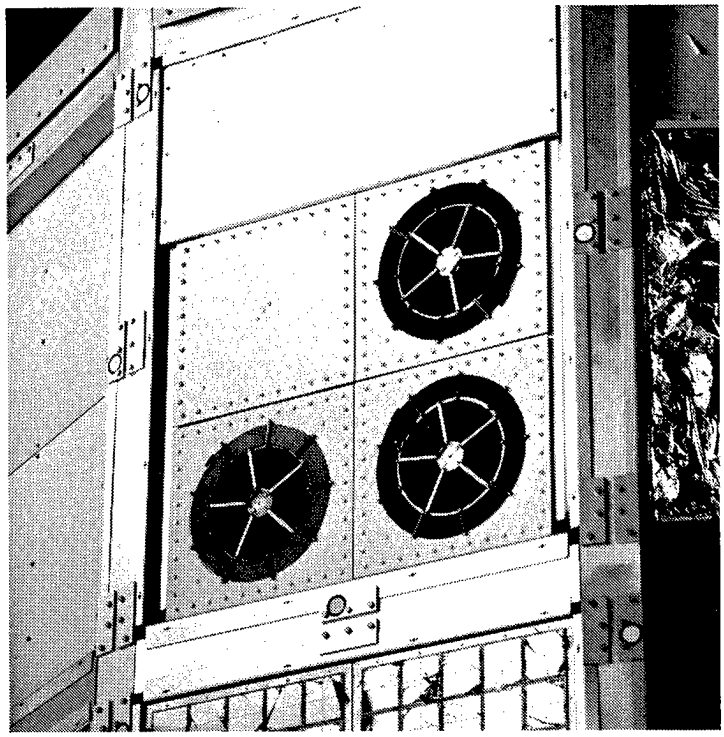

Figure 4.4.2.4-1. Fiber Optics System Experiment (M0004)

cladding and changing the refractive index versus wavelength characteristic that reduces the numerical aperture of the fiber with decreasing temperature, ultimately cutting off optical transmission or, (2) by mechanical changes in the cable polymers that induce microbending at low temperatures. Johnston writes that for future systems, careful attention must be given to improving the temperature stability of cable structures, and to qualification testing to verify their performance (ref. 103).

In addition, the M0003-8 experiment (which was shielded from direct exposure) showed a small temperature dependence, which was attributed to slight mechanical movements in the multiconnector with temperature. Total variation since 1978 was about 0.2 dB during the flight phase (ref. 104).

Finally, two of the experimenters (S0109 and M0004) discussed the expectation that using today's improved radiation hard fiber optic cable would enable space missions to experience longer runs and higher doses of radiation, and suggest that fiber optic systems can be successfully used in low orbits (refs. 105 and 106). The data from these LDEF experiments provides for improved radiation exposure data and performance predictions for future use of fiber optics in space.

4.4.2.5 Detectors

Four LDEF experiments contained detectors to test their resistance to space environmental exposure. Most detectors were not degraded by the space exposure, with one notable exception: triglycine sulfide, which had a 100% detectivity failure rate on both the control and flight samples. Details from each experiment follow:

A0135: Effect of Space Exposure on Pyroelectric Infrared Detectors. Post-flight measurements and comparisons revealed that the pyroelectric detectors made of lithium-tantalate and strontium-barium-niobate suffered no measurable loss of performance. Detectors made of triglycine-sulfide suffered complete loss of performance on both the control and flight sample, suggesting a shelf-life problem. In addition, the KRS-5 windows on the detector were degraded, underscoring the importance of window selection for detectors (ref. 107).

S0050: LDEF Active Optical System Components Experiment. HgCdTe detectors, InGaAsP photodiodes, large area silicon photodiodes, and PIN diodes had good performance and no apparent degradation effects (ref. 108).

M0003-6: Space Environment Effects on Spacecraft Materials. Preliminary pulse response results on avalanche photodiodes show some shift in breakdown voltage (10%). Additional testing is in progress to verify these results (ref. 109).

M0003-8: LDEF Fiber Optics Experiment. The Vactec large area detectors included with this experiment performed well (ref. 110).

4.4.2.6 Reflectometers and Radiometers

Certain LDEF experiments described the performance of radiometers and reflectometers for the measurement of solar and thermal properties. In general, all of the measuring instruments met their performance criteria and provided valuable data on incident radiation. Following are short summaries from each LDEF experiment, including follow-on programs for measuring optical properties in space.

S0069: Thermal Control Surfaces Experiment (TCSE). Reflectometers were used on the TCSE to measure the spectral reflectance from 250 to 2500 nm in order to determine the solar absorptance and total hemispheric emittance. In addition, three radiometers on the TCSE monitored the direct radiance from the Sun, reflected Earth albedo, and Earth-emitted infrared (IR) incident on the TCSE. Calorimeters measured the in-space temperature of the test sample, and irradiance monitors measured the external heat inputs. These measurements provided the inputs to the heat balance equation and made calculation for solar absorptance and total emittance for the flight samples possible. A functional test of the reflectometer subsystem followed the component-level functional tests to determine overall system health. The reflectometer operated normally. The post-flight reflectance data for the near-infrared data from 2500 nm to about 600 nm looked reasonable with signal levels on the same order as preflight values; however, a little more noise was evident in the data. From 600 nm to 400 nm, signal levels were significantly lower and noisier but some data were used.

Below 380 nm, where the deuterium lamp is used, the data was considered suspect as it did not agree with ground measurements (ref. 111).

Three follow-on programs to LDEF for measuring optical properties in space were exhibited at a poster session at the LDEF First Post-Retrieval Symposium by S0069 Experimenters (ref 112). According to the poster, the objective of their program is to develop and prove the concepts for in-space inspection instruments to measure the optical properties of spacecraft surfaces. Phase I of the NASA Small Business Innovative Research (SBIR) program was completed in August 1990. Phase II began July 1991. An outline of their projects follows:

- Optical Properties Monitor on Eureka. NASA In-Space Technology Program that will do spectral total hemispheric reflectance, total integrated scatter, vacuum ultraviolet transmittance and reflectance, as well as environmental monitors for molecular contamination, atomic oxygen, and irradiance monitors (radiometers).
- Laboratory Portable Spectro-Reflectometer (LPSR-102). A handheld instrument to measure reflectance of large surfaces.
- Space Portable Spectro-Reflectometer (SPSR), which is a portable instrument to measure the reflectance of large surfaces.

S0014: Advanced Photovoltaic Experiment (APEX). This experiment contained an absolute cavity radiometer. Post-flight results showed the cavity radiometer was unchanged in regards to sensitivity, reflectance, and overall condition (ref 113).

A0147: Passive Exposure of Earth Radiation Budget Experiment (ERB) Components. Unlike the previous two experiments, this experiment contained solar and Earth flux components for the ERB radiometer including thermopiles, interference filters, and fused silica windows. The objective of the experiment was to expose ERB channel components to the environment and, upon retrieval, resubmit them to radiometric calibration with experiment configuration, as shown in figure 4.4.2.6-1. The cavity radiometer performance (located on S0014) appeared to be unaffected by space exposure, even though there was visible change to the interior cavity coating, where the Z302 coating exhibited some puckering (ref. 114).

4.4.2.7 Optical Sources

Several kinds of optical sources flew on LDEF including solid and gas lasers, flashlamps, standard lamps, and light-emitting-diodes (LED). Experiments S0050, M0003-8, S0069, M0004, and M0006 carried examples of these four optical source types. The results indicate that most optical sources operated nominally, meeting their performance criteria, except for two gas lasers (HeNe and CO2) which were carried passively (but would not fire post-flight), and a flickering deuterium lamp arc. Summaries of experiments containing optical sources are described below:

S0069: Thermal Control Surfaces Experiment (TCSE). The TCSE contained two light sources: a deuterium UV lamp and a tungsten filament in a quartz envelope lamp, as an integral part of its integrating spectroreflectometer. The

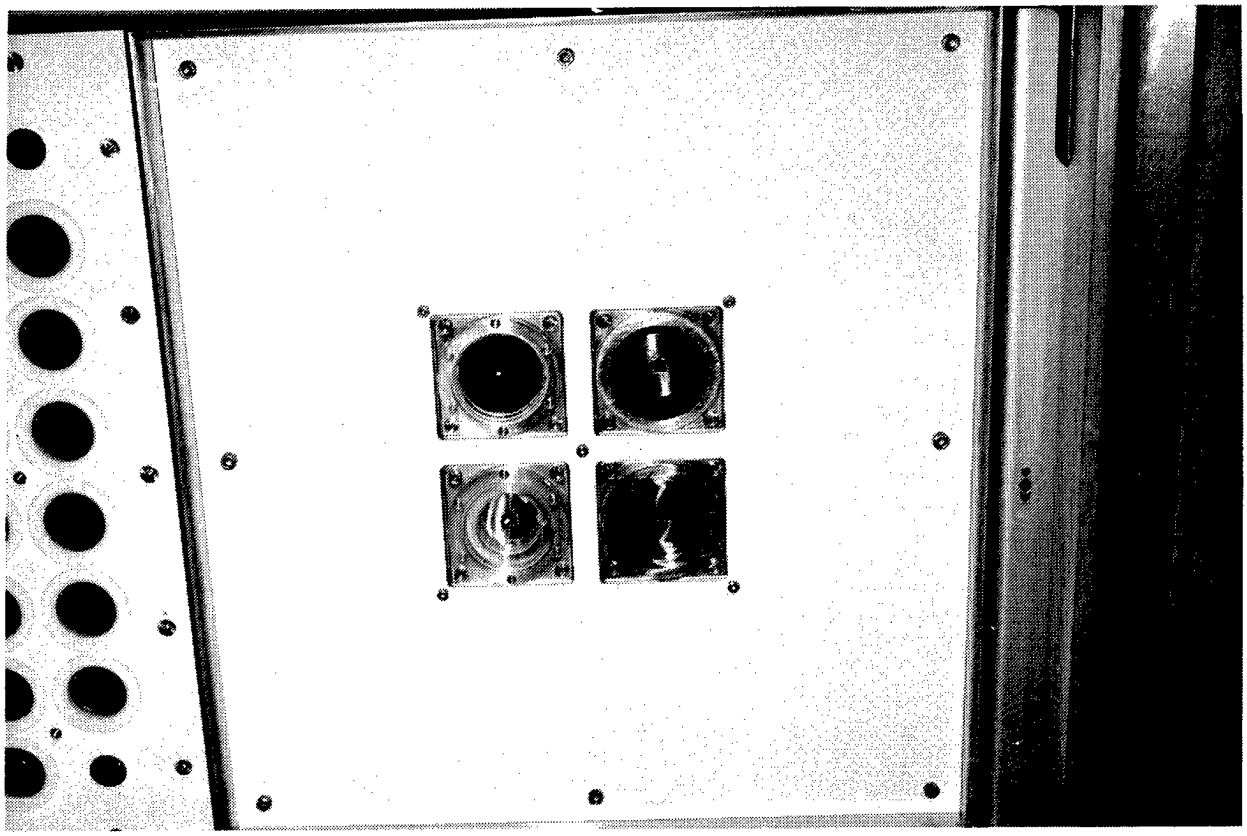

Figure 4.4.2.6-1. Passive Exposure of Earth Radiation Budget Experiment (A0147) Earth Flux Channel Components

component functional post-flight test results of the two lamps and power supplies were nominal; they responded to computer control as designed. There were no measured atypical power transients. The tungsten lamp irradiated normally at power on, and a visual check in the integrating sphere verified the visible spectrum between 500 and 700 nm. The deuterium lamp irradiance appeared slightly unstable due to flickering of the lamp arc. No visible inspection was possible of the UV energy from the monochromator (ref 115).

S0050: Investigation of the Effects of Long-Duration Exposure on Active Optical Systems Experiment. This experiment contained several kinds of laser components including HeNe and CO_2 gas laser tubes, GaAlAs semiconductor diode lasers, GaAsP light emitting diodes, and YAG laser rods. Post-flight testing of the HeNe and CO_2 laser tubes was performed in May, 1990. No laser action could be obtained from the tubes. The characteristics of the tubes suggested that the mixture of fill gas had changed during the period between pre-flight and post-flight testing. While the extended period in orbit was unplanned, the experiment result is consistent with changes expected from gas diffusion though the glass tube. The tubes were in good physical condition and survived the launch and recovery phases without apparent degradation (ref. 116).

The GaAlAs semiconductor diode lasers were tested with a circuit containing a silicon controlled rectifier which provided low-voltage high-current pulses at a rate controlled by an external pulse generator. Diode radiation output was monitored by a silicon photodiode. Post-flight measurements indicated greater light output from all devices, a result believed caused by the improved diode properties. The performance of the devices relative to one another also did not change significantly.

The GaAsP light emitting diode (LED) showed some indentations in the plastic dome of the unit exposed to space as compared to a companion diode stored over the time period of the LDEF mission. The indents are assumed to be a result of meteoroid or debris impacts. Other performance characteristics of these devises were unchanged.

The YAG laser rods remain to be tested. Presently, the special laser cavity and test fixture for evaluating the rods are being reconfigured and aligned for post-flight measurements

M0003-8: Fiber Optics Experiment. Post-flight spectral output measurements of the LED showed peak output of 905 nm, with a broad peak as is expected of an LED of this type and vintage Further, the LED indicated no change between preflight and post-flight forward voltage measurements (ref 117).

M0004: Space Environmental Effects on Operating Fiber Optic Systems. Optical sources used in this experiment are presently under investigation. No data were available for review.

4.4.2.8 "Lessons Learned" Concluding Remarks

The various experiments have revealed that contamination, micrometeroid and debris impacts, atomic oxygen, radiation, and synergistic conditions were all significant environmental factors affecting the LDEF optical hardware. As indicated by the principal investigators' initial results, the final interpretation of the environmental effects on optics could become quite complex. The true consequences of these effects on optical elements and systems must await the outcome of many precise optical measurements by experimental investigators.

Contamination was one of the most frequently discussed environmental factors causing degradation of the LDEF optical materials and optical system performance. These findings underscore the need for further research into prevention and control of contaminants on flight optical hardware. Provided in Appendix B is a discussion of current research in optical systems contamination control.

To facilitate the collection and distribution of current and future results, the LDEF Optical Experiments Database is available for quick and easy access to available experimental findings. The database is described in greater detail in the following section 4.4.3., and a complete list of its file information in its current state of completion is provided in Appendix D.

4.4.3. Optical Experiments Database

One of the main objectives of the Systems SIG is to develop a database that identifies the optical hardware flown, summarizes experimental results and conclusions, and provides a system analysis overview and future design suggestions. Compiling this information into an easily accessible database format and making it available to the space community is a major task accomplished by the System SIG Optics effort.

After a trade study of the Boeing standard software packages, Filemaker Pro was chosen as the Optical Experiments Database software application program. Filemaker Pro is a database manager for the Macintosh computer produced by Claris Corp (ref. 137). It is a flat, text-retrievable database that provides access to the data via an intuitive user interface, without tedious programming. "Relational" databases were examined for this application, but found to have many features and capabilities unnecessary for this application. Although this software is available only for the MacIntosh at this time, copies of the database can be saved to a format that is readable on a personal computer (PC) as well.

Within the Filemaker Pro application, the LDEF Optical Systems information is placed in a file called "LDEF-data". Within that file, each individual LDEF experiment has its own "record" (for example S0109, A0138-7, M0006 and M0004). Each record contains specific information using "field name" headings, from which one can view or print reports from the provided layout. The database layout was designed with the following characteristics in mind: (1) user friendly, (2) data traceable, (3) authors are acknowledged (4) data are upgradeable, and (5) access privileges allow full viewing but not editing. Appendix B contains the information required to access the LDEF Optics Database using Filemaker Pro.

5.0 REFERENCES

1. O'Neal, R.L., E.B. Lightner, "Long Duration Exposure Facility - A General Overview", *LDEF 69 Months in Space; First LDEF Post-Retrieval Conference, NASA CP-3134, February 1992.*

2. *Proceedings of the Solar Max Repair Mission Degradation Study Workshop*, Goddard Space Flight Center, 408-SMRM-79-0001, May 1985

3. *Test and Evaluation of the Surveyor III Television Camera Returned from the Moon by Apollo XII*, Hughes Aircraft Company, December 1970.

4. Albjerg, M., *LDEF Cargo Systems Manual: 41C*, Johnson Space Center, JSC Report # JSC-19016, March 1984.

5. Clark, L.G., W. H. Kinard, D.J. Carter, J.L.Jones, *The Long Duration Exposure Facility Mission 1 Experiments*, NASA SP-473, 1984.

6. Bourassa, R. J. and J. R. Gillis, "Atomic Oxygen Exposure of LDEF Experiment Trays, " NAS1-19247, Task 1, Boeing Defense & Space Group, Seattle, WA ,1992.

7. See, T.H., Allbrooks, M.A., Atkinson, D.R., Simon, C.G. and Zolensky, M., *Meteoroid and Debris Impact Features Documented on the Long Duration Exposure Facility, A Preliminary Report*, Publication #84, JSC #24608, 583 pp.

8. Dursch, H.W, *LDEF Systems Special Investigation Group Investigation Plan*, Boeing Defense and Space Group, February 1990.

9. Mason, J.B., H.W.Dursch, J.Edelman, "Systems Special Investigation Group Overview", *LDEF 69 Months in Space; First LDEF Post-Retrieval Conference, NASA CP-3134, February 1992.*

10. *LDEF Systems Special Investigation Group Interim Report*, Boeing, January 1991.

11. Warren, J..L. and 10 co-authors, "The Detection and Observation of Meteoroid and Space Debris Impact Features on the Solar Max Satellite," Proc. Lunar Planet. Sci. Conf. 19th, p. 641-657, 1989.

12. See, T.H., Allbrooks, M.A., Atkinson, D.R., Simon, C.G. and Zolensky, M., "Meteoroid and Debris Impact Features Documented on the Long Duration Exposure Facility, A Preliminary Report," Publication #84, JSC #24608, 583 pp, 1990.

13. Zook, H.A., "On Cosmic Dust Trajectory Measurements and Experiment Pointing Considerations, in Progress Towards a Cosmic Dust Collection Facility on Space Station," Mackinnon, I.D. and Carey, W.C., eds., Lunar and Planetary Institute, LPI Technical Report 88-01, p. 76-77, 1990.

14. Zook, H.A., "Meteoroid Directionality on LDEF and Asteroidal Versus Cometary Sources (abstract)", Lunar Planet. Sci. XXII, Lunar and Planetary Institute, Houston, Tx., p. 1577-1578, 1991.

15. Peterson, R.B., "Instrument Pointing Considerations; Report to Cosmic Dust Collection Facility Open Forum." Lunar and Planetary Science Institute, unpublished, 1991.

16. Zolensky, M., Atkinson, D., See, T.H., Allbrooks, M., Simon, C., Finckenor, and Warren, J., "Meteoroid and Orbital Debris Record of the Long Duration Exposure Facility's Frame," J. Spacecraft and Rockets, v.28, no. 2, p. 204-209, 1991.

17. Bourassa, R.J., J. R. Gillis and K. W. Rousslang, "Atomic Oxygen and Ultraviolet Radiation Mission Total Exposures for LDEF Experiments," *LDEF 69 Months in Space; First LDEF Post-Retrieval Conference, NASA CP-3134, February, 1992.*

18. Bourassa, R.J., and J. R. Gillis, "Atomic Oxygen Exposure of LDEF Experiment Trays, " NAS1-19247, Task 1, Boeing Defense & Space Group, Seattle, WA ,1992.

19. Rutledge, Sharon K., "Durability Evaluation Of Photovoltaic Blanket Materials Exposed On LDEF Tray (S1003)", *LDEF 69 Months in Space; First LDEF Post-Retrieval Conference, NASA CP-3134, February 1992.*

20. Gregory, J.C., "LDEF Attitude Measurement Using A Pinhole Camera With A Silver/Oxygen Atom Detector," *LDEF 69 Months in Space; First LDEF Post-Retrieval Conference, NASA CP-3134, February 1992.*

21. deGroh, Kim K., "Atomic Undercutting Of LDEF Aluminized Kapton Multilayer Insulation," *LDEF 69 Months in Space; First LDEF Post-Retrieval Conference, NASA CP-3134, February 1992.*

22. Jursa, A.S.,Editor, *Handbook of Geophysics and the Space Environment*, p. 1-5, Air Force Geophysics Laboratory, 1985.

23. Berrios, W.M., and Thomas Sampair, "Long Duration Exposure Facility Solar Illumination Data Package," Orbital Environment Data Group, NASA LaRC,1991.

24. Smith, G. Louis, David Rutan and T. Dale Bess , "Atlas of Albedo and Absorbed Solar Radiation Derived From Nimbus 7 Earth Radiation Budget Data Set," November 1978 to October 1985 , NASA Reference Publication 1231, 1990.

25. Bourassa, R. J., and J. R. Gillis, "Solar Exposure of Long Duration Exposure Facility Experiment Trays" NAS1-18224, Task 12, Boeing Defense & Space Group, Seattle, WA (1990).

26. Berrios, W.M., "Use of LDEF's Thermal Measurement System for the Verification of Thermal Models," *LDEF 69 Months in Space; First LDEF Post-Retrieval Conference, NASA CP-3134, February 1992.*

27. Duckett, R.J., Gilliland, C.S., "Variable Anodic Thermal Control Coating on Aluminum, " AIAA-83-1492, June 1983.

28. Crutcher, E. R. and W. W. Wascher: "Particle Types and Sources Associated with LDEF." *LDEF 69 Months in Space; First LDEF Post-Retrieval Conference, NASA CP-3134, February 1992.*

29. Crutcher, E. R., L. S. Nishimura, K. J. Warner, and W. W. Wascher: "Quantification of Contaminants Associated with LDEF." *LDEF 69 Months in Space; First LDEF Post-Retrieval Conference, NASA CP-3134, February 1992.*

30. Crutcher, E. R. and K. J. Warner: "Molecular Films Associated with LDEF." *LDEF 69 Months in Space; First LDEF Post-Retrieval Conference, NASA CP-3134, February 1992.*

31. Crutcher, E. R., L. S. Nishimura, K. J. Warner, and W. W. Wascher: "Silver/Teflon Blanket: LDEF Tray C-08"., *LDEF 69 Months in Space; First LDEF Post-Retrieval Conference, NASA CP-3134, February 1992.*

32. Crutcher, E. R., L. S. Nishimura, K. J. Warner, and W. W. Wascher: "Migration and Generation of Contaminants From Launch Through Recovery: LDEF Case History." *LDEF 69 Months in Space; First LDEF Post-Retrieval Conference, NASA CP-3134, February 1992.*

33. Assie, Jean-Pierre, Conde,E., "Mircrowelding of Various Metallic Materials under Ultra-Vacuum," *LDEF 69 Months in Space; First LDEF Post-Retrieval Conference, NASA CP-3134, February 1992.*

34. Dursch, H. W., Spear, W. S., "On-orbit Coldwelding - Fact or Friction?," *LDEF 69 Months in Space; First LDEF Post-Retrieval Conference, NASA CP-3134, February 1992.*

35. *Final Report for the Post-Flight Evaluation of the Magnetically Anchored Viscous Damper,* General Electric Astro Space Division, Contract No. 02N0139514, October 1990

36. Durin, Christian, "French Cooperative Passive Payload (FRECOPA) System Results," *LDEF 69 Months in Space; First LDEF Post-Retrieval Conference, NASA CP-3134, February 1992.*

37. *An Evaluation of Rod End Bearings, Astro P/N ADNE4J, Flown on LDEF,* New Hampshire Ball Bearings, April 1991.

38. Steckel, G.C. and Le, T.D., "M0003-10: LDEF Advanced Composites Experiment," *LDEF 69 Months in Space; First LDEF Post-Retrieval Conference, NASA CP-3134, February 1992.*

39. Young, P.R., Slemp , W.S., Witt, W.G., and Shen, J.Y., "Characterization of Selected Polymer Matrix Composite Materials," 36th International SAMPE Symposium, April 1991.

40. Tennyson, R.C., Mabson, G.E., Morrison, W.D., and Kleimon, J., "Preliminary Results from the LDEF/VTIAS Composite Material Experiment," *LDEF 69 Months in Space; First LDEF Post-Retrieval Conference, NASA CP-3134, February 1992.*

41. *LDEF Experimenter Users Handbook,* LDEF Project Office, Langley Research Center, Hampton, VA.

42. "Experiment Initiate System Checkout at Kennedy Space Center, February 23-24, 1990," S. Sokol, NASA Langley Research Center, October 1980.

43. "Experiment Power Data System for Long Duration Exposure Facility," August 1, 1978 (as Updated March 14, 1979), Flight Electronics and Systems Engineering Divisions, NASA Langley Research Center, Hampton, Virginia.

44. Tennyson, R. L. and G. E. Mabson, "Thermal-Vacuum Effects on Polymer Matrix Composite Materials," *LDEF 69 Months in Space; First LDEF Post-Retrieval Conference, NASA CP-3134, February 1992.*

45 Raman, "Experimentation and Destructive Physical Analysis for the Space-Exposed Lithium-Sulfur Dioxide (Li/SO_2) From the Long Duration Exposure Facility (LDEF)," SAFT America, Inc. Attachment 1, pp. (1)-1,2, 1991.

46. Thaller, L., (Memo Report) "Discharge of LDEF Li/SO2 Cells," Aerospace Corporation, January 1991.

47. Deligiannis, F., Presentation to Lithium Battery Safety Committee, Jet Propulsion Laboratory, July 1991.

48 Lewis, H. L. and V. L. Hammersley, "Long Duration Exposure Facility (LDEF) Lithium Carbon Monofluoride (LiCF) Cells -- Analytical Comparison To Earth Based Cells," The Seventh Annual Battery Conference, California State University, Long Beach, CA. January 21-23, 1992.

49. "Thermal Control Surfaces Experiment Initial Flight Data Analysis Final Report," June 1991, pp. 49-52, AZ Technology Report No. 90-1-100-2.

50. Tiller, S. L. and D. Sullivan, "Long Duration Exposure Facility Low-Temperature Heat Pipe Experiment Package Power System Results," *LDEF 69 Months in Space; First LDEF Post-Retrieval Conference, NASA CP-3134, February 1992.*

51. Brinker, D.J., R.E. Hart, and J.R. Hickey, "Preliminary Results from the Advanced Photovoltaic Experiment Flight Test," *LDEF 69 Months in Space; First LDEF Post-Retrieval Conference, NASA CP-3134, February 1992.*

52. Whitaker, A.F., and L.E. Young, "An Overview of the First Results on the Solar Array Passive LDEF Experiment (SAMPLE)," A0171, *LDEF 69 Months in Space; First LDEF Post-Retrieval Conference, NASA CP-3134, February 1992.*

53. Trumble, T.M., "Experiment M0003-4, Advanced Solar Cell and Coverglass Analysis, An Overview," L*LDEF 69 Months in Space; First LDEF Post-Retrieval Conference, NASA CP-3134, February 1992.*

54. Tiller, S.E., and D. Sullivan, "LDEF Low-Temperature Heat Pipe Experiment Package Power System Results," *LDEF 69 Months in Space; First LDEF Post-Retrieval Conference, NASA CP-3134, February 1992.*

55. Preuss, L. "Evaluation of LDEF Experiment S1002," *LDEF 69 Months in Space; First LDEF Post-Retrieval Conference, NASA CP-3134, February 1992.*

56. Stella, P., "LEO Effects on Conventional and Unconventional Solar Cell Cover Materials," Conference Record of the 21st IEEE Photovoltaic Specialists Conf.,1991, Las Vegas.

57. Anspaugh, B.E. and R.G. Downing, "Radiation Effects in Silicon and Gallium Arsenide Solar Cells Using Isotropic and Normally Incident Radiation," Conf. Rec. of the 17th IEEE Photovoltaics Specialists Conf., 23, 1984.

58. Linton, Roger C., Rachel R. Kamenetzky, John M. Reynolds and Charles L. Burris, LDEF Experiment A0034: "Atomic Oxygen Stimulated Outgassing;" *LDEF 69 Months in Space; First LDEF Post-Retrieval Conference, NASA CP-3134, February 1992.*

59. Berrios, William M. "Use Of The Long Duration Exposure Facility's Thermal Measurement System for the Verification Of Thermal Models;" *LDEF 69 Months in Space; First LDEF Post-Retrieval Conference, NASA CP-3134, February 1992.*

60. Wilkes, Donald R. M. John Brown, Leigh L. Hummer and James M. Zwiener,"Initial Materials Evaluation of the Thermal Control Surfaces Experiment (S0069); "*LDEF 69 Months in Space; First LDEF Post-Retrieval Conference, NASA CP-3134, February 1992.*

61. LDEF Spaceflight Environmental Effects Newsletter, Vol. II, No. 3, June 15, 1991

62. Tennyson, R. C. G. E. Mabson, W. D. Morrison and J. Kleiman, "Preliminary Results from the LDEF/UTIAS Composite Materials Experiment;" *LDEF 69 Months in Space; First LDEF Post-Retrieval Conference, NASA CP-3134, February 1992.*

63. Grote, Michael G. "Results From The LDEF/A0076 Cascaded Variable Conductance Heat Pipe Experiment;" *LDEF 69 Months in Space; First LDEF Post-Retrieval Conference, NASA CP-3134, February 1992.*

64. Shular, David, Transverse Flat Plate Heat Pipe Experiment;" *LDEF 69 Months in Space; First LDEF Post-Retrieval Conference, NASA CP-3134, February 1992.*

65. Stein, Bland A., and H. Gary Pippin, "Preliminary Findings Of The LDEF Materials Special Investigation Group;" *LDEF 69 Months in Space; First LDEF Post-Retrieval Conference, NASA CP-3134, February 1992.*

66. Lonny Kauder; "Preliminary Results For LDEF/HEPP Thermal Control Samples;" Internal memo, NASA GSFC Thermal Engineering Branch, September 12, 1990

67. McIntosh, Roy and Patrick J. Brennan, "Long Duration Exposure Facility (LDEF) Low Temperature Heat Pipe Experiment Package (HEPP);" *LDEF 69 Months in Space; First LDEF Post-Retrieval Conference, NASA CP-3134, February 1992.*

68. Brinza, David E., Ranty H. Liang and Albert E. Stiegman "VUV-Induced Degradation Of FEp Teflon Aboard LDEF;" *LDEF 69 Months in Space; First LDEF Post-Retrieval Conference, NASA CP-3134, February 1992.*

69. deGroh, Kim J, and Bruce A. Banks, "Atomic Oxygen Undercutting Of LDEF Aluminized-Kapton Multilayer Insulation;" *LDEF 69 Months in Space; First LDEF Post-Retrieval Conference, NASA CP-3134, February 1992.*

70. Hickey, J. R." Passive Exposure Of Earth Radiation Budget Experiment Components LDEF Experiment AO-147: Post-Flight Examinations And Tests;" *LDEF 69 Months in Space; First LDEF Post-Retrieval Conference, NASA CP-3134, February 1992.*

71. Wilkes, Donald R., Leigh L. Hummer and James M. Zwiener "Thermal Control Surfaces Experiment - Flight Systems Performance;" *LDEF 69 Months in Space; First LDEF Post-Retrieval Conference, NASA CP-3134, February 1992.*

72. Golden, Johnny L., "Results Of Examination Of The A276 White And Z306 Black Thermal Control Paint Disks Flown On LDEF;" *LDEF 69 Months in Space; First LDEF Post-Retrieval Conference, NASA CP-3134, February 1992.*

73. Parcelier, Michel and Jean Pierre Assié "Effect Of Space Environment On Composite Materials And Thermal Coatings A0138-9);" *LDEF 69 Months in Space; First LDEF Post-Retrieval Conference, NASA CP-3134, February 1992.*

74. Charlier, Jean "Vacuum Deposited Optical Coatings Experiment;" *LDEF 69 Months in Space; First LDEF Post-Retrieval Conference, NASA CP-3134, February 1992.*

75. Sampair, Thomas R. and William M. Berrios "Effects Of Low Earth Orbit Environment On The Long Duration Exposure Facility Thermal Control Coatings;" *LDEF 69 Months in Space; First LDEF Post-Retrieval Conference, NASA CP-3134, February 1992.*

76. Zwiener, James M. , Kenneth A. Herren, Donald R. Wilkes, Leigh L. Hummer and Edgar R. Miller, "Unusual Materials Effects Observed On The Thermal Control Surfaces Experiment (S0069)"; *LDEF 69 Months in Space; First LDEF Post-Retrieval Conference, NASA CP-3134, February 1992.*

77. Plagemann, Walter L., "Space Environmental Effects on the Integrity of Chromic Acid Anodized Coatings;" *LDEF 69 Months in Space; First LDEF Post-Retrieval Conference, NASA CP-3134, February 1992.*

78. Hurley, Charles J., "Long Duration Exposure Facility Experiment M0003-5, Thermal Control Materials;" *LDEF 69 Months in Space; First LDEF Post-Retrieval Conference, NASA CP-3134, February 1992.*

79. Brinker, David J., John R. Hickey and David A. Scheiman "Advanced Photovoltaic Experiment, S0014: Preliminary Flight Results And Post-Flight Findings;" *LDEF 69 Months in Space; First LDEF Post-Retrieval Conference, NASA CP-3134, February 1992.*

80. Crutcher, E.R., L.S. Nishimura, K.J. Warner and W.W. Wascher, "Migration and Generation of Contaminants From Launch Through Recovery: LDEF Case History," NASA Contract Report NAS1-18224, Task 12.

81. Rouslang, K., E.R. Crutcher, and H.G. Pippin, "Results of Examination of Silvered Teflon from the LDEF", *LDEF 69 Months in Space; First LDEF Post-Retrieval Conference, NASA CP-3134, February 1992.*

82. Harvey, Gale "Effects of Long Duration Exposure on Optical Systems Components," *LDEF 69 Months in Space; First LDEF Post-Retrieval Conference, NASA CP-3134, February 1992.*

83. Vallimont, John and Keith Havey, "Effect of Long Term Exposure on Optical Substrates and Coatings," *LDEF 69 Months in Space; First LDEF Post-Retrieval Conference, NASA CP-3134, February 1992.*

84. Hickey, John "Passive Exposure of Earth Radiation Budget Experiment Components LDEF Experiment A0147 Post Flight Examination and Tests," *LDEF 69 Months in Space; First LDEF Post-Retrieval Conference, NASA CP-3134, February 1992.*

85. Hawkins, Gary, John Seeley and Roger Hunneman, "Exposure to Space Radiation of High Performance Infrared Multilayer Filters and Materials Technology," *LDEF 69 Months in Space; First LDEF Post-Retrieval Conference, NASA CP-3134, February 1992.*

86. Kinser, Donald et.al., "Contamination of Optical Surfaces in Earth Orbit," *LDEF LDEF 69 Months in Space; First LDEF Post-Retrieval Conference, NASA CP-3134, February 1992.*

87. Wiedlocher, David, et.al., "Mechanical Properties of Silicate Glasses Exposed to a Low-Earth Orbit," *LDEF 69 Months in Space; First LDEF Post-Retrieval Conference, NASA CP-3134, February 1992.*

88. Clark, Lenwood, et.al., Long Duration Exposure Facility (LDEF) Mission 1 Experiments, NASA SP-473, Langley Research Center, 1984.

89. Mooney, Thomas A. and Ali Smajkiewicz, "Transmittance Measurement of Ultraviolet and Visible Wavelength Filters Flown Aboard LDEF," *LDEF 69 Months in Space; First LDEF Post-Retrieval Conference, NASA CP-3134, February 1992.*

90. Vallimont, John and Keith Havey, ibid.

91. Hawkins, Gary, John Seeley and Roger Hunneman, "Exposure to Space Radiation of High Performance Infrared Multilayer Filters and Materials Technology," *LDEF 69 Months in Space; First LDEF Post-Retrieval Conference, NASA CP-3134, February 1992.*

92. Preuss, Ludwig "Evaluation of LDEF Experiment S1002," *LDEF 69 Months in Space; First LDEF Post-Retrieval Conference, NASA CP-3134, February 1992.*

93. Charlier, Jean "Vacuum Deposited Optical Coatings Experiment," *69 Months in Space*, First LDEF Post-Retrieval Conference, NASA CP-3134, 1992.

94. Donovan, Terry M., J.M. Bennett, et.al. "Space Environmental Effects on Coated Optics," *LDEF 69 Months in Space; First LDEF Post-Retrieval Conference, NASA CP-3134, February 1992.*

95. Trumble, Terry M. "Experiment M0003-4 Advanced Solar Cell and Coverglass Analysis," *LDEF 69 Months in Space; First LDEF Post-Retrieval Conference, NASA CP-3134, February 1992.*

96. Whitaker, Ann F. "An Overview of the First Results on the Solar Array Passive Experiments," *LDEF 69 Months in Space; First LDEF Post-Retrieval Conference, NASA CP-3134, February 1992.*

97. Brinker, David J., John Hickey and Davide Scheiman "Advanced Photovoltaic Experiment S0014," *LDEF 69 Months in Space; First LDEF Post-Retrieval Conference, NASA CP-3134, February 1992.*

98. Johnston, A.R. , L.A. Bergman and R. Hartmayer, "LDEF Fiber Optic Exposure Experiments S0109," *LDEF 69 Months in Space; First LDEF Post-Retrieval Conference, NASA CP-3134, February 1992.*

99. Taylor, E.W., J.N. Berry et. al. "Preliminary Analysis on WL Experiment #701 Space Environment Effects on Operating Fiber Optic System," *LDEF 69 Months in Space; First LDEF Post-Retrieval Conference, NASA CP-3134, February 1992.*

100. Mulkey, Owen "Final Report on the LDEF M0003-8 Fiber Optics Experiment," *LDEF 69 Months in Space; First LDEF Post-Retrieval Conference, NASA CP-3134, February 1992.*

101. Taylor, ibid.

102. Johnston, ibid.

103. Johnston, ibid.

104. Mulkey, ibid.

105. Taylor, ibid.

106. Johnston, ibid.

107. Robertson, James B. "Effect of Space Exposure of Pyroelectric Infrared Detectors," *LDEF 69 Months in Space; First LDEF Post-Retrieval Conference, NASA CP-3134, February 1992.*

108. Blue, M.D., "LDEF Active Optical System Components Experiment," *LDEF 69 Months in Space; First LDEF Post-Retrieval Conference, NASA CP-3134, February 1992.*

109. Hodgson, Randall and James Holsen "Post-Flight Characterization of Optical System Samples, Thermal Control Samples and Detectors from LDEF Experiment M0003,"*LDEF 69 Months in Space; First LDEF Post-Retrieval Conference, NASA CP-3134, February 1992.*

110. Mulkey, ibid.

111. Wilkes, Donald R., "Thermal Control Surfaces Experiment Initial Flight Data Analysis Final Report," NASA subcontract NAS8-36289-SC03, AZ Technology, June 1991.

112. AZ Technology Developed for NASA Marshall Space Flight Center, 3322 Memorial Parkway, Huntsville, AL. 35801.

113. Brinkley, David J., John Hickey and David Scheiman, "Advanced Photo-Voltaic Experiment," *LDEF 69 Months in Space; First LDEF Post-Retrieval Conference, NASA CP-3134, February 1992.*

114. Hickey, J.R. "Passive Exposure of Earth Radiation Budget Experiments Components, LDEF Experiment A0147: Post Flight Examinations and Tests," *LDEF 69 Months in Space; First LDEF Post-Retrieval Conference, NASA CP-3134, February 1992.*

115. Wilkes, ibid.

116. Blue, M.D. "LDEF Optical System Component Experiment," *LDEF 69 Months in Space; First LDEF Post-Retrieval Conference, NASA CP-3134, February 1992.*

117. Mulkey, Owen, ibid.

118. Guregian, James J., Robert T. Benoit and Wallace K. Wong, "An Overview of Contamination Effects on the Performance of High Straylight Rejection Telescopes," Proc. SPIE 1329, pp. 7, 1991.

119. Chuan, Raymond and W. L. Bowers, "A Non-Optical Real-Time Particle Fallout Monitor," Optical System Contamination: Effects, Measurements, Control II, A. Glassford, Proc. SPIE 1329, pp. 168 (1990).

120. Bowers, William and R.L. Chuan, "A 200 MHz Surface Acoustic Wave Microbalance," Optical System Contamination: Effects Measurements, Control, A.Peter Glassford, Editor, Proc. SPIE 1329, pp. 179 (1990).

121. Darnton, Lane, R.Champetier et.al., "Ultrasensitive Dust Monitor for the Advanced X-Ray Astrophysics Facility (AXAF)," Optical System Contamination: Effects, Measurement , Control II, Proc. SPIE 1329, pp. 211 (1990).

122. Pezzaniti, J.L., D. Wilkes, J. Bennett, et.al. "Total integrated scatter instrument for in-space monitoring of surface degradation," Optical System Contamination, Proc. SPIE 1329, pp. 200 (1990).

123. Bowers W. and R. Chuan, "A 200 MHz Surface Acoustic Wave Mass Microbalance," Optical System Contamination: Effects, Measurements, Control, P. Glassford, editor, Proc. SPIE 1329, pp. 7 (1990).

124. Guregian, J.J., R. Benoit and W. Wong, "An Overview of Contamination Effects on Performance of High Stray Light Rejection Telescope," Optical Contamination, Proc. SPIE 1329, pp. 7, (1990).

125. Pezzaniti, J.L., D.Wilkes, J.Bennett, et.al., ibid.

126. Pezzaniti, J. L., D. Wilkes, J. Bennett, et.al., ibid.

127. Fischer, R.F., P.M.George, et.al., "Ion Beam Cleaning of Contaminated Optics," Optical System Contamination, A.Peter Glassford, editor, Proc. SPIE 1329, pp. 86 (1990).

128. George, P.M., "Your Mirrors Are In Space and Uou Have to Clean Them," Research and Development, October 1988, pp.109-114.

129. Peterson, R.V. and C.W.Bowers, "Contamination Removal by Jet-spray," Optical System Contamination, A.Peter Glassford, Editor, Proc. SPIE 1329, pp. 72 (1990).

130. Shaw, C., "Contamination Removal by Ion Sputtering," Optical System Contamination, A. Peter Glassford, editor, Proc. SPIE 1329, pp. 100 (1990).

131. Piper, L.G., M.Frisch, et.al.,"Laser Cleaning of Cryogenic Optics," Optical System Contamination, A.Peter Glassford, editor, Proc. SPIE 1329, pp. 110-125 (1990).

132. Osiecki, R.A. and T.J. Magee, "Ultraviolet Laser Cleaning of Mirrored Surfaces," Optical System Contamination, A.Peter Glassford, Editor, Proc. SPIE 1329, pp. 127-134 (1990).

133. Pierce, V. G., M. Frish et.al., "Laser Mirror Cleaning in a Simulated Space Environment," Optical System Contamination, A.Peter Glassford, Editor, Proc. SPIE 1329, pp. 134-140 (1990).

134. Arnold, G.S., R.C. Young Owl and David Hall, "Optical Effects of Photochemically Deposited Contaminant Films," Optical System Contamination, A. Peter Glassford, editor, Proc. SPIE 1329, pp. 225-265 (1990).

135. Howard, T. P.George and R.Fischer, "BRDF Measurements for Contamination Assessment in a Spacecraft Environment," Optical Systems Contamination, A. Peter Glassford, Editor, Proc. SPIE 1329, pp. 266-279 (1990).

136. Folkman, M.A., L.A. Darnton, et.al., "Optical Scatter and Contamination Facility," A. Peter Glassford, Editor, Proc. SPIE 1329, pp. 225.

137. Customer Relations, Claris Corp., 5201 Patrick Henry Drive, Santa Clara, CA 95052-8168. (Tel. 1-800-735-7393)

138. Armstrong, T.W., B. L. Colborn, "Scoping Estimates of the LDEF Satellite Induced Radioactivity, "SAIC Report No. 90/1462, NASA Contract Report NAS8-38427 (1990)' "Predictions of Induced Radioactivity for Spacecraft in Low Earth Orbit," Nuclear Tracks and Radiation. Measurements, Paramon Press, 20, 75 (1992).

139. Benton, E.V., W. Heinrich (Eds.), "Ionizing Radiation Exposure of LDEF," University of San Francisco Report TR-77 (1990); E. V. Benton, et.al., "Ionizing Radiation Exposure of LDEF (Pre-Recovery Estimates)", Nucl. Tracks Radia. Meas. Pengamon Press 20.75 (1992).

141. Harmon, B.A., et.al, "LDEF Radiation Measurements: Preliminary Measurements," Nucl. Tracks Radiat. Meas. Pergamon Press, 20, 131 (1992).

142. Csige,I., et al., "Charged Particle LET-Spectra Measurements Aboard LDEF", *LDEF 69 Months in Space; First LDEF Post-Retrieval Conference, NASA CP-3134, February 1992.*

143. Parnell, T. A., "Summary of Ionizing Radiation Analysis on the LDEF"

144. Banks, B, " LDEF Yaw and Pitch Angle Estimates", LDEF Materials Workshop, November, 1991

APPENDIX A - HARDWARE FLOWN ON LDEF

The following lists show the various types of hardware that were flown on LDEF. This hardware was either an experiment specimen or used in support of an experiment. The lists are approximately 90% complete.

MECHANICAL HARDWARE:

LUBRICANTS

(Unless otherwise noted, the following lubricants were not exposed to the exterior LDEF environment)

Everlube 620C (MIL-L8937, Form A), MoS2 dry film with phenolic binder
M0003, exposed to exterior trailing edge

Vespel SP-1
M0003,exposed to exterior trailing edge

Vespel SP-21 washers
A0187-1

Vespel insulated bushings
A0147

Vespel spacer insulation
S1002

Lubribond A (MIL-L-23398)
M0003, exposed to exterior trailing edge

Braycote 601 (flew as 3L-38RP)
A0187-1, cycled few times on-orbit, located exterior surfaces, near trailing edge

Vac Kote 21207 Ball Aerospace Systems Group (BASG)
S0069, MoS2 without binder

Vac Kote 18.07 BASG
S0069? sealed monochrometer
MoS2 with polyimide binder
Application method for 21207?

MoS2
A0175, applied to nut plates

MIL-L-23398D Solid film, air cured, lubricant
Belleville washers, EECC's
Drive shaft and linkages, EECC's

MoS2, physical vapor deposited
A0138-10 used on stacked specimens

Cetyl alcohol

A0175
applied to nut plates
removed on-orbit

Tungsten disulfide on both grapples

Microseal, moly dry film lubricant (probably Microseal 200-1, E/M Lubricants)
A0187-1 sliding surface, includes deposition process.

Molykote Z (Dow Corning)
A0138-10 used on stacked specimens

Silver plated nuts, MS21046 C4 through C14
Primary structure

GREASES

Ball Brothers 44177
Thrust races and thrust bearings on the EECC's

Dow Corning DC-1102 thermal grease
S1001 and P0005

ANDOK C , Exxon channeling petroleum grease
S0069
approx 1 oz on recorder, hemetically sealed, backfilled with 90% N, 10% He

Apiezon- L high vacuum grease (Fisher Scientific 206-852-9030)
A0180 used on O-rings

Apiezon -T
M0001

Apiezon - H thermal grease
4 oz, thermal coating between experiment modules

Dow Corning -340 heat sink compound, greaselike filled with heat conductive metal oxides
A0133, Inside sealed electronics box
M0001

Mobil 28 grease, non-channeling silicone grease
MTM (Lockheed) bearings contain 25% grease fill, bearing within elastomeric sealed enclosure backfilled with 95% N & 5% He.

SEALS AND SEALANTS

DC6-1104 controlled volatility sealant
A0187-2, A0178

RTV 3140 clear silicone protective coating
S1001

Silicon rubber sealant GE 567 RTV

A0054

RTV 566 Sealant
A0076, S1002

Viton O-ring
A0134/S0010, MIL-R-83248
A0138-2, Skega Mfg
A0138-2, Vacour Mfg
A0189
M0001, Parker V747-15
M0002, C 76
P0005
A0139A, AMS 7280
A0180
S0069, recorder
A0015, Viton B
MTMs

Buna-N O-rings, M0006

Butyl 4154
A0138-1, butyl seal for FRECOPA box

Butyl, Parker Seal B-612-70
EECC
P0004

Metal "V" Seal
EECC

EPDM rubber, 053A, Kirkhill
P0005

NBR rubber, V-45, Kirkhill
P0005

Silicon rubber gaskets, Chorlastic R-500
S0050, EPDS

Silicon rubber, SN 3500-41
M0004

Neoprene gasket
A0139A

FASTENERS

AISI SAE 1037
A0015 nuts have polyamid inlet for self locking

AISI helicoils
A0015

Loctite adhesive
A0019, A0138-1, M0003

Kaylock clinchnuts, No K7001-3-6
A0019

Teflon washers, Seastrom Mfg
A0034

Kel - F washer
A0114

Inconel wavy spring washers
A00134/S0010

Epon 828 (Epoxy plus Versamid)
A0056, locking of structure fasteners

Extensive list of fasteners on A0172, A0015, A0180, A0023, A0034, M0003.

Self locking KAYNAR
S0109

Keensert blind end fasteners
S1003

Fiberglass washers, G-10, A0038

Nylon screws and nuts
EPDS, S1002

Nickel plated fasteners
S1002

Self locking features
A0034, A0172, S1006

Helicoils, 909F4-0250, Permathread insert, KAYNAR
Tray Clamps

Silver plated nuts, MS21046 C4 through C14
Primary structure

Cadmium
M0003

MECHANIMS AND MOTORS

Delrin AF gears
A0138-1

Piston and check valve

P0005

Gear boxes / DC motors
A0139A

DC motor, Pittman #98-938
EECC

Kel - F bushing
A0114

Solenoids
A0176

Bearing, angular contact; flexiable shaft coupling, slip liner bearing, needle bearing, etc
A01878-1

Bearings on A0133 were alcohol cleaned and run dry

ELECTRICAL/ELECTRONIC HARDWARE:

LDEF SYSTEMS

EPDS: CMOS digital microcircuits (MIL-STP-883, Class B)
analog microcircuits: ADC, MUX, op amps
diodes, transistors, transformers
capacitors, resistors, connectors, etc.
conformal coatings (Conathane CF-1155)
circuit boards, solder joints
heat shrinkable tubing
relays
hardware, potting compound
shields and coatings

MTM (tape recorder):
DC motor, magnetic speed sensor
ferrite heads, bias oscillator
control and record electronics

EIS: 1 system with 24 outputs to turn on/off experiments
timing and power switching circuitry
CMOS microcircuits and discrete components
(diodes, transistors, etc.)
latching relays, status indicators

Batteries:
LiSO2 cells combined into 7.5V, 12V, and 28V units

EXPERIMENT ELECTRICAL SYSTEMS

Typical sub-system assemblies:
Signal conditioning
Power distribution and timing
DC/DC converters, including high voltage supplies (up to 1.2kV)
Memories (volatile and non-volatile
Tape recorders (one 4 track, all others 2 track

Microcircuits:
CMOS (CD4000A and B series), 54 Cxx series digital
54LSxx series digital
Linear: op amps, comparators, ADC's, DAC's, switches, regulators
EEPROM's, PROM's, RAM's

Discrete Components:
Tansistors, diodes (including SCR's)
MOSFET switches
Relays
Capacitors: ceramic, tantalum (dry and wet slug)
Transformers and inductors
Resistors
Oscillator crystals
E-cells (electrolytic current integration)

Solar cells and sensors; photodiodes
Fiber optics and optical isolators
LED's
Thermistors
DC motors
Connectors
Thermocouples

Conformal Coatings:
Solithane 113 with and without curing agent:
A0056 also used as mating compound between structure components and for locking of fasteners.
A0138-1, A0038, S0014, S1001, S1002
A0054 used as potting compound
Sylgard 184: A0138-2
Nytrile phenolic: A0133
Versamid 140/Epicote 808, PCB coating: A0139A
Conap CE-1155, polyurethane: EPDS
Hysol PC 18: M0003
PRC 1568: EECC

Potting Compounds:
Crest: A0180
PRC 1535: A0038, A0201

Solder:
SN63, QQ-S-S71E, EPDS, A0201
L-Sn 60/63 PB, A0139A, S0014
Eutectic solder, #157, Ag-Sn, P0003
Silver solder, A0172
Indium solder #1 & #3
E-solder, silver filled, Epoxylite Corp, M0001

Wiring:
H-film (Kapton) insulated - S1005
Copper #22 gauge w Teflon insulation - S1005
TFE/FEP wiring - S1005
Teflon wiring, TFT -200 24 AWG, EPDS
Kynar insulated, A0054
TFE insulated, A0076
TFE insulated, MIL-W-16878, A0133, M0003, M0004
Raychem 44, MIL-W-80144 (shielded and unshielded), A0139A , S1002
TFE 20 gauge, A0139A
TFE insulated wiring, Alpha 5855, 5856, & 5858, A0180
PTFE, A0187-1
Teflon wire, TFT-200, 20-22 AWG, MIL-W-22759, A0201
TFE Teflon coated 26 gauge, S0014
TFE wire #20 & #22, S1001
Habia, Deutsche, ZT 2607 Tefcell insulation, 99.9% silver, used inside EECC, S1002
Thermocouple wire, Teflon insulation & outer jacket, P0003
Stycast 2850 filled epoxy or wire?, P0003
PTFE and polyimide coated wiring, Filotex Mfg, A0038-1

Connectors:

Deutsch:

A0201 - 38131-12-8pn
P0003 - MIL-B-131F
EPDS - 38007-12A-3014
A0054 - Unknown part #
A0076 - Unknown part #

Cannon:

S1001 - DEM-9P-NMC 76 gold plated
S0014 - MTB2-40PL1, Royal D series, DEMA-25P-NMB-A106, DEMA-25S-NMB-A106
EPDS - MTB-XXPL1, MTB-XXSL1, DDM-S0S-NMB-K56, DC50906-1, DC50907-1, 50908-1
A0076 - Unknown part #

Bendix:

S0014 - JT02A-14-37P (005) (MS27473)
A0201 - MS3470 L 20-41 S

Elco:

A0201 - 7023-047-000-001, 7038-047-217-001
EPDS - 7022-047-000-118, 7008-047-163-106

Amphenol:

A0201 - MS3470 122 10 S, MS3470 122 8 S , MS3470 20 41 P, MS3470 L 14-19 S

Amp:

S1001 - MIL-C-24308, MIL-G-45204

Sunbank:

EPDS - SE54F1208 A12N

Thermal Hardware:

A. Instrumentation
- thermocouples
- thermistors
- passive temperature indicators (liquid crystal)
- adhesives (RTV 560, EC57, Y966)
- heaters
- platinum resistance thermometers
- thermostats
- radiometers, reflectometers, and calorimeters

B. Insulation
- MLI (aluminized Mylar or Kapton)
  - with and without Dacron separators
- Betacloth
- ceramic insulators
- phenolic thermal panel insulators

C. Heat Pipes
- low temperature fixed conductance (ethane)
- low temperature thermal diode (ethane)
- cascade variable conductance (ammonia)
- transverse flat plate (ammonia)

D. Thermal Control
- Surface Coatings
  - Chromic Acid Anodize
  - Magnesium Fluoride layers
  - Conductive ITO and VDA layers
  - Thermal Grease
- Metallized Polymeric Films
  - Silver Teflon
  - Aluminized Teflon
  - Aluminized Kapton
  - SnO_2/In_2O_3 Kapton
  - SiO_x Kapton
  - Silver Inconel
- Conductive and Non-conductive Pigmented Coatings
  - White Paints - Z93, S13, S13G/LO, YB71, A276, RTV615
  - Black Paints - Z306, D111, Z302
  - Goddard Green (sodium/potassium-silicate binder coatings)

E. Phase Change Material (PCM)
- n-heptane

Optical Hardware:

Glasses and crystals [UV-VIS-IR]:
Aluminosilicate, borosilicate, lead silicate, potash borosilicate, SiO_2, soda lime silica, soda potash lime, titanium silicate, , black glass [low scatter], CaF_2, CdTe, Ge, Si, KRS-5, KRS-6, ZnSe, BaF_2, Al_2O_3, Corning 7940, Suprasil W, Ge (polycrystalline, high purity), molybdenum mirror, diamond turned copper mirror.
UV transmissive windows [MgF_2, Sapphire (Al_2O_3), CaF_2, LiF, SiO_2]

Filters [UV-VIS-IR]:
CdSe, Ge, PbTe, PbF_2, KRS-5, SiO, ZnS, Cryolite on SiO_2, PbF_2 on SiO_2, SiO on SiO_2, Ag on SiO_2, ThF_2 on SiO_2, ZnS on SiO_2, AR coating on MgF_2, assorted optical bandpass between 0.3 and 1.1 microns [Schott glasses], Al on SiO_2, neutral density [manufacturer: Corion], narrow band [Corion], hot mirrors [Corion visible transmitting], Lyman alpha and 1600 and 1600 angstrom UV filters, Al_2O_3 on SiO_2, magnesium difluoride on SiO_2, assorted filters [manufacturer: OCLI], SiO on SiO_2, $SiFl_2$ on SiO_2, Ge on SiO_2, Ag on SiO_2.

Metal films [substrates specified if known]:
Indium oxide [In_2O_3], aluminum oxide, Au plated Al [2024-T351], Au plated Al [6003], Au on SiO_2, Ir on SiO_2, Nb on SiO_2, Os on SiO_2, Pt on SiO_2, Cu on SiO_2, Ag on C, Ag on SiO_2, Ta on SiO_2, W on SiO_2, Sn on SiO_2, Zn on SiO_2, OSR mirrors [Au, Al, Ag]

Optical Sources:
CO_2 waveguide laser, Nd+:YAG laser [glass rod], HeNe laser, laser diodes [AlGaAs and an array], flash lamp, 3-GaAs LED's [830nm nominal], one sealed emitter module [1300nm], pre- and non-irradiated LED's [probably 830nm, GaAs]

Optical Detectors:
Si and UV-enhanced Si [PIN], PMT [UV response], pyroelectrics [lithium tantalate (LiTaO3), strontium barium niobate (SBN), triglycine sulfate (TGS)], numerous photovoltaics [Si, PbSnTe arrays, GaAsSb, HgCdTe, InSb], various photoconductors [HgCdTe, PbS, PbSe], solar cells [including $CuInSe_2$ and other thin film types], numerous solar cells [Si based], GaAs and GaAlAs/GaAs solar cells, at least one channeltron array [original trademarked name for a micro-channel plate (MCP)], pre- and non-irradiated photodiodes.

Fiber optics:
Numerous fibers [nominally 10, silica core, unknown core diameter; reportedly both step and graded index types] with various cladding materials; 4 multimode silica core fibers.

Appendix B: Survey Of Current Research In Optical Systems Contamination Control

LDEF optical materials and optica systems exhibited performance degradation due to contamination which underscores the need for further research into contamination prevention and control. Current research in optical systems contamination control for space environments includes the following fields of study: (1) contamination monitoring, (2) on-orbit cleaning, (3) contamination characterization techniques (especially cryogenic and photodeposited molecular films), and, (4) instituting new screening methodologies to select low outgassing materials for spaceborne optical materials. Some recent advances in these fields are described below.

Contamination monitoring requirements for optical materials has stimulated research into new techniques including a portable bidirectional reflectance distribution function (BRDF) instrument (ref. 118), elutriator/quartz crystal microbalance (ref. 119), surface acoustic wave microbalance (ref. 120), grazing incidence telescope dust monitor (ref. 121), and the total integrated scatter (TIS) instrument for in-space monitoring (ref. 122). These research instruments greatly extend the contamination monitoring capability for optical materials in space. They promise a greater mass sensitivity to contaminants (ref. 123), portability (ref. 124), and have demonstrated the potential to accurately measure changes in the scattering intensity due to atomic oxygen (ref. 125) and may even be able to differentiate scatter effects from atomic oxygen roughening or from particulate contamination (ref. 126).

Promising research with on-orbit cleaning techniques also exists including ion beam cleaning of cryogenic surfaces (refs. 127 & 128), CO_2 jet spray (ref. 129), radio frequency (RF) plasma sputtering (ref. 130), and a variety of laser cleaning techniques (refs. 131, 132, and 133). These techniques have demonstrated the ability to clean some contaminants from optical surfaces, but require further study to determine the full range of contaminants that can be cleaned effectively without damaging the surface of the optical material. In addition, these techniques require some engineering development to translate the technology into practical devices for use both on ground and space.

The LDEF optical material experiments also demonstrated the need for data that characterizes the impact of various contaminants, especially cryo- and photodeposited molecular films, on properties like transmission, reflection, and scatter from optical surfaces. Additional research studies would certainly include characterizing outgassing products from spacecraft materials and components, or further research into photochemical deposition effected by solar vacuum ultraviolet light.

To perform characterization analysis, laboratory systems have been developed for simulating contamination processes typical of spacecraft environments (refs. 135 and 136). For example, the Contamination Effects Vacuum Chamber is described as being used to record BR/TDF of cryo- and photodeposited molecular films as a function of molecular material, deposition rate, sample/TQCM temperature, and UV

flux. And, future LDEF-type missions may be required to run experiments in actual space environments that will verify the simulation findings.

The next step after gathering characterization data is to provide screening methodologies which can assist design engineers in selecting low outgassing materials for spaceborne optical instruments, and to minimize the detrimental effects of contamination. Published standard references on low outgassing materials will certainly prevent many sources of contamination.

And finally, the optical components on the LDEF mission have shown how important it is to consider contamination control throughout the mission experiment---from the beginning of the mission with the design of the optical system, followed by construction, development, assembly, transportation, launching and operation of the spacecraft-----so that contamination does not exceed acceptable levels.

APPENDIX C: OPTICS DATABASE USER'S GUIDE

Presented below is a short LDEF User's Manual for the LDEF Optical Experiments Database to assist in accessing the data provided on computer diskette with this final report. The LDEF User's Manual contains pertinent excerpts from the Claris Filemaker Pro manual on specifically how to access and work with the LDEF optical information. It will not describe installation of the Filemaker Pro application software, the steps taken to create this database, nor how to upgrade the database. (The readers are encouraged to consult the Claris manual for full Filemaker Pro information.) The LDEF User's Manual is divided up into six sections:

1. Computer start-up and database password access
2. Working with information
    a. finding information
    b. browsing records
    c. moving from record to record
    d. sorting information
3. Previewing and Printing
4. Exchanging Information
5. Help function
6. Quitting Filemaker Pro

1. Computer start-up and database password access

If you are working from a hard disk, open your Filemaker Pro folder and click on the Filemaker Pro application icon. If you do not have a hard disk, insert your working copy of the Filemaker Pro application disk in one drive, double click the disk icon, and double click the Filemaker Pro application icon. Highlight the filename LDEF data and click it open. Type the password "OPTICAL" and click okay. This password gives you the access to all the information, but does not give you the ability to edit information in the database.

2. Working with information

To find all the LDEF experiment records for viewing, choose Find All from the Select menu. Filemaker Pro displays one of the twenty-four LDEF optical experiment records stored in the database. To move from one record to the next, click either the bottom or top page of the book (to the left of the screen) to view each record. Or slide the bookmark up and down to move more quickly through the records.

To find a specific record, choose Find from the Select menu. An empty LDEF layout appears on the screen. Depending on what information you have to begin your search (PI name, experiment number, etc.) click on the field name box where the computer will search. For example, click on the Experiment Number box, and you will see the indicator bar begin blinking in that box. Put in the number of the experiment you are looking for (ex. A0056) and than click Enter or Find. The database instantly retrieves the A0056 experiment record. You could just as easily have typed the Principal Investigators name in the Present Principal Investigator box, and it would have found the same experiment record.

You will notice that to the left it says the computer found one record out of the twenty-four total records that satisfied your search request. If you had chosen instead

a search item that is shared by a couple of different records, than the computer will find all those experiments that satisfy your search request. For example, if you inputted A0138 in the Experiment Number box, the computer search would have resulted in 4 records being found. As you page through these records, you will see they are A0138-3, A0138-4, A0138-5 and A0138-7; all subexperiments of A0138.

In contrast, you can limit the search by inputting items in more than one Field name. For instance, if you had inputted A0138 in the Experiment Number box, and inputted the name Bourrieau in the Original Principal Investigator box, the computer would have searched and found only one record...A0138-7.

Filemaker Pro lets you put in actual values, like Cumulative Sun Hours for searching. In addition, the database allows you to search the database within a range of values, (e.g. between 11,000 and 15,000 Sun Hours), by using the range symbol (...). For example, you would type "11,000.15,000", in the Sun Hours box and than click "Find". You would see that the computer found thirteen LDEF experiment records with Cummulative Sun Hours between 11,000 and 15,000.

3. Previewing and Printing

In preparing the LDEF material you have exhibited on the screen for printing, Filemaker Pro needs to know what printer and pre-defined paper size you are going to use. To specify a printer, use the Chooser function on the Apple menu. Then choose Page Setup from the File menu, where you can choose the paper size and other options you want, then click okay.

You can check how a report will look when printed by previewing it before you begin to print. Previewing lets you catch many errors without wasting time or paper. To do this:

a) Open LDEF data
b) Browse records you want to print
c) Choose Preview from the Select menu.

Your records look exactly as they will be printed. Move from page to page by clicking the pages in the book or dragging the bookmark. Use the zoom controls to zoom in to see objects on the screen in detail, or zoom out to get an overview. To return to Browse, choose Browse from the Select menu. In summary, to print copies of the LDEF records, follow this sequence of steps:

a) Use Chooser on the Apple Menu to select printer, if necessary.
b) Browse the records you want to print. Use Find, Omit, or Find All as necessary.
c) Sort the records, if necessary. Filemaker Pro prints the records in the order of the LDEF database layout, unless you use the sort command to change the order.
d) Choose Page Setup from the file menu, and make your choices in the Page Setup dialog box.
e) Use Preview to check report before printing.
f) Go to File menu and choose Print.

g) A screen will appear asking you further questions about what you want printed. You can choose to print just this record, or all being browsed for example. When you have made your choices, click Okay. The screen will tell you when the printer has begun to print.

4. Exchanging Information

Filemaker Pro allows you to exchange information between Filemaker Pro and many other programs. To import data, means you bring data from another application or Filemaker Pro file into a Filemaker Pro file. To export data, means you take data from a Filemaker Pro file and make it accessible to another application. Here are the steps to follow for each.

To import a Filemaker Pro file:

a. Open the file to which you want to add records.
b. In Browse, choose Import from the File menu. (You will see the Import dialog box.)
c. Click "Import records from file on disk."
d. Choose Filemaker Pro from the file type pop-up menu.
e. Select the file you want to import.
f. Click Open. (You will see a dialog box telling you how many text, number, date, picture, or calculation fields there are in the import file; and how many test, number, date or picture fields names and compatible field types in the current file match field names in the import file.
g. Click an option to tell Filemaker Pro how to input values in repeating fields. (Keeping them in the original record or splitting them into separate records.)
h. Click okay. (After the import is copied into the current file, Filemaker Pro changes to Browse. The status panel shows the total number of records now in the current file, and the total number of records found.)

You might want to Exchange information with other applications. Filemaker Pro can import from and export to the following formats:

-tab-separated text (word processing)
-comma-separated text (ASCII characters)
-SYLK (spreadsheets like Microsoft Excel and WINGZ)
-DBF (dBASE format)
-DIF (spreadsheets like Visicalc and AppleWorks)
-WKS (worksheet format used by Lotus 1-2-3)
-BASIC (variant of comma-separated text is a format developed to conform to the Microsoft BASIC standard)
-Merge file (similar to the comma-separated text file format, this format can be used in creating personalized form letters and other standard documents).

To export a Filemaker Pro file:

When Filemaker Pro saves your records, the records are saved in a special format used by Filemaker Pro. However Filemaker Pro lets you save your records in formats that can be used to export other applications.

1. Open the file you want to export.
2. In Browse, choose Export from the File menu. (The Export dialog box appears.)
3. Type a name for the export file, and specify where you want it saved.
4. Choose the file type you want from the pop-up menu.
5. Click New. (You see the Field Order Dialog box.)
6. Move the fields into the order you want to export them.
7. Choose whether you want the fields formatted.
8. Click okay. (A copy of the data is saved in this format.)

5. Help function

The Apple menu supplies on-line information about Filemaker Pro. On this menu, the Help command displays the window for the Filemaker Pro Help System, which provides information about Filemaker Pro commands and dialog boxes and step-by-step procedures for most common tasks. When open, Help appears in the Window menu. You can switch back and forth between Help and your Filemaker Pro file by clicking the window you want to make active.

6. Quitting Filemaker Pro

Choose Quit from the File menu. You do not have to save your file. Filemaker Pro automatically saves your work as you go, and does so again as part of quitting.

APPENDIX D: PAPER COPY OF SYSTEMS SIG OPTICAL DATABASE

An LDEF Optical Experiment Database was created (using Filemaker Pro database software) that provides for quick and easy access to available experimenter's optic's related findings. The database contains a file for each of the LDEF experiments that possessed optical hardware (database currently contains 29 files). Each file contains various fields that identify the optical hardware flown, describe the environment seen by that hardware, summarizes experimenter findings and list references for additional information. This Appendix is a paper copy of the database.

Experiment Number: A0034

Experiment Title: Atomic Oxygen Simulated Outgassing Experiment

Tray Location: C9 Leading Edge (8.1 degrees off RAM incidence angle), C3 Trailing Edge (171.9 degrees off RAM incidence angle)

Experiment Objective:

To determine if the impingement of atomic oxygen in near-Earth orbit is a major factor in producing optically damaging outgassed products. [Ref 1]

AO Fluence (atoms/cm2): C9 = 8.71E + 21, C3 = 1.33E + 03 [Ref 2]

Radiation Flux:

Temperatures (C):

Experiment Tray Sun Hours: C9 = 11,200 and C3 = 11,100 [Ref 3]

M/D Impact Density:

Original Principal Investigators:

Robert L. Scott, Jr.
Southern University
Baton Rouge, LA.

Roger C. Linton
NASA George C. Marshall Space Flight Center
Huntsville, Al.

Present Principal Investigators:

Roger C. Linton
Code EH12
NASA Marshall Space Flight Center
Alabama, 35812
Tel. (205)544-2526
FAX (205)544-0212

Charles C. Burris
Southern University
Baton Rouge, LA

Robert L. Scott, Jr.
Ciba-Geigy
Saint Gabriel, LA.

Optical Materials Flown on LDEF:

Coatings on borosilicate or fused silica windows:
Z-93 whitepaint (IITRI) zinc oxide in potassium silicate binder
A-276 white paint; titanium dioxide pigment in polyurethane binder
S-13G (IITRI); zinc oxide in RTV602 silicone binder
S-13G/LO (IITRI); zinc oxide in RTV602 silicone binder, improved formulation for outgassing
Z-306 Chemglaze; black, titanium dioxide and carbon in polyurethane binder
Z-326 Chemglaze;
YB71 zinc ortho titanate (ZOT) (IITRI)
anodized aluminum protective cover
[Ref 4 and 5]

Measurements Performed on Samples:

1. solar absorptance and emittance for Al protective cover
2. optical transmission for windows
3. black light exposure test for fluoresence
4. reflectance of mirrors

[Ref 4]

Results Summary:

The effects of extended space exposure on thermal control coatings of LDEF Experiment A0034 are dependent on several factors, including the type or composition of the coating and the combination of incident environmental factors. For a few specimens,variant response to the same environmental exposure indicates influences of specific coating formulation or preparation. LDEF leading edge exposure, characterized by the degree of atomic oxygen exposure, apparently reversed the damage induced by incident solar radiation. The principal exception is one of the S13G specimens (01-41) exposed under an open aperture on the leading edge. [Ref 5]

The visual appearance and optical properties of the polyurethane coatings exposed under open apertures on the leading edge were little changed despite the eroison of binder material by atomic oxygen. Significant degradation of the A276 specimen exposed under a quartz window appears to be duplicated in an area of the open aperture specimen that was shadowed from direct atomic oxygen impingement. [Ref 5]

The most significant degradation to the zinc oxide or zinc orthotitanate coatings was found in specimens of S13G and S13G-Lo exposed to the aperture-limited level of solar radiation and the minimal atomic oxygen fluence on the trailing edge. Specimens of Z-93 coatings were least affected of all by exposure on the leading or trailing edge modules. Specimens of YB-71 coatings were affected to a degree only slightly more than Z-93

coatings. Preliminary results of BRDF and surface profiling measurements indicate that the atomic oxygen exposure on these coatings does not significantly alter the diffuse properties. Observations of fluorescence changes induced in the exposed coatings provide additional evidence of environmental interaction. [Ref 5]

Conclusions:

System Analysis and Future Design Considerations:

Published Experiment Reports:

PI's Database:

References:

1. Clark, Lenwood, et.al., THE LONG DURATION EXPOSURE FACILITY (LDEF), NASA SP-473, NASA Langley Research Center, 1984, pg. 11.
2. Bourassa, Roger, J. and J.R. Gillis, "Data Summary: Atomic Oxygen Flux and Fluence Calculation for Long Duration Exposure Facility (LDEF)", LDEF MSIG, Boeing Defense and Space Group, NASA Contract NAS1-1824, Jan. 18, 1991.
3. Bourassa, Roger, J. and J.R. Gillis,"Solar Exposure of Long Duration Exposure Facility Experiment Trays", LDEF MSIG", Boeing Defense and Space Group, June 26, 1991, NASA Contract 1-1824-Task 12.
4. Linton, Roger C., First LDEF Post Retrieval Symposium presentation entitled, "Atomic Oxygen Simulated Outgassing", June 2-8, 1991, Kissimee, Florida, NASA CP-3134, 1991.
5. Linton, Roger C., Effects of Space Exposure on Thermal Control Coatings, American Institute of Aeronautics and Astronautics, AIAA 92-0795, Advance copy of the paper for the 30th Aerospace Sciences Meeting, January 6-9, 1992, Reno, Nevada.

Experiment Status:

Hardware Archive:

Data Upgrade Date: 1/28/92

Experiment Number: A0056

Experiment Title: Exposure to Space Radiation of High Performance Infrared Multilayer Filters and Materials

Tray Location: G12 Earth End (90.8 degrees off RAM incidence angle), B8 (38.1 degrees off RAM incidence angle)

Experiment Objective:

To maximize the exposure of particular optical materials and filters known to be useful in atmospheric and planetary remote sensing satellites, to ascertain their suitability for spacecraft use and to permit an understanding of degradation mechanisms. [Ref 1]

AO Fluence (atoms/cm2): G12 = 3.05E + 20, B8 = 6.93E + 21 [Ref 2]

Radiation Flux:

Temperatures (C):

Experiment Tray Sun Hours: G12 = 4,500 and B8 = 9,400 [Ref 3]

M/D Impact Density:

Original Principal Investigators:

John S. Seeley, R. Hunneman and A. Whatley
Department of Cybernetics, University of Reading
Reading, Berks, UNITED KINGDOM

Derek R. Lipscombe
British Aerospace Corporation
Stevenage, Hartfordshire, UNITED KINGDOM

Present Principal Investigators:

Gary J. Hawkins, John Seeley, Roger Hunneman
The University of Reading, Infrared Multilayer Laboratory
Department of Cybernetics, Whiteknights
Reading, Berkshire, RG6 2AY, ENGLAND
Tel. 9011 0734 318 224
FAX 9011 0734 318 220

Optical Materials Flown on LDEF:

UNCOATED CRYSTALS AND MATERIALS
Calcium Fluoride (CaF_2)
Magnesium Fluoride (MgF_2)
Germanium (Ge)
Silicon (Si)
Cadmium Telluride (CdTe)
Sapphire (Al_2O_3)
Y-cut Quartz
Z-cut Quartz
KRS-5
KRS-6
SOFT SUBSTRATE/ COATING MATERIALS
KRS-5 with 61-layer AS2S3/KRS-5
KRS-6 with 33-layer ZnS/KRS-5 & ZnSe/KRS-5
KRS-5 with 61-layer CdTe/KRS-5 & AS2S3/KRS-5
HARD SUBSTRATE / FILTER COATINGS
Ge with PbTe/ZnSe
Ge with PbTe/ZnS
Al_2O_3 with Ge/SiO
ZnSe with PbF_2
Si with SiO
[Ref 1]

Measurements Performed on Samples:

Spectral reflectance and transmittance (2.5 to 40 um)
Linear transmittance versus linear wavenumber
Statistical spectral comparison (average transmission in coincident regions and wavenumber correlations).
Spectral displacement (comparing wave number diplacement between pre- and post-flight)
Visual examination and photographic record (inspections at all stages of the LDEF experiment) [Ref1]

Results Summary:

UNCOATED: Correlation of average transmittance was very high between pre- and post-flight measurements. A consistent loss in transmission (-0.765%), was indicated but this was sufficiently close to zero to infer no change within the transmission accuracy envelope permitted. Although complete fracture occured from an impact onto one uncoated sample, most other impacts produced only localized coating delamination around the periphery of the impact site.

SOFT-COATED: Comparison of pre- and post-flight average transmittance values were made from samples from both sites, and the correlation was very low (-0.168); indicating no correlation between pre- and post-flight sample spectra. This was also evident from visual inspections, where gross physical degradation and delamination of the coatings and substrate materials was evident, having occured as a result of excess space exposure and the effects of atomic oxygen bombardment. Post-flight visual and spectral analysis of the soft materials showed that less degradation had occured in the Earth-facing tray (G12) than in the leading edge tray (B8). The meteroid/debris impact on the calcium floride sample (B8-2) occured near the edge of the sample holder. The impact crater was about 1 mm in diameter with a spallation zone diameter of about 5.5 mm. The substrate cleaved in two directions outwards from the crater site to the opposite sides of the sample, and at an angle of about 75 degrees, breaking the sample into three pieces. Although other samples had impact craters of this size with large spallation diameters and small fractures, this was the only sample which showed evidence of complete fracture, verifying the fragile and brittle nature of calcium flluoride as a substrate material , whilst remaining optically funtional.

HARD-COATED MATERIALS: Pre- and post-flight comparisons were well correlated. They showed a small and consistent loss in transmission for both, within the accuracy envelope. These samples are considered stable and show no degradation for the exposure. A PbTe/ZnS-based sample was cleaned in 1,1,1,-Trichloroethane and 2-propanol and remeasured. The spectrum remained unchanged and it was deduced that the surface was not contaminated by exposure to space; its loss of transmission therefore must be ascribed to another mechanism.

[Ref 1]

Conclusions:

The effects of space exposure on the high-performance filters flew on LDEF were neglible. No significant changes were found either in transmission or spectral position of any hard-coated II-VI / PbTe-based multilayers on germanium substrates, or in uncoated substrates.

The softer materials were adversely affected in their physical and optical properties by the long exposure in space, varying from a reduced transmission to a complete opacity.

Although impacts by micrometeoroid damaged some samples, these did not detract from their function and performance as an optical component. Likewise, atomic oxygen and space radiation caused no detectable spectral effect, other than in soft material smples which were exposed beyond that intended.

[Ref 1]

System Analysis and Future Design Considerations:

Published Experiment Reports:

1. Hawkins G.J., Hummeman R., Seeley J.S.,"Space Exposure of Infrared Filters and Materials on the NASA Long Duration Exposure Facility (LDEF)", University of Reading (1990), ISBN 077049 04098.
2. Hawkins G.J., Hunneman R., Seeley J.S.; "Preliminary Results from Infrared Multilayer Filters and Materials Exposed to the Space Environment on the NASA LDEF Mission" Proc. SPIE 1320 pp 407-419 (1990).

PI's Database:

References:

1. Hawkins, Gary J., et.al., "Exposure to Space Radiation of High Performance Infrared Multilayer Filters and Materials Technology Experiment (A0056), First LDEF Post-Retrieval Symposium Proceedings, NASA CP-3134, 1991.
2. Bourassa, Roger, J. and J.R. Gillis, "Data Summary: Atomic Oxygen Flux and Fluence Calculation for Long Duration Exposure Facility (LDEF), LDEF MSIG, Boeing Defense and Space Group, NASA Contract NAS1-1824, Jan. 18, 1991.
3. Bourassa, Roger, J. and J.R. Gillis, "Solar Exposure of Long Duration Exposure Facility Experiment Trays", LDEF MSIG, Boeing Defense and Space Group, June 26, 1991, NASA Contract 1-1824-Task 12.

Experiment Number: A0056

Experiment Status:
Hardware Archive:
Data Upgrade Date: 1/28/92

Experiment Title: Effect of Space Exposure on Pyroelectric Infrared Detectors

Tray Location: E5 (128.1 degrees off RAM incidence angle)

Experiment Objective:

To determine the effects of long duration exposure and launch environment on the performance of pyroelectric detectors. This will be valuable information to potential users of pyroelectrics for predicting performance degradation, setting exposure limits, or determining shielding requirements. [Ref 1]

AO Fluence (atoms/cm2): 3.72E + 12 [Ref 2]

Radiation Flux:

Temperatures (C):

Experiment Tray Sun Hours: 8,200 [Ref 3]

M/D Impact Density:

Original Principal Investigators:

James B. Robertson, Ivan O. Clark, and Roger K. Crouch
NASA Langley Research Center
Hampton, Virginia

Present Principal Investigators:

James B. Robertson and Ivan O. Clark
NASA Langley Research Center M/S152E
Hampton, Virginia 23665-5225
Tel. (804) 864-6643
FAX (804)864-3800

Optical Materials Flown on LDEF:

Twenty pyroelectric-type infrared detectors were flown onboard LDEF. The detector chips were of three different pyroelectric materials: lithium-tantalate, strontium-barium-niobate and triglycine-sulfide. [Ref 4]

Measurements Performed on Samples:

The experiment was passive; no measurements were taken during the flight. Performance of the detectors was measured before and after flight [Ref 4], using detector parameters signal strength, noise and detectivity which is calculated from signal and noise data. [Ref 6]

Results Summary:

Post flight measurements and comparison revealed that detectors made of lithium-tantalate and strontium-barium- niobate suffered no measureable loss of performance. Detectors made of triglycine-sulfide suffered complete loss of performance, but so did the control samples of the same material. [Ref 4]

A white substance was seen on the KRS-5 (thallium-bromide-iodide) detector windows. Other window materials were flown (Irtran II and germanium), but the effect was seen only in the KRS-5. Chemical analysis revealed silicate over all of the KRS-5 flight windows and a higher concentration of thallium in the damaged regions of flight windows than in either the control window or in less damaged regions of the flight windows. If the detector had survived, the detectivity was expected to be lower due to the decrease in transmission of the windows. [Ref 6]

Conclusions:

1. Strontium-barium-niobate and lithium-tantalate are suitable materials for pyroelectric detectors for longterm space applications.
2. The triglycine-sulfide detectors are not recommended because of their apparent short shelf life.
3. The choice of detector window and lens materials is of major importance.

[Ref 5]

System Analysis and Future Design Considerations:

Window and lens materials are of major importance. In space use, a detector will be part of a detection system and located behind a lens or window of some sort, and damage to the lens or window will most likely play a larger role than damage to the detector in the degradation of the system performance. [Ref 6]

Published Experiment Reports:

PI's Database:

References:

1. Clark, Lenwood G., THE LONG DURATION EXPOSURE FACILITY (LDEF), NASA Langley Research Center,

NASA SP-473, 1984, pg.158.
2.Bourassa, Roger J. and J.R.Gillis, "Data Summary: Atomic Oxygen Flux and Fluence Calculation for Long Duration Exposure Facility (LDEF)", LDEF MSIG, Boeing Defense and Space Group, NASA Contract NAS1-1824, Jan. 18, 1991.
3. Bourassa, Roger J. and J.R. Gillis, Solar Exposure of Long Duration Exposure Facility Experiment Trays", LDEF MSIG, Boeing Defence and Space Group, June 26, 1991, NASA Contract 1-1824-Task 12.
4. Robertson, James B., First LDEF Post-Retrieval Symposium Abstracts, NASA Conference Publication 10072, June 1991, pg. 106.
5. Robertson, James B., "Effects of Space Exposure on Pyroelectric Infrared Detectors", presentation at the First LDEF Post-Retrieval Conference, Kissimee, Florida, June 2-8, 1991.
6. Robertson,James B., "Effect of Space Exposure of Pyroelectric Infrared Detectors", an extended abstract for the First LDEF Post-Retrieval Symposium Proceedings, NASA CP-3134, 1991.

Experiment Status:

Additional work to be performed on transmission studies on window materials. [Ref 5]

Hardware Archive:

Data Upgrade Date: 1/28/92

Experiment Number: A0138-3

Experiment Title: Thin Film Metal Film and Multilayer Experiment

Tray Location: B3 Trailing Edge (171.9 degrees off RAM incidence angle)

Experiment Objective:

This experiment investigates the effects of space environment on vacuum UV optical components (EUV thin films, UV gas filters, photocathodes, and UV crystal filters) for use in the development and qualification of new UV components. [Ref 1]

AO Fluence (atoms/cm2): 1.33E + 03 [Ref 2]

Radiation Flux:

Temperatures (C): from -23C to 66C (about 34000 orbits) [Ref 3]

Experiment Tray Sun Hours: 11,100 [Ref 4]

M/D Impact Density: 90 impacts/m2 > 50 um

Original Principal Investigators:

J.P Delaboudiniere and J.M. Berset
CNRS/LPSP
Verrieres le Buisson, France

Present Principal Investigators:

J.P. Delaboudiniere
CNRS/LPSP
Verrieres le Buisson, France

Optical Materials Flown on LDEF:

EUV thin films
UV gas filters
photocathodes
UV crystal filters

Measurements Performed on Samples:

Results Summary:

Conclusions:

System Analysis and Future Design Considerations:

Published Experiment Reports:

PI's Database:

References:

1. Clark, Lenwood, et.al., THE LONG DURATION EXPOSURE FACILITY (LDEF), NASA SP-473, NASA Langley Research Center, 1984.
2. Bourassa, Roger, J. and J.R. Gillis, "Data Summary: Atomic Oxygen Flux and Fluence Calculation for Long Duration Exposure Facility (LDEF), LDEF MSIG, Boeing Defense and Space Group, NASA Contract NAS1-1824, Jan. 18, 1991.
3. Durin, Christian, "French Cooperative Passive Payload", C.N.E.S., First LDEF Post-Retrieval Symposium viewfoil copies, June 1991.
4. Bourassa, Roger, J. and J.R. Gillis, "Solar Exposure of Long Duration Exposure Facility Experiment Trays", LDEF MSIG, Boeing Defense and Space Group, June 26, 1991, NASA Contract 1-1824-Task 12.

Experiment Status:

Hardware Archive:

Data Upgrade Date: 1/28/92

Experiment Number: A0138-4

Experiment Title: Vacuum - Deposited Optical Coatings Experiment

Tray Location: B3 Trailing Edge (171.9 degrees off RAM incidence angle)

Experiment Objective:

To analyze the stability of various vacuum-deposited optical coatings exposed to the space environment. [Ref 1]

AO Fluence (atoms/cm2): 1.33E + 03 [Ref 2]

Radiation Flux:

Temperatures (C): from -23C to 66C (about 34000 orbits) [Ref 3]

Experiment Tray Sun Hours: 11,100 [Ref 4]

M/D Impact Density: 90 impacts/m2 > 50 um [Ref 3]

Original Principal Investigators:

A. Malherbe
Optical Division
Matra, SA
Rueil Malmaison, FRANCE

Present Principal Investigators:

Jean Charlier
Matra Defense
DET/DTO
17, rue Paul Dautier
78140 Velizy Villacoublay
FRANCE
tel. (33-1)39.46.97.86
FAX (33-1)39.46.64.87

Irenee Alet
CNES/Centre Spatial de Toulouse 18
Avenue Edouard Belin
31055 Toulouse Cedex
FRANCE
telephone: 33 612 73780
FAX: 33 612 74099

Optical Materials Flown on LDEF:

See page 162 Table 18 in Reference 1 for complete details. Below is a summary of the materials:

Metallic interference filter made in ultrahigh vacuum, wavelength = 121.6 nm
Metallic interference filter made in classical vacuum, wavelength = 121.6 nm
Metallic interference filter, wavelength = 130 nm
Dielectric interference filter, wavelength = 500 nm
Bandpass interference filter, wavelength = 15 um
Al + MgF_2 metallic mirror on glass substrate measured at 121 nm
Al + MgF_2 metallic mirror on Kanigen substrate at 121 nm
Al + LiF metallic mirror on glass substrate at 102 nm
Al + LiF metallic mirror on Kanigen substrate
Platinum mirror at 121 nm
Au mirror at 121 nm
Ag + ThF_4 metallic mirror on glass substrate at 450 nm
Ag + ThF_4 metallic mirror on Kanigen substate at 450 nm
Dielectric mirror at wavelength = 250 nm
Dielectric mirror at wavelength = 170 nm
Metallic selective mirror at wavelength = 170 nm
SiO_2-TiO_2 dielectric mirrors
Antireflection coating in 14- to 16-um region
Antireflection coating in 8- to 13-um region
Dichrometric separation in visible and infrared region at 10 um

Measurements Performed on Samples:

Spectral transmission and reflectance measurements on pre- and post-flight samples, controls and reference samples.

Results Summary:

See transmission and reflectance charts in Reference 5.

Conclusions:

1. UV filters and mirrors were sensitive to space exposure; the MgF_2 material is probably the main factor for the weakness.

2. Components and coatings for visible and infrared applications have been little or not affected in their optical performances by space exposure.
3. Coatings including many highly-stressed layers (oxides and fluorides) show an evident risk of mechanical degradation (vacuum cycling).
[Ref 5]

System Analysis and Future Design Considerations:

Published Experiment Reports:

PI's Database:

References:

1. Clark, Lenwood, et.al., THE LONG DURATION EXPOSURE FACILITY (LDEF), NASA SP-473, NASA Langley Research Center, 1984.
2. Bourassa, Roger, J. and J.R. Gillis, "Data Summary: Atomic Oxygen Flux and Fluence Calculation for Long Duration Exposure Facility (LDEF)", LDEF MSIG, Boeing Defense and Space Group, NASA Contract NAS1-1824, Jan. 18, 1991.
3. Durin, Christian, "French Cooperative Passive Payload", C.N.E.S., First LDEF Post Retrieval Symposium viewfoil copies, June 1991.
4. Bourassa, Roger, J. and J.R. Gillis,"Solar Exposure of Long Duration Exposure Facility Experiment Trays", LDEF MSIG, Boeing Defense and Space Group, June 26, 1991, NASA Contract 1-1824-Task 12.
5. Charlier, Jean., "Vacuum Deposited Optical Coatings Experiment", First LDEF Post Retrieval Synposium Proceedings NASA CP-3134,1991.

Experiment Status:

Hardware Archive:

Data Upgrade Date: 1/24/92

Experiment Number: A0138-5

Experiment Title: Ruled and Holographic Gratings Experiment

Tray Location: B3 Trailing Edge (171.9 degrees off RAM incidence angle)

Experiment Objective:

To test the behavior of grating coatings after extended exposure to the space environments, by examining coatings for changes and differentiating the influence of vacuum and solar illumination. [Ref 1]

AO Fluence (atoms/cm2): 1.33E + 03 [Ref 2]

Radiation Flux:

Temperatures (C): from -23C to 66C (about 34000 orbits) [Ref 3]

Experiment Tray Sun Hours: 11,100

M/D Impact Density: 90 impacts/m2 > 50 um [Ref 3]

Original Principal Investigators:

Gilbert Moreau
Jobin-Yvon Division
Instruments, SA
Longjumeau, FRANCE

Present Principal Investigators:

Francis Bonnemason
Instruments SA
Jobin Yvon
Longjumeau, FRANCE

Renee Alet
CNES/Centre Spatial de Toulouse 18
Avenue Edouard Belin
31055 Toulouse Cedex, FRANCE
Telephone: 33 612 73780
FAX: 33 612 74099

Optical Materials Flown on LDEF:

- Replica from ruled grating (glass blank + epoxy photoresist + coating) Type G. Grating characteristic is 1200 G/MM blazed at 250 nm, Al-coated.
-Original master holographic grating (glass blank + sensitive photoresist + coating) Type H. Grating characteristic is 3600 G/MM 50-150 nm spectral range, platinum-coated.
-Ion etched original master grating (glass blank + coating) Type HU. Grating characteristic is 1200 G/MM blazed at 250 nm, Al-coated.
-Control mirrors (glass blank + coating) Type W.
[Ref 5]

Measurements Performed on Samples:

-wavefront planarity (Michelson interferometer)
-light efficiency (photogoniometer)
-stray light level (monochromator)
[Ref 6]

Results Summary:

Reference Samples:

I. Coatings--Control Mirrors: no reflectance degradation for Al and Pt coatings (>2% loss)

II. Gratings: No degradation in wavefront planarity. Absolute efficiency losses as follows: Type G3 10% at 220 nm; Type HU3 Very slight decrease and shift of the efficiency curve on the whole spectral range (220-600 nm); Type H3 Correct preservation and distribution of energy.

Vacuum Samples:

I. Coatings--Control Mirrors Aluminum showed reflectivity loss < or = to 10% on the whole spectral range. Platinum showed around 10% loss at the three wavelengths of the test.

II. Gratings: No degradation in wavefront planarity. Absolute efficiency losses as follows: Type G1.2 showed < or = to 10% on whole spectral range. Type HU1.2 showed < or = to 10% on the 220 - 300 nm spectral range. Type H1.2 showed 10% at 58.4 and 73.4 nm and 25% at 121.6 nm.

Space Exposed Samples:

I. Coatings--Control mirrors: Aluminum showed a reflectivity loss of 30% at 220 nm. Platinum showed a reflectivity loss of 30% at 121.6 nm.

II. Gratings: No degradation in wavefront planarity. Absolute efficiency losses as follows: Type G1.1 had 35% loss at 220 nm. Type HU1.1 had 30% at 220 nm. Type H1.1 had correct behavior at 58.4 and 74.4 nm; 40% loss at 121.6 nm. [Ref 5]

Conclusions:

Wavefront planarity and efficiency tests have been performed using the same instrumentation as before the flight, on the reference samples (stored on earth in the same container under air-nitrogen pressure) and loaded sets of mirrors and gratings. We have noticed no wavefront degradation on the gratings. This indicates that the materials used for manufacturing the standard gratings (glass blanks, photoresist for holographic recording, epoxy photoresist for replication process and coatings) are suitable for the thermal conditions in space. Control reference samples revealed an alteration of efficiency (10%) on the 220-300 nm spectral range with the ruled grating replica. Both holographic and ion-etched originals remained in good condition. Long exposure to space vacuum has affected the tested coating (Al and Pt) reflectivity, around 10%. The same is true with all the gratings, except the holographic grating at 121.6 nm, which showed 25% degradation of the Pt coating. Long exposure to space environemnts (sun radiation, cosmic dusts) has damaged the coatings, 30% loss at 220 nm for Al and 30% at 121.6 nm for Pt. We note similar degradation with the Al coated components (35% at 220 nm for the ruled grating replica). The Pt coated holographic grating presented a higher damage; 40% at 121.6 nm. [Ref 5]

System Analysis and Future Design Considerations:

In actual use, loaded spectroscopic systems are not exposed to solar radiation and cosmic dust. Under protected conditions, gratings should not present significant deterioration, with respect to wavefront and efficiency tests. However, when exposed to solar radiation and cosmic dust, the wavefront quality and efficiency is notably degraded in the UV region. [Ref 5]

The aluminum and platinum coatings of the ruled and holographic gratings have shown good resistence against the extended long duration space environmental factors as measured by wavefront planeity and absolute efficiency. [Ref 6]

Published Experiment Reports:

PI's Database:

References:

1. Clark, Lenwood, et.al., THE LONG DURATION EXPOSURE FACILITY (LDEF), NASA SP-473, NASA Langley Research Center, 1984.
2. Bourassa, Roger, J. and J.R. Gillis, "Data Summary: Atomic Oxygen Flux and Fluence Calculation for Long Duration Exposure Facility (LDEF)", LDEF MSIG, Boeing Defense and Space Group, NASA Contract NAS1-1824, Jan. 18, 1991.
3. Durin, Christian, "French Cooperative Passive Payload", C.N.E.S., First LDEF Post-Retrieval Conference viewfoil copies, June 1991.
4. Bourassa, Roger, J. and J.R. Gillis, "Solar Exposure of Long Duration Exposure Facility Experiment Trays", LDEF MSIG, Boeing Defense and Space Group, June 26, 1991, NASA Contract 1-1824-Task 12.
5. Bonnemason, Francis, "Ruled and Holographic Gratings Experiment", First LDEF Post-Retrieval Conference Viewfoil copy, June 1991.
6. Bonnemason, Francis, "Ruled and Holographic Diffraction Gratings Experiment, First LDEF Post-Retrieval Proceedings, NASA CP-3134, 1991.

Experiment Status:

Stray light level analysis must still be performed. [Ref 6]

Hardware Archive:

Data Upgrade Date: 1/28/92

Experiment Number: A0138-7

Experiment Title: Optical Fibers and Components Experiment

Tray Location: B3 Trailing Edge (171.9 degrees off RAM incidence angle)

Experiment Objective:

Evaluate fiber optics permanent damage induced by ionizing radiation after a long exposure in space and after laboratory tests. Waveguides exposed to the space environment will be used to develop laboratory tests to simulate space radiation effects. [Ref 1]

AO Fluence (atoms/cm2): 1.33E + 03 [Ref 2]

Radiation Flux:

Temperatures (C): -23C to 86C (about 34000 orbits) [Ref 3]

Experiment Tray Sun Hours: 11,100 [Ref 4]

M/D Impact Density: 90 impacts/m2 > 50 um [Ref 3]

Original Principal Investigators:

J. Bourrieau
CERT/ONERA-DERTS
Toulouse, FRANCE

Present Principal Investigators:

J. Bourrieau
CERT/ONERA-DERTS
Toulouse, FRANCE

Irenee Alet
CNES/Centre Spatial de Toulouse 18
Avenue Eduoard Belin
31055 Toulouse Cedex, FRANCE
Telephone: 33 612 73780
FAX: 33 612 74099

Optical Materials Flown on LDEF:

Two optical fiber waveguides (one step index and one graded index) of some 60 cm length with connectors.

Measurements Performed on Samples:

Results Summary:

Conclusions:

System Analysis and Future Design Considerations:

Published Experiment Reports:

PI's Database:

References:

1.Clark, Lenwood, et.al., THE LONG DURATION EXPOSURE FACILITY (LDEF), NASA SP-473, NASA Langley Research Center, 1984.

2. Bourassa, Roger, J. and J.R. Gillis, "Data Summary: Atomic Oxygen Flux and Fluence Calculation for Long Duration Exposure Facility (LDEF)", LDEF MSIG, Boeing Defense and Space Group, NASA Contract NAS1-1824, Jan. 18, 1991.

3. Durin, Christian, "French Cooperative Passive Payload", C.N.E.S., First LDEF Post-Retrieval Conference viewfoil copy, June 1991.

4. Bourassa, Roger, J. and J.R. Gillis, "Solar Exposure of Long Duration Exposure Facility Experiment Trays", LDEF MSIG, Boeing Defense and Space Group, June 26, 1991, NASA Contract 1-1824-Task 12.

Experiment Status:

Hardware Archive:

Data Upgrade Date: 1/24/92

Experiment Title: Passive Exposure of Earth Radiation Budget Experiment Components

Tray Location: B8 (38.1 degrees off RAM incidence angle), G12 Earth End (90.8 degrees off RAM incidence angle), B9 (8.1 degrees off RAM incidence angle)

Experiment Objective:

To assure the measurement accuracy of solar and Earth flux measurement devices. [Ref 1]

AO Fluence (atoms/cm2): B8 = 6.93E + 21, G12 = 3.05E + 20, B9 = 8.71E + 21 [Ref 2]

Radiation Flux:

Temperatures (C):

Experiment Tray Sun Hours: B8 = 9,400; G12 = 6,800 ; B9 = 11,200 [Ref 3]

M/D Impact Density:

Original Principal Investigators:

John R. Hickey and Francis J. Griffin
The Eppley Laboratory, Inc.
Newport, Rhode Island

Present Principal Investigators:

John R. Hickey
The Eppley Laboratory, Inc.
P.O. Box 4419, Newport, RI 02840
Tel. (401)847-1020
FAX (401) 847-1031

Thomas A. Mooney and Ali Smajkiewicz
Barr Associates
2 Lyberty Way
Westford, MA 01886
Tel. (508)692-7513
FAX (508)692-7443

Optical Materials Flown on LDEF:

SOLAR SENSORS [Channel # / filter / spectral band in um / thermopile]
1S fused silica 0.18 to 3.8 N3 thermopile
2S fused silica 0.18 to 3.8 N3 thermopile
3S None (total rad.) < 0.2 to >50 N3 flat plate
4S OG-530 glass 0.526 to 2.8 N3
5S RG-695 glass 0.698 to 2.8 N3
6S Interference filter 0.395 to 0.510 N3
7S Intereference filter 0.344 to 0.460 N3
8S Interference filter 0.300 to 0.410 N3
9S Interference filter 0.285 to 0.365 K2
10S Intereference filter 0.250 to 0.320 K2
10C None (total rad.) <0.2 to >50 HF cavity
EARTH FLUX SENSORS [Channel No. / filter /spectral band in um / thermopile]
11E None (total rad.) <0.2 to >50 N3 Flat plate
12E None (total rad.) <0.2 to >50 N3 flat plate
13E Fused silica hemispheres 0.2 to 3.8 N3
14E RG-695 glass hemispheres 0.695 to 2.8 N3
EPPLEY LAB METAL AND DIELECTRIC COATING MATERIAL [Coating Material/ Cements/ Substrates/Covers]
Zirconium Oxide Epon 828 with Versamid 140 Hardener Fused Silica (Amersil T08)
Zinc Sulfide Apco R313
Thorium Fluoride
Cryolite (Sodium Aluminum Fluoride)
Lead Flluoride
Lead Chloride
[Ref 4]

Measurements Performed on Samples:

Observations and microscopy analysis
Lamp-thermopile exposure evaluation (test configuration repeatability)
Thermopile resistence tests
spectral transmittance
pyrheliometric calibration
cavity reflectance
[Ref 4]

Results Summary:

1. Laboratory thermopile repeatability = 0.33%
2. Pre- and post-flight thermopile resistence measurement variation = < 2 ohms for the N3 thermopiles
   = < 10 ohms for the K2 thermopiles
3. Percent change in ERB solar channel module exposure between pre- and post-flight signal (mV):
   1S-03 = 1.63
   2S-03 = -0.70
   3S-03 = 0.57
   4S-03 = -0.28
   5S-03 = 1.00
   6S-03 = 0.63
   7S-03 = 0.18
   8S-03 = 0.18
   9S-03 = -0.92
   10S-03 = -0.16
4. Spectral transmittance curves are available for the fused silica windows and the interference filters in Ref 4.
5. Cavity heater resistence between pre- and post-flight was unchanged at 152.2 ohms.
6. Cavity thermopile resistence 354.7 ohms up 0.3 ohms for the preflight values.
7. The sensor vacuum to air ratio changed 0.16% from preflight measurements.
8. Data ratios to the World Radiation Reference: APEX/LDEF Instrument SN21185 = 1.00069
   EPLAB refrence SN14915 = 1.00002
9. Cavity reflectance: 250 +/- 80 ppm for the APEX/LDEF cavity
   270 +/- 80 ppm for a new cavity of the same type
   [All results above taken from Ref 4]
10. Eppley sample spectral profiles are available in Reference 5.

Conclusions:

Results of preliminary testing of the ERB components exposed aboard the LDEF indicate the following conclusions. Thermopile sensors were virtually unaffected by the space exposure, including the painted receivers of the directly exposed units. The filter and window materials experienced changes in spectral transmittance, some due to contamination and some due to UV exposure or other factors. Identification of the amounts due to each cause is under investigation. There appeared to be a contaminant which was later cleaned by atomic oxygen on most of the exterior exposed components. Very little of the LDEF contaminant was found on the sensors disscussed here. The cavity radiometer performance appears to be unaffected within our ability to assess change even though there is visible change to the cavity coating. It remains to relate the LDEF results to the results of the Nimbus ERB mission in a quantitative manner. These results should be useful to those planning similar future measurements from space. [Ref 4]

Concluding remarks about the Eppley samples follow. With the exception of the lead compounds, the coatings survived very well. The lead-containing components revealed a decrease in spectral transmission due to increased absorption by the lead compounds. In an instrument, signal would be lost but spectral stability maintained. These materials, however, are no longer being incorporated into spaceborne filters. The Epon cement degraded somewhat at 500 nm (other wavelengths are masked by the filter). The filters containing aluminum layers experienced an increase in transmission that can be attributed to the pinholes which developed during the LDEF exposure. This form of failure would reduce signal-to-noise but would not influence spectral band position or width. [Ref 5]

System Analysis and Future Design Considerations:

Filters containing lead compounds show reductions in transmission, which may be due to elevated temperatures, suggesting a thermal effect. In an instrument, signal would be lost but spectral stability maintained. These materials are no longer used in spaceborne filters. [Ref 5]

Published Experiment Reports:

PI's Database:

References:

1. Clark, Lenwood, et.al., THE LONG DURATION EXPOSURE FACILITY (LDEF), NASA SP-473, NASA Langley Research Center, 1984.
2. Bourassa, Roger, J. and J.R. Gillis, "Data Summary: Atomic Oxygen Flux and Fluence Calculation for Long

Duration Exposure Facility (LDEF), LDEF MSIG, Boeing Defense and Space Group, NASA Contract NAS1-1824, Jan. 18, 1991.
3. Bourassa, Roger, J. and J.R. Gillis, Solar Exposure of Long Duration Exposure Facility Experiment Trays, LDEF MSIG, Boeing Defense and Space Group, June 26, 1991, NASA Contract 1-1824-Task 12.
4. Hickey, John L., "Passive Exposure of Earth Radiation Budget Experiment Components LDEF Experiment A0147: Post Flight Examinations and Tests", First Post-LDEF Symposium Proceedings, NASA CP-3134, 1991.
5. Mooney, Thomas A. and Ali Smajkiewicz, "Transmittance Measurements of Ultraviolet and Visible Filters Flown Aboard LDEF", First Post-Retrieval LDEF Symposium Proceedings NASA CP-3134,1991.

Experiment Status:

Spectral transmittance change due to contaminants still under investigation. Work is continuing on comparing LDEF data to the Nimbus ERB mission in a quantitative fashion.

Hardware Archive:

Data Upgrade Date: 1/28/92

Experiment Number: A0171

Experiment Title: Solar Array Materials Passive LDEF Experiment

Tray Location: A8 (38.1 degrees off RAM incidence angle)

Experiment Objective:

To evaluate the synergistic effects of space environment on various solar-array materials, including solar cells, coverslips with various antireflective coatings, adhesives, encapsulants, reflector materials, substrate strength materials, mast and harness materials, structural composites, and thermal control treatments. [Ref 1]

AO Fluence (atoms/cm2): 6.93E + 21 [Ref 2]

Radiation Flux:

Temperatures (C): about 32,000 cycles (temperature to be determined) [Ref 2]

Experiment Tray Sun Hours: 9,400 [Ref 3]

M/D Impact Density: 2-7 impacts per composite, less than 1 mm in diameter [Ref 2]

Original Principal Investigators:

Ann F. Whitaker, Charles Smith, Jr. and Leighton Young
NASA George C. Marshall Space Flight Center
Huntsville, Alabama

Present Principal Investigators:

Ann F. Whitaker and Leighton E. Young
NASA Marshall Space Flight Center
MSFC, Al 35812
Tel (205)544-2510
FAX (205)544-0212

Optical Materials Flown on LDEF:

This passive experiment contains a total of about 100 materials and material processes which address primarily solar array materials, including solar cells, composites, thin films, paints, metals and other polymers. This database will record results concerningthe solar cells only. Seven separate MSFC photovoltaic (solar cells) were flown on this experiment. All test articles underwent substantial atomic oxygen erosion of their polyimide (Kapton) substrate structures with the effect that one module was lost prior to Orbiter rendezvous with LDEF; one came loose and drifted away when LDEF was grappled; and one (M3) was attached at only one corner when LDEF was retrieved. The latter was found on the floor of the cargo bay when LDEF was removed. A description of the solar cell test articles on hand for post-flight analysis are described below. [Ref 2]

SOLAR CELL TEST ARTICLES

M3 ASEC 12 Cell Module
- Applied Solar Energy Corp. (ASEC) 200 microns, 2 cm x 4 cm silicon N on P, 2 ohm-cm, back reflector cells
- Chemically Vapor Deposited (CVD) dielectric, wrap-around contacts
- 150 micron microsheet coverslides with UV filters and AR coatings
- Rear surface of module facing space

M4 ASEC 6 Cell Module
- ASEC 550 micron, 2 cm x 4 cm silicon N on P, 10 ohm-cm back-surface field cells
- Wrap-around contacts with wrap-around junction
- 2 each 50 micron, 4.7 x 6.7 cm coverslides
- cells mounted facing space

Cells C6 through C10- ASEC cells same as M3 but with coverslides as follows:
- C6 none
- C7 150 micron microsheet with AR coating
- C8 150 micron microsheet with UV filter and AR coating
- C9 150 micron frosted fused silica with UV filter and AR coating
- C10 150 micron fused silica with UV filter and AR coating

Note: Each test article has a copper interconnect system laminated between 2 sheets of Kapton that comprises the structural substrate for the solar cells. [Ref 2]

Measurements Performed on Samples:

preflight electrical performance
post flight electrical performance
visual examination [Ref 2]

Results Summary:

Atomic oxygen degradation was obvious from visual examination of the polyimide substrates of the cells. However, some portions of the Kapton substrate containing acrylic adhesives are still intact and require more evaluation to determine the reasons for their survival. Solar cell to solar cell interconnect bonds withstood the effects of thermal cycling well with no debonding found at the parallel-gap weld of the copper interconnect to the cell contact pads. The module that was retrieved from from the cargo bay had 5 (of 12) cells that contained cracks in either the solar cell or cell cover. Micrometeroids/space debris impacts were evident on all the test articles. These ranged from small nicks to solar cell coverslide breakage and rather deep penetrations within the cells. [Ref 2]

Solar cell and solar cell module maximum power point (Pmp) degradation ranged from 4.3% to 80% with 76% of the single cells tested having less than 10% degradation. There were four cells out of 17 that had Pmp degradation greater than 20%. Three of these were from modules which were retrieved from the cargo bay. The other was cell (C6) which was flown without a coverslide. Discounting these cells, the average cell Pmp degradation was 6.5% with a standard deviation of 1.75%. The thin cell module (M4), which was retrieved intact but with severe damage to its Kapton substrate degraded 5.2% in Pmp. Four cells had discernible degradation in open circuit voltage (Voc) which is typical of a decrease in cell shunt resistence. Three of these were from the module retrieved from the cargo bay with the other being the cell flown without a coverslide. Two of the cells with Voc degradation were from the four which degraded more than 20%. Three cells showed evidence of severe series resistence increases. All three of these were from the cargo bay module. Two are from the four having discernible degradation in Voc. [Ref 2]

Conclusions:

Power degradation in the experimental solar cells was consistent with the exposure environment and appears to be produced principally by the radiation and atomic oxygen environments. Atomic oxygen erosion dominated for the most part in materials that were expected to be both atomic oxygen and ultraviolet vulnerable. Silicone coatings appear to protect Kapton, and adhesive systems contained under photon opaque materials were surprisingly environmentally resistant. New synergistic effects of the space environment were noted in the interaction of atomic oxygen and copious amounts of contamination and in the induced luminescence of many materials. A high density of small micrometeroid/space debris impacts were observed on mirrors, protective coatings, paints and composites. At this time, no correlation between cell/module electrical performance and meteroid impacts has been established. [Ref 2]

System Analysis and Future Design Considerations:

Acrylic adhesives remained intact on some portions of the Kapton substrate, where all other materials were degraded by atomic oxygen. More research is required to determine the reasons for their survival in the atomic oxygen environment.

Published Experiment Reports:

PI's Database:

References:

1. Clark, Lenwood G, et.al., THE LONG EXPOSURE FACILITY (LDEF): Mission 1 Experiments, NASA SP-473, NASA Langley Research Center, pg. 86-87, 1984.
2. Whitaker, Ann and Leighton Young, "An Overview of the First Results on the Solar Array passive LDEF Experiment", First Post-Retrieval LDEF Synposium Proceedings, NASA CP-3134, 1991.
3. Bourassa, Roger J. and J.R.Gillis, "Solar Exposure of Long Duration Exposure Facility Experiment Trays", LDEF MSIG, Boeing Defense and Space Group, June 26, 1991, NASA Contract 1-1824-Task 12.

Experiment Status:

Hardware Archive:

Data Upgrade Date: 1/28/92

Experiment Number: A0172

Experiment Title: Effects of Solar Radiation on Glasses

Tray Location: D2 (141.9 degrees off RAM incidence angle), G12 Earth end (90.8 degrees off RAM incidence angle)

Experiment Objective:

To determine the effects of solar radiation and space environment on glasses in space flight by exposing glass specimens to the space environment and analyzing the optical, mechanical, and chemical property changes that occur after differing cumulaltive solar radiation exposure. [Ref 1]

AO Fluence (atoms/cm2): D2 = 4.81E + 08, G12 = 3.05E + 20 [Ref 2]

Radiation Flux:

Temperatures (C):

Experiment Tray Sun Hours: D2 = 9,600 ; G12 = 4,500 [Ref 3]

M/D Impact Density: D2 average frequency = 0.002 impacts/cm2 year [Ref 4]

Original Principal Investigators:

Ronald Nichols	Donald Kinser
NASA /MSFC	Vanderbilt University
Huntsville, AL	Nashville, TN

Present Principal Investigators:

D. Kinser, R. Weller, M.Mendenhall, D. Wiedlocher
Vaderbilt University,
Nashville, TN.

R.Nichols, D.Tucker and A. Whitaker
Marshall Space Flight Center
MSFC, AK 35812

Optical Materials Flown on LDEF:

commercial optical fused silica
low iron soda-lime-silica glass
Pyrex 7740 glass
Vycor 7913 glass
BK-7 glass
Zerodur glass ceramic
[Ref 4]

Measurements Performed on Samples:

mechanical testing (ASTM-F-394 piston on 3 ball method in a liquid nitrogen environment)
statistical analysis
optical microscopy
back scatter spectrometry

Results Summary:

Samples were exposed on LDEF in two locations corresponding to: 1) the negative velocity vector (52 samples) and 2) approximately perpendicular to the velocity vector facing earth (68 samples). Samples located in the tray affixed to the second row of the LDEF module, primarily receiving direct solar radiation, received seven micrometeorite impacts on glass samples and four impacts on the tray structure. Impacts were observed on all glass types with the exception of the Vycor. Two Zerodur samples were affected with one suffering two impact events. The observed frequency of impact events averaged over the exposure time was 0.002 impacts/cm2 year. [Ref 4]

Weibull analysis as well as standard statistical evaluation were conducted. The Weibull analysis revealed no differences between control samples and the two exposed groups. This was confirmed through optical microscopy evaluation of the fracture initiation origin. Statistical analysis including Student's t test for confidence interval. We thus concluded that radiation components of the Earth orbit did not degrade the mechanical strength of the samples examined within the limits of experimental error. [Ref 4]

Statistical problems arising from the low frequency and location of micrometeroite or space debris impacts upon the samples precluded statistically valid measurement of impacted sample strengths. Upper bounds for the magnitude of the impact event damage upon strengths for impacted samples were determined using calculated values of stress corresponding to the actual stress present of the impact site during testing. The upper bound of strength degradation for meteorite impacted samples based upon this analysis and the

observations was 50%. [Ref 4]

The glass and glass ceramic samples exposed to low earth orbit environment for approximately 5-1/2 years on LDEF were found to display limited degradation in optical transmission. Commercial optical quality fused silica samples display decreases in transmission in the 200 to 400 nm wavelength region and this degradation appears to be a consequence of surface contamination. The contamination, found only on internal surfaces of samples, was measured by medium back scattering spectrometry and found to be primarily carbon. Additional thin film contamination by a species with atomic mass near 64, which was present at the level of about 8E + 14/cm2, has not been identified. [Ref 5]

These observations are consistent with the interpretation that organic binders used in the black absorbing paint (ChemGlaze Z-306) inside the sample holding tray were concentrated in the vicinity of the samples and photolytically cracked by solar UV radiation. The resulting decomposition products were deposited on the interior sample surface and gave rise to the optical transmission loss. [Ref 5]

No detectable contamination was observed on the external or space exposed surfaces of the samples. No measurable damage was detected which could be atributed to the direct action of gamma or UV radiation on the glass. [Ref 5]

Conclusions:

System Analysis and Future Design Considerations:

These results emphasize the need for special precautions in the preparation of spacecraft carrying precision optical components on long duration exposure missions. [Ref 5]

Published Experiment Reports:

A paper describing this work is being submitted to the Journal of the American Ceramic Society, and should appear in early 1992.

PI's Database:

References:

1. Clark, Lenwood, et.al., THE LONG DURATION EXPOSURE FACILITY (LDEF) NASA SP-473, NASA Langley Research Center, 1984, pg. 88.
2. Bourassa, Roger J. and J.R.Gillis, "Data Summary: Atomic Oxygen Flux and Fluence Calculation for Long Duration Exposure Facility (LDEF)", LDEF MSIG, Boeing Defense and Space Group, NASA Contract NAS1-1824, Jan. 18, 1991.
3. Bourassa, Roger J. and J.R. Gillis, "Solar Exposure of Long Duration Exposure Facility Experiment Trays", LDEF MSIG, Boeing Defense and Space Group, June 26, 1991, NASA Contract 1-1824-Task 12.
4. Wiedlocher, D.E., D.S.Tucker, R.Nichols and D.Kinser, "Mechanical Properties of Silicate Glasses Exposed to a Low Earth Orbit" (an extended abstract), First LDEF Post-Retrieval Symposium Proceedings, CP-3134, 1991.
5. Kinser, D, R.Weller, M.Mendenhall, and D.Wiedlocher, "Contamination of Optical Surfaces in Earth Orbit" (an extended abstract), First LDEF Post-Retrieval Symposium Proceedings, CP-3134, 1991.

Experiment Status:

Hardware Archive:

Data Upgrade Date: 1/28/92

Experiment Title: Radiation Sensitivity of Quartz Crystal Oscillators Experiment for the Long Duration Exposure

Tray Location: D2 (141.9 degrees off RAM incidence angle)

Experiment Objective:

To determine whether there is a correlation between defect cluster concentrations observed for different grades of quartz examined by TEM and the electrical stability of quartz resonators exposed to the complex radiation associated with an orbital LDEF environment. [Ref. 1]

AO Fluence (atoms/cm2): 4.81E + 08 [Ref. 2]

Radiation Flux: Estimated to be 1E + 03 [Ref. 3]

Temperatures (C): Estimated to be less than 30C [Ref. 3]

Experiment Tray Sun Hours: 9,600 [Ref. 4]

M/D Impact Density:

Original Principal Investigators:

Ronald L. Nichols
NASA George C. Marshall Space Flight Center
Huntsville, Alabama

Donald L. Kinser
Vanderbilt University
Nashville, Tennessee

Present Principal Investigators:

J. S. Ahearn and J.D.Venables
Martin Marietta Laboratories
1450 S. Rolling Rd.
Baltimore, MD 21227
Tel. (301)247-0700
FAX (301) 247-4939

Optical Materials Flown on LDEF:

quartz crystal oscillators (swept premium Q-quartz and natural quartz) [Ref. 3]

Measurements Performed on Samples:

transmission electron microscopy (quantification of electron exposure and micrographs)
resonant frequency shift
[Ref. 3]

Results Summary:

SUMMARY OF AGING DATA

Quartz Type	Aging Rate (Hz/day)	Total Freq. Shift upon Aging (Hz)	Sample Type
Swept Q	3.2E - 11	6.1E - 9	Shielded
Swept Q	1.1E - 10	2.1E - 8	Unshielded
Natural	3.4E - 11	6.5E - 9	Shielded
Natural	3.2E - 11	6.1E - 9	Unshielded

The data indicates that the shielded swept premium Q resonators showed the same drift rate before and after the flight. However, the unshielded swept premium Q resonators exhibited a larger frequency drift in all of the post-flight aging tests than in the pre-flight tests. The magnitude of the frequency shift is 2.1E - 8 Hz for the unshielded case compared to 6.1E - 9 in the shielded case.

All of the natural quartz pre- and post-flight aging tests were similar within the scatter of the experimental data. In addition, all of the natural quartz resonators, and the pre-flight and shielded post-flight swept premium Q resonators behaved in a similar manner within the scatter of the experiment. [Ref. 3]

Conclusions:

Quartz materials were examined in the transmission electron microscope (TEM) and classified as to their sensitivity to radiation damage by establishing the rate of damage caused by the electron beam in the microscope. All of the space-exposed resonators fabricated with swept premium Q material exhibited a frequency shift above that of the control resonators; none of the resonators fabricated from the natural quartz material exhibited such a shift.The marked contrast in behavior between the swept premium Q resonators and the natural quartz resonators correlates with the pre-flight TEM observations, where the Q quartz exhibited a lower density of strain centers than in the natural quartz but with a more rapid development and larger size of the strain centers after a given electron

dose. [Ref. 3]

System Analysis and Future Design Considerations:

The need for high-precision quartz oscillator clocks (and filters) for communication satellites, missiles, and space probes makes it necessary to improve the radiation stability of materials used for these applications. These results suggest that TEM can be used to classify grades of quartz according to their suitability for use in radiation-hard resonators. Moreover using this technique, it may be possible to identify the impurities that are responsible for the radiation-induced frequency drift associated with irradiated quartz crystal resonators. [Ref. 3]

Published Experiment Reports:

1. Ahearn, J.S. and Venables, J.D. "Radiation Sensitivity of Quartz Crystal Oscillators: Experiment for the LDEF", March-May 1978, Monthly Progress Report #1-3 on contract NAS 1-15263.
2. Ahearn, J.S. and Venables, J.D., "Radiation Sensitivity of Quartz Crystal Oscillators Experiment for the Long Duration Exposure Facility, First LDEF Post-Retrieval Conference Proceedings, NASA CP 3134, 1991.

PI's Database:

None available.

References:

1. Clark, Lenwood G. et. al., "The Long Duration Exposure Facility (LDEF) Mission 1 Experiments", NASA SP SP-473, NASA Langley Research Center, 1984, pg. 170.
2. Bourassa, Roger J. and J.R. Gillis, "Data Summary: Atomic Oxygen Flux and Fluence Calculation for Long Duration Exposure Facility (LDEF)", LDEF MSIG, Boeing Defense and Space Group, NASA Contract NAS1-1824, Jan. 18, 1991.
3. Ahearn, J.S. and J.D. Venables, "Radiation Sensitivity of Quartz Crystal Oscillators Experiment", LDEF Post-Retrieval Symposium Proccedings, NASA CP-3134, 1991.
4. Bourassa, Roger, J. and J.R.Gillis, "Solar Exposure of Long Duration Exposure Facility Experiment Trays", LDEF MSIG, Boeing Defense and Space Group, June 26, 1991, NASA Contract 1-1824-Task 12.

Experiment Status:

The experiment objective was met. Further experiments are underway to understand the absence of the effect (change in resonant frequency) in the natural quartz resonators.

Hardware Archive:

Data Upgrade Date: 1/28/92

Experiment Title: Space Environmental Effects on Spacecraft Materials

Tray Location: D3 Trailing Edge (171.9 degrees off RAM incidence angle), D4 (158.1 degrees off RAM incidence angle), D8 (38.1 degrees off RAM incidence angle), D9 Leading Edge (8.1 degrres off RAM).

Experiment Objective:

To understand the changes in the properties and structure of materials after exposure to the space environment and to compare these changes with predictions based on laboratory experiments. To improve the performance and usage of existing materials and to decrease the lead times for application of new materials on DOD space systems. [Ref. 1]

AO Fluence (atoms/cm2): See individual M0003 subexperiment database record.

Radiation Flux: See individual M0003 subexperiment database record.

Temperatures (C): See individual M0003 subexperiment database record.

Experiment Tray Sun Hours: See individual M0003 experiment

M/D Impact Density: See individual M0003 subexperiment database.

Original Principal Investigators:

Paul Schall (overall manager of the nineteen individual M0003 experiments)
The Aerospace Corporation
El Segundo, California

Present Principal Investigators:

See individual experiments M0003-1 to M0003-8, M0003-11 and M0003-14.

Optical Materials Flown on LDEF:

The following entry lists all the subexperiments under the M0003 experiment for reference. Optical materials were flown on the following subexperiments: -1, -2, -4, -6, -7, -8, -11 and -14. Each of these optical materials subexperiments has its own record in this database.

M0003-1 Radar camouflage and electro-optical signature coatings
M0003-2 Laser optics
M0003-3 Structural materials
M0003-4 Solar-power components
M0003-5 Thermal control materials
M0003-6 Laser communication components
M0003-7 Laser mirror coatings
M0003-8 Composites materials, electronic piece parts, and fiberoptics
M0003-9 Thermal control materials
M0003-10 Advanced composities
M0003-11 Contamination monitoring
M0003-12 Radiation dosimetry
M0003-13 Laser-hardened materials
M0003-14 Quartz crystal microbalance
M0003-15 Thermal control materials
M0003-16 Advanced composities
M0003-17 Radiation dosimetry
M0003-18 Thermal control coatings
M0003-19 Electronic devices
[Reference 1]

Measurements Performed on Samples:

Typical analyses included the measurement of optical properties (reflectance, transmittance, and refractive index), macrophysical properties, and microstructural properties. [Reference 1] See individual subexperiments for details.

Results Summary:

See individual subexperiment records.

Conclusions:

See individual subexperiment record.

System Analysis and Future Design Considerations:

See individual subexperiment record.

Published Experiment Reports:

M. J. Meshishnek, S.R.Gyetvay and C.H. Jaggers, LONG DURATION EXPOSURE FACILITY EXPERIMENT M0003 DEINTEGRATION FINDINGS AND IMPACTS, First LDEF Post Retrieval Symposium Proceedings, Kissimee, Florida, June 2-8, 1991.

PI's Database:

M0003 Database compiled by Sandy Gvetnay, et. al. , The Aerospace Corporation, El Segundo, CA.

References:

1. Clark, Lenwood, et.al., THE LONG DURATION EXPOSURE FACILITY (LDEF), NASA SP-473, NASA Langley Research Center, 1984.

Experiment Status:

Hardware Archive:

Data Upgrade Date: 1/28/92

Experiment Number: M0003-1

Experiment Title: Radar Camouflage Materials and EO Signature Coatings

Tray Location: D3 Trailing Edge (171.9 degrees off RAM), D4 (158.1 degrees off RAM incidence angle), D8 (38.1 degrees off RAM incidence angle), D9 Leading Edge (8.1 degrees off RAM incidence angle)

Experiment Objective:

AO Fluence (atoms/cm2): D3 = 1.33E +03; D4 = 9.34E +04; D8=6.93E + 21; D9 = 8.71E +21 [Ref 1]

Radiation Flux:

Temperatures (C):

Experiment Tray Sun Hours: D3 = 11,100; D4 = 10,500; D8 = 9,400; D9 = 11,200 [Ref 2]

M/D Impact Density:

Original Principal Investigators:

G. Grider and E. Pelton
AFWAL Avionics Laboratory

Present Principal Investigators:

Richard Porter
WL/SNA
Wright Patterson AFB, OH 45433-6533
(513)255-5076

Optical Materials Flown on LDEF:

Measurements Performed on Samples:

Results Summary:

Conclusions:

System Analysis and Future Design Considerations:

Published Experiment Reports:

PI's Database:

References:

1. Bourassa, Roger J. and J.R.Gillis, "Data Summary: Atomic Oxygen Flux and Fluence Calculation for Long Duration Exposure Facility (LDEF)", LDEF MSIG, Boeing Defense and Space Group, NASA Contract NAS1-1824, Jan. 18, 1991.
2. Bourassa, Roger J. and J.R. Gillis, "Solar Exposure of Long Duration Exposure Facility Experiment Trays", LDEF MSIG, Boeing Defense and Space Group, June 26, 1991, NASA Contract 1-1824-Task 12.

Experiment Status:

Hardware Archive:

Data Upgrade Date: 1/24/92

Experiment Number: M0003-2

Experiment Title: Laser Optics

Tray Location: D3 Trailing Edge (171.9 degrees off RAM incidence angle), D4 (158.1 degrees off RAM incidence angle), D8 (38.1 degrees off RAM incidence angle), D9 Leading Edge (8.1 degrees off RAM) [Rf1]

Experiment Objective:

1) Determine adverse effects of natural space environment on laser optical component materials; 2) assess environmental hazards peculiar to a LEO space exposure (AO erosion); 3)Anchor codes for space effects prediction and simulartions, and 4) Suggest methods and approaches to minimize optical performance degradation in space. [Ref 3]

AO Fluence (atoms/cm2): D3 = 1.33E +03; D4 = 9.34E +04; D8=6.93E + 21; D9 = 8.71E +21 [Ref 2]

Radiation Flux:

Temperatures (C): 160 F delta T, 15 cycles per day (evidence for greater delta T on PL samples) [Ref 3]

Experiment Tray Sun Hours: D3 = 11,100; D4 = 10,500; D8 =9,400; D9=11,200 [Ref 4]

M/D Impact Density: 2,273 Impacts/m2 averaged all sizes; 5,000 > 0.3 mm dia holes; 30,000 < 0.3 mm dia [Ref3]

Original Principal Investigators:

A. Stewart and A.H. Guenther
Air Force Weapons Lab

Present Principal Investigators:

Linda De Hainaut
PL/LTC
Kirtland AFB, NM 87117-6008
(505) 844 0626
[Ref 5]

Optical Materials Flown on LDEF:

Ten sets of six samples each (120 surfaces); each set uniquely exposed; two control sets not flown. Each set contains:
uncoated fused silica (T22 Supersil-W1, Amersil, Inc., finished at Perkin Elmer)
MgF2 coated fused silica (coating is M.G.D.A by E.M Chemical Co; 1/2 wavelength at 1.06 um; Perkin Elmer coater)
bare polished molybdenum (low carbon ARC casted bar stock; Amax Specialty metal)
molybdenum coated with Cr,Ag & ThF4 (ThF5-Cerac, 99% pure; Ag-Marz Wire, 99.99% pure; Cr-Electronic Spare
Products, 99.99% pure)
diamond turned copper (OFHC)
diamond turned Ni plated Cu (Northrup?)

Four sets on Leading Edge exposed for: 70 months, 3 months, 6 months and 9 months

Four sets on Trailing Edge exposed for: 0 months, 3 months, 6 months and 9 months

Two sets control samples never flown

[Ref 3]

Measurements Performed on Samples:

Preflight characterization (visual, microscopic, surface roughness, scatter, reflectance, transmittance/absorption)
Phase 1 -Postflight examination plan (visual, photography, scatter photography, Normarski microscopy, total integrated scatter, BRDF, total hemispherical reflection, reflectance vs. incidence angle, absorption, transmission, elipsometry, profilometry)
Phase 2-Post flight examination (XPS/Auger, SEM, RBS, SIMS, ESCA, laser damage)

Results Summary:

Conclusions:

System Analysis and Future Design Considerations:

Published Experiment Reports:

PI's Database:

References:

1. Bourassa, Roger, Incidence Angles for LDEF Tray and Longeron Locations paper copy
2. Bourassa, Roger, J. and J.R. Gillis, "Data Summary: Atomic Oxygen Flux and Fluence Calculation for Long Duration Exposure Facility (LDEF)", LDEF MSIG, Boeing Defense and Space Group, NASA Contract NAS1-1824, January 18, 1991.
3.DeHainaut, Linda L.,"Degradation of Optical Components in a Space Environment", a copy of a viewfoil presentation given to Gail Bohnhoff-Hlavacek for inclusion into the database at the LDEF Materials Conference by Linda DeHainaut, November 1991.
4.Bourassa, Roger J. and J.R. Gillis, "Solar Exposure of Long Duration ExposureFacility Experiment Trays", LDEF MSIG, Boeing Defense and Space Group, June 26, 1991, NASA Contract 1-1824-Task 12.
5.FAX from Michael Meshishnek showing list of LDEF SSD 802 investigators as of 09/11/91.

Experiment Status:

Visual, photography and Nomarski have been performed post-flight. Some scatter measurements (TIS,BRDF) have been performed on the fused silica.

Hardware Archive:

Data Upgrade Date: 1/28/92

Experiment Title: Advanced Solar Cell and Coverglass Analysis

Tray Location: D3 Trailing Edge (171.9 degrees off RAM incidence angle), D4 (158.1 degrees off RAM incidence angle), D8 (38.1 degrees of RAM incidence angle), D9 Leading Edge (8.1 degrees off RAM)

Experiment Objective:

To understand changes in the properties and structure of materials after exposure to the space environment and to compare these changes with predictions based on laboratory experiments. And, further to improve the performance and usage of existing materials and decrease the lead times for application of new materials on DOD space systems. [Ref 1]

AO Fluence (atoms/cm2): D3 = 1.33E + 03, D4 = 9.34E + 04, D8 = 6.93E + 21, D9 = 8.71E + 21 [Ref 2]

Radiation Flux:

Temperatures (C):

Experiment Tray Sun Hours: D3=11,100; D4=10,500; D8=9,400; D9=11,200 [3]

M/D Impact Density:

Original Principal Investigators:

Joseph F. Wise and Kenneth Masloski
AFWAL Aeropropulsion Laboratory
Wright Patterson Air Force Base, OH 45433

Present Principal Investigators:

Terry M. Trumble
Aerospace Power Division
Aero Propulsion and Power Directorate
WL/POOC-2
Wright Patterson Air Force Base, OH 45433-6533
(513)255-6236
(513)476-4781

Optical Materials Flown on LDEF:

The experiment consists of 48 coverglass samples and 12 solar cell strings. Sixteen (16) of the coverglass samples were on the leading edge and 16 on the trailing edge, and 16 on the backside of a tray protected from direct exposure to the LEO environment. An additional 15 samples were used as control samples and were not flown. [Ref 4]

Measurements Performed on Samples:

photographic survey
microscopy (Nomarski)
optical transmission
optical reflectance
optical absorbance
electrical properties
[Ref 4]

Results Summary:

OPTICAL PROPERTIES

The full results of the transmission, reflection and absorption are being analyzed and will be presented in a later publication. Following is a brief summary of the results from Ref 4. There are more pronounced changes in the optical properties on the trailing edge than on the leading edge. The existing surface contamination did not interfere with the optical properties measurements made on the coverglass samples. The short wavelength cutoff of the optical samples has moved noticeable toward the longer wavelengths. Changes noted otherwise have been primarily in absorptance. [Ref 4]

SURFACE ANALYSIS

The leading edge analysis of the MgF_2 indicates the presence of fluoridated organic contaminants. The fluorine contamination found on the LDEF is likely to be an organic derived fromTeflon. It also appears that oxygen has replaced some of the fluorine in the material. There is no thick layer of oxide as was observed for the ThF_4 samples, however. Analysis of the ThF_4 sample indicates that almost all of the fluorine has been removed from the leading edge ThF_4 sample. SiO_2 appears to be unchanged. All of the trailing edge samples have experienced a layer of greater than 100 Angstroms of contamination. There are also high levels of Si, C and O with about half of the samples showing trace amounts of N, F and Sn. There is contamination of this type on the

leading edge, but to a lesser degree. There is evidence on the trailing edge of silicone-based material contamination. [Ref 4]

PHOTOGRAPHIC SURVEY

The Tedlar mounting rings for the coverglass samples account for a portion of the contamination. This material was not a space qualified material. A second photographic survey confirmed earlier information showing micrometeroid damge, thermal cycling stresses and considerable amounts of loose surface contamination. [Ref 4]

SOLAR CELL ANALYSIS

A visual comparison of cell strings indicated that the fabrication process used for the metallization of each of the cell strings had a large effect on the lifetime of the cells themselves. Metal migration and contamination between the coverglass and the cell proper were two of the main concerns. Loss of silver, or considerable oxidation for unprotected silver appears to be a problem. Contamination, discoloration, shows up mainly on the cell contacts and interconects. [Ref 4]

ELECTRICAL PROPERTIES

Have not been measured at this time. [Ref 4]

Conclusions:

None available at this time.

System Analysis and Future Design Considerations:

There is concern that ThF_4 and MgF_2 will require a passivating coating to survive in Low Earth Orbit (LEO). [Ref 4]

Published Experiment Reports:

Meshishnek M.J., S.R. Gyetvay and C.H. Jaggers, "Long Duration Exposure Facility Experiment M0003 Deintegration Findings and Impacts", First LDEF Post-Retrieval Symposium Proceedings, Kissimee, Florida, June 2-8, 1991.

PI's Database:

Experiment M0003 database compiled by M.Meshishnek, et.al., The Aerospace Corporation.

References:

1. Clark, Lenwood G. et.al., "The Long Duration Exposure Facility: Mission 1 Experiments", NASA SP-473, NASA Langley Research Center, 1984, pg.44-48.
2. Bourassa, Roger J. and J.R.Gillis, "Data Summary: Atomic Oxygen Flux and Fluence Calculation for Long Duration Exposure Facility (LDEF)", LDEF MSIG, Boeing Defense and Space Group, NASA Contract NAS1-1824 Jan. 18, 1991.
3. Bourassa, Roger J. and J.R. Gillis, "Solar Exposure of Long Duration Exposure Facility Experiment Trays", LDEF MSIG, Boeing Defense and Space Group, June 26, 1991, NASA Contract 1-1824-Task 12.
4. Trumble, Terry, "Advanced Solar Cell and Coverglass Analysis", First LDEF Post-Retrieval Symposium Proceedings, NASA CP-3134, 1991.

Experiment Status:

The first phase of the optical studies has been completed. The full results of the transmission, reflectance and absorptance are being analyzed and will be presented in a publication within a few months. Tape recorder data is being analyzed and selected cell strings are being evaluated for their electrical properties.

Hardware Archive:

Data Upgrade Date: 1/28/92

Experiment Number: M0003-6

Experiment Title: Laser Communications Components

Tray Location: D3 Trailing Edge (171.9 degrees off RAM incidence angle), D4 (158.1 degrees off RAM incidence angle), D8 (38.1 degrees off RAM incidence angle), D9 Leading Edge (8.1 degrees off RAM)

Experiment Objective:

AO Fluence (atoms/cm2): D3 = 1.33E +03; D4 = 9.34E +04; D8=6.93E + 21; D9 = 8.71E +21 [Ref 2]

Radiation Flux:

Temperatures (C):

Experiment Tray Sun Hours: D3 = 11,100; D4 = 10,500; D8 =9,400; D9=11,200

M/D Impact Density:

Original Principal Investigators:

I.Otero, S. Rockholm, and R. Linford
Air Force Space Division and the McDonnell Douglas Astronautics Co.

Present Principal Investigators:

James Holsen
McDonnell Douglas Astronautics Co.
Dept. E465, Bldg. 287/3/309H
P.O. Box 516
St. Louis, MO 663266
(314)234-5510
[Ref 5]

Optical Materials Flown on LDEF:

Measurements Performed on Samples:

Results Summary:

Conclusions:

System Analysis and Future Design Considerations:

Published Experiment Reports:

PI's Database:

References:

1. Clark, Lenwood G. et.al., "The Long Duration Exposure Facility: Mission 1 Experiments", NASA SP-473, NASA Langley Research Center, 1984.
2. Bourassa, Roger, J. and J.R. Gillis, "Data Summary: Atomic oxygen Flux and Fluence Calculation for LOng Duration Exposure Facility (LDEF)", LDEF MSIG, Boeing Defense and Space Group, NASA Contract NAS1-1824, January 18, 1991.
3.Bourrassa, Roger J. and J.R. Gillis, "Solar Exposure of Long Duration ExposureFacility Experiment Trays", LDEF MSIG, Boeing Defense and Space Group, June 26, 1991, NASA Contract 1-1824-Task 12.
5.FAX from Michael Meshishnek showing list of LDEF SSD 802 investigators as of 09/11/91.

Experiment Status:

Hardware Archive:

Data Upgrade Date: 1/28/92

Experiment Number: M0003-7

Experiment Title: Space Environmental Effects on Coated Optics

Tray Location: D8 (38.1 degrees off RAM incidence angle), D4 (158.1 degrees off RAM incidence angle), D3 Trailing Edge (171.9 degrees off RAM incidence angle), D9 Leading Edge (8.1 degrees off RAM)

Experiment Objective:

To validate laboratory simulation results of natural space radiation on high reflectance mirrors and an output window, and to further determine the added effects of atomic oxygen, thermal cycling, meteroids and debris, and spacecraft contamination on optical performance. [Ref 1]

AO Fluence (atoms/cm2): D8 = 6.93E + 21, D4 = 9.34E + 04, D3 = 1.33E +03, D9 = 8.71E + 21 [Ref 2]

Radiation Flux:

Temperatures (C):

Experiment Tray Sun Hours: D8=9400; D4=10,500; D3=11,100; D9=11,200 [3]

M/D Impact Density:

Original Principal Investigators:

Terry M. Donovan
Naval Weapons Center
China Lake, CA 93555

Present Principal Investigators:

Terry M. Donovan, J.M.Bennet, R.Z. Dalbey and D.K.Burge
Thin Film Physics Section Code 33818
Naval Weapons Center
China Lake, CA 93555
Tel. (619)939-1401 or (619) 939-1424
FAX (619)939-1409

Optical Materials Flown on LDEF:

SAMPLE #	DESIGN	POSITION	EXPOSURE (months)
1	$(Si/Al_2O_3)3/Ag/Si$	D8	3
2	$(Si/Al_2O_3)2/Ag/Mo$	D4	3
3	$(ZnS/Al_2O_3)4/Ag/Mo$	D8	9
4	$(ZnS/ThF_4)Ag/Mo$	D8	6
5	$(ZnS/ThF_4)5Ag/Mo$	D4	9
6	$(Al_2O_3)/CaF_2$	D3	70

[Ref 1]

Measurements Performed on Samples:

Spectral reflectance
Absorption (calormetric)
Total integrated scatter calculations
Solar UV and charged particle simulations
Microscopical evaluation
OTHER RELATED TESTS:
Environmental durability tests (adhesion, humidity, thermal cycling, abrasion resistence and absorption)
Talystep surface profiler
Contamination evaluation
Scanning electron microscopy (SEM)
Auger profiling
X-ray photoemission spectroscopy [Ref 1]

Results Summary:

MIRROR RESULTS

1. A slight decrease in post-flight reflectance of silicon/aluminum oxide coated mirror compared with a laboratory control was noted. However, the reflectance degradation was on the same order as the reflectance loss due to aging effects on the control samples. The reflectance loss of the test sample at longer wavelengths is somewhat greater and possibly relates to absorption caused by surface oxidation.

2. Post-flight reflectance decreased significantly (0.7%) on the zinc-aluminum oxide coating compared with a laboratory control at the design wavelength. Also significant is an apparent shift of the high reflectance band to shorter wavelengths, and may be the result of a reduction in the optical thickness of the outer coating layer(s).
3. A sputter profile of the zinc sulfide/thorium fluoride coating showed an apparent reduction (about 50%) in the thickness of the outer zinc sulfide layer. The sputter profile also indicated the presence of a copper contamination layer, possibly coming from nearby copper mirrors in the vaccum cassette. This feature appears to be related to a second phenomena, dendritic formation. Further, an apparent shift of the spectral curve to shorter wavelengths was documented. [Ref 1]

CALCIUM FLUORIDE WINDOW

1. Post-flight examination of the calcium fluoride window showed very little damage. An FTIR transmission plot showed little or no change from the pre-flight condition. [Ref 1]

IMPACT CRATERS

1. All samples were examined for the presence of impact craters. No features that could be associated with the space environment could be found on either sample #1 or 2. Impact sites were found on samples #3-5. The character of the impact sites differed throughout the samples: the multilayer structure of the coating design is revealed in some sites, and not in others; some sites showed evidense of melting others didn't; some samples showed evidence of impact splatter around the site while others didn't. [Ref1]

Conclusions:

The high reflectance silicon/aluminum oxide coated mirror exposed for three months on the leading edge of LDEF performed as expected with minimal reduction in reflectance at longer wavelengths, i.e., 3-4 um. No impact sites were observed on either the leading edge or trailing edge on samples of this design.

Both zinc sulfide-based coating designs, samples #3-5, showed significant reductions in reflectance at the design wavelength, apparent large spectral shifts of the reflectance maxima, and dendrite formation. The dendrite formation was related to a thin copper contamination layer which was found only on samples in the vacuum cassette on the leading edge. Concentration gradients of copper between dendrite and dendrite-free regions provided excellent contrast in the SEM. No oxidation was found in the contaminated area but was found as expected in contamination free regions. A combination of thermal cycling and irradiation effects probably provided energy for the dendrite process.

Small impact sites were found on both the leading and trailing edge zinc sulfide samples . Finally, the aluminum oxide coated calcium fluoride window, sample #6, remained essentially unchanged after 70 months exposure on the trailing edge. [Ref 1]

System Analysis and Future Design Considerations:

Published Experiment Reports:

1." Natural and Induced Space Radiation Effects on Optical Coatings and Materials", Final Report on Contracts N00123-78-C-0989 and N60530-79-C-0263 to the Naval Weapons Center by L.B.Fogdall, et.al. of the Boeing Radiation Effects Laboratory, April 1981.

PI's Database:

None available .

References:

1. Donovan, T.M., J.M. Bennett, R.Z.Dalbey and D.K.Burge, SPACE ENVIRONMENTAL EFFECTS ON COATED OPTICS, First long Duration Exposure Facility Post-Retrieveal Symposium, Kissimee, Florida, June 2-8, 1991, NASA CP-3134, 1991.
2. Bourassa, Roger, J. and J.R. Gillis, "Data Summary: Atomic Oxygen Flux and Fluence Calculation for Long Duration Exposure Facility (LDEF)", LDEF MSIG, Boeing Defense and Space Group, NASA Contract NAS1-1824, Jan. 18, 1991.
3. Bourassa, Roger, J. and J.R. Gillis, "Solar Exposure of Long Duration Exposure Facility Experiment Trays", LDEF MSIG, Boeing Defense and Space Group, June 26, 1991, NASA Contract 1-1824-Task 12.

Experiment Status:

Hardware Archive:

Data Upgrade Date: 1/28/92

Experiment Title: LDEF M0003-8 Fiber Optics Experiment

Tray Location: D9 Leading Edge (8.1 degrees off RAM incidence angle)

Experiment Objective:

To gather data on the effects of the launch, flight and recovery operations on fiber optics components. Primarily to investigate the stability of fiber optic multi contact connectors. In addition, since this was an active experiment, another objective was to monitor the effects of space exposure on the source and detectors used. [Reference 1]

AO Fluence (atoms/cm2): 8.71E + 21 [Reference 2]

Radiation Flux:

Temperatures (C):

Experiment Tray Sun Hours: 11,200 [Reference 3]

M/D Impact Density:

Original Principal Investigators:

Owen Mulkey and Leo Buldharpt
Boeing Aerospace Company
P.O. Box 3999
Seattle, WA 98124
[Reference 4]

Present Principal Investigators:

Gary Pippin
Boeing Defense and Space Group
P.O. Box 3999 M/S 82-32
Seattle, WA 98124
Tel. (206)773-2846
FAX (206)773-4946

Optical Materials Flown on LDEF:

1. Hughes 20 contact C-21 series connector (multi contact connector) which accomodated size #16 fiber optic termini.
2. Spectronix (now Honeywell) SPX 2231-012 LED operating at 905 nm wavelength, coupled to a one to two power splitter built into a modified Hughes size contact which mated to a SMA source mount.
3. The optical fiber used in the reference path (about 18") and the test connector path (about 80") was a Gallite 3000, considered a low loss fiber at the time (1978) made by Gailleo Electro Optics Corporation with the following characteristics:

attentuation	80 dB/km @ 500-900 nm
NA	0.48
core diameter	88 um
cladding dia	110 um
core index of refraction	1.61

The fiber was unjacketed and the fiber length in the connector path was approximately 2 meters (80"). The fiber attentuation was about 0.16 dB, which was inconsequential for the purpose of the experiment.

4.The detectors were Vactec (now EG&G) VTP 1013's which were relatively large area silicon detectors and were operated at 2.125 volts reverse bias (half the supply voltage).

[Reference 1]

Measurements Performed on Samples:

Pre-flight data (voltage, current, resistence)
Flight data (board temperature, bursts, voltage)
Post-flight (temperature, voltage, mechanical, visual, LED spectral output)
No significant optical performance measurements were made on the optical fibers because of the shortness of the fiber length and because there was no preflight data available for comparison.

[Reference 1]

Results Summary:

PREFLIGHT DATA
V analog 1.67 volts DC
V reference diode 2.90 volts DC

Supply voltage 4.26 volts DC
Supply current 28 mA
LED forward voltage 1.28 volts DC
Thermister resistence 10.3 K ohms

The 1.67 VDC analog voltage corresponded to approximately equal values on the unknown and reference channels. For zero volts at the unknown, the V analog was equal to 0.91 VDC: for V analog equal to twice the reference, the output was equal to 2.04 VDC. The total signal range was 1.13 volts.

The flight test tapes and digitized tape data provided a plot of max/min readings of the 32 readings per burst for the 111 recording bursts for V analog and the the board's temperature from the first 410 days of the mission. A superposition of the analog signal plot on the temperature plot, shows a strong correlation between the two.

The plots of V analog and temperature versus time for each burst indicate that Vanalog is inversely related to the board temperature but the resolution is quite poor due to quantizing effects of the experiments A/D to D/A conversion and the additional A/D conversion of the tape system data. In examining the over 3000 readings of V analog supplied on the data disk, only 15 different voltage readings occured, varying from 1.678080 to 1.705408. These were in steps of 1.952 mV and were obviously the quantized voltages of the A/D converter to a 1 microvolt resolution. These 15 steps then represented the change in the steps of the output D/A Converter (DAC) of the experiment which were in 4.4 mV steps. No accuracy was lost in the conversion process, but the data looked very irregular when viewed in detail.

This data indicates that the total swing of the Vanalog voltage during the recorded portion of the flight was from 1.68 to 1.70 volts. When this is related to a change in dB it comes out to be from +0.05 dB to + 0.20 dB with respect to the preflight reading of 1.67 in 1978.

Post flight tests were run on the board to determine the relationships between temperature, time and various board voltages, to better characterize the circuit. This was done after all mechanical and visual examinations were complete. The only change in the data is that of the supply current which appears to have dropped from 28 mA to 21.26 mA. A check of the original pre-flight data indicates that the current was actually measured at 5.0V instead of 4.26V. A measurement of the supply current at 5.0V gave a post flight current of 2711 mA which is reasonable.

Temperature data was plotted to show the effect of temperature on the system's performance. V analog shows a very slight variation with temperature because the tracking of V unknown and V reference compensate the circuit. V unknown along with the V reference voltage show an increase with a decrease in temperature and vice versa. Vcc/2 remains constant at 2.140 volts throughout test. V diode shows a -5mV/C slope with temperature which is consistent with the vendors data sheet. V thermister shows the exact voltage predicted by the manufacturers data sheet, and so inicates that the values of temperature recorded in flight and on this post flight test are correct.

Post-flight visual exam of the board and components revealed no changes, except for a slight dulling of the black paint on the box where it was not covered by the lid. No evidence of fiber pistoning, which is the failure of the fiber and terminus adhesive bond and subsequent protrusion or intrusion of the fiber was noted in any of the thirteen termini in the experiment. Post-flight mechanical examination revealed about 0.02dB change and is considered normal and probably better than expected. The spectral output of the LED was tested and had a peak output of 905 nm with a broad peak. This is to be expected of an LED of this type and vintage.

[All paragraphs from Ref.1]

Conclusions:

The experiment suffered little or no degradation either prior to, during or after flight. Variations in output power as reflected by the V analog voltages were very slight, showed a small temperature dependence, which was probably due to slight mechanical movements in the multi contact connector with temperature. Total variation since 1978 was about a 0.2dB increase during the flight phase. The unit tested the same in November 1990 as it did in December of 1978, a span of nearly 12 years. The experiment operated in a relatively benign environment and was designed to perform reliably, which it did. [Reference 1]

System Analysis and Future Design Considerations:

None available at this time.

Published Experiment Reports:

M.J. Meshishnek, S.R. Gyetvay and C.H. Jaggers, "Long Duration Exposure Facility Experiment M0003 Deintegration Findings and Impacts, First LDEF Post Retrieval Symposium Proceedings, NASA CP-3134.

PI's Database:

References:

1. Mulkey, Owen, "Final Report on the LDEF M0003-8 Fiber Optics Experiment", LDEF Post Retrieval Symposium Proceedings, NASA CP-3134, 1991.
2.Bourassa, Roger J. and J.R.Gillis, "Data Summary: Atomic Oxygen Flux and Fluence Calculation for Long Duration Exposure Facility (LDEF)", LDEF MSIG, Boeing Defense and Space Group, NASA Contract NAS1-1824, Jan. 18, 1991.
3.Bourassa, Roger J. and J.R.Gillis, "Solar Exposure of Long Duration Exposure Facility Experiment Trays", LDEF MSIG, Boeing Defense and Space Group, June 26, 1991, NASA Contract 1-1824-Task 12.
4.Clark, Lenwood, et al. THE LONG DURATION EXPOSURE FACILITY (LDEF), NASA SP-473, 1984.

Experiment Status:

Experiment is complete.

Hardware Archive:

Data Upgrade Date: 1/28/92

Experiment Number: M0003-11

Experiment Title: Contamination Monitoring

Tray Location: D3 Trailing Edge (171.9 degrees off RAM incidence angle), D4 (158.1 degrees off RAM incidence angle), D8 (38.1 degrees off RAM incidence angle), D9 Leading Edge (8.1 degrees off RAM) Ref 1

Experiment Objective:

AO Fluence (atoms/cm2): D3 = 1.33E +03; D4 = 9.34E +04; D8=6.93E + 21; D9 = 8.71E +21 [Ref 2]

Radiation Flux:

Temperatures (C):

Experiment Tray Sun Hours: D3 = 11,100; D4 = 10,500; D8 =9,400; D9=11,200 [Ref3]

M/D Impact Density:

Original Principal Investigators:

E. Borson
The Aerospace Corporation

Present Principal Investigators:

Eugene Borson
The Aerospace Corporation
P.O. Box 92957 M2/250
Los Angelew, CA 90009
(213)336-6943

Optical Materials Flown on LDEF:

Measurements Performed on Samples:

Results Summary:

Conclusions:

System Analysis and Future Design Considerations:

Published Experiment Reports:

PI's Database:

References:

1. Bourassa, Roger, Viewfoil showing incidence angles for LDEF tray and longeron locations.
2. Bourassa, Roger, J. and J.R. Gillis, "Data Summary: Atomic oxygen Flux and Fluence Calculation for LOng Duration Exposure Facility (LDEF)", LDEF MSIG, Boeing Defense and Space Group, NASA Contract NAS1-1824, January 18, 1991.
3.Bourrassa, Roger J. and J.R. Gillis, "Solar Exposure of Long Duration ExposureFacility Experiment Trays", LDEF MSIG, Boeing Defense and Space Group, June 26, 1991, NASA Contract 1-1824-Task 12.

Experiment Status:

Hardware Archive:

Data Upgrade Date: 1/28/92

Experiment Number: M0003-14

Experiment Title: QCM Monitor

Tray Location:

Experiment Objective:

AO Fluence (atoms/cm2):

Radiation Flux:

Temperatures (C):

Experiment Tray Sun Hours:

M/D Impact Density:

Original Principal Investigators:

D.Wallace
Berkeley Industries

Present Principal Investigators:

Donald A. Wallace
QCM Research
2825 Laguna Canyon Road
P.O. Box 277
Laaguna Beach, CA 92652
(714)494-9401

Optical Materials Flown on LDEF:

Measurements Performed on Samples:

Results Summary:

Conclusions:

System Analysis and Future Design Considerations:

Published Experiment Reports:

PI's Database:

References:

Experiment Status:

Hardware Archive:

Data Upgrade Date: 1/24/92

Experiment Title: Space Environment Effects on Operating Fiberoptic Systems

Tray Location: F8 (38.1 degrees off RAM incidence angle)

Experiment Objective:

To assess the performance survivability of hardened fiberoptic data link design for application in future spacecraft systems and to collect, analyze, and document the effects of space environmental conditions on link performance. [Reference 1]

AO Fluence (atoms/cm2): 6.93E + 21 [Reference 2]

Radiation Flux: Total dose varying from 238 rad(Si), to 25 Krad(Si) [Reference 3]

Temperatures (C): External tray temperatures varied from +57 C to -29 C [Reference 3]

Experiment Tray Sun Hours: 9,400 [Reference 4]

M/D Impact Density: 29 large craters (>300um), and 264 small craters (>100um) [Reference 3]

Original Principal Investigators:

Edward W. Taylor
Air Force Weapons Laboratory
Kirtland Air Force Base
Albuquerque, NM

Present Principal Investigators:

Edward W. Taylor
Air Force Systems Command Phillips Laboratory
Directorate of Space and Missles Technologies
Optoelectronics section, PL/SQT, Code NT
Kirtland Air Force Base, NM. 87117-6008
Tel. (505) 846-4746 FAX (505) 844-3888

Optical Materials Flown on LDEF:

ACTIVE EXPERIMENTS: Four active links were exposed to space. One of these consisted of 45 m of cabled glass fiber incorporating a hermetically sealed emitter and detector operating at a wavelength of 1.3 um. The remaining active links consisted of three cabled plastic-coated silica fiber links using LED's and PIN photodiodes operating at a wavelength of 830 nm. Two of these links were 20 m long and the remaining link was 48 m long. Optical waveguide, connectors, and other experimental equipment consisted of components selected according to results of Air Force studies. A 1-m optical data link was used for recording the relative temperature of the tray inner volume.

PASSIVE EXPERIMENTS: Three 10-m links were located within the tray volume. The links had been preirradiated and were evaluated upon LDEF retrieval for increased radiation damage. These links served primarily as comparison links to the active-link experiments. The components experiment contained preirradiated and nonirradiated LED's and photodiodes rigidly mounted within a section of the tray volume. [Reference 1]

Table 1 in Reference 3 describes the material and technical characteristics of space-exposed optical fibers prior to launch.

Measurements Performed on Samples:

IN SITU ANALYSIS (AT KSC)- visual, photodocumentation, color change evaluation, microscopy, IR detection, fiber link activation, energy emission from impactor sites

IN ORBIT OPICAL DATA TRANSMISSION- signal strength (and hence signal-to-noise ratio), burst error runs (examination of bit stream for errors)

IMPACT DENSITY STUDIES- microscopy, photomicrography, transmitted laser light in failed fiber, optical time-domain reflectometer (OTDR)

NON-OPTICAL MEASUREMENTS- in orbit temperature cycling, in-orbit radiation dosimeter measurements. [Reference 3]

Results Summary:

Early photographs provided by the Columbia crew, indicated numerous micrometeroid and debris (M/D) impacts experienced on the LDEF surface. In situ visual analysis performed at KSC showed subtle changes to the optical fiber cabling including color changes, and numerous micrometeroroid and/ or debris impacts. [Ref. 3] It was also observed that some of the tightly wound fibers did begin to sag, and a brown discoloration was present (contamination). [Ref 2]. All four of the M/D impacted cabled fiber links were activated within four hours of deintegration and three links were found to be fully operational. The fourth data link (Link #4) could not be operated at KSC. [Reference 3]. The data indicate that Link #3 and #4 experienced approximately 1.0dB and

0.2dB deviation, respectively in signal-to- noise ratio (SNR) during the first year in orbit. The reduction of SNR data in links 1 and 2 is still under analysis. [Reference 3]. The space exposed optical fibers experienced a radiation dose varying from 238 rad (Si), to 25 Krad (Si), depending on the shielding provided by the fiber cabling materials and hold down clamps. The fiber doses resulted primarily from geo-magnetically trapped electrons, since the galactic cosmic ray contribution was estimated to constitute approximately 1% to 3% of the trapped proton dose at typical shieldings (greater than 1 g/cm2). Therefore, for a shielding of less than 1.0 g/cm2, trapped electrons dominate the surface absorbed dose. While the fiber links were calculated to have received a substantial dose over the 2114 days in orbit, no direct evidence of permanent induced radiation damage has been observed to date. [Reference 3]. The external tray temperatures--extrapolated from the internal measurements and calibrations--ranged from approximately +57 C to -29C. Effects due to temperature dependence are currently under investigation. [Ref. 3]

Conclusions:

Analyses to date confirm that the four space exposed fiber optic links performed within their expected performance profile under temperature cycling extremes and direct space exposure to galactic and trapped radiations, atomic oxygen, and ultraviolet radiation. Activation of the experiment at KSC some 2185 days following its April 1984 deployment into low-earth orbit resulted in excellent performance by three of the four space-exposed links. The links continue to operate, thus providing a benchmark and invaluable database for on-going and future space photonics programs and for fiber optics space survivability and reliability studies. Despite numerous micrometeroid and debris impacts experienced by the cabled fibers and experiment surfaces, only a single optical fiber was observed to be severed over the 2115 days in orbit. This event occurred after the data acquisition portion of the mission was completed. Thus, the experiment operation and demonstration of technology concept were both fully successful.

Perhaps the most profound conclusion that may be drawn from the preliminary data presented, is that this experiment demonstrated that the1978-1980 era fiber optic technology can and did operate excellently in space for a prolonged time period. One need only apply the much improved technology and advances in fiber optic or photonic technologies during the past decade to fully realize fiber optic applications in space. This experiment demonstrated for the first time, under severe and deliberate space exposure conditions, that fiber optic systems can survive in a prolonged space orbit. [Ref 3.]

System Analysis and Future Design Considerations:

Published Experiment Reports:

D.S. McKnight, R.E. Dueber and E.W.Taylor, "Space Debris and Micrometeorite Events Experienced By WL EXP 701 in Prolonged Low-Earth Orbit" , 8 June 1990, accepted for publication by the JOURNAL OF GEOPHYSICAL RESEARCH SPACE PHYSICS, Sept. 1990.

A.R. Johnston, L.A.Bergman, E.W.Taylor, FIBER OPTIC EXPERIMENT FOR THE SHUTTLE LONG DURATION EXPOSURE FACILITY, SPIE Vol. 296, August 1982, pp. 40-50.

PI's Database:

References:

1. E.W. Taylor, SPACE EFFECTS ON FIBER OPTICS SYSTEMS, NASA SP-473, The Long Duration Exposure Facility, Mission 1, Experiments, edited by L.G. Clark et. al., Washington, D.C., 1984, pp.182-184,
2. E.W. Taylor oral technical presentation at the LDEF First Post-Retrieval Conference, June 4, 1991.
3. E.W.Taylor, et.al., PRELIMINARY ANALYSES OF WL EXPERIMENT #701, SPACE ENVIRONMENT EFFECTS ON OPERATING FIBER OPTIC SYSTEMS, The First LDEF Post-Retrieval Symposium, June 2-8, Kissimee, Florida, NASA CP #3134, 1991.

Experiment Status:

Temperature dependence of fiber optic links currently under investigation.

Hardware Archive:

Data Upgrade Date: 1/24/92

Experiment Title: Space Environmental Effects

Tray Location: C3 Trailing Edge (171.9 degrees off RAM)

Experiment Objective:

To examine the effects of long-term exposure of the near-Earth space environment on advanced electro-optial and radiation sensor components, and to observe the effect of long-duration space flight on the germination rate of selected terrestrial plant seeds. Only the electro-optical experiment will be discussed here. [Ref. 1]

AO Fluence (atoms/cm2): 1.33E + 03 [Ref 2]

Radiation Flux:

Temperatures (C):

Experiment Tray Sun Hours: 11,100 [Ref 3]

M/D Impact Density:

Original Principal Investigators:

Joseph A. Angelo, Jr. and Richard G. Madonna, Air Force Technical Applications Center, Patrick Air Force Base, Florida.
Lynn P. Altadonna, Perkin-Elmer, Danbury, Connecticut.
Michael D'Agostino and Joseph Chang, Grumman Aerospace Corp., Bethpage, New York.
Robert R. Alfano and Van L. Caplan, The City College, New York, New York.

Present Principal Investigators:

Mike Steskal
U.S. Air Force
HQ AFTAC/DOSOP
Patrick Air Force Base, Florida 32925
Tel. (407) 494-4178
FAX (407)494-2560
(See additional analysts participating in this experiment under the Optical Measurements field name.)

Optical Materials Flown on LDEF:

1. Nd+:Glass laser rod (1)
2. Buna-N Rubber O-Rings (3) (-65F to 250F degrees)
3. Mirror (1) and Buna-N Rubber O-rings laser energy 100R at 1.06 um
4. Perkin-Elmer Beryllium Mirror (1) and BUNA-N Rubber O-Rings
5. Mirror (1) and Buna-N Rubber O-Rings CVI output cavity mirror 55R at 1.06 um
6. Fused silica DY mirror (1) and Buna-N Rubber O-Rings
7. Fiber optic cable (1)
8. Meth-polymethacrylate polymer film (1)
9. Polyethylene terephthalate polymer film (1)
10. Polystyrene polymer film (1)
11. Polypyronelletimile polymer film (1)
12. CdSe semiconductor (1), RIIIA, high resistance, sulfur contaminated, C axis 11-surface
13. CdSe semiconductor (1), MIV A, low resistence, sulfur contaminated, C-axis 11-surface
14. p-GaAs semiconductor (1), 6.42 E + 18 Zn /cm3 sample #9-16, u = 103, p = 0.0106
15. n-GaAs semiconductor (1), 1.4 E + 16/cm3, sample #249
16. GaAs #1 semiconductor (1), compensated, epitaxial, defective density: 10E + 5, high resistance, p = 4E +7 Ohm-cm
17. n-GaAs semiconductor (1), 2-4E + 18 Si/cm3, (100) +/- 5 degrees, p = .001, density < 100/cm2
18. GaAs semiconductor (1), Si doped (100), #7189P, EPD = 5200 /cm2, p = .0013 Ohm-cm, u = 1662 cm2/volt-sec, N = 2.9E + 118 /cm3
19. GaAs semiconductor (1), Si doped (100), #7476P, EPD = 1500 /cm2, p = .0015 Ohm-cm, u = 1995 cm2/volt-sec, N = 2.1E + 118 /cm3
20. GaAs semiconductor (1), Si doped (100), #4018P, EPD = 4900/cm2, p = .0028 ohm-cm, u = 2411 cm2/volt-sec, N = .92E + 18/cm3
21. GaAs semiconductor (1), Si doped (100), #6744P, EPD = 5300/cm2, p = .0037 ohm-cm, u = 2534 cm2/volt-sec, N = .66E + 18/cm3

22-26. 6061T6 aluminum alloy and seeds 27. Lithium fluoride (LiF) radiation dosimeters (Ref. 4)

Measurements Performed on Samples:

Items 1-6, 8-21, 23-26 and the exposure cannister were analyzed by the Air Force Materials Lab, Wright Patterson AFB, OH , Lt. Michele Jones (513)255-8097. Item 7 was analyzed by Mr. Ed Taylor of the Air Force Weapons Lab, Kirtland Air Force Base, NM (505)844-7099. Item 22 was analyzed by EPCOT Center, THE LAND, Lake Buena Vista, FL , Mr. Andrew Schugar (407)560-7256. Item 27 was analyzed by Grumman Beathpage, NY, Dr. Chang (516)575-0605. [Ref. 4]

Results Summary:

Conclusions:

System Analysis and Future Design Considerations:

Published Experiment Reports:

PI's Database:

References:

1. Clark, Lenwood, et.al., THE LONG DURATION EXPOSURE FACILITY (LDEF), NASA SP-473, NASA Langley Research Center, 1984.
2. Bourassa, Roger, J. and J.R. Gillis, "Data Summary: Atomic Oxygen Flux and Fluence Calculation for Long Duration Exposure Facility (LDEF)", LDEF MSIG, Boeing Defense and Space Group, NASA Contract NAS1-1824, Jan. 18, 1991.
3. Bourassa, Roger, J. and J.R. Gillis, "Solar Exposure of Long Duration Exposure Facility Experiment Trays", LDEF MSIG, Boeing Defense and Space Group, June 26, 1991, NASA Contract 1-1824-Task 12.
4. FAX correspondence from Mike Steskal to H.Dursch, 27 July 1990.

Experiment Status:

Hardware Archive:

Data Upgrade Date: 1/24/92

Experiment Title: Advanced Photovoltaic Experiment (APEX): Preliminary Flight Results and Post-Flight Findings

Tray Location: E9 Leading Edge (8.1 degrees off RAM incidence angle)

Experiment Objective:

To provide information on the performance and endurance of advanced and conventional solar cells, to improve reference standards for photovoltaic measurements, and to measure the energy distribution in the extraterrestrial solar spectrum. [Ref 1]

AO Fluence (atoms/cm2): 8.71 + 21 [Ref 2]

Radiation Flux:

Temperatures (C):

Experiment Tray Sun Hours: 11,200 [Ref 3]

M/D Impact Density:

Original Principal Investigators:

Henry W. Brandhorst, Jr. and A.F. Forestieri
NASA Lewis Research Center
Cleveland, Ohio 44135

Present Principal Investigators:

David J. Brinker, John Hickey and David Scheiman
NASA Lewis Research Center
Cleveland, Ohio 44135
Tel. (216)433-2236
FAX (216)433-6106

The Eppley Laboratory, Inc.
Newport, RI 02840
Tel. (401)847-1020
FAX (401)847-1031

Optical Materials Flown on LDEF:

APEX SOLAR CELL TYPES
Silicon: BSR/BSF, violet, vertical junction, textured, 5.9 cm PEP, 2 mil thick
Gallium arsenide: LPE
Standards: Balloon, rocket, airplane, radiation damaged
Coverglass: fused silica, V- and U-grooved, ceria doped microsheet

ABSOLUTE CAVITY RADIOMETER
DIGITAL ANGLE SUN SENSOR
[Ref 4]

Measurements Performed on Samples:

prelight and post-flight performance of solar cells
preflight and post-flight analysis and calibration of cavity radiometer (sensitivity, reflectance, and overall condition)
preflight and post-flight analysis of digital sun angle sensor (resolution, sensitivity)
post-retrieval visual observations
(Ref 4)

Results Summary:

Post-flight analysis of the Advanced Photovoltaic Experiment indicates that it sucessfully completed its mission and returned 325 days of valid solar intensity and spectrum data. A number of physical changes are readily apparent, including micrometeroid and debris impact craters, loss of black paint from the surface of the experiment and a contaminating film similar in nature to that found over most of the LDEF. Detailed post-flight analysis and calibration of many of the sensors and components of APEX has been conducted. The cavity radiometer is unchanged with regards to sensitivity, reflectance, and overall condition. The Digital Angle Sensor has not changed in either resolution or sensitivity. The post-flight performance of the solar cells analyzed thus far has revealed no unexpected behavior. Cell illuminated performance has been remeasured using the laboratory solar simulators after removal from APEX.

More specifically, although the contaminating film was found over much of LDEF, and has coated many of the cells to varying degrees, no loss or changes in coverglasses or antireflection coatings was observed. Some discoloration of the RTV used to fasten cell wiring is seen. A number of cells have sustained cratering from micrometeroid and/or debris, the severity of the crater varying from a tiny chip in the coverglass to penetration of the coverglass, cell and aluminum substrate. Illuminated current-voltage characteristics varied depending on the severity of the damage. One example described a solar cell with a crack on the the cell and the coverglass.

There was loss in fill factor, but the short-circuit current and open circuit voltage are unchanged. Another example describes a solar cell with a large crater extending into the silicon cell through the coverglass, although neither the cell nor cover are cracked. Simulator data showed a 100 mV drop in open circuit voltage due to shunting of the cell pn junction at the sight of the crater. The 5% drop in current is due to area loss associated with the crater and a contaminating layer evident of the cell. [Ref4]

Conclusions:

System Analysis and Future Design Considerations:

Published Experiment Reports:

PI's Database:

References:

1. Clark, Lenwood, et.al., THE LONG DURATION EXPOSURE FACILITY (LDEF), NASA SP-473, NASA Langley Research Center, 1984, pg. 88.
2. Bourassa, Roger J. and J.R.Gillis, "Data Summary: Atomic Oxygen Flux and Fluence Calculation for Long Duration Exposure Facility (LDEF)", LDEF MSIG, Boeing Defense and Space Group, NASA Contract NAS1-1824, Jan. 18, 1991.
3. Bourassa, Roger J. and J.R. Gillis, "Solar Exposure of Long Duration Exposure Facility Experiment Trays", LDEF MSIG, Boeing Defense and Space Group, June 26, 1991, NASA Contract 1-1824-Task 12.
4. Brinker, David J., John R. Hickey and David A. Scheiman,"Advanced Photovoltaic Experiment, S0014: Preliminary Flight Results and Post-Flight Findings", First LDEF Post-Retrieval Symposium Proceedings, NASA CP-3134, 1991.

Experiment Status:

The APEX analysis is continuing with emphasis on the interpretation of flight data, post-flight inspection of the numerous solar cells, and investigation of materials science issues.

Hardware Archive:

Data Upgrade Date: 1/24/92

Experiment Title: Effects of Long Duration Exposure on Active Optical System Components

Tray Location: E5 (128.1 degrees off RAM incidence angle)

Experiment Objective:

To quantify the effects of long duration space exposure on the performance of lasers, radiation detectors, and selected optical components performance; and, to evaluate the results and implications of the measurements, and establish guidelines for selection of space electro-optical systems. Also see subexperiments S0050-1 and -2. [Ref 1]

AO Fluence (atoms/cm2): 3.72E + 12 [Ref 2]

Radiation Flux: <300 krads on uncovered;<500 rads on inverted flat pack;<300 rads on covered filter [Ref 3]

Temperatures (C): calculated maximum temperature of 66C +/- 10C [Ref 3]

Experiment Tray Sun Hours: 8,200 [Ref 4]

M/D Impact Density:

Original Principal Investigators:

M. Donald Blue, James J. Gallagher, R.G. Shackkelford
Georgia Institute of Technology
Engineering Experiment Station
Atlanta, Georgia 30332

Present Principal Investigators:

M. Donald Blue
Georgia Tech. Res. Institute
Georgia Inst. of Technology
Atlanta, GA 30332
Tel. (404)894-3646
FAX (404)894-5073

Note: See subexperiments S0050-1 and S0050-2 in this database for further investigators.

Optical Materials Flown on LDEF:

PASSIVE COMPONENTS	ACTIVE COMPONENTS	DETECTORS
Black Paint Samples	ADP Modulators	Silicon PIN
Neutral Density Filters	Channeltron Array	Silicon PV
Narrow-Band Filters	GaAlAs Laser Diodes	Silicon Gamma-Ray
Laser Mirrors	GaAsP LED	InGaAsP PV
Hot-Mirror Filter	Nd:YAG Rods	InSb PV
Lyman-Alpha Filter	CO_2 Waveguide Laser	PbS
UV Filter 1600A	HeNe Laser	PbSe
LiF Window	Holographic Crystals	HgCdTe PV
$AlMgF_2$ Mirror	Laser Flash Lamps	HgCdTe PC
Optical Glasses		PdSi Arrays
MgF_2 Window		Pyroelectrics
Al_2O_3 Window		UV PMT
35-mm UV Film		UV Silicon
Various Optical Glasses		
Black Polyethylene		

[Reference 3]

Measurements Performed on Samples:

Infrared detectors: resistance and capacitance
Infrared modulators: transmission, half-wave voltage, frequency roll-off
Lasers: output radiation
LEDs: voltage,current and light emission
Optical black paints: reflectivity
Optical interference films: interference minima and/or maxima, bandpass
Neutral density filters: transmission
Mirrors: reflectivity [Reference 5]

Results Summary:

GENERAL OBSERVATIONS: The tray came to GTRI in pristine condition (except for the stain described below) and without fingerprints. All components survived the trip without mechanical damage. Micrometeroid impacts were seen on a wide variety of components. The green epoxy-fiberglass mounting strips were changed to a walnut brown where they were exposed to the space environment. Where covered, the original green color was maintained. The tray was covered with a light coating of nicotine stain which is believed by NASA to be the result of Z306 thermal-control black paint outgassing in the space environemnt and becoming fixed in place by the effects of solar UV. The weight density of this material on the GTRI tray has been estimated by Dr. Gale Harvey of NASA LaRC to be 0.2 mgm/cm2. [Reference 5]

COMPONENT CHARACTERISTICS:

Lasers- No laser action could be obtained from the HeNe and CO_2 tubes, although they were in good physical condition, suggesting that the mixture of fill gas had changed during the period between initial and post-flight tests. The GaAlAs diode lasers indicated greater light output, believed to be due to the new experimental arrangement, rather than improved diode performance. The GaAsP LED characteristics were unchanged between initial and post-flight tests. YAG laser rods remain to be tested. [Reference 3]

Modulators- No measureable changes in optical transmission were found with the ADP light modulator. The half-wave voltage and roll-off frequency were unchanged within experimental errors. [Reference 3]

Detectors- HgCdTe detector indicates it performs better than previous measurements, again due to improved test set-up. Measurements of an InGaAsP photodiode indicate good performance. No space-related degradation effects were found. Several large-area silicon photodiodes and PIN diodes were remeasured. The original current-voltage and capacitance-voltage characteristics of these devices were reproduced. Active areas of these devices were directly exposed to the space environment, and show the effects of micrometeroroid impacts. Pyroelectric detectors showed no space-related degradation. [Reference 3]

Optical Filters- Narrow and broad band optical filters showed a small but significant reduction in transmission, and is believed to be related to degradation of the cement used in the filter construction. [Reference 3] Neutral density filters (inconel films) show increased transmission, likely due to erosion of the deposited layer. Organic deposits are seen on the films. The deposits are greater in the center along the rim where the samples were covered. [Reference 5]

Paints- The post recovery data indicate reduced reflectivity and, more importantly, low reflectivity at extreme infrared wavelengths. Degradation of pigment and binder is the suspected cause of these changes. [Reference 3]

Conclusions:

None available at this time.

System Analysis and Future Design Considerations:

1. Gas lasers for long-term space applications must not be sealed systems, due to changes expected from gas diffusion through the glass envelope. [Reference 3]
2. The space environment as experienced by the LDEF does not degrade active components such as detectors, laser diodes, and modulators at ambient temperature. [Reference 3]
3. Black paints for sensor baffle coatings will not only survive in the space environment, but will provide enhanced performance with aging.[Reference 3]
4. Narrow band and broad band optical filters exposed directly to the space environment may have a small but significant reduction in transmission . This is believed to be related to degradation of the cement used in their construction. [Reference 3]
5. In general, where the specimens are rigid, sealed or passivated, and unaffected by UV, expect that space exposure will not cause degradation to their electro-optic characteristics. If the specimens are deposited thin-film based, or contain organics, expect degradation. (Reference 5]

Published Experiment Reports:

See subexperiments S0050-1 and S0050-2.

PI's Database:

None available.

References:

1. Clark, Lenwood, et.al., THE LONG DURATION EXPOSURE FACILITY (LDEF), NASA SP-473, NASA Langley Research Center, 1984.
2. Bourassa, Roger, J. and J.R. Gillis, "Data Summary: Atomic Oxygen Flux and Fluence Calculation for Long Duration Exposure Facility (LDEF)", LDEF MSIG, Boeing Defense and Space Group, NASA Contract NAS1-1824,

Jan. 18, 1991.
3. Blue, M.D., "LDEF Active Optical System Components Experiment", Proceedings from the First Long Duration Exposure Facility Post-Retrieval Symposium, June 2-8, 1991 Kissimee, Florida. To be published in the NASA Conference Publication No.3134, 1991.
4.Bourassa, Roger, J. and J.R. Gillis,"Solar Exposure of Long Duration Exposure Facility Experiment Trays", LDEF MSIG, Boeing Defense and Space Group, June 26, 1991, NASA Contract 1-1824-Task 12..
5. Blue, M.D. verbal and written inputs to the Systems SIG Optical Survey.

Experiment Status:

Hardware Archive:

Data Upgrade Date: 1/24/92

Experiment Number: S0050-1

Experiment Title: Effects of Long Duration Exposure on Optical Systems Components

Tray Location: E5 (128.1 degrees off RAM incidence angle)

Experiment Objective:

To determine quantitatively the effects of long duration space exposure on fifteen optical components selected as representative of components used in Earth-looking ultraviolet spectroscopy from low Earth-orbit. The spectrum of interest was 100 nm to 300 nm. This subexperiment describes the optical windows examined. [Ref 1]

AO Fluence (atoms/cm2): 3.72E + 12 [Ref 2]

Radiation Flux: <300 krads on uncovered; <500 rads on inverted flat pack; <300 rads on covered filters [Ref 3]

Temperatures (C): 41C Max [Ref 4]

Experiment Tray Sun Hours: 8,200 [Ref5]

M/D Impact Density:

Original Principal Investigators:

M. Donald Blue, James J. Gallagher, R.G. Shackkelford
Georgia Insitute of Technology
Engineering Experiment Station
Atlanta, Georgia

Present Principal Investigators:

Gale A. Harvey
NASA Langley Research Center
Hampton, VA 23665-5225
Tel. (804)864-6742
FAX (804)864-7790

Optical Materials Flown on LDEF:

OPTICAL WINDOWS
CaF_2
MgF_2
LiF
Al_2O_3 (synthetic sapphire)
SiO_2 (fused silica)
[Ref 1]

Measurements Performed on Samples:

Microscopical evaluation and photodocumentation
optical transmission
[Reference 1]

Results Summary:

WINDOW	3.4 ABSORPTION RESULTS	UV TRANSMISSION RESULTS
CaF_2	Organic film present on both sides of the window.	Transmission increasing from almost zero at 200 nm to more than 50% at 380 nm. Catastrophic loss in UV transmission.
MgF_2	Organic film present on front side of window.	Higher transmission of MgF_2 window compared to CaF_2 or LiF because the back film is missing on the MgF_2. Still catastrophic loss in UV transmission.
LiF	Organic films present on both sides of the window.	Similar transmission to CaF_2. Catastrophic loss in UV transmission.
Al_2O_3	Methyl absorption stronger here than on CaF2, MgF2, and LiF; also nonhydro-carbon organic contaminant on window.	Substrate does not transmit below 150 nm. Near UV not measured.
SiO_2	Absence of 3.4 um absorptions, suggests a substrate selectivity	Substrate does not transmit below 150 nm. Near UV not measured.

(film deposition dependent on substrate.
[Reference 1]

Conclusions:

Surface contamination is the only deterioration seen on Experiment S0050-1 optical windows in Tray E5 on LDEF. A faint brown stain is present on the front surface of all six windows. A brittle film is also present on the back surface of the three UV transmitting fluoride windows. The change in vacuum ultraviolet transmission of the fluroide windows is catastrophic. The absence of 3.4 u absorptions on the SiO_2 window indicates the film deposition were dependent on the substrates. [Ref 1]

System Analysis and Future Design Considerations:

Published Experiment Reports:

1.Harvey, G.A., Raper, J.L. and Messier, R.N., "Microcontamination of IR Spacecraft Optics," in Proceedings of Microcontamination Conference and Exposition, Anaheim, CA, pp. 237-259, October 1989.

2. Harvey, G.A. and Raper, J.L. "Halogen Occultation Experiment (HALOE)Optical Witness-Plate Program,"NASA TM 4081, February 1989.

PI's Database:

References:

1. Harvey, Gale , "Effects of Long Duration Exposure on Optical Systems Components", First Post-Retrieval LDEF Symposium Proceedings, NASA CP-3134, 1991.

2. Bourassa, Roger, J. and J.R. Gillis, "Data Summary: Atomic Oxygen Flux and Fluence Calculation for Long Duration Exposure Facility (LDEF)", LDEF MSIG, Boeing Defense and Space Group, NASA Contract NAS1-1824, Jan. 18, 1991.

3. Blue, M.D., "LDEF Active Optical System Components Experiment", Proceedings from the First Long Duration Exposure Facility Post-Retrieval Symposium, June 2-8, 1991 Kissimee, Florida, NASA CP-3134, 1991.

4. ?

5. Bourassa, Roger, J. and J.R. Gillis, "Solar Exposure of Long Duration Exposure Facility Experiment Trays", LDEF MSIG, Boeing Defense and Space Group, June 26, 1991, NASA Contract 1-1824-Task 12.

Experiment Status:

Hardware Archive:

Data Upgrade Date: 1/24/92

Experiment Title: Effects of Long Term Exposure on Optical Substrates and Coatings

Tray Location: E5 (128.1 degrees off RAM incidence angle)

Experiment Objective:

To determine the effects of long term space exposure on optical substrates and coatings. See additional experiment description under the S0050 record. [Ref 1]

AO Fluence (atoms/cm2): 3.72E + 12 [Ref 2]

Radiation Flux: <300 krads on uncovered; <500 rads on inverted flat pack; <300 rads on covered filter [Ref 3]

Temperatures (C): calculated maximum temperature of 66C +/- 10C [Ref 4]

Experiment Tray Sun Hours: 8,200 [Ref 5]

M/D Impact Density:

Original Principal Investigators:

M. Donald Blue, James J. Gallagher, R.G. Shackkelford
Georgia Institute of Technology
Engineering Experiment Station
Atlanta, Georgia 30332

Present Principal Investigators:

John Vallimont and Keith Havey
Eastman Kodak Company
Rochester, NY
Tel. (716)253-2402 or (716)253-2236
FAX (716)253-7277

Optical Materials Flown on LDEF:

Kodak included 12 substrate and coating samples on the LDEF structure. There were 3 fused silica and 3 Ultra Low Expansion (ULE) uncoated glass samples, 2 ULE samples with a high reflectance silver coating,and 2 fused silica samples coated with an antireflectance (AR) coating, and 2 fused silica samples with a solar rejection coating. The samples were 32 mm diameter by 1 mm thick. A set of duplicate control samples was also manufactured and stored in a controlled environment for comparison purposes. ULE glass is described as not tolerant of the radiation environment, and was expected to show some radiation darkening. [Reference 1]

Measurements Performed on Samples:

Microscopical evaluation and photodocumentation
Spectral transmission (preflight, post-flight and after cleaning)
Spectral reflectance (pre-flight, post-flight and after cleaning)
Contamination analysis (x-ray photoelectron spectroscopy (XPS)
[Reference 1]

Results Summary:

XPS analysis showed the substrates and coatings to be covered with a thin layer of polymer which contained silicon. For most of the samples the contaminant was silica-like in nature, but on the ULE(tm) substrate and the AR coating, the contaminant was visibly darker and appeared similar in structure to the silicon of the rubber gasket which was used to mount the optics. However, neither the relative atomic percentages or the relative sizes of the silicon and oxygen peaks from the XPS conclusively prove that the contaminant is a residue from the mounting rubber gasket. Other silicon sources must be considered as well.

A micrometeroid impact site was found on one of the samples. The impact crater measured .3 mm in diameter by .03 mm deep. Multiple fractures occured in the glass at the impact site.

No radiation darkening was evident on either the ULE (tm) or the fused silica glass.
[Reference 1]

After post-flight spectral measurements, the samples were cleaned using toluene, followed by a methanol rinse, and then measured again for spectral transmission and reflectance from .3 -1.2 um. This was repeated again (or again) with rubbing where necessary to clean the samples enough to return them to pre-flight measurements. All samples were cleaned effectively with this technique, except the AR coated samples. The contamination on the AR coatings can not be cleaned with the toluene and methanol solvents. In addition, measurements indicate a spectral shift. Additional analyses is underway at this time. [Reference 6]

Conclusions:

A preliminary evaluation of the flight samples for effects from the 5 year mission showed that a contaminant was deposited on the samples, a micrometeroid impact ocurred on one of the samples, and the radiation darkening

which was expected for the glass did not occur. After cleaning the contaminant, the optical performance of the coatings returned to the pre-flight measurements (except AR coatings). [Reference 1]

System Analysis and Future Design Considerations:

Not available at this time.

Published Experiment Reports:

None available at this time.

PI's Database:

None available at this time.

References:

1. Vallimont, John, "Effects of Long Term Exposure on Optical Substrates and Coatings", First LDEF Post Retrieval Symposium Proceedings, NASA CP-3134, 1991.
2. Bourassa, Roger J. and J.R. Gillis, "Data Summary: Atomic Oxygen Flux and Fluence Calculation for Long Duration ExposureFacility (LDEF)", LDEF MSIG, Boeing Defense and Space group, NASA Contract NAS1-1824, Jan. 18, 1991.
3. Blue, M.D. "LDEF Active Optical System Components Experiment", First LDEF Post Retrieval Symposium Proceedings, NASA CP-3134, 1991.
4. ?
5. Bourassa, Roger J. and J.R.Gillis, "Solar Exposure of Long Duration Exposure Facility experiment Trays", LDEF MSIG, Boeing Defense and Space Group, June 26, 1991, NASA Contract 1-1824-Task 12.
6. Telephone conversation with John Vallimont and Keith Havey, September 19, 1991.

Experiment Status:

Hardware Archive:

Data Upgrade Date: 1/24/92

Experiment Title: Thermal Control Surfaces Experiment (TCSE)

Tray Location: A9 Leading Edge (8.1 degrees off RAM incidence angle)

Experiment Objective:

Spectral reflectance measurements were used to determine the effects of near-Earth orbital and Shuttle-induced environments on spacecraft thermal surface samples. [Ref 1]

AO Fluence (atoms/cm2): 8.71E + 21 [Ref 2]

Radiation Flux: 3.0E + 5 rads [Ref 6]

Temperatures (C): 3.3E + 4 thermal cycles [Ref 6]

Experiment Tray Sun Hours: 11,200 [Ref 3]

M/D Impact Density:

Original Principal Investigators:

Donald R. Wilkes and Harry M. King
NASA George C. Marshall Space Flight Center
Huntsville, Alabama

Present Principal Investigators:

Donald R. Wilkes
AZ Technology
Building 600, Suite 93
3322 Memorial Pkwy.
Huntsville, AL 35801
Tel. (205)880-7481
FAX 205 880-7483

James Zwiener
NASA George C. Marshall Space Flight Center
Marshall Space Flight Center
Alabama 35812
(205)544-2528

Optical Materials Flown on LDEF:

Silver Teflon
Silver Teflon (diffuse)
S13G-LO (IITRI)
Z93 (IITRI)
YB71 (IITRI)
YB71(over Z93) (IITRI)
D111 Black (IITRI)
A276 (MSFC/EH)
A276/OI 650 (MSFC/EH)
A276/RTV 670 (MSFC/EH)
Z302 (MSFC/EH)
Z302/OI 650 (MSFC/EH)
Z302/RTV 670 (MSFC/EH)
Tedlar (MSFC/EH)
Silver (MSFC/Peters)
KRS-5 IR Crystal
Chromic Acid Anodize
[Ref 4]

S0069 included the most complete thermal and optical measurement system flown on the LDEF. This system included three radiometers using flat black thermopile detectors and domed collection optics. Quartz lenses were used on the solar and Earth albedo radiometers, and a germanium lens was used on the Earth infrared radiometer. This experiment also contained a calorimeter and a reflectometer containing tungsten and deuterium lamps, a scanning prism monochrometer, and a 4.5 inch diameter integrating sphere coated with barium sulfate. [Ref 5].

Measurements Performed on Samples:

In orbit: solar absorptance, total emittance, spectral reflectance (0.25 to 2.5 um)
Post-flight: post retrieval photographs, post-flight functional equipment tests on flight hardware absorptance, emittance, spectral reflectance, fluorescence
[Ref 4]

Results Summary:

Post-flight functional tests were performed on the reflectometer, calorimeter, radiometer and monochrometer flight hardware. These tests showed the systems to be in surprisingly good health. Most subsystems and

components are in good enough shape for the system to perform both reflectance and daily measurement functions. From these tests and analyses of flight data, there a number of anomalies that will require detailed analysis. These include: 1) Failure of a relay in the flight recorder which resulted in loss of one third of the flight data, 2) Premature latch-up of the 25th clock bit, 3) Hanging of the carousel during rotation at sample 25 resulting in loss of some reflectance data, 4) the bad or excessively noisy data in some of the UV reflectance measurements both in-flight and post-flight measurements.
[Reference 4.]

Conclusions:

While the TCSE system still functions after its extended space mission, this does not say that all components did not change. Some components are surely changed from the TCSE mission and, in some more demanding applications, could contribute to a system failure or compromised performance. Both subsystem and component tests and analyses should be carried out on the TCSE hardware to better understand the longterm effects of the space environment.[Reference 4]

System Analysis and Future Design Considerations:

[See Conclusion section.]

Published Experiment Reports:

1. Wilkes, D. R., POST FLIGHT SYSTEM FUNCTIONAL CHECK-OUT FINAL TEST REPORT, Report Np. 90-2-103-1, October 10, 1990.
2. Wilkes, D.R., MEASUREMENT AND ANALYSIS OF TCSE FLIGHT SAMPLES, REPORT NO. 90-2-107-1, February 1991.
3. Wilkes, D.R., TCSE INITIAL FLIGHT DATA ANALYSIS SUMMARY, Report No. 90-1-100-2, June 1991.

PI's Database:

None available.

References:

1. Clark, Lenwood, et.al., THE LONG DURATION EXPOSURE FACILITY (LDEF), NASA SP-473, NASA Langley Research Center, 1984.
2. Bourassa, Roger, J. and J.R. Gillis, "Data Summary: Atomic Oxygen Flux and Fluence Calculation for Long Duration Exposure Facility (LDEF)", LDEF MSIG, Boeing Defense and Space Group, NASA Contract NAS1-1824, Jan. 18, 1991."Solar Exposure of Long Duration Exposure Facility Experiment Trays", LDEF MSIG, Boeing Defense and Space Group, June 26, 1991, NASA Contract 1-1824-Task 12.
4.Wilkes, D.R., THERMAL CONTROL SURFACE EXPERIMENT: POST FLIGHT SYSTEM FUNCTIONAL CHECK-OUT FINAL TEST REPORT, Report No. 90-2-103-1.
5. Edelman, J. "LDEF Systems Special Investigative Group Thermal Analysis", Draft report to Boeing Defense and Space Group, October 4, 1991.
6. Wilkes, Donald and Leigh Hummer, "Thermal Control Surfaces Experiment: Initial Flight Data Analysis Final Report", prepared for George C. Marshall Space Flight Center, NAS8-36289-SC03, June 1991.

Experiment Status:

Hardware Archive:

Data Upgrade Date: 1/24/92

Experiment Title: LDEF Fiber Optic Exposure Experiment

Tray Location: C12 (81.9 degrees off RAM incidence angle)

Experiment Objective:

To study the effects of the low earth-orbit space environment on optical fiber cable and connector samples, in hopes of providing an increased level of confidence in the use of optical fiber technology in future NASA spacecraft and military satellites. [Ref 1]

AO Fluence (atoms/cm2): 1.28E + 21 [Reference 2]

Radiation Flux: Total flux estimated at around 300 rads for internal samples, and 7500 rads for the external samples. [1]

Temperatures (C): Estimated to be between 0-90F inside tray; between -85 and 185F at surface [Ref1].

Experiment Tray Sun Hours: 6,800 [Ref. 3]

M/D Impact Density: See results section for details.

Original Principal Investigators:

Alan R. Johnston and Larry A. Bergman
Jet Propulsion Laboratory
Pasadena, California

Present Principal Investigators:

A.R. Johnston, L.A. Bergman, R. Hartmayer
(818)354-4054 (818)354-4689 (818)354-1925
Jet Propulsion Laboratory
California Institute of Technology
Pasadena, California 91109
FAX (818)393-4820

Optical Materials Flown on LDEF:

Following are excerpts from a more complete Table 1 provided in Reference 1 of the optical fibers flown on LDEF. (External fiber cable samples are identified by the letter "P", while internal samples are identified by the letter "C" in the sample designation.) All cables were off-the-shelf products, available in the early 1980's, except the single mode fiber, which was a developmental item, cabled in an off-the-shelf cable type. All the major fiber types, plastic-clad, large core, graded index and single-mode, were represented. For each flight sample, an identical control fiber sample was kept at JPL for post-flight comparisons.

CABLE	CORE/CLADDING	BUFFER	TUBE MATERIAL	STRENGTH MEMBER/CABLE JACKET
P-1	Ge-doped silica/silica	Acrylate	Hytrel tight	Kevlar/polyurethane
P-2	Glass/glass	Polymer coat/	Hytrel tight	Kevlar/polyurethane
P-3	Silica/proprietary	Acrylate soft coat	Acrylate Hard	--/urethane
P-4	Silica/borosilicate	Acrylate	--	Kevlar/polyurethane
C-1	Ge-doped silica/silica	Acrylate	Hytrel tight	Kevlar/polyurethane
C-2	Silica/borosilicate	silicone	Hytrel tight	Kevlar/polyurethane
C-3	Borosilicate/borosilicate	Halar 300	Polyester loose	Fiberglass/polyurethane
C-4	Silica/borosilicate	Acrylate	–	Kevlar/polyurethane
C-5	Silica/RTV silicone	RTV silicone	Tefzel tight	Kevlar hytrel
C-6	Quartz/quartz	Polyacrylate	Nylon loose	Kevlar/PVC

Measurements Performed on Samples:

Visual and photodocumentation
Microscopy and photomicrography
Micrometeroid counts (with hand lens)
Color changes
Optical time domain reflectometry (OTDR)
Comparison measurements between flight and control samples (study attentuation and photobleaching)
Spectral loss
[Ref 1]

Results Summary:

POST FLIGHT OBSERVATIONS

There were no changes in the components mounted inside of the experiment tray that could be seen by comparing before and after photographs. However, external samples exhibited color changes, slight staining, physical displacement from the surface of the mounting plate. During dismanteling of the tray at JPL, many micrometeroid impacts were detected on the surface of the tray, the sample plates, and on the fiber cables. None of the micrometeroid impacts caused any detectable damage to the optical fiber. Four of the twenty connector termination show evidence of contamination on the polished end surface of the termination, though not in the small, optically important core area of the fiber on any of the four. The unknown contaminant appears to have been extruded through microcracks in the epoxy used to secure the fiber in the connector ferrule. Certain flight samples exhibited a noticeable stiffening, and were more difficult to strip. [Ref 1]

EXPERIMENTAL DATA

1. Photobleaching: The attentuation change observed at 1300 nm after photobleaching was measured using a non-contact technique on six samples was averaged, the result being -0.027 +/- 0.05dB. The precision of the sample to control comparison was about 0.05 dB or 1%. Therefore, no measurable photobleaching effect was detected between the flight and control samples.
2. Direct and OTDR Attentuation Comparison: For the control samples, the difference between direct and PTDR attentuation values, averaged over all samples (except the single mode fiber) was 0.07 +/- 0.08dB., leading to the conclusion that the overall accuracy is approximately +/- 0.1 dB. For the flight samples, the same difference is 0.15 +/- 0.11 dB, indicating on the average, the flight samples incurred a small (between 0.1 and 0.2 dB) increase in loss. To summarize the loss data at 830 nm, four of the six internally mounted samples showed no increase in loss, within the estimated measurement increase. The remaining two had a small increase, on the order of 0.5 dB, Three of the four external samples exhibited a larger increase, 2 to 4 dB. The fourth external sample showed no loss increase.
3. Spectral loss: The samples tested to date show a broad absorption near 600 nm, which is typical for radiation damaged fibers.
4.Temperature: The temperature was estimated to range between 0 and 90F inside tray; and between -85 and 185F at surface of tray. The LDEF tray was exposed to about 30,000 thermal cycles during the course of the mission.
5. Loss vs Temperature: The typical attentuation versus temperature data exhibited a hysteresis type behavior because of the large rate of change of temperature during the test cycle.
6. Attentuation Data Conversion: Converting the attentuation data presented earlier to dB/km and combining it with the rough preflight estimate of dose, they obtained for P-1 a loss increment of approximately 10E -3 db/km-rad, and for C-1 approximately 2.5E -2 dB/km-rad. Sample P-1 was a germanium-doped core fiber with a small amount of phosphorus along the axis of the core. The core of sample C-1 was doped with germanium and phosphorus throughout. The other three external samples suffered loss increases between 1 and 3E-2 dB/km-rad, consistent with expectations for a Ge-P doped fiber, but they do not yet know their composition.
7. Micrometeroid Impacts: There were three impact craters approximately 0.5mm in diameter on different cables. The average number of impacts larger than 0.01 mm, was 33 on a sample plate, 21 on the fiber cable sample coil, and 2 on each of the fiber mounting clamps. None of the micrometroid impacts caused any detectable damage to the optical fiber.

[Ref 1]

Conclusions:

1) All samples were functional with the proper optical power design margin, all of them would have performed well in a system function for the duration of the mission.
2) Tentatively, damage from ionizing radiation appears consistent with the laboratory experiments. Measurements producing an annealing curve extending to 1 day or more in duration appear useful to predict damage over missions as long as LDEF.
3) The choice of the most radiation resistent fibers available now, by extrapolation, will enable missions with significantly higher dose and longer runs to be achievable.
4) Internally located connectors performed well. However, contamination thought to be volatiles derived from the cable materials was observed. Additional thermal-vac tests aimed at understanding this phenomenon are desirable.
5) Three micrometeroid pits about 0.5 mm in diameter were observed on our four external cables, but the fibers were not damaged. An exposed 1 km fiber cable would have seen the order of 10 such impacts per year, with unknown risk to the fiber.
6) No photobleaching (or conversely no incomplete annealing of radiation damage) was observed.

7) A better understanding of the long-term effects of the space environment (vacuum and heat) on polymer material (both mechanical and optical materials is needed.
[Ref 1]

System Analysis and Future Design Considerations:

1. Temperature dependent fiber attentuation loss will be an important design consideration for future systems. In this experiment, an increase in loss with decreasing temperature, becoming much steeper near the lower end of our temperature range, was observed in most (but not all) fiber cables. The typical attentuation versus temperature data exhibited a hysteresis type behavior because of the large rate of change of temperature during the test cycle.
2. LDEF exposure adds to the overall bulk of data for predicting the effect of much longer exposures.
3. LDEF exposure has subjected samples to a real space environment with a combination of effects occuring.
4. Present day rad-hard fibers are considerably better than those used on LDEF, so it appears reasonable to expect much longer runs to be possible in the future, even for missions that may have an order of magnitude larger total radiation dose.
5. For future systems, careful attention must be given to improving the temperature stability of cable structures, and to qualification testing to verify their performance.
6. Should understand the possible sources and mechanisms for the observed contamination in order to eliminate the possiblity of degradation in performance.
7. Further invesigation into polymer aging is necessary, for the materials in fiber cables, the fiber buffer, the cladding in PCS fibers and the cements used in making up a connector termination may all undergo changes in optical or mechanical properties which would affect performance. [Ref 1]
8. For longterm use in space, Johnston recommends using radiation hard fibers, shield ing and protecting them from temperature extremes. [Ref 4]

Published Experiment Reports:

PI's Database:

References:

1. Johnston, A.R. , "LDEF Fiber Optic Exposure Experiment S0109", LDEF First Post-Retrieval Symposium Proceedings, NASA CP-3134.
2. Bourassa, Roger, J. and J.R. Gillis, "Data Summary: Atomic Oxygen Flux and Fluence Calculation for Long Duration Exposure Facility (LDEF)", LDEF MSIG, Boeing Defense and Space Group, NASA Contract NAS1-1824, Jan. 18, 1991.
3. Bourassa, Roger, J. and J.R. Gillis, "Solar Exposure of Long Duration Exposure Facility Experiment Trays", LDEF MSIG, Boeing Defense and Space Group, June 26, 1991, NASA Contract 1-1824-Task 12.
4. Johnston, A.R., "LDEF Fiber Optic Exposure Experiment S0109", LDEF First Post-Retrieval Synposium verbal presentation, Kissimee, Florida, June 1991.

Experiment Status:

Hardware Archive:

Data Upgrade Date: 1/28/92

Experiment Number: S1002

Experiment Title: Investigations of Critical Surface Degradation Effects on Coatings and Solar Cells

Tray Location: E3 Trailing Edge (171.9 degrees off RAM incidence angle)

Experiment Objective:

To qualify these coatings under realistic space environment conditions. In addition, the experiment will provide design criteria, techniques, and test methods to insure control of the combined space and spacecraft environmental effects, such as contamination, electrical conductance, and optical degradation, on the coatings. [Ref. 1]

AO Fluence (atoms/cm2): 1.33E + 03 [Ref 2]

Radiation Flux: 7 E + 11 equivalent 1 MeV electrons for solar cells [Ref.3]

Temperatures (C):

Experiment Tray Sun Hours: Tray 11,100 [Ref 4]; the coatings/ solar cells 1440 [Ref3]

M/D Impact Density:

Original Principal Investigators:

Ludwig Preuss
Space Division, Messerschmitt-Bolkow-Blohm
Munich, Federal Republic of Germany

Present Principal Investigators:

Ludwig Preuss
Deutsche Aerospace AG-MBB
Munich, Federal Republic of Germany
Tel. 089-60727297
FAX 089-60727252

Optical Materials Flown on LDEF:

TEST COMPONENTS [from Ref 1, unless otherwise noted]

1. Second-surface mirror with Ag reflector and Inconel protection layer on rear; interference filter on front face.
2. Second-surface mirror with Ag reflector and Inconel protection layer on rear; interference filter on front face; doped In_2O_3 layer on interference filter.
3. Chromium black selective absorbers (Chemglaze Z306 as described in Ref. 2)
4. Solar-cell modules with doped In_2O_3 layer on cover glass
5. Quartz crystal microbalance

REFERENCE COMPONENTS [from Ref 1 unless otherwise noted]

1. Second-surface mirror with Ag reflector and Inonel protection layer on rear.
2. Optical solar reflector with Ag reflector and Inconel protection layer on rear .
3. Solar-cell module.

[from Reference 1 unless otherwise noted]

Measurements Performed on Samples:

OPTICAL MEASUREMENTS [Ref. 3]
Visual inspection
Thermooptical measurements (absorptance, emittance)
OTHER MEASUREMENTS [Ref. 3]
Electrical measurements (current, resistence, voltage, beat-frequency)
Chemical investigations (EDX, XPS, IR)
Metallurgical investigations (SEM)

Results Summary:

THERMOOPTICAL CHARACTERISTICS OF SINGLE COMPONENTS [Ref. 2]

Component	Solar abs.	Change in abs (%)	Emittance	Change in Emittance (%)
Flight- SSM/1F1	0.11+/-0.02	0	0.77 +/-0.04	0
Flight- SSM/1F 2	0.11+/-0.02	0	0.77 +/-0.04	0
Control (1&2 mean)	0.11+/-0.02	0	0.77 +/-0.04	0
Flight-SSM/1F/LS 3	0.16 +/0.02	14	0.75+/-0.04	0
Flight-SSM/1F/LS 4	0.16 +/-0.02	14	0.75 +/-0.04	0
Control (5&6 mean)	0.14 +/0.02	0	0.75 +/-0.04	0
Flight-SSM 5	0.11 +/-0.02	10	0.78 +/-0.04	1

Control- SSM 9	0.10 +/-0.02	0	0.77 +/-0.04	0
Flight- OSR 6	0.09 +/-0.02	13	0.79 +/-0.04	1
Control- OSR 10	0.08 +/-0.02	0	0.78 +/-0.04	0
Flight -Chemglaze 7	0.94 +/-0.01	2	0.89 +/-0.05	1
Control-Chemglaze12	0.96 +/-0.01	0	0.90 +/- 0.05	0
Flight-OTS SC 13	0.83 +/-0.01	1	0.79 +/-0.04	0
Control-OTS SC 5	0.82 +/-0.01	0	0.79 +/-0.04	0
Flight-GEOS SC 12	0.81 +/-0.01	0	0.77 +/-0.04	0
Flight-GEOS SC 11	0.81 +/-0.01	0	0.77 +/-0.04	0
Control GEOS SC 10	0.81 +/-0.01	0	0.77 +/-0.04	0
Control GEOS SC 1	0.81 +/- 0.01	0	0.77 +/- 0.04	0

Legend:
SSM Second surface mirror
IF Interference filter
SC Solar cell
LS Conductive layer (In_2O_3)
OSR Optical solar reflector
Chemglaze Z306 black coating
QCM Quartz crystal microbalance
GEOS, OTS Satelllites
[Ref 2]

Conclusions:

All space exposed sulfuric acid anodized surfaces turned a yellow color, with a resulting increase in solar absorptivity (values increased up to 25%) due to contamination. A particularly intensive yellow coloring can be detected in areas where the adhesive residue had not been removed completely. (The intensity of the color increased with increasing thickness.) The emittance values on the anodized surfaces did not show any significant change within the error of the measurements. QCM measurements and physical surface analyses indicate a contamination layer between 1 and 8 nm on all space exposed surfaces. [Ref 3]

A small number of micrometeroid impacts were seen, the diameters varying from 0.1 to 0.5 mm, except for one impact that measured 1 X 3 mm in size, which was attributed to a debris impact. No atomic oxygen degradation was detected. [Ref. 3]

Though a contamination layer was expected on the individual optical components, the XPS analyses indicated a contamination layer of less than 1 nm on the SSM/IF/LS .The effect on the emittance values was neglible and the increase in absorptance values for the nine month exposure period was within the measurement error of the technique, except for the dark yellow areas on the calorimeter support. In conclusion, absorptance and emittance values for the optical coatings (SSM/IF, SSM/IF/LS, SSM, OSR and Chemglaze) showed good behavior during the nine month exposure. Solar cells also showed good behavior during the nine month exposure. L. Preuss concludes, that considering both laboratory and the results of the LDEF mission, it can be concluded that the coatings and solar cell components investigated are space qualified. [Ref. 3]

System Analysis and Future Design Considerations:

Anodized surfaces are very sensitive to contamination, and will show an increase in solar absorbtivity. [Ref. 3]

Published Experiment Reports:

PI's Database:

References:

1. Clark, Lenwood, et.al., THE LONG DURATION EXPOSURE FACILITY (LDEF), NASA SP-473, NASA Langley Research Center, 1984.
2. Bourassa, Roger, J. and J.R. Gillis, "Data Summary: Atomic Oxygen Flux and Fluence Calculation for Long Duration Exposure Facility (LDEF)", LDEF MSIG, Boeing Defense and Space Group, NASA Contract NAS1-1824, Jan. 18, 1991.
3. Preuss, Ludwig, "Evaluation of LDEF Experiment S1002", LDEF First Post-Retrieval Symposium Proceedings, NASA CP-3134, 1991.
4. Bourassa, Roger, J. and J.R. Gillis, "Solar Exposure of Long Duration Exposure Facility Experiment Trays", LDEF MSIG, Boeing Defense and Space Group, June 26, 1991, NASA Contract 1-1824-Task 12. LDEF Mission 1 book.

Experiment Number: S1002

Experiment Status:

Hardware Archive:

Data Upgrade Date: 1/28/92

(Color version of black and white photograph on p. 26)

Near Trailing Edge

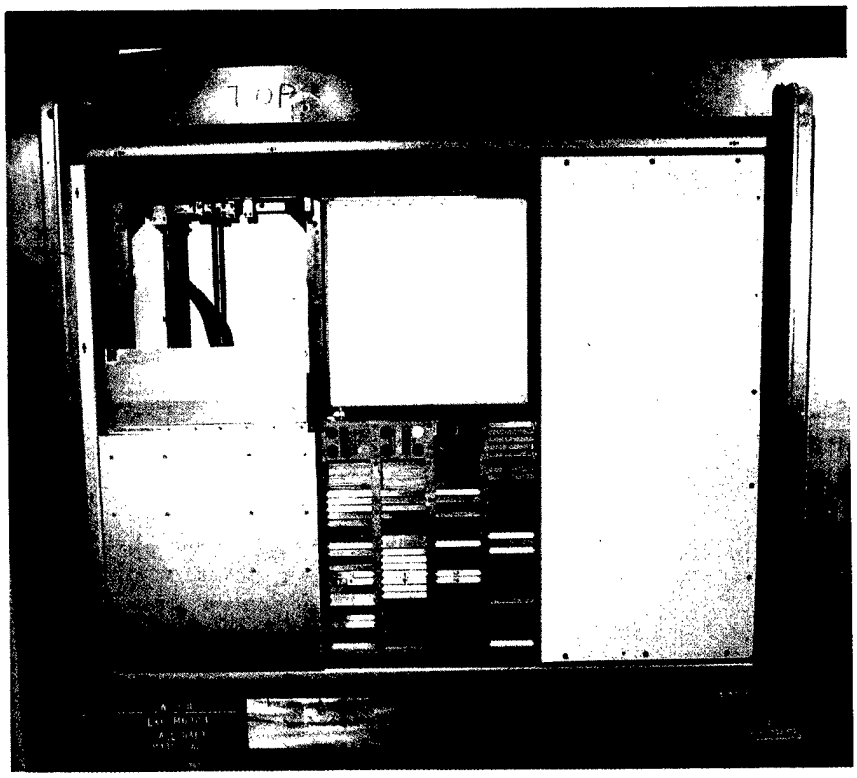

Near Leading Edge

Figure 3.0-1. Effect of Solar UV on Thermal Control Coatings

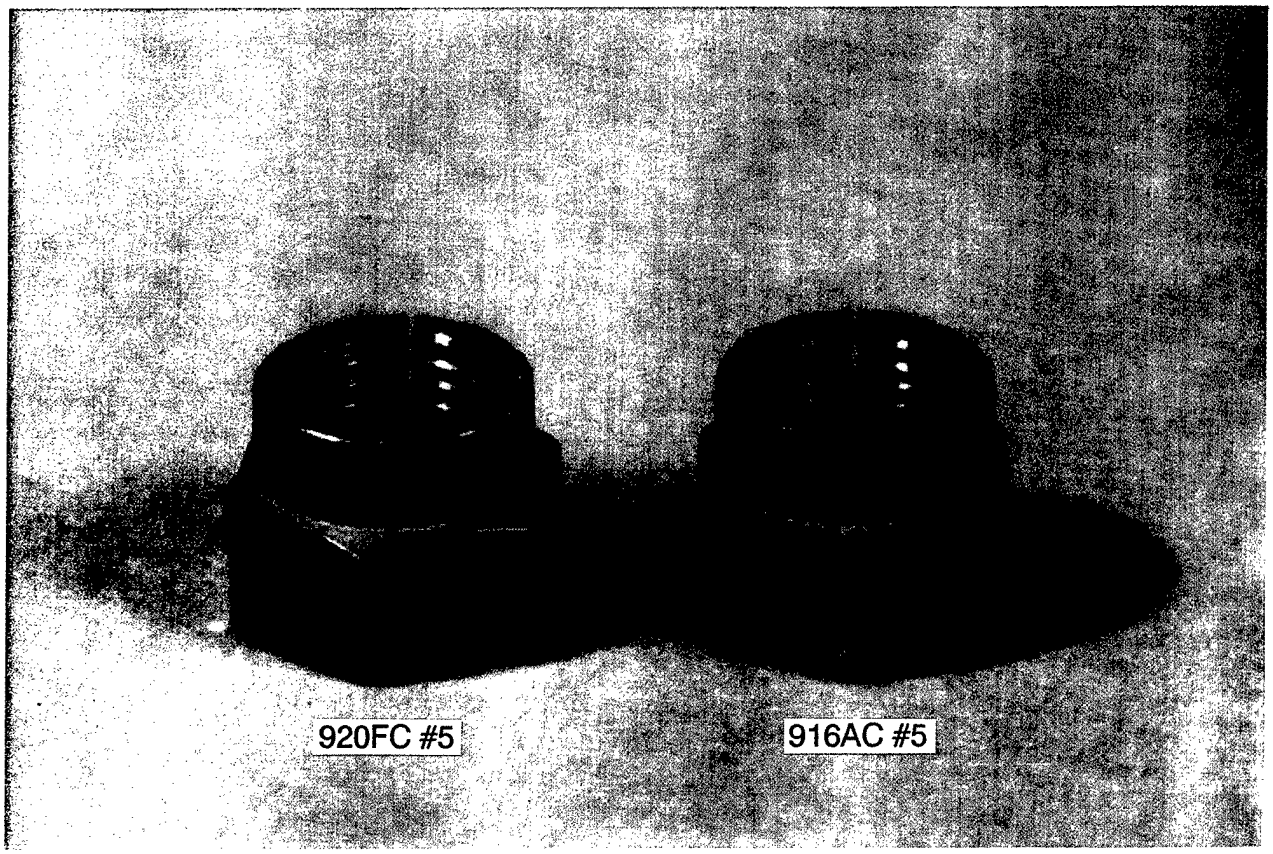

Figure 4.1.3.1-4. Photograph of silver plated nuts—All exterior nut surfaces had a brown contaminant film, some more than others. The discoloration of the nut was not atomic oxygens caused oxidation.

(Color version of black and white photograph on p. 58)

(Color version of black and white photograph on p. 92)

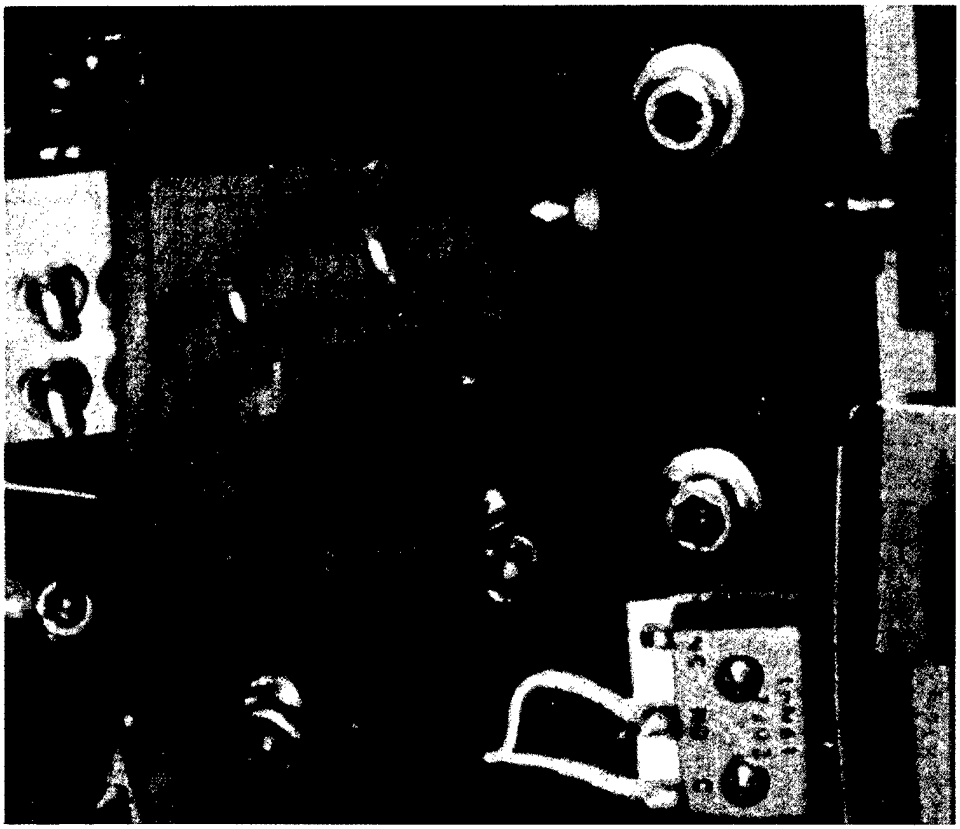

Figure 4.1.7-1. Offgassing Diffraction Pattern of Ball Brothers Lubricant 44177

radiation. Thermal analysis (differential scanning calorimetry and thermal gravimetric analysis) of the extracted oil revealed a new endotherm at approximately 106° C. This may be attributable to moisture effects. The LDEF grease also had a new endotherm at 211° C. This has not been explained at this time. Further testing is planned.

Dow Corning 340 heat sink compound was used on two experiments on LDEF; A0133, Effect of Space Environment on Space Based Radar Phased Array Antenna, and M0001, Heavy Ions in Space. The heat sink compound in both experiments performed as expected, transferring heat from one surface to another. Neither application exposed the Dow Corning 340 to U.V. radiation or to atomic oxygen, but both experiments saw hard vacuum and mild thermal cycling. The infrared spectra of a sample of Dow Corning 340 from experiment M0001 was unchanged compared to that of a control sample.

Dow Corning 1102, used on Experiment S1001, Low Temperature Heat Pipe, is an obsolete heat sink compound that was composed of 85% mineral oil, 10% Bentonite, 3% MoS_2, and 3 percent acetone. Postflight visual examination of the material showed no change from the initial condition.

Dow Corning Molykote Z was used on Experiment A0138. No results have been reported.

Exxon Andok C was used in Experiment S0069, Thermal Control Surfaces Experiment. No results have been reported.

BOEING ELECTRONIC COMPONENT EXPERIMENT: PARTS FLOWN

A. Plastic Encapsulated Devices Experiment

20	CD4068BE 8-input NAND gate (CMOS)
20	DM54LS30N 8-input NAND gate (low power Schottky)
100	1 uf, 50V ceramic capacitors
100	10MegOhm, 1/4 watt, 1% resistors
50	2N2222A-type transistors
100	1N4005 diodes

B. Hybrid Integrated Circuits Experiment

This contained 63 miscellaneous hybrids, including assorted circuits, resistor test patterns (CrSi, NiCr, thick films), and assorted substrates (A1203, Be0, etc.)

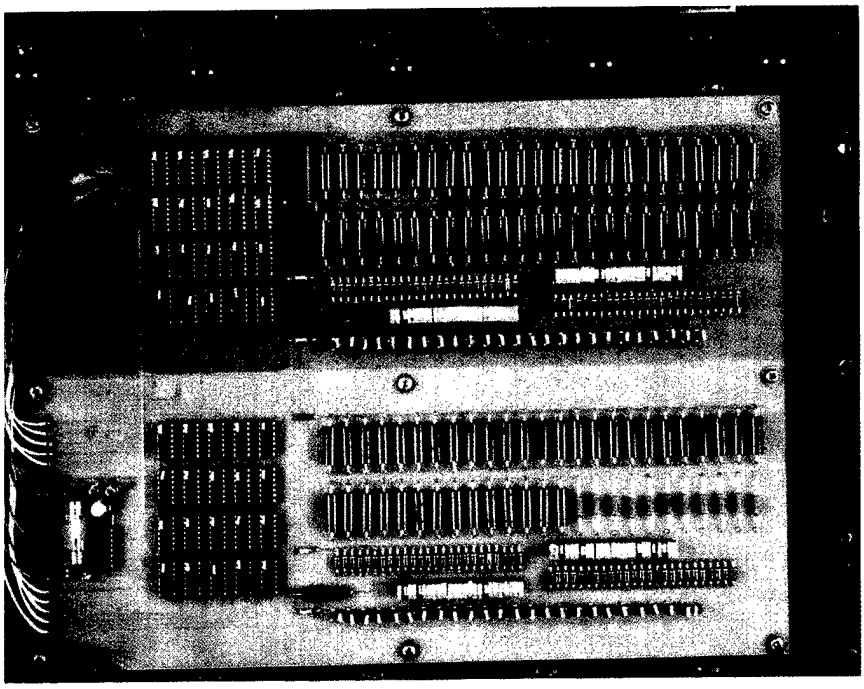

Figure 4.2.8-1. Boeing LDEF Circuit Board After Flight and Recovery

(Color version of black and white photograph on p. 158)

(Color version of black and white photograph on p. 170)

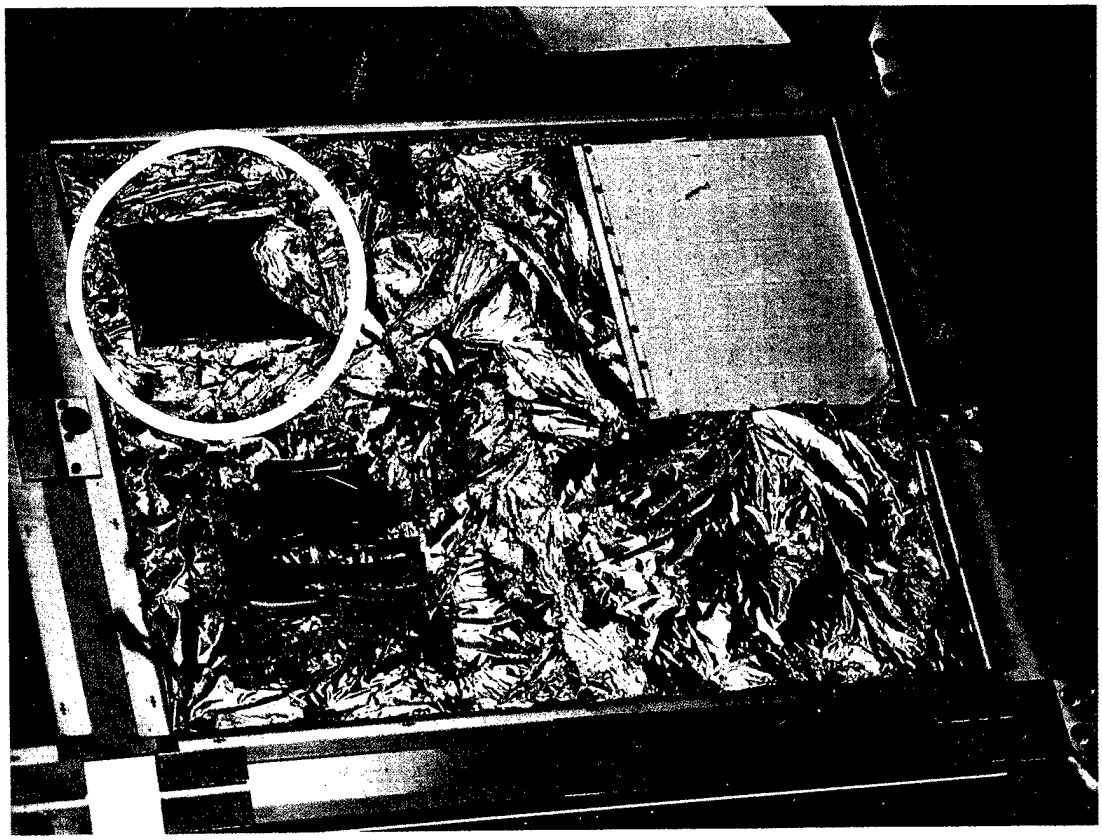

Figure 4.3.2.2-2. On-Orbit Photograph of Experiment A0076

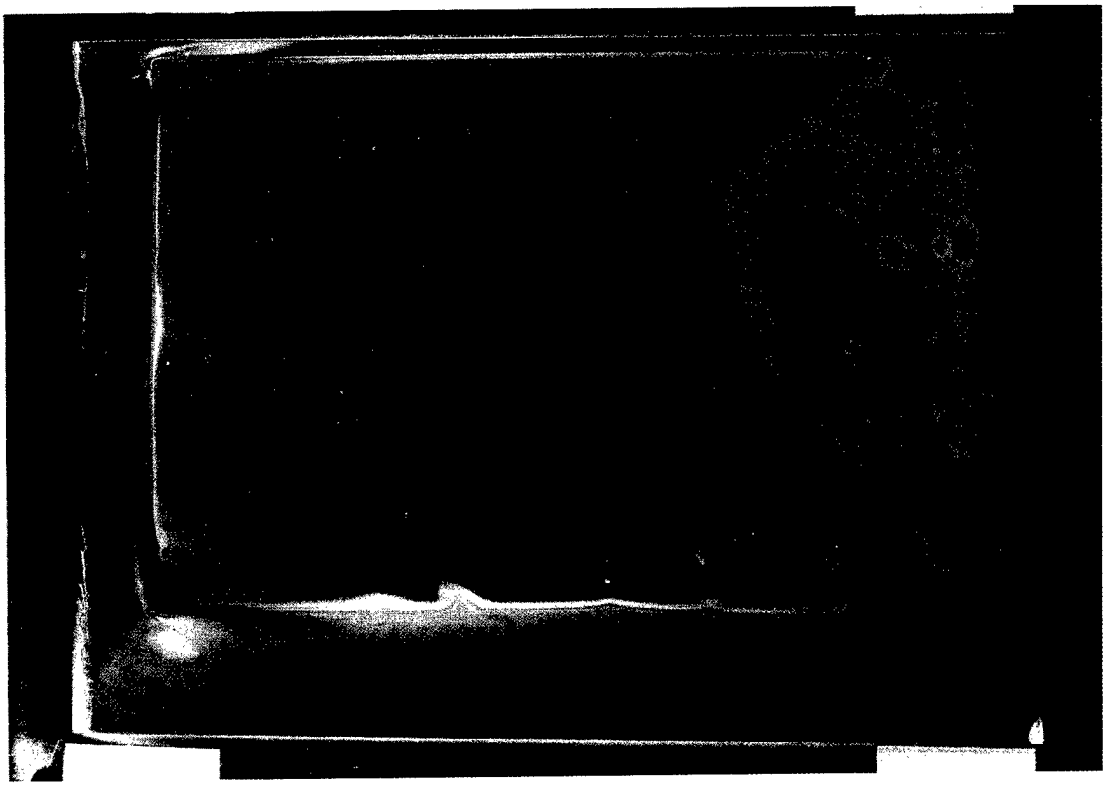

Figure 4.3.2.2-3. Close-Up of Solar Collector After Removed From the Experiment

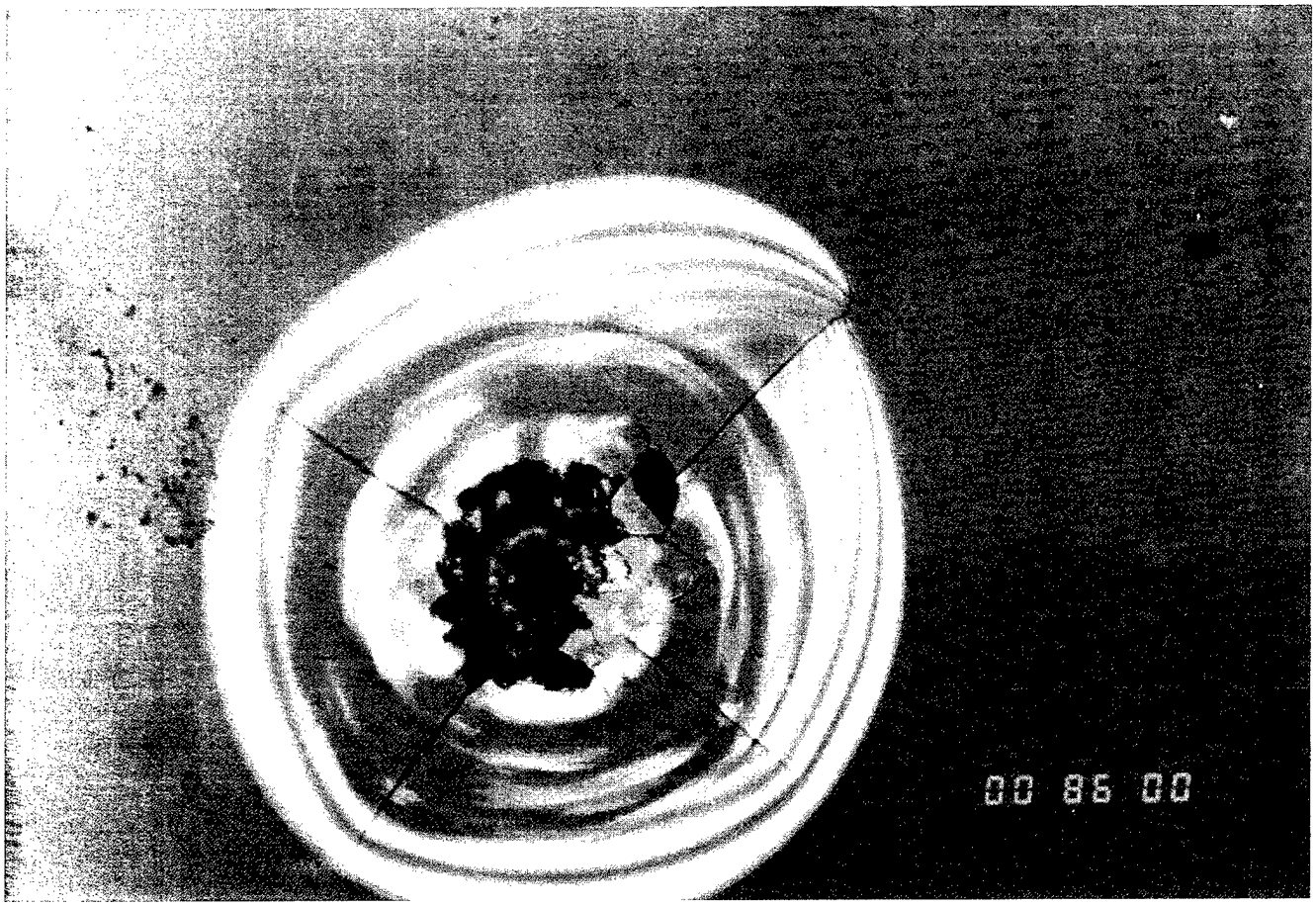

Figure 4.4.2.1-1. Impact Crater With Surrounding Localized Damage on a Transparent Dielectric-Fused SiO_2 Glass Substrate (Photograph Courtesy of The Aerospace Corporation)

(Color version of black and white photograph on p. 184)

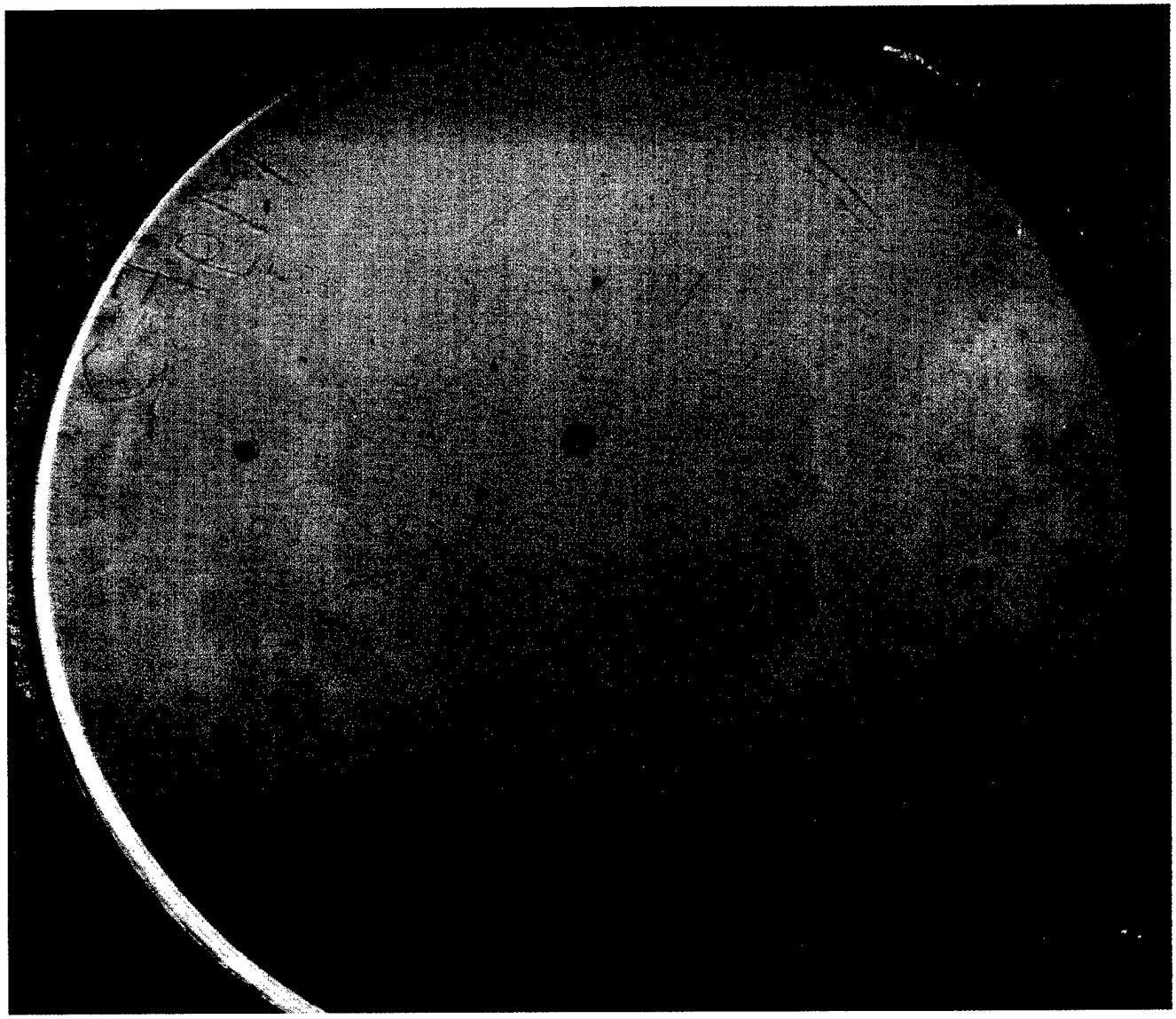

Figure 4.4.2.1-3. Effects of Long Exposure on Optical Systems Components (S0050-1) Contaminated MgF_2 Optical Window

(Color version of black and white photograph on p. 186)

(Color version of black and white photograph on p. 189)

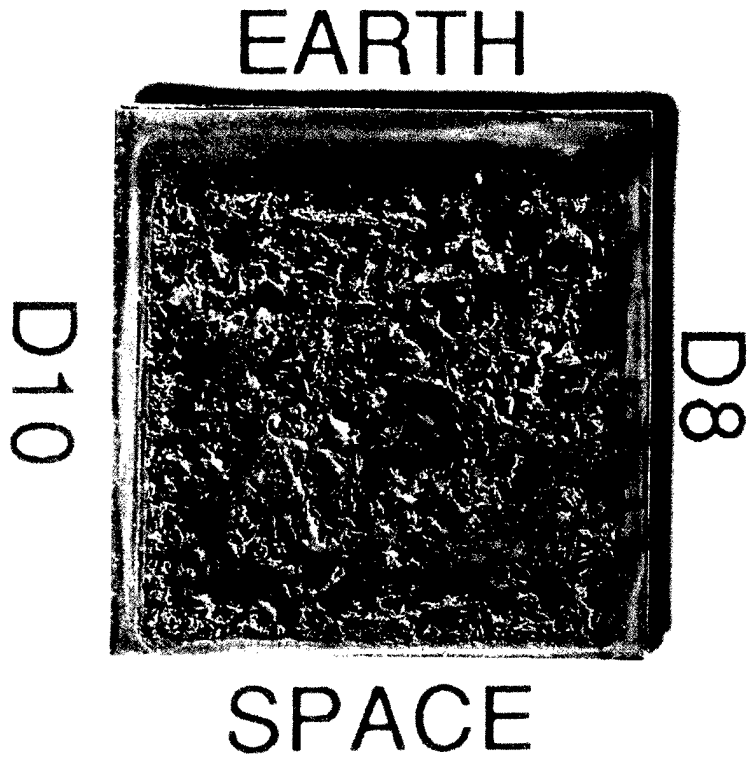

Figure 4.4.2.2 -1. Severely Corroded and Peeling Optical Solar Reflector Silver Mirror (Photograph Courtesy of The Aerospace Corporation)

Figure 4.4.2.2-2. Contamination on Laser Mirror Photographed at SAEF-2 at the Nomarski Microscope Workstation. (Courtesy of E. R. Crutcher)

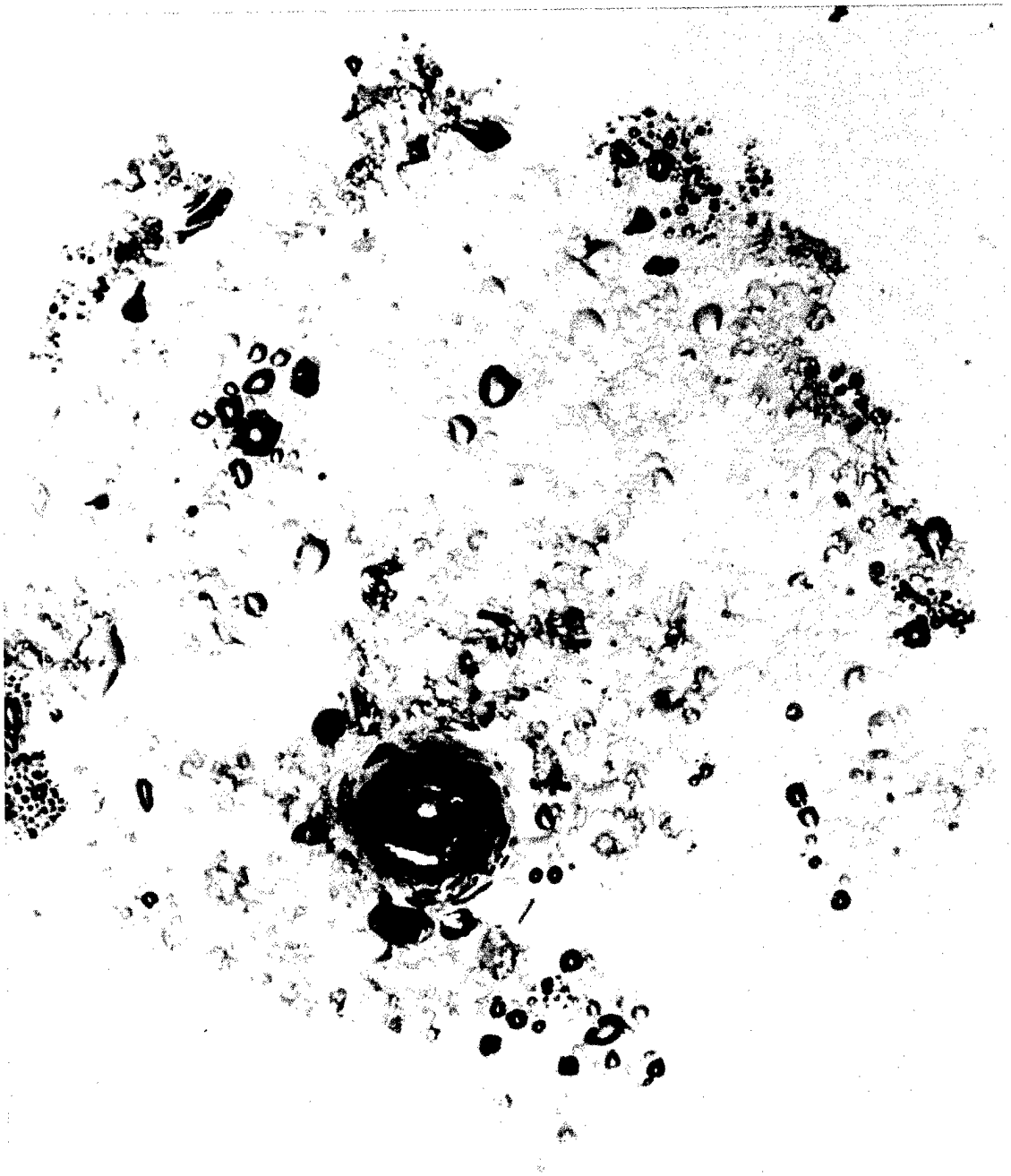

Figure 4.4.2.2 -3. An Impact Crater With an Expanded, Asymetric Area of Damage. The substrate is molybdenum with a Cr/Ag/ThF_4 coating. (Photograph courtesy of The Aerospace Corporation)

(Color version of black and white photograph on p. 191)

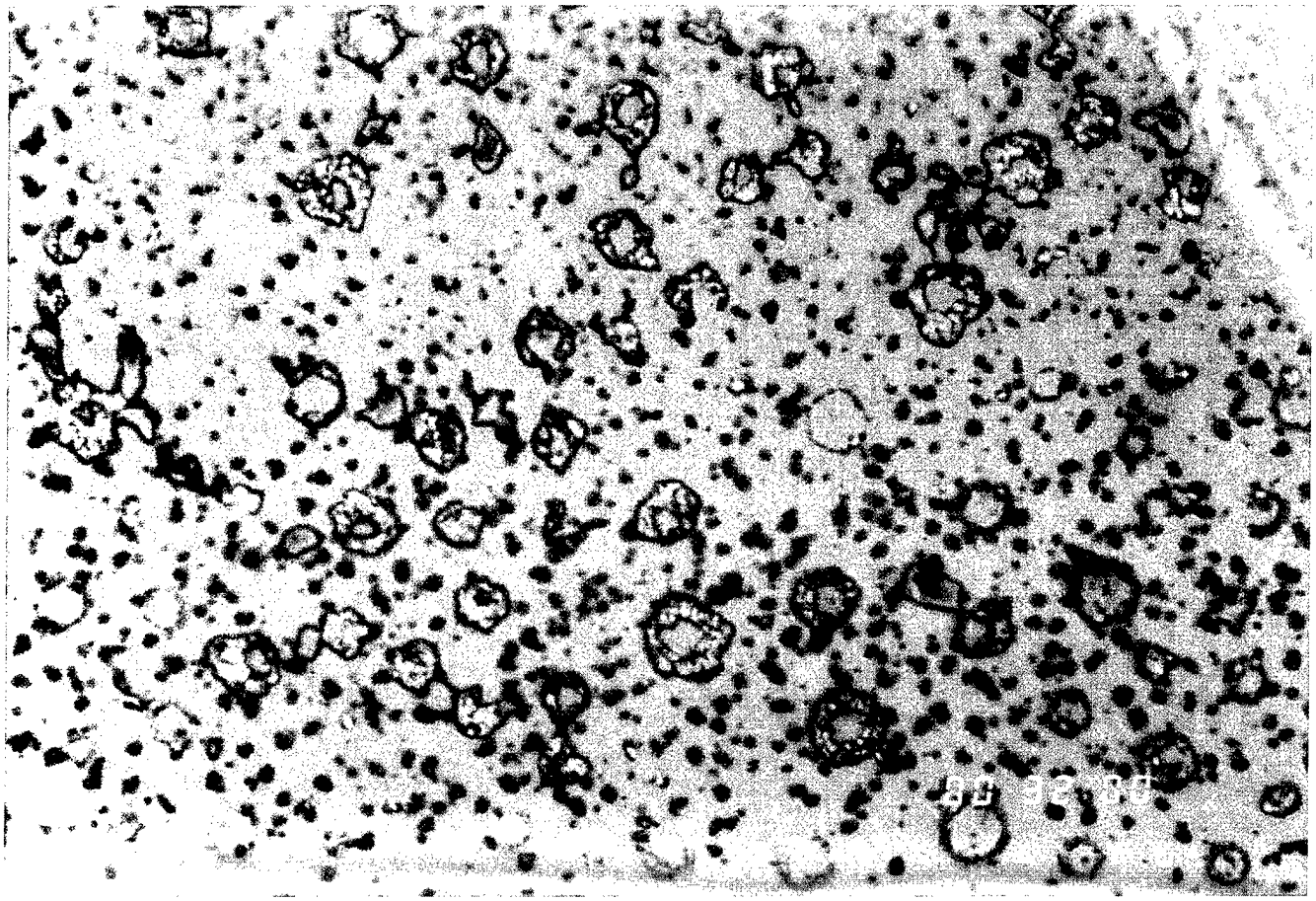

Figure 4.4.2.2-4. Degraded ZnS Coating on a SiO_2 Substrate (Courtesy of The Aerospace Corporation)

(Color version of black and white photograph on p. 193)

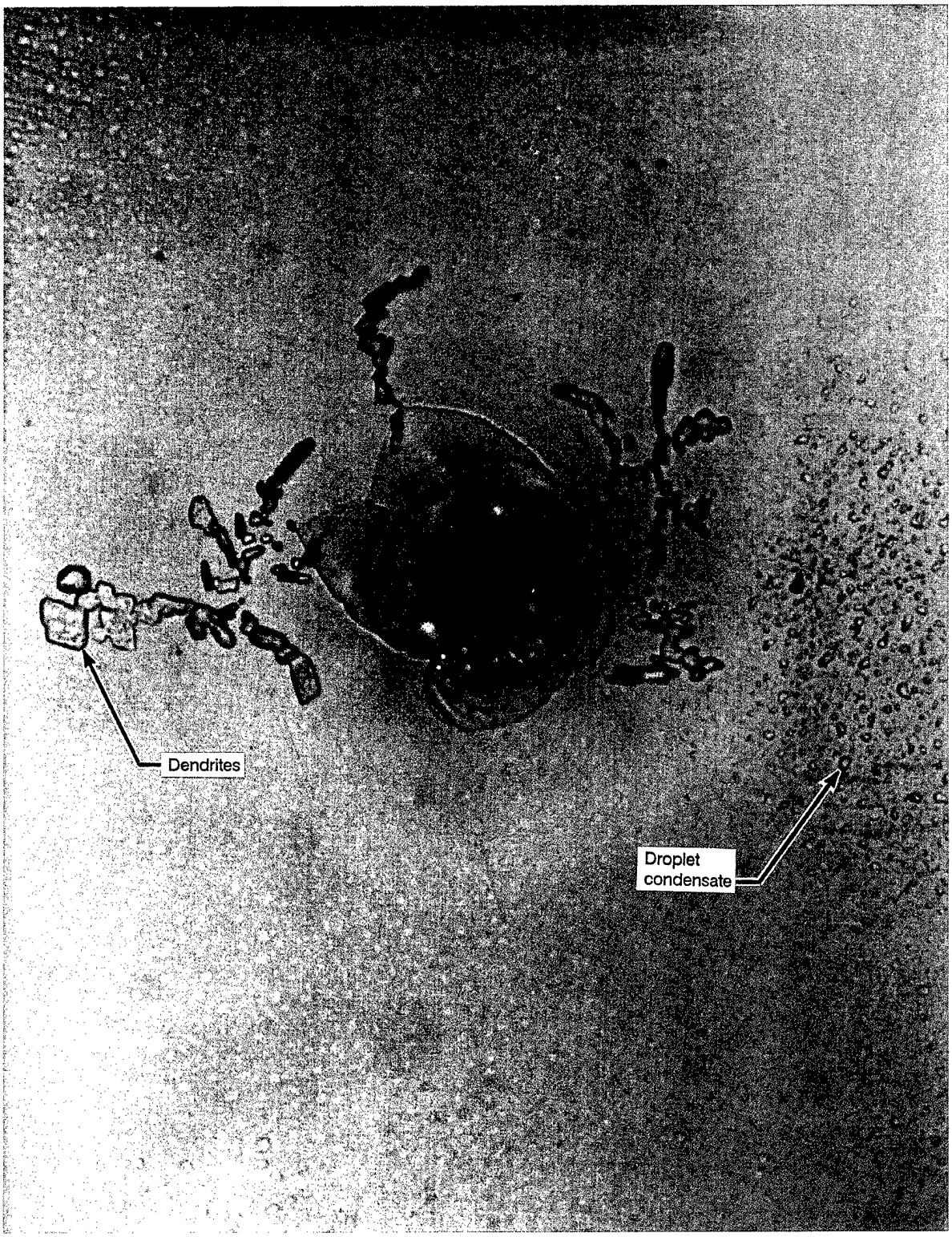

Figure 4.4.2.3-1. Damaged Area of a Coated Solar Cell Coverglass on a Silicon Wafer, Surrounded by What Appears to Be Dendrites and a Droplet Condensate (Courtesy of The Aerospace Corporation)

(Color version of black and white photograph on p. 197)

REPORT DOCUMENTATION PAGE

Form Approved
OMB No. 0704-0188

Public reporting burden for this collection of information is estimated to average 1 hour per response, including the time for reviewing instructions, searching existing data sources, gathering and maintaining the data needed, and completing and reviewing the collection of information. Send comments regarding this burden estimate or any other aspect of this collection of information, including suggestions for reducing this burden to Washington Headquarters Services, Directorate for Information Operations and Reports, 1215 Jefferson Davis Highway, Suite 1204, Arlington, VA 22202-4302, and to the Office of Management and Budget, Paperwork Reduction Project (0704-0188), Washington, DC 20503

1. AGENCY USE ONLY *(Leave blank)*

2. REPORT DATE
April 1992

3. REPORT TYPE AND DATES COVERED
Contractor Report

4. TITLE AND SUBTITLE
Analysis of Systems Hardware Flown on LDEF - Results of the Systems Special Investigation Group

5. FUNDING NUMBERS
C NAS1-19247
WU 506-48-91-08

6. AUTHOR(S)
Harry W. Dursch, W. Steve Spear, Emmett A. Miller, Gail L. Bohnhoff-Hlavacek, and Joel Edelman

7. PERFORMING ORGANIZATION NAME(S) AND ADDRESS(ES)
Boeing Defense & Space Group
P. O. Box 3999 M/S 82-32
Seattle, WA 98124-2499

8. PERFORMING ORGANIZATION REPORT NUMBER

9. SPONSORING / MONITORING AGENCY NAME(S) AND ADDRESS(ES)
NASA
Langley Research Center
Hampton, VA 23665-5225

SDIO
Materials & Structrues Off.
Washington, DC 20301-7100

10. SPONSORING / MONITORING AGENCY REPORT NUMBER
NASA CR-189628

11. SUPPLEMENTARY NOTES
Langley Technical Monitor: Louis A. Teichman

12a. DISTRIBUTION / AVAILABILITY STATEMENT
Unclassified - Unlimited

Subject Category 18

12b. DISTRIBUTION CODE

13. ABSTRACT *(Maximum 200 words)*

The Long Duration Exposure Facility (LDEF) was retrieved after spending 69 months in low Earth orbit (LEO). LDEF carried a remarkable variety of mechanical, electrical, thermal, and optical systems, subsystems, and components. The Systems Special Investigation Group (Systems SIG) was formed to investigate the effects of the long term exposure to LEO on systems related hardware and to coordinate and collate all systems analysis of LDEF hardware. This report discusses the status of the LDEF Systems SIG investigation through the end of 1991.

14. SUBJECT TERMS
LDEF, Low Earth Orbit, Spacecraft Systems

15. NUMBER OF PAGES
298

16. PRICE CODE
A13

17. SECURITY CLASSIFICATION OF REPORT
Unclassified

18. SECURITY CLASSIFICATION OF THIS PAGE
Unclassified

19. SECURITY CLASSIFICATION OF ABSTRACT

20. LIMITATION OF ABSTRACT